Convection in Fluid and Porous Medium under Modulation

THESIS

Submitted to
Babasaheb Bhimrao Ambedkar University
(A Central University)
Lucknow

BABASAHEB
BHIMRAO
AMBEDKAR
UNIVERSITY

LUCKNOW
प्रज्ञा शील करुणा
ESTABLISHED 1996

for the award of the Degree of

Doctor of Philosophy

in

APPLIED MATHEMATICS

Under the supervision of
Prof. B.S. BHADAURIA

Research Scholar
AJAY SINGH
Enrollment No. 057/13

DEPARTMENT OF APPLIED MATHEMATICS
SCHOOL FOR PHYSICAL SCIENCES
BABASAHEB BHIMRAO AMBEDKAR UNIVERSITY
(A CENTRAL UNIVERSITY)
VIDYA VIHAR, RAEBARELI ROAD, LUCKNOW-226 025
UTTAR PRADESH, INDIA

2017

Convection in Fluid and Porous Medium under Modulation

THESIS

Submitted to
Babasaheb Bhimrao Ambedkar University
(A Central University)
Lucknow

BABASAHEB
BHIMRAO
AMBEDKAR
UNIVERSITY
LUCKNOW
प्रज्ञा शील करुणा
ESTABLISHED 1996

for the award of the Degree of

Doctor of Philosophy

in

APPLIED MATHEMATICS

Under the supervision of
Prof. B.S. BHADAURIA

Research Scholar
AJAY SINGH
Enrollment No. 057/13

DEPARTMENT OF APPLIED MATHEMATICS
SCHOOL FOR PHYSICAL SCIENCES
BABASAHEB BHIMRAO AMBEDKAR UNIVERSITY
(A CENTRAL UNIVERSITY)
VIDYA VIHAR, RAEBARELI ROAD, LUCKNOW-226 025
UTTAR PRADESH, INDIA

2017

Dedicated

to

My Family Members

DECLARATION

I declare that the work embodied in this Ph.D. thesis entitled as **"Convection in Fluid and Porous Mediun under Modulation"** is carried out by me under the supervision of Prof. B.S. Bhadauria, Department of Applied Mathematics, Babasaheb Bhimrao Ambedkar University (A Central University) Lucknow, India. The information presented in this Ph.D. thesis has not been submitted for the award of any degree or diploma. I declare that I have faithfully acknowledged, given credit to and referred to the research workers whenever their works have been cited in the text and the body of the thesis. I further declare that I have not willful lifted up some others work, para, text, data, results, etc. reported in the journals, books, magazines, reports, dissertations, thesis, etc., or available at websites and included them in this thesis and cited my own work.

Date: 04-12-2017

Ajay Singh

(Research Scholar)

CERTIFICATE

This is to certify that the thesis titled **"Convection in Fluid and Porous Medium under Modulation"** submitted by **Mr. Ajay Singh** is an original research work and has not been previously submitted in part or full for the award of any other degree or diploma to this or any other university.

The thesis submitted to the Babasaheb Bhimrao Ambedkar University Lucknow satisfies all the requirements as stipulated in the *Doctor of Philosophy (Ph.D.) regulations -1999 as amended in 2010* and it is fit for submission and evaluation for the award of the degree of Doctor of Philosophy of the University.

Date: 04-12-2017

Supervisor

Dr. B. S. Bhadauria
Professor of Mathematics
Department of Applied Mathematics
B.B. Ambedkar University, Lucknow

Head of the Department

Professor B. S. Bhadauria
Head
Department of Applied Mathematics
B.B. Ambedkar University, Lucknow

ACKNOWLEDGEMENT

First of all, I would like to give thank to Almighty God, without whose blessing it would have been difficulty to achieve this precious moment in my life.

I am gratefully beholden to my supervisor, Prof. B.S. Bhadauria, Professor and Head, Department of Applied Mathematics, Babasaeb Bhimrao Ambedkar University, Lucknow for providing me the opportunity to undergo this research work. He not only guided my research work but also gave me strength during the course of time. His continuous motivation, cooperation, assistance and moral support, I fulfilled my dreams to make my present venture. His devotion to duty will remain an ideal to me in future.

My grateful thanks are due to Dr. B.K. Singh and Dr. Rahul Varshney, Assistant Professor of Mathematics and Statistics respectively of the Babasaeb Bhimrao Ambedkar University, Lucknow for providing me necessary facilities during the course of research and timely encouragement.

I am thankful to my seniors (Palle Kiran, Alok Srivastava), for their co-operation at various stages of my research work.

I am also grateful to my dear friends Manoj, Vineet and Promod for their suggestion, inspiration and help in the completing this work.

I thank all the staff members, Mr. Rakesh and Mr. Vinay Kumar Sahu of the Department for their cooperation and help during the period of my research work time to time.

I express my sincere gratitude to my parents for their overwhelming support and encouragement to accomplish this task.

Ajay Singh

PREFACE

The thesis entitled **"Convection in Fluid and Porous Medium under Modulation"** comprising of analytical/numerical solutions of some problems related with the topic, is an outcome of the research work carried out by me during the course of investigations under the supervision of Prof. B.S. Bhadauria, Professor, Department of Applied Mathematics, School for Physical Sciences, Babasaheb Bhimrao Ambedkar University, Lucknow.

Rayleigh-Bénard convection is an example of convective thermal instability, introduced by Chandrasekhar(1961) in ordinary fluid layers worldwide since last one century. The porous media corresponding to this problem is known as Horton-Rogers-Lapwood convection and it has many applications in various fields of engineering, thermal sciences and geophysics. Regulating the convective phenomenon in thermal sciences is of considerable importance due to its numerous application, such as in engineering problems, in industries, etc. Therefore, the relevant studies on regulation of heat and mass transfer in the following chapters is performed. For more detailed analysis on thermal instability, refer some excellent books: Ingham and Pop(2005), Nield and Bejan(2012) and vafai(2000).

The **first problem** deals with the thermorheological effect of temperature dependent viscous fluid in the presence of imposed time periodic gravity modulation for double diffusive convection. The temperature dependent viscosity fluid gives rise to variation in top and bottom structures and referred as a non-Boussinesq effect. A weakly non-linear analysis of thermal instability under gravity modulation, with temperature dependent viscosity, using the power series expansion in terms of the amplitude of gravity modulation, which is considered to be small, is carried out for double-diffusive convection in porous media. Nusselt number and Sherwood number are calculated numerically through the non-autonomous equation involving amplitude of convection using Ginzburg-Landau equation. By exploring the non-linear effect of solute Rayleigh number (Ra_s), Lewis number (L_e), Vadász number (Va), thermorheological parameter and amplitude of gravity modulation analytically. The curves for heat and mass transfer with respect to slow time variation are depicted graphically. Further, streamlines, isotherms and isohalines for different values of time are also

drawn.

In the **second problem**, the combined effect of internal heating and time periodic gravity modulation on oscillatory convection in a viscoelastic fluid layer, using complex non-autonomous Ginzburg-Landau equation, is studied. A weakly non-linear stability analysis has been performed by using power series expansion in terms of the amplitude of gravity modulation. The Nusselt number has been obtained in terms of the amplitude for oscillatory mode of convection. The influence of relaxation (λ_1) and retardation (λ_2) time of viscoelastic fluid, on heat transfer, have been discussed. It is found that modulation has a destabilizing effect at low frequencies and stabilizing effect at high frequencies. Further, it is also found that overstability advances the onset of convection more with internal heating, hence increases heat transfer. The subcritical Hopf bifurcation and Pitchfork bifurcation are also studied.

The **third study** deals with the effect of various parameters on chaotic convection in an anisotropic porous medium, under gravity modulation, is investigated. For this, the problem is reduced into Lorenz system (nonautonomous) by employing truncated Galerkin expansion method. It is found that the system shows either chaotic or periodic nature for suitable values of scaled Rayleigh number (R). The influence of amplitude of modulation (δ) is to advance the chaotic nature in the system while that of frequency of modulation (Ω) has tendency to delay the chaotic behaviour. The effects of Péclet (P_e) number and anisotropic parameters on the chaotic system are also studied and found that they delay the chaotic nature. The phase portrait and time domain diagrams of the Lorenz system for suitable parametric values have been used to analyse the system.

The **fourth study** deals with the investigation on thermal instability in a couple-stress fluid saturated rotating porous medium under temperature modulation for oscillatory as well as chaotic convection by adopting complex Ginzburg-Landau equation and Lorenz system. Couple-stress fluid is a kind of non-Newtonian fluid having polar effects. To study oscillatory mode, a weakly non-linear stability analysis has been carried out in terms of the amplitude of temperature modulation(assumed to be small quantity), using power series

expansion. Here, three cases of temperature modulation are considered; In-phase modulation, Out-phase modulation and Lower-boundary modulation for oscillatory convection. The Nusselt number has been obtained in terms of the small amplitude for oscillatory mode of convection to govern the heat transport in the system. On the other hand, for chaotic convection, the governing equations are reduced into a (non-autonomous) Lorenz system by using truncated Galerkin expansion method. The effects of Vadász number, Couple-stress parameter (C_1) and amplitude of modulation are found to have destabilizing effect, whereas the frequency of modulation and Taylor number (Ta) show a stabilizing effect on oscillatory convection. Further, it is found that the effect of scaled Rayleigh number R and amplitude of modulation δ are to advance the chaotic convection while scaled Taylor number (T_A) is to delay the chaotic convection.

In the **fifth problem**, the effect of temperature modulation on chaotic convection in a viscoelastic fluid saturated porous medium has been investigated. For this, the problem is reduced into Lorenz system by employing truncated Galerkin expansion method. The effect of scaled Rayleigh number R on the chaotic system is studied and found that it has periodic and chaotic both nature in a defined interval. Amplitude of modulation is to advance the chaotic nature in the system. The effects of scaled relaxation (Γ) parameter and retardation parameter (Λ') on the system are also studied. The phase portrait and time domain diagrams of the Lorenz system for suitable parametric values have been used to analyse the system.

In the **last problem**, a nonlinear convection in nanofluid saturated porous medium is studied in the presence of effective throughflow and internal heating under gravity modulation. Nanofluid is mixture of a base fluid and nanoparticles. A weakly nonlinear stability analysis has been carried out to obtain the Nusselt number, which is found to be the function of various parameters related to heat and mass transport across the porous medium. The time periodic vertical vibration is used to regulate the thermal instability in the system. The parameters arise due to nanofluid like Le, Na, Rn are destabilizing the system. The effects of remaining parameters are also studied thoroughly.

Contents

List of Figures **v**

Nomenclature **xii**

1 Introduction **1**

1.1 Basic Definitions 1

1.1.1 Heat transfer 1

1.1.2 Rayleigh Bénard convection 3

1.1.3 Porous medium 3

1.1.4 Anisotropic porous medium 4

1.1.5 Saturated porous medium 4

1.1.6 Unsaturated porous medium 4

1.1.7 Porosity 4

1.1.8 Permeability 5

1.1.9 Hoton-Rogers-Lapwood convection 5

1.1.10 Mechanism of thermal instability 5

1.1.11 Newtonian and non-Newtonian fluids 6

1.1.12 Throughflow mechanism 7

1.1.13 Couple-stress fluid 7

1.1.14 Rotation 8

1.1.15 Internal heating 8

1.1.16 Nanofluid 9

1.1.17 Doubble diffusive convection 9

1.1.18 Chaos . . . 9
1.1.19 Modulation . . . 10
1.2 Hydrodynamic equations for fluid layer . . . 12
1.3 Hydrodynamic equations for porous medium . . . 14
1.3.1 Darcy law . . . 14
1.3.2 Brinkman-extended Darcy model . . . 15
1.4 Boundary conditions . . . 15
1.5 Methods of solution . . . 15
1.5.1 Analytical methods . . . 15
1.5.2 Numerical methods . . . 17
1.6 Some earlier work . . . 18
1.6.1 Temperature modulation in fluid layer . . . 18
1.6.2 Temperature modulation in porous medium . . . 19
1.6.3 Gravity modulation in fluid layer . . . 21
1.6.4 Gravity modulation in porous medium . . . 21
1.7 Applications . . . 23

2 An analytical study of heat and mass transport in Bénard-Darcy convection with G-jitter and variable viscosity liquids in porous media 24
2.1 Introduction . . . 24
2.2 Governing equations . . . 26
2.3 Amplitude equation and heat and mass transport for stationary instability . 30
2.4 Results and Discussion . . . 33
2.5 Conclusions . . . 41

3 Stability analysis and internal heating effects on oscillatory convection in a viscoelastic fluid layer under gravity modulation 44
3.1 Introduction . . . 44
3.2 Mathematical structure . . . 46
3.3 Basic state . . . 47
3.4 Analysis of the periodic solutions . . . 49

3.5 Bifurcation analysis . . . 53
3.5.1 Hopf bifurcation . . . 53
3.5.2 Pitchfork bifurcation . . . 54
3.6 Results and Discussion . . . 55
3.7 Conclusions . . . 63

4 Throughflow and G-jitter effects on chaotic convection in an anisotropic porous medium 64

4.1 Introduction . . . 64
4.2 Mathematical structure of the problem . . . 65
4.3 Method of solution . . . 66
4.4 Results and Discussion . . . 69
4.5 Conclusions . . . 79

5 Oscillatory and chaotic convection in a couple-stress fluid saturated rotating porous medium under temperature modulation 82

5.1 Introduction . . . 82
5.2 Mathematical formulation of the problem . . . 84
5.3 Formulation of Ginzburg-Landau (amplitude) equation . . . 86
5.4 Formulation of the Lorenz system . . . 91
5.5 Results and discussion . . . 93
5.6 Conclusions . . . 105

6 Numerical study on chaotic convection in a viscoelastic fluid saturated porous medium under temperature modulation 106

6.1 Introduction . . . 106
6.2 Mathematical structure of the problem . . . 107
6.3 Basic state . . . 108
6.4 Method of solution . . . 109
6.5 Results and Discussion . . . 111
6.6 Conclusions . . . 117

7 Nonlinear g-jitter thermal instability in nanofluid in the presence of throughflow and heat source **119**

7.1 Introduction 119

7.2 Mathematical structure of the problem 120

7.3 Basic state 123

7.4 Perturbed state 123

7.5 Non-linear stability analysis 123

7.6 Nusselt number for heat and mass transport 125

7.7 Results and Discussion 126

7.8 Conclusions 129

Bibliography **130**

List of Publications **148**

List of Conferences **149**

List of Figures

1.1 All kind of heat transfer 2

1.2 Rayleigh Bénard convection 3

1.3 A sketch of porous medium 4

1.4 Mathematical diagram of thermal instability 6

1.5 Physical assumptions for throughflow model 7

1.6 A diagram for chaotic motion 10

2.1 Physical configuration of the problem 26

2.2 Variation of Nusselt number with time for different values of V 33

2.3 Variation of Nusselt number with time for different values of Le 34

2.4 Variation of Nusselt number with time for different values of Ra_S 34

2.5 Variation of Nusselt number with time for different values Va 34

2.6 Variation of Nusselt number with time for different values δ 36

2.7 Variation of Nusselt number with time for different values Ω 36

2.8 Variation of Sherwood number with time for different values of V 36

2.9 Variation of Sherwood number with time for different values of Le 37

2.10 Variation of Sherwood number with time for different values of Ra_S 38

2.11 Variation of Sherwood number with time for different values Va 38

2.12 Variation of Sherwood number with time for different values δ 38

2.13 Variation of Sherwood number with time for different values Ω 39

2.14 Streamlines at (a) $\tau = 0.1$, (b) $\tau = 1$, (c) $\tau = 2$, (d) $\tau = 3$, (e) $\tau = 4$, (f) $\tau = 5$, (g) $\tau = 6$, (h) $\tau = 7$, (i) $\tau = 8$ 40

2.15 Isotherms at (a) $\tau = 0.1$, (b) $\tau = 1$, (c) $\tau = 2$, (d) $\tau = 3$, (e) $\tau = 4$, (f) $\tau = 5$, (g) $\tau = 6$, (h) $\tau = 7$, (i) $\tau = 8$ 41
2.16 Isohalines at (a) $\tau = 0.1$, (b) $\tau = 1$, (c) $\tau = 2$, (d) $\tau = 3$, (e) $\tau = 4$, (f) $\tau = 5$, (g) $\tau = 6$, (h) $\tau = 7$, (i) $\tau = 8$ 42

3.1 Physical configuration of the problem 46
3.2 Effect of R_i on Nu for fixed other parameters 56
3.3 Effect of P_r on Nu for fixed other parameters 56
3.4 Effect of λ_1 on Nu for fixed other parameters 57
3.5 Effect of λ_2 on Nu for fixed other parameters 57
3.6 Effect of δ on Nu for fixed other parameters 57
3.7 Effect of Ω on Nu for fixed other parameters 58
3.8 Comparison between internal and non-internal heating system 58
3.9 Streamlines at (a) $s = 0.0$, (b) $s = 0.4$, (c) $s = 0.8$, (d) $s = 1.0$, (e) $s = 1.2$, (f) $s = 1.5$ 59
3.10 Isotherms at (a) $s = 0.0$, (b) $s = 0.4$, (c) $s = 0.8$, (d) $s = 1.0$, (e) $s = 1.2$, (f) $s = 1.5$ 60
3.11 An unstable limit cycle (red) is created through Hopf bifurcation. The origin is asymptotically stable. $P_r = 1, R_i = 1, \lambda_1 = 0.4, \lambda_2 = 0.1, \delta = 0.3, \Omega = 50$ . . 60
3.12 Hopf bifurcation diagram. $P_r = 1, R_i = 1, \lambda_1 = 0.47, \lambda_2 = 0.1, \delta = 0.3, \Omega = 50$ 61
3.13 The origin is unstable. $P_r = 1, R_i = 1, \lambda_1 = 0.5, \lambda_2 = 0.1, \delta = 0.3, \Omega = 50$ . . 61
3.14 $P_r = 1, R_i = 1, \lambda_1 = 0.4, \lambda_2 = 0.1, a = 2.61411, \Omega = 1, s = 1000$ 62
3.15 supercritical pitchfork bifurcation. $P_r = 1, R_i = 1, \lambda_1 = 0.5, \lambda_2 = 0.1, a = 2.61411, \Omega = 1, s = 2000$ 62
3.16 subcritical pitchfork bifurcation. $P_r = 1, R_i = 1, \lambda_1 = 0.5, \lambda_2 = 0.1, a = 2.61411, \Omega = 1, s = 2100$ 62

4.1 Physical configuration of the problem 66
4.2 Phase portrait and time domain diagrams for the system (4.3.6) with parameters $R = 5$ and $\zeta = 0.4$, $\chi_1 = 0.4$, $P_e = 1.0$, $\delta = 0.1$, $\Omega = 5$ 68

4.3 Phase portrait and time domain diagrams for the system (4.3.6) with parameters $R = 8.5$ and ζ= 0.4, $\chi_1 = 0.4$, $P_e = 1.0$, $\delta = 0.1$, $\Omega = 5$ 69
4.4 Phase portrait and time domain diagrams for the system (4.3.6) with parameters $R = 15$ and ζ= 0.4, χ_1=0 .4, $P_e = 1.0$, $\delta = 0.1$, $\Omega = 5$ 69
4.5 Phase portrait and time domain diagrams for the system (4.3.6) with parameters $R = 23$ and ζ= 0.4, $\chi_1 = 0.4$, $P_e = 1.0$, $\delta = 0.1$, $\Omega = 5$ 70
4.6 Phase portrait and time domain diagrams for the system (4.3.6) with parameters $R = 24$ and ζ= 0.4, $\chi_1 = 0.4$, $P_e = 1.0$, $\delta = 0.1$, $\Omega = 5$ 70
4.7 Phase portrait and time domain diagrams for the system (4.3.6) with parameters $R = 200$ and ζ= 0.4, $\chi_1 = 0.4$, $P_e = 1.0$, $\delta = 0.1$, $\Omega = 5$ 70
4.8 Phase portrait and time domain diagrams for the system (4.3.6) with parameters P_e =5 and ζ= 0.4, $\chi_1 = 0.4$, R=15, $\delta = 0.1$, $\Omega = 5$ 71
4.9 Phase portrait and time domain diagrams for the system (4.3.6) with parameters P_e =6 and ζ= 0.4, $\chi_1 = 0.4$, R=15, $\delta = 0.1$, $\Omega = 5$ 71
4.10 Phase portrait and time domain diagrams for the system (4.3.6) with parameters P_e =7 and ζ= 0.4, $\chi_1 = 0.4$, R=15, $\delta = 0.1$, $\Omega = 5$ 72
4.11 Phase portrait and time domain diagrams for the system (4.3.6) with parameters ζ= 0.4 and P_e =1, $\chi_1 = 0.4$, R=15, $\delta = 0.1$, $\Omega = 5$ 72
4.12 Phase portrait and time domain diagrams for the system (4.3.6) with parameters ζ= 0.7 and P_e =1, $\chi_1 = 0.4$, R=15, $\delta = 0.1$, $\Omega = 5$ 73
4.13 Phase portrait and time domain diagrams for the system (4.3.6) with parameters ζ= 0.9 and P_e =1, $\chi_1 = 0.4$, R=15, $\delta = 0.1$, $\Omega = 5$ 73
4.14 Phase portrait and time domain diagrams for the system (4.3.6) with parameters $\chi_1 = 0.5$ and P_e =1, ζ= 0.4, R=15, $\delta = 0.1$, $\Omega = 5$ 74
4.15 Phase portrait and time domain diagrams for the system (4.3.6) with parameters $\chi_1 = 0.7$ and P_e =1, ζ= 0.4, R=15, $\delta = 0.1$, $\Omega = 5$ 74
4.16 Phase portrait and time domain diagrams for the system (4.3.6) with parameters $\chi_1 = 0.9$ and P_e =1, ζ= 0.4, R=15, $\delta = 0.1$, $\Omega = 5$ 75
4.17 Phase portrait and time domain diagrams for the system (4.3.6) with parameters $\Omega = 10$ and P_e =1, ζ= 0.4, R=15, $\delta = 0.1$, $\chi_1 = 0.4$ 75

4.18 Phase portrait and time domain diagrams for the system (4.3.6) with parameters $\Omega = 40$ and P_e =1, ζ= 0.4, R=15, $\delta = 0.1$, $\chi_1 = 0.4$ 76
4.19 Phase portrait and time domain diagrams for the system (4.3.6) with parameters $\Omega = 80$ and P_e =1, ζ= 0.4, R=15, $\delta = 0.1$, $\chi_1 = 0.4$ 76
4.20 Phase portrait and time domain diagrams for the system (4.3.6) with parameters $\delta = 0.01$ and P_e =1, ζ= 0.4, R=15, $\Omega = 5$, $\chi_1 = 0.4$ 77
4.21 Phase portrait and time domain diagrams for the system (4.3.6) with parameters $\delta = 0.2$ and P_e =1, ζ= 0.4, R=15, $\Omega = 5$, $\chi_1 = 0.4$ 77
4.22 Phase portrait and time domain diagrams for the system (4.3.6) with parameters $\delta = 0.4$ and P_e =1, ζ= 0.4, R=15, $\Omega = 5$, $\chi_1 = 0.4$ 78
4.23 Phase portrait and time domain diagrams for the system (4.3.6) with parameters $\delta = 0.0$ and P_e =1, ζ= 0.4, R=5, $\Omega = 5$, $\chi_1 = 0.4$ 78
4.24 Phase portrait and time domain diagrams for the system (4.3.6) with parameters $\delta = 0.1$ and P_e =1, ζ= 0.4, R=5, $\Omega = 5$, $\chi_1 = 0.4$ 79
4.25 Phase portrait and time domain diagrams for the system (4.3.6) with parameters $\delta = 0.0$ and ζ= 1.5, R=16, $\chi_1 = 0.6$, $\sigma = 5$ 80
4.26 Phase portrait and time domain diagrams for the system (4.3.6) with parameters $\delta = 0.1$ and P_e =1, ζ= 1.5, R=16, $\Omega = 5$, $\chi_1 = 0.6$, $\sigma = 5$ 80

5.1 Physical configuration of the problem 85
5.2 Effect of Ta on Nu for IPM case ($\theta = 0$) 93
5.3 Effect of Va on Nu for IPM case ($\theta = 0$) 93
5.4 Effect of C_1 on Nu for IPM case ($\theta = 0$) 93
5.5 Effect of Ta on Nu for OPM case ($\theta = \pi$) 94
5.6 Effect of Va on Nu for OPM case ($\theta = \pi$) 94
5.7 Effect of C_1 on Nu for OPM case ($\theta = \pi$) 94
5.8 Effect of δ on Nu for OPM case ($\theta = \pi$) 95
5.9 Effect of Ω on Nu for OPM case ($\theta = \pi$) 95
5.10 Effect of Ta on Nu for LBMO case ($\theta = -i\infty$) 96
5.11 Effect of Va on Nu for LBMO case ($\theta = -i\infty$) 96

5.12 Effect of C_1 on Nu for LBMO case ($\theta = -i\infty$) 97
5.13 Effect of δ on Nu for LBMO case ($\theta = -i\infty$) 97
5.14 Effect of Ω on Nu for LBMO case ($\theta = -i\infty$) 97
5.15 Comparison of stationary and oscillatory systems 98
5.16 Phase portrait diagrams and time domain for the system (5.4.8) with parameters $R = 10, T_A = 0.1, \delta = 0.1$ 98
5.17 Phase portrait diagrams and time domain for the system (5.4.8) with parameters $R = 25.5, T_A = 0.1, \delta = 0.1$ 99
5.18 Phase portrait diagrams and time domain for the system (5.4.8) with parameters $R = 33, T_A = 0.1, \delta = 0.1$ 99
5.19 Phase portrait diagrams and time domain for the system (5.4.8) with parameters $R = 75, T_A = 0.1, \delta = 0.1$ 100
5.20 Phase portrait diagrams and time domain for the system (5.4.8) with parameters $R = 33, T_A = 0.2, \delta = 0.1$ 100
5.21 Phase portrait diagrams and time domain for the system (5.4.8) with parameters $R = 33, T_A = 0.5, \delta = 0.1$ 101
5.22 Phase portrait diagrams and time domain for the system (5.4.8) with parameters $R = 33, T_A = 0.8, \delta = 0.1$ 101
5.23 Phase portrait diagrams and time domain for the system (5.4.8) with parameters $R = 33, T_A = 0.2, \delta = 0.01$ 102
5.24 Phase portrait diagrams and time domain for the system (5.4.8) with parameters $R = 33, T_A = 0.2, \delta = 0.1$ 102
5.25 Phase portrait diagrams and time domain for the system (5.4.8) with parameters $R = 33, T_A = 0.2, \delta = 0.2$ 103
5.26 Phase portrait diagrams and time domain for the system (5.4.8) with parameters $R = 13.1, T_A = 0.1, \delta = 0.0$ 103
5.27 Phase portrait diagrams and time domain for the system (5.4.8) with parameters $R = 13.1, T_A = 0.1, \delta = 0.1$ 104

6.1 Physical configuration of the problem 107

6.2 Phase portrait and time domain diagrams for the system (6.4.6) with parameters $R = 10$ and $\Gamma = 1$, $\Lambda' = 0.7$, $\delta = 0.1$ 111
6.3 Phase portrait and time domain diagrams for the system (6.4.6) with parameters $R = 11$ and $\Gamma = 1$, $\Lambda' = 0.7$, $\delta = 0.1$ 112
6.4 Phase portrait and time domain diagrams for the system (6.4.6) with parameters $R = 200$ and $\Gamma = 1$, $\Lambda' = 0.7$, $\delta = 0.1$ 112
6.5 Phase portrait and time domain diagrams for the system (6.4.6) with parameters $\Gamma = 0.6$ and $R = 11$, $\Lambda' = 0.7$, $\delta = 0.1$ 113
6.6 Phase portrait and time domain diagrams for the system (6.4.6) with parameters $\Gamma = 1.5$ and $R = 11$, $\Lambda' = 0.7$, $\delta = 0.1$ 113
6.7 Phase portrait and time domain diagrams for the system (6.4.6) with parameters $\Gamma = 3$ and $R = 11$, $\Lambda' = 0.7$, $\delta = 0.1$ 114
6.8 Phase portrait and time domain diagrams for the system (6.4.6) with parameters $\Lambda' = 0.5$ and $\Gamma = 1$, $R = 15$, $\delta = 0.1$ 114
6.9 Phase portrait and time domain diagrams for the system (6.4.6) with parameters $\Lambda' = 0.7$ and $\Gamma = 1$, $R = 15$, $\delta = 0.1$ 115
6.10 Phase portrait and time domain diagrams for the system (6.4.6) with parameters $\Lambda' = 0.9$ and $\Gamma = 1$, $R = 15$, $\delta = 0.1$ 115
6.11 Phase portrait and time domain diagrams for the system (6.4.6) with parameters $\delta = 0.01$ and $\Gamma = 1$, $R = 11$, $\Lambda' = 0.7$ 116
6.12 Phase portrait and time domain diagrams for the system (6.4.6) with parameters $\delta = 0.1$ and $\Gamma = 1$, $R = 11$, $\Lambda' = 0.7$ 116
6.13 Phase portrait and time domain diagrams for the system (6.4.6) with parameters $\delta = 0.3$ and $\Gamma = 1$, $R = 11$, $\Lambda' = 0.7$ 117
6.14 Phase portrait and time domain diagrams for the system (6.4.6) with parameters $\delta = 0.0$ and $\Gamma = 1$, $R = 1.1$, $\Lambda' = 0.1$ 117
6.15 Phase portrait and time domain diagrams for the system (6.4.6) with parameters $\delta = 0.1$ and $\Gamma = 1$, $R = 1.1$, $\Lambda' = 0.1$ 118

7.1 Physical configuration of the problem 121

7.2 Effect of Le on heat and mass transfer 126
7.3 Effect of N_A on heat and mass transfer 126
7.4 Effect of Rn on heat and mass transfer 127
7.5 Effect of P_r on heat and mass transfer 127
7.6 Effect of P_e on heat and mass transfer 127
7.7 Effect of δ on heat and mass transfer 128
7.8 Effect of Ω on heat and mass transfer 128
7.9 Effect of R_i on heat and mass transfer 129
7.10 Comparison between modulated and unmodulated system 129

Nomenclature

Latin symbols

$A(s)$	amplitude of convection
a	wave number
a_c	critical wave number
d	depth of fluid layer
L	length of porous layer
$\vec{g}$	acceleration due to gravity
P_e	P*é*clet number
R	scaled Rayleigh number
Nu	Nusselt number
p	reduced pressure
K	permeability
Ra	thermal Rayleigh-number
Ra_s	solute thermal Rayleigh-number
D_B	Brownian diffusion
D_T	thermophoretic diffusion coefficient
Le	Lewis number
N_A	modified diffusivity ratio
N_B	modified particle density increment
Rm	basic-density Rayleigh number
Rn	concentration Rayleigh number
T	temperature

ΔT	temperature difference across the fluid layer
t	time
$\mathbf{q}$	fluid velocity(u, v, w)
Q	internal heat source
Ta	Taylor number
C_1	couple-stress parameter
R_i	internal Ryleigh number
X	rescaled amplitude
Y	rescaled amplitude
Z	rescaled amplitude
(x, z)	horizontal and vertical co-ordinates

Greek symbols

δ	amplitude of gravity modulation
α_T	coefficient of thermal expansion
χ	perturbation parameter
κ_T	effective thermal diffusivity
K_x	permeability in x direction
K_z	permeability z direction
η	thermal anisotropic parameter κ_{Tx}/κ_{Tz}
ξ	mechanical anisotropic parameter K_x/K_z
Ω	frequency of modulation
ω	dimensionless oscillatory frequency
$\overline{\lambda_1}$	stress relaxation time
$\overline{\lambda_2}$	strain retardation time
μ	dynamic viscosity of the fluid
μ_c	material constant for couple stress fluid
$(\rho c)_f$	heat capacity of fluid
$(\rho c)_p$	effective heat capacity of the nanoparticle

ϕ	nanoparticle volume fraction
ϵ	porosity
ν	kinematic viscosity
ρ	fluid density
θ	phase angle
ψ	stream function
s	slow time scale
τ	fast time scale

Other symbols

∇^2	$\frac{\partial^2}{\partial x^2}+\frac{\partial^2}{\partial y^2}+\frac{\partial^2}{\partial z^2}$
∇^2_η	$\eta\frac{\partial^2}{\partial x^2}+\frac{\partial^2}{\partial z^2}$
∇^2_ξ	$\frac{\partial^2}{\partial x^2}+\frac{1}{\xi}\frac{\partial^2}{\partial z^2}$
∇	$\hat{i}\frac{\partial}{\partial x}+\hat{j}\frac{\partial}{\partial y}+\hat{k}\frac{\partial}{\partial z}$

Subscripts

b	basic state
c	critical
0	reference value

Superscripts

’	perturbed quantity
*	dimensionless quantity

Chapter 1

Introduction

Initially, we write some definitions, hydrodynamic equations and laws, methods, literature review and applications beautifully to comprehend the upcoming chapters.

1.1 Basic Definitions

1.1.1 Heat transfer

When heat moves from a high temperature object to a lower temperature object, then heat transfer occurs in that object. Thermal instability occurs in any kind of system due to this. There are mainly three types of heat transfer process, as given below.

- **Radiation**

  Radiation is the transmission of energy in the form of electromagnetic waves through a material medium. Sunshine is one of the live example of radiation in our life.

- **Conduction**

  Conduction is the transfer of energy, which takes place from more energetic to the less energetic particles of a substances due to interaction between the particles. In this process temperature gradient exists in a stationary medium, which may be a solid or a fluid. For example, a spoon in a cup of hot tea becomes warmer because heat moves from tea to spoon in the form of conduction.

- **Convection**

  Convection is a kind of heat transfer (hot to cool) which is found in fluids or gases. There are two types of convective mechanisms, such as energy transfer due to fluid particle's irregular motion in the fluid, form of bulk (diffusion) and another way of heat transfer is due to temperature gradient. Making of tea, boiling of milk are daily life examples of convective heat transfer. Figure 1.1, is the best example to understand all types of heat transfer.

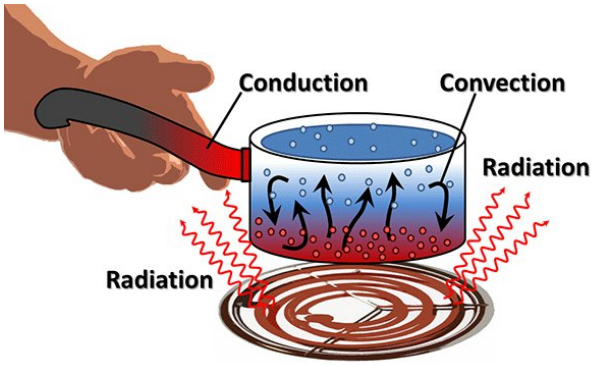

Figure 1.1: All kind of heat transfer

We can divide the convective mechanism into the following convection.

- **Natural convection** is a physical phenomenon in which heat can be transported in fluid due to density differences, occurring by means of temperature gradient without any external appliances. The examples are mantle convection, boiling water and oceanic circulation etc.

- **Forced convection** is another form of heat transport in which fluid motion is driven by external forces. The use of a fan to provide forced convection, air cooling of hot electrical components on a stack of printed circuit boards is an example of forced convection.

- **Mixed convection**, when convection and forced convection occurred simultaneously, the physical phenomenon is known as mixed convection. Mixed convection would result if a fan is used to force air upward through the circuit boards, thereby opposing the buoyancy flow, or downward, thereby opposing the buoyancy flow.

1.1.2 Rayleigh Bénard convection

Rayleigh Bénard convection is basically natural convection, taking place in horizontal fluid layer heated from below in which fluid attains regular patterns of convection cells known as Bénard cells. These convective cells are generated from the buoyant force acting between the fluid layers due to temperature gradient, see hypothetical Figure 1.2. Its analytical and experimental is common in real world scenario. Rayleigh Bénard convection depends on the buoyancy force, viscous force and defined as $Ra = \frac{\alpha_T g \Delta T d^3}{\nu \kappa_T}$, a non-dimesionlised quantity. Where d is the depth of fluid layers, ΔT is the temperature difference between the fluid layers, ν is the kinematic viscosity of fluid, κ_T is the thermal diffusivity of the fluid, α_T is the coefficient of thermal expansion and g is the acceleration due to gravity. The classical Rayleigh-Bénard convection is found to be an interesting phenomenon introduced by Chandrasekhar(1961), due to bottom heating of a fluid layer. When the Rayleigh number exceeds a certain value, known as critical Rayleigh number the convection takes place in the system.

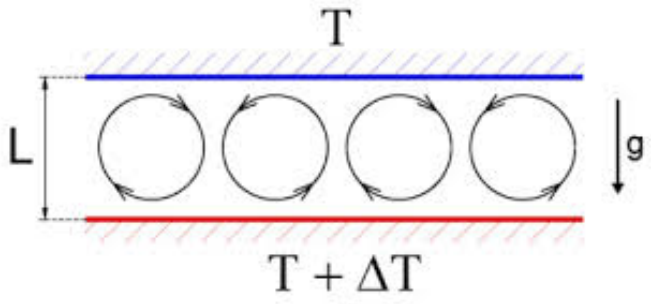

Figure 1.2: Rayleigh Bénard convection

1.1.3 Porous medium

A material which contains interconnected void space (pore) such that the fluid motion is possible in it, is known as porous material or porous medium. The example of porous medium are rocks, soils, biological tissues (e.g. bones), cement, foams, sand, wood, human lung and ceramics. In a porous medium, the distribution of pores with respect to shape and size is irregular. The shape of porous medium is depicted in Figure 1.3.

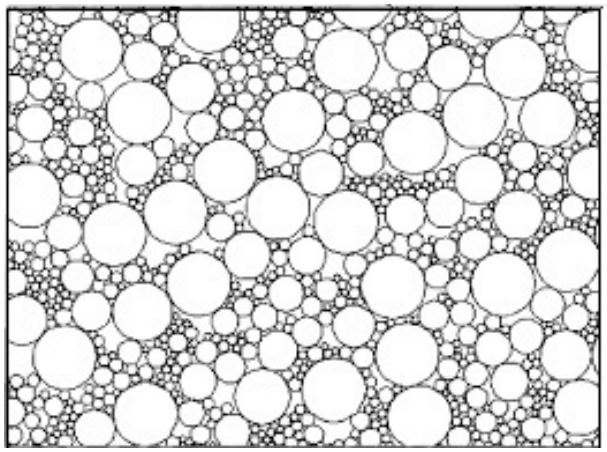

Figure 1.3: A sketch of porous medium

1.1.4 Anisotropic porous medium

It is defined as a porous medium having different permeability in different direction. It is used in chemical engineering process and for insulating purpose. Epherre(1977) was the first to study the anisotropic porous medium.

1.1.5 Saturated porous medium

A porous medium is said to be saturated porous medium if its pore volume is connected and occupied by a specific fluid.

1.1.6 Unsaturated porous medium

A porous medium is said to be unsaturated porous medium if its pore volume is not fully occupied by a fluid.

1.1.7 Porosity

It is ratio of the volume of the voids to the total volume of the porous medium. The porosity of any porous domain lies in the interval $(0, 1)$. Let, V_f denotes the volume of the fluid

(voids), and V_m denotes the volume of the material (total volume), then the porosity ϵ is given by,

$$\epsilon = \frac{V_f}{V_m}. \tag{1.1.1}$$

In general, we assume that all the void space is connected. If in fact one has to deal with a medium in which some pore space is disconnected, then one has to introduce an **effective porosity** defined as the ratio of connected void space to total volume.

1.1.8 Permeability

It is a measure of the ease with which a fluid can flow through a porous medium. The degree to which porous within the material is inter-connected is known as effective porosity. In this work we consider it, as parameter K.

1.1.9 Hoton-Rogers-Lapwood convection

Horton and Rogers(1945) and Lapwood(1948) studied the Rayleigh Bénard convection in a horizontal porous medium, therefore named as Hoton-Rogers-Lapwood convection or Darcy Bénard convection. The non-dimensionlised Darcy Rayleigh number is defined in this case as $Ra_D = \frac{\alpha_T g \Delta T K d}{\nu \kappa_T}$, here K is permeability. Thermal convection in porous media has attracted the researchers during the last three decades due to its huge applications in various fields such as petroleum industry, chemical engineering and geophysics, etc. Interested authors can read the unique books (problem related to thermal instability in a fluid saturated porous medium) are given by Ingham and Pop(2005), Nield and Bejan(2012) and Vafai(2000).

1.1.10 Mechanism of thermal instability

We consider an infinitely extended horizontal fluid layer of depth d, confined between two parallel planes, the lower plane at $z = 0$ while upper one is at $z = d$. A Cartesian frame of reference is adopted in such a way that the origin lies on the lower plane and z axis

is vertically upward. The fluid layer is heated from below and cooled from above. The physical configuration of the system is depicted in Figure 1.4. After getting sufficient heat fluid molecules expand, become lighter and so they are pushed by heavy molecules to move up and void space is formed due to these molecules, filled by neighbouring molecules. The repetition of this process starts the motion in the fluid layer. When the temperature gradient is so enough between the fluid layers, a small pocket of fluids starts to move up into the colder region of higher density. During this period onset of convection occurs in the system. Bénard(1900), gave the first quantitative experiments of thermal instability in fluid layers. Lord Rayleigh(1916) gave the first theoretical treatment to the theory of Bénard experiments.

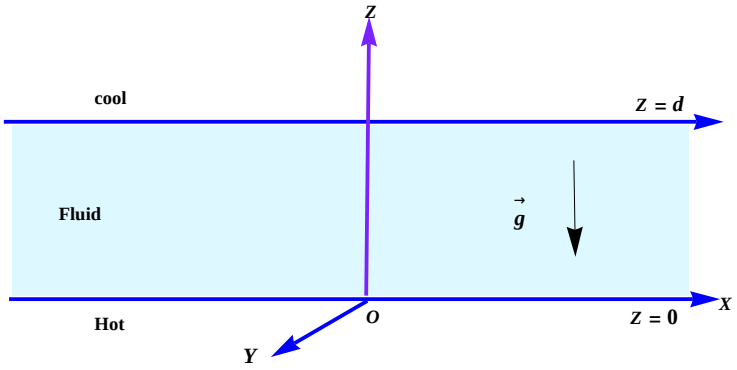

Figure 1.4: Mathematical diagram of thermal instability

1.1.11 Newtonian and non-Newtonian fluids

In the **Newtonian** fluid, viscosity is proportional to shear stress. Water, mineral oil and alcohol are some examples of Newtonian fluid. An opposite effect is followed in **non-Newtonian** fluid i.e. there is no linear relation between viscosity and shear stress. For example cream, paint, glue etc. Further, **viscoelastic** fluid is also a kind of non-Newtonian fluid which is centre point of research and industrial applications. There are some viscoelastic fluids, given by

- Maxwell fluid.
- Rivlin-Ericksen fluid.

- Jeffrey (Oldroyd) fluid.

1.1.12 Throughflow mechanism

The concept of throughflow is used to control the convective mechanism in engineering sciences, industries, geophysics etc. The basic state temperature profile of throughflow changes from linear to non-linear with layer height, which affects the stability of the system. In this study, we find a convective parameter P_e (Péclet number) which handles the heat and mass transport in the system. This term is included in the energy equation and shows dual nature, according as $P_e > 0$ (upward throughflow) or $P_e < 0$ (downward throughflow), on the system. Mathematically, it is expressed and depicted in Eq.(1.1.2) and Figure 1.5 respectively

$$P_e = \frac{w_0 d}{\kappa_T}, \tag{1.1.2}$$

where w_0= fluid velocity at basic state in z direction, κ_T= thermal diffusivity and d= depth of fluid layer.

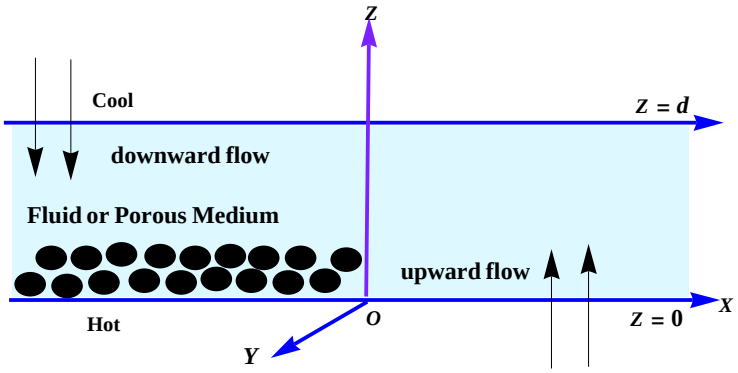

Figure 1.5: Physical assumptions for throughflow model

1.1.13 Couple-stress fluid

Couple-stress fluid is a kind of non-Newtonian fluid having polar effects. The application of couple-stress fluid is in the study of mechanisms of lubrication of synovial joints. The synovial fluid has been modelled as a couple-stress fluid in human joints by Walicki and Walicka(1999). Some more applications of couple-stress fluids are in the fields of industrial

sciences, solidification of liquid crystals, cooling of metallic plate in a bath etc. Stokes(1966) was the first to propose the model for couple-stress fluid. The couple-stress parameter affects the momentum equation of the system. Let C_1 is the couple-stress parameter, then

$$C_1 = \frac{\mu_c}{\mu d^2}, \tag{1.1.3}$$

where μ, μ_c are fluid viscosity and couple stress viscosity respectively.

1.1.14 Rotation

The effect of rotation on the onset of thermal instability introduces a new parameter into the problem known as Taylor number, Ta. The effect of rotation can be explained by certain general theorems, relating to vorticity, in the dynamics of fluids. Mathematically, we can write

$$Ta = \left(\frac{2\Omega_1 d}{\nu}\right)^2, \tag{1.1.4}$$

where Ω_1 is a characteristic angular velocity, d is depth of fluid layer, and ν is the kinematic viscosity. Generally, the studies corresponding to rotation represent a stabilizing behaviour.

1.1.15 Internal heating

Internal heat is the main source of energy for celestial bodies caused by nuclear fusion and decaying of radioactive materials, which keeps the celestial objects warm and active. It is due to the internal heating of the earth that there exists a thermal gradient between the interior and exterior of the earth's crust, saturated by multi-components fluids which helps convective flow. Therefore, the role of internal heat generation becomes very important in several applications that include geophysics, reactor safety analyses, metal waste form development for spent nuclear fuel. This term affects the energy equation of convective system. In this work, we consider it as a convective parameter R_i, which shows a destabilize effect and given by

$$R_i = \frac{Qd^2}{\kappa_T}, \tag{1.1.5}$$

where Q is the internal heat coefficient.

1.1.16 Nanofluid

Nanofluids are engineered colloids. It is mixture of a base fluid (like water or ethylene-glycol) and nanoparticles (like metallic or metallic oxide: Cu, Cuo, Al_2O_3). Nanoparticles are particles having diameters between 1-100 nm. and are made of metal or metallic oxides, such as copper and alumina. The base fluid is usually a conductive fluid, such as water or ethylene glycol. The thermal conductivity and convective properties of nanofluid over the properties of the base fluid is good enough. Heat transfer coefficient enhances up to 40% in case of nanofluids. Its uses are in medical sciences, auto-mobiles and engineering fields etc. Choi(1995) was the first to propose the term "nanofluid".

1.1.17 Doubble diffusive convection

When the convective phenomenon of fluid is driven by two different density gradients, it is known as double-diffusive convection. These density variations may by caused by gradients in the composition of fluid or by temperature differences. In the oceanography, heat and salt concentrations are present having different gradients. In this case, the thermal and concentration (solute) gradients are present, so Boussineq approximation is revised as in the form

$$\rho = \rho_0[1 - \alpha_T(T - T_0) + \beta_T(S - S_0)], \tag{1.1.6}$$

where α_T and β_T are the thermal and solute expansion coefficients, T and S are the temperature and the solute content, respectively.

1.1.18 Chaos

Some problems of dynamical system in non-linear case are so difficult to be solved directly. Poincaré(1890) was the first to study the dynamical system generated by the three body problem, is quite sensitive to the initial conditions exhibiting chaotic behaviour. The chaotic systems are mainly unpredictable and their solutions may show either periodic or chaotic

nature. For the chaotic mode, there is no guarantee for converge of its solution. Today chaotic motion is a growing subject for research and applications field as many scientists and industries are taking interest in it. There are some live examples of chaotic motion in daily life such as: the ring of smoke, signal of any receiver and in weather sciences etc. In fluid dynamics, to study chaotic convection, the basic model is to be converted into Lorenz model. In chapter four, all mechanism related to chaotic system is given. In Eq.(1.1.7) a particular dynamical system for chaotic motion is considered as

$$\begin{cases} \frac{dx}{d\tau} = F_1(x, y, z), \\ \frac{dy}{d\tau} = F_2(x, y, z), \\ \frac{dz}{d\tau} = F_3(x, y, z), \end{cases} \tag{1.1.7}$$

where x, y, z are dynamical variables and τ is time.

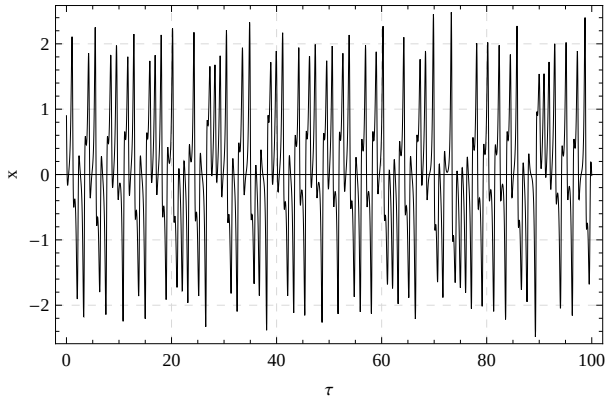

Figure 1.6: A diagram for chaotic motion

It is clear from the Figure 1.6 that in chaotic motion, solution does not repeat its previous value.

1.1.19 Modulation

Controlling of the convective phenomenon is much necessary for industrial research to save money, energy and time etc. Keeping this in mind, scientists are now giving the theory and doing research with modulation effect for application purpose. Hence **modulation** is

a tool to handle the convective phenomenon. Many types of modulations are used by the authors in their studies such as **temperature**, **gravity** and **magnetic** modulation. When we apply modulation theory, we get the two additional terms like amplitude and frequency of modulation. These terms help to control the convective mechanism either by increasing or decreasing the values of these parameters.

- **Temperature Modulation**

  In many practical problems, the temperature at the boundaries found to be non-uniform (periodic) in transient heating or cooling. Consequently, the basic temperature field depends explicitly on position and time, this is known as thermal modulation problem. Mathematically, we express as

$$T = \begin{cases} T_0 + \frac{\Delta T}{2}[1 + \chi^2 \delta cos(\Omega t)], & at \quad z = 0, \\ \\ T_0 - \frac{\Delta T}{2}[1 - \chi^2 \delta cos(\Omega t + \theta)], & at \quad z = d, \end{cases} \tag{1.1.8}$$

  where the physical variables are given in the nomenclature.

- **Gravity Modulation**

  The time dependent gravitational field, one of the complex forces, is of interest in space laboratory experiments, in areas of crystal growth, atmospheric sciences, etc. The idea of using mechanical vibration as a tool to improve the heat transfer rate has received much attention. However, the regulation of convection is important from the applications point of view and thermo-gravitational vibration is known to be an effective means of controlling instabilities. The gravity modulation of the system leads to the variable coefficients in the momentum equation of thermal instability and involves the vertical time periodic vibrations of the system, and is known as G-jitter in literature. Eq.(1.1.9) represents the mathematical form of gravity modulation as

$$\mathbf{g} = g_0(1 + \chi^2 \delta cos(\Omega t), \tag{1.1.9}$$

  where g_0 is the constant gravity field.

- **Magnetic modulation**

  In general, the magnetic fluids differ from the ordinary fluids by showing magnetic as well as flow properties. The magneto convection arises due to the interaction of electrically conducting fluid flow and the applied magnetic field. Convection can also take place in these fluids due to temperature dependence of their magnetization. This property is useful in space research, where the role of gravity can be replaced by a magnetic body force. The magnetic force can be used to create circulation in small passages where natural convection is either absent or ineffective. Generally, the magnetization depends on the magnetic field, temperature and density. Hence, the magnetic force depend on the thermal state of the fluid and may lead to convection. Mathematically, it is defined as

$$H = H_0(1 + \chi^2 \cos(\Omega t)), \tag{1.1.10}$$

where H_0 is the mean value of magnetic field.

1.2 Hydrodynamic equations for fluid layer

In fluid dynamics, the following are the basic properties that every fluid obeys, where the hydrodynamical flow of a viscous fluid is governed by varying density and temperature:

(a) Equation of continuity

The continuity equation states that, the rate of generation of mass within a given volume must be balanced by an equal net outward flow of mass through the volume. The differential form of equation of continuity is given by

$$\frac{\partial \rho}{\partial t} + \nabla.(\rho \vec{q}) = 0. \tag{1.2.1}$$

For incompressible fluid, the above expression is reduces to

$$\nabla.\vec{q} = 0, \tag{1.2.2}$$

where $\vec{q}$ is fluid velocity and ρ is fluid density.

(b) Momentum equation

$$\frac{\partial \vec{q}}{\partial t} + (\vec{q}.\nabla)\vec{q} = -\frac{1}{\rho}\nabla p + \nu\nabla^2\vec{q} + F, \tag{1.2.3}$$

where ν is kinetic viscosity, p is pressure, F is the body force term, represents an external forces that act on the fluid, for example: gravity, wind, etc.

(c) Energy or temperature equation

$$\frac{\partial T}{\partial t} + (\vec{q}.\nabla)T = \kappa_T\nabla^2 T + Q(T - T_0). \tag{1.2.4}$$

It is based on the law of conservation of energy. κ_T is the thermal conductivity which is proportional constant in Fourier's law of heat conduction. Q is coefficient of internal heat.

(d) Boussinesq approximation

The Boussinesq approximation is a common method to solve the convective problems. This approximation states that, the density differences are sufficiently small to be neglected everywhere except where they appear in terms of multiplied by $\vec{g}$, the acceleration due to gravity. Mathematically, we define as

$$\rho = \rho_0[1 - \alpha_T(T - T_0)]. \tag{1.2.5}$$

Here α_T is the thermal expansion coefficient, and subscript 0 is the reference value.

1.3 Hydrodynamic equations for porous medium

(a) Equation of continuity

$$\nabla.\vec{q} = 0. \tag{1.3.1}$$

(b) Momentum equation

$$\frac{\rho}{\epsilon}\frac{\partial \vec{q}}{\partial t} = -\nabla p - \frac{\mu}{K}\vec{q} + \rho_f g. \tag{1.3.2}$$

(c) Energy or temperature equation

$$\frac{\partial T}{\partial t} + (\vec{q}.\nabla)T = \kappa_T \nabla^2 T. \tag{1.3.3}$$

(d) Oberbeck-Boussinesq approximation

$$\rho_f = \rho_0[1 - \alpha_T(T - T_0)], \tag{1.3.4}$$

where ϵ is porosity of the porous medium, μ is the dynamic viscosity, K is permeability and κ_T is overall thermal conductivity.

1.3.1 Darcy law

The fluid flow in a porous medium is governed by this law, which is given by Henry Darcy in (1856). He found that there is a proportionality relation between flow rate and the applied pressure difference. Mathematically defined as

$$\vec{q} = -\frac{K}{\mu}\nabla p, \tag{1.3.5}$$

where all the parameters already discussed in above sections.

1.3.2 Brinkman-extended Darcy model

The above Darcy law is valid for only sufficiently small and linear seepage velocity ($\vec{q}$). Thus for high velocity i.e. for high Reynold numbers, the extension of Darcy law is given by

$$\nabla p = -\frac{\mu}{K}\vec{q} + \overline{\mu}\nabla^2\vec{q}, \tag{1.3.6}$$

where $\overline{\mu}$ is a quantity having the dimension of viscosity and it is known as the effective viscosity. The effective viscosity is not expected to be the same as the viscosity of the fluid.

1.4 Boundary conditions

To study any dynamical system, the boundary conditions are used to calculate the dependent variables. On the basis of lower and upper boundaries of a convective system, we have given below some different types of boundary conditions such as rigid-rigid, free-free, rigid-free and free-rigid.

1. Zero normal velocity: $\omega = 0$, for both rigid and free boundaries.
2. (a) Zero tangential velocity (no slip): $\frac{\partial\omega}{\partial z} = 0$, for rigid boundaries.

   (b) Zero tangential stress: $\frac{\partial^2\omega}{\partial z^2} = 0$, for free boundaries.
3. **Conducting (isothermal)**: For isothermal boundary wall, the temperature disturbances must be zero at the boundary.
4. **Insulated (adiabatic)**: For adiabatic boundary wall, the temperature of the wall change, but there should be no through-flow of temperature.

1.5 Methods of solution

1.5.1 Analytical methods

Stability analysis: The stability of any flow depends upon the nature of acting infinitesimal disturbances. If the initial disturbances are small, the governing equations may be

linear. For analysing the stability there are two methods, given below:

- **Energy method**

  We calculate the kinetic energy of the perturbations in this method, and if this kinetic energy increases along with time, then the flow is unstable, and if it decays with time then the flow is stable. This method is fail to provide the information of unstable system, so it is not generally used for convective problems.

- **Normal mode method**

  In this method, an arbitrary disturbance is expressed as a superposition of certain possible modes, and then the stability of the system with respect to each of these modes is investigated, based on oscillations theory. Mathematically, we write the expression $exp[i(k_x x + k_y y) + st]$ for normal mode method, where s is the frequency of perturbation and $k^2 = k_x^2 + k_y^2$ is the wave number. The stability analysis is performed by using frequency of perturbation (s). If $Re(s > 0)$, then the disturbance will grow exponentially with time, and it will represent an unstable system. If $Re(s = 0)$, then the system will be neutrally stable. If $Re(s < 0)$, then it shows a stable system as the disturbance reduces exponentially with time.

Perturbation method: Some time, we face difficulties in solving the engineering problems, mathematical non-linear governing equations in real life directly. In this method, the solution is represented by the initial few terms of an asymptotic expansion. The expansions may be carried out in terms of introduced parameter which appears in the considered equation, known as perturbation parameter. Here, we suppose χ as a perturbation parameter such that the solution is available and reasonably simple for $\chi = 0$, this process known as regular perturbation method. There is one more kind of perturbation method, known as singular perturbation method, where the solution cannot be approximated by setting the parameter value to zero. Mathematically, we can write an expression for approximation to the solution of U

$$U = U_0 + \chi U_1 + \chi^2 U_2 + ..., \tag{1.5.1}$$

where U_0 would be the known solution to the exactly solvable initial problem and $U_1, U_2, ..$ are represent the higher-order terms which may be found by successive iterations.

A truncated representation of Fourier series method: The linear stability analysis is sufficient to find the stability condition of the motionless solution and the corresponding eigenfunctions describing qualitatively the convective flow, it cannot give information related to the values of the convection amplitudes, nor regarding the rate of heat and mass transfer. In order to get this additional information, we perform the non-linear analysis, which will help in understanding the physical mechanism with minimum amount of mathematical analysis and is a step forward toward understanding full non-linear problem. The Fourier expressions for the physical variables such as stream function, temperature and nanoparticle fraction, are given by

$$\psi = \sum_{n=1}^{\infty}\sum_{m=1}^{\infty} A_{mn}(\tau)\sin(max)\sin(n\pi z), \tag{1.5.2}$$

$$T = \sum_{n=1}^{\infty}\sum_{m=1}^{\infty} B_{mn}(\tau)\cos(max)\sin(n\pi z), \tag{1.5.3}$$

$$\phi = \sum_{n=1}^{\infty}\sum_{m=1}^{\infty} C_{mn}(\tau)\cos(max)\sin(n\pi z). \tag{1.5.4}$$

1.5.2 Numerical methods

Galerkin method: This method is used for converting a continuous operator problem to a discrete problem. Galerkin method is mainly a weighted residual method used to solve boundary value problems. Some basic steps of this method are given below:

(a) Expand the unknown solution in a set of basis functions, with unknown coefficients or parameters; it is known as the trial solution.

(b) Check whether the trial solution satisfy the boundary conditions as well as initial conditions.

(c) Define the residual, set the weighted residual to zero and solve the equations.

(d) Find out the error by taking successive approximations, and show convergence as the number of basis functions increases.

Runge-Kutta method: It is well known method of numerical analysis. The Runge-Kutta methods are used in family of implicit and explicit iterative methods for the approximation of solutions of ordinary differential equations. The mathematicians C. Runge and M.W. Kutta(1900) introduced this wonderful technique.

1.6 Some earlier work

1.6.1 Temperature modulation in fluid layer

The effect of temperature modulation on thermal stability in a viscous fluid layer was first considered by Venezian(1969). He performed a linear stability analysis of small amplitude temperature modulation and derived the onset criteria using a perturbation expansion in powers of the amplitudes of oscillations. His results showed that the onset of convection can be delayed or advanced by the out of phase or in-phase modulation of the boundary temperatures respectively, as compared to the unmodulated system. A similar problem was studied earlier by Gershuni and Zhukhovitskii(1963), for a temperature profile obeying the rectangular law. Rosenblat and Herbert(1970), investigated the low-frequency modulation of thermal instability of a Boussinesq fluid heated from below. They considered the applied temperature gradient as the sum of a steady component and a low frequency sinusoidal component. Rosenblat and Tanaka(1971) studied the effect of thermal modulation on the onset of Rayleigh-Bénard convection using Gelerkin technique and discussed the stability of the system using Floquet theory. Theoretical and experimental investigation of thermal modulation in a horizontal fluid layer has been performed by Finucane and Kelly(1976). They found both experimentally and numerically that at low frequencies, the modulation is destabilizing, whereas at high frequencies it is stabilizing. Bhadauria and Bhatia(2002),

studied the time-periodic heating (temperature modulation) of Rayleigh-Bénard convection using rigid-rigid boundaries and compared the results for various temperature profiles. The shift in the critical Rayleigh number is calculated and it is found that it is possible to advance or delay the onset of convection. Bhadauria(2006a), investigated the convective instability in a horizontal layer of electrically conducting fluid heated from below in the presence of an applied vertical magnetic field. The temperature gradient between the walls of the fluid layer consists of a steady part and a time dependent oscillatory part. The temperature of both walls is modulated. It is found that the effect of magnetic field has a stabilizing influence on the onset of thermal instability. Further, it is also found that it is possible to advance or delay the onset of convection by proper tuning of the frequency of modulation of the walls temperature. Bhadauria et al.(2009), examined the stability of a horizontal fluid layer heated from below. The temperature gradient between the walls of the fluid layer consists of a steady part and a time-dependent part, which is oscillatory. By considering the weekly non-linear analysis, it is shown that the modulation produces a range of stable hexagons near the critical Rayleigh number. Raju and Bhattacharyya(2010), studied thermal instability in a horizontal fluid layer with the boundary temperature modulated sinusoidally in time. This was extension of the Venezian(1969) work for rigid-rigid boundaries. Perturbation technique was used to calculate the correction in the value of the critical Rayleigh number. Bhadauria and Kiran(2014c), sudied weakly nonlinear double diffusive magneto-convection in a Newtonian liquid under temperature modulation. Bhadauria and Kiran(2014d), studied heat and mass transfer for oscillatory convection in a binary viscoelastic fluid layer subject to temperature modulation by using complex Ginzburg-Landau equation. **Recently**, Bhadauria and Kiran(2016), gave a model for weakly non-linear oscillatory convection in a rotating fluid layer under temperature modulation.

1.6.2 Temperature modulation in porous medium

The porous media analogue of Rayleigh-Bénard convection is known as Horton Rogers Lapwood convection, and was first studied by Horton and Rogers(1945) and by Lapwood(1948),

independently. Horton and Rogers studied the convection of a fluid through permeable medium as the result of a vertical temperature gradient, the medium being in the shape of a fluid layer bounded above and below by perfectly conducting media. Lapwood examined the breakdown of a stability of a fluid subject to a vertical temperature gradient in a porous medium and also discussed the possibility of convective flow. A detailed study on the effect of temperature modulation on convection in a porous medium was given by Caltagirone(1976), Chhuon and Caltagirone(1979). Rudraiah and Malashetty(1990), analyzed the effect of temperature modulation on convection in a sparsely packed porous medium. Malashetty and Basavaraja(2002), investigated the effect of time periodic temperature modulation at the onset of convection in a Boussinesq fluid saturated anisotropic porous medium using a linear stability analysis. Brinkman flow model with effective viscosity larger than the viscosity of the fluid is considered to give a more general theoretical result. It is shown that the small anisotropy parameter has a strong influence on the stability of the system. Shivakumara et al.(2011) examined theoretically linear stability of Walters B viscoelastic fluid saturated horizontal porous layer, when the walls of the porous layer are subjected to time periodic temperature modulation. The effect of all three types of modulations is found to be destabilizing as compared to the unmodulated system. Malashetty and Begum(2011), studied the effect of thermal modulation on the onset of convection in a Maxwell fluid saturated porous layer. A theoretical analysis of thermo convective instability in a densely packed porous medium is carried out when the boundary temperatures vary with time in a sinusoidal manner by Siddheshwar et al.(2013), by performing a weakly non linear stability analysis. A new result that shows that asynchronous temperature modulation may be used to either enhance or reduce heat transport by suitably adjusting the frequency and phase difference of the modulated temperature. **Recently**, Suthar et al.(2016) studied the onset of thermally modulated Darcy-Bénard convection. The correction in the critical Darcy-Rayleigh number was computed and depicted graphically.

1.6.3 Gravity modulation in fluid layer

Gresho and Sani(1970) have studied the linear stability of a fluid layer with rigid boundaries and found influence of the gravitational modulation on the convection threshold of the system. Biringen and Peltier(1990) investigated the nonlinear three dimensional Rayleigh-Bénard problem under gravity modulation numerically, and confirmed the results obtained by Gresho and Sani(1970). Clever et al.(1993), considered the problem of two dimensional oscillatory convection in a graviatationally modulated fluid layer. Chen and Chen(1999) studied the effect of gravity modulation on the stability of convection in a vertical slot. They examined the stability for fluids of different Prandtl numbers. Shu et al.(2005), examined the effects of modulation of gravity and thermal gradients on natural convection in a cavity, numerically as well as experimentally. It is found that for low Prandtl number fluids, modulations in gravity and temperature produce the same flow field both in structure and in magnitude. Gravity modulation in a fluid layer has been investigated by Bhadauria (2006b). Siddheshwar et al.(2012a), studied a weakly non-linear stability problem of magneto-convection in an electrically conducting Newtonian fluid, confined between two horizontal surfaces, under a constant vertical magnetic field, and subjected to an imposed time-periodic boundary temperature or gravity modulation. Siddheshwar and Revathi(2013), studied the effect of gravity modulation on weakly non-linear stability of stationary convection in a dielectric liquid. Gupta et al.(2016a) studied a local nonlinear stability analysis of modulated double diffusive stationary convection in a couple stress liquid. **Recently**, Kiran et al.(2017) studied weakly nonlinear oscillatory convection in an electrically conduction fluid layer under gravity modulation. It is found that modulation is used as a controller for the convective system.

1.6.4 Gravity modulation in porous medium

Malashetty and Padmavathi(1997), investigated the stability of a horizontal fluid and porous layer heated from below for the case of a time dependent buoyancy force generated by gravity modulation. By performing a linear stability analysis they showed that the gravity modulation can significantly affect the stability limits of the system. Govender(2004),

investigated the effect of low amplitude gravity modulation on the onset convection in a porous layer heated from below. It is noticed that on increasing the frequency of modulation stabilizes the convection. Govender(2005a) used linear stability theory to investigate analytically the effects of gravity modulation on convection in a homogenous porous layer heated from below. The linear stability results were presented for both, the synchronous and subharmonic solutions, and the exact point for the transition from synchronous to subharmonic solutions was computed. He demonstrated that increasing the excitation frequency, rapidly stabilizes the convection up to the transition point from synchronous to subharmonic convection. Beyond the transition point, the effect of increasing the frequency is to slowly destabilize the convection. Saravanan and Kumar(2010) studied the effect of gravity modulation on the onset of convection in a horizontal fluid saturated porous layer heated from below. They focused on low amplitude gravity modulation and the thresholds were found using Mathieu's functions. The emergence of instability via the synchronous and subharmonic modes and the transition between them are discussed. Malashetty and Swamy(2011), studied the effects of G-jitter on the convection in a fluid or porous layer using linear stability analysis. They found that, the onset of convection can be advanced or delayed by proper tuning of various convective parameters. Bhadauria and Kumar(2012), studied stability analysis of Temperature/Gravity-Modulated stationary Rayleigh-Bénard convection in a rotating porous medium. **Recently**, Kiran et al.(2016) studied thermal convection in a nanofluid saturated porous medium with internal heating and gravity modulation. They performed linear and nonlinear stability analyses to investigate the onset of convection and heat and mass transfer in the system. It was found that gravity modulation can be used effectively to regulate heat and mass transfer in the system.

1.7 Applications

Convection in porous media is of practical importance in modern science and engineering. Scientists and Engineers study flow aspects like momentum and heat and mass transfer in porous media to apply them to a huge spectrum of modern industrial fields which include:

(a) Petroleum industries need knowledge of flow mechanism in order to increase the recovery.

(b) It is known that the earth has huge amount of energy resources trapped in it, specially near the centre. This heat needs to be brought upto the surface from deep interiors travelling its way through porous rocks. Here seems to be a need for effective thermal conductive fluids.

(c) Chemical engineers require the knowledge for mass transfer and chemical reaction processes in porous reactors.

(d) Nuclear scientists require porous media knowledge, effective coolants and mass transfer fluids for efficient functioning of nuclear rectors.

Chapter 2

An analytical study of heat and mass transport in Bénard-Darcy convection with G-jitter and variable viscosity liquids in porous media

2.1 Introduction

Rayleigh-Bénard convection in porous media commonly called Horton-Rogers-Lapwood convection has its own importance due to its wide range of applications in mechanical engineering, chemical engineering, geophysics and real problems. Double-diffusive convection in porous media concerns instability in fluid-saturated porous media with two diffusing components like temperature and salt contributing to the instability in an opposing sense and with the components having unequal diffusivity coefficients. Applications of this problem is found in metallurgy, solidification of polymeric liquids, geothermal energy extraction, oil recovery process, nuclear waste disposal and the migration of

This chapter is based on the research article: An analytical study of heat and mass transport in Bénard-Darcy convection with G-jitter and variable viscosity liquids in porous media, accepted in STRPM (Begell House-2017).

moisture through air contained in fibrous insulation. Neild and Bejan(2012), Ingham and Pop(2005), Vadász(2008), Vafai(2010), Vafai(2015) provide an excellent review in this area. Studies related to stability analysis have been done by Nield(1968), Taunton(1972), Griffith(1981), Rudraiah(1982), Poulikakos(1986), Rudraiah and Siddheshwar(1998), Mulone and Straughan(2006), Kuznetsov and Nield(2008), Kuznetsov and Nield(2010), Kuznetsov and Nield(2011), Nield and Kuznetsov(2011a), Bhadauria(2012).

The temperature dependent viscosity fluid gives rise to variation in top and bottom structures and referred as a non-Boussinesq effect. Non-linear energy stability theory has been derived by Richardson and Straughan (1993) for the problem of convection in porous medium when the viscosity depends on the temperature for vanishingly small initial data thresholds, Payne (1999) derived unconditional non-linear stability for temperature sensitive fluid in porous media. Qin and Chadam (1996), Nield (1996), Holzbecher (1998), Rees(2002), Siddheshwar and Chan(2004), Vanishree and Siddheshwar (2010) and Siddheshwar and Vanishree(2012) studied the effect of variable viscosity on convection problems in a porous medium, Srivastava(2013) studied the effect of variable viscosity in the presence of internal heat source and gravity modulation, Bhadauria and Kiran(2013) investigated the effect of variable viscosity in the presence of temperature modulation.

Research articles related to the gravity modulation are provided by Malashetty and Padmavathi(1997), Rees and Pop(2000), Rees and Pop(2001), Rees and Pop(2003), Malashetty and Basavaraja(2005), Govender(2004), Govender(2005), Govender(2005a), Kuznetsov(2005), Kuznetsov(2006a), Kuznetsov(2006b), Siddhavaram and Homsy(2006), Strong(2008a), Strong(2008b), Razi(2009), Saravanan and Purusothaman(2009), Saravanan and Arunkumar(2010), Saravanan and Sivakumar(2010), Saravanan and Sivakumar(2011), Siddheshwar(2012) Bhadauria(2013), Swamy(2014) and Matta(2016).

Most of the studies concern linear stability of the thermal or double-diffusive system in porous media in the absence/presence of gravity modulations, and hence address only questions on onset of convection. If one were to quantify heat and mass transports in

porous media in the presence of gravity modulations, then the linear stability analysis is inapplicable and the nonlinear stability analysis becomes inevitable. There are no reported studies on this aspect of the problem. In the light of the above, we make a weakly nonlinear analysis of the problem using the Ginzburg-Landau equation and, in the process, quantify the heat and mass transports in terms of the amplitude governed by the Ginzburg-Landau equation.

2.2 Governing equations

We consider an infinitely extended horizontal anisotropic porous layer saturated by variable viscosity Newtonian fluid with temperature-dependent viscosity confined between the planes $z = 0$ and $z = d$, which is heated and salted from below. We choose a Cartesian frame of reference as, origin in the lower boundary and the z-axis vertically upward direction. The gravity force is acting in vertically downward direction, we consider only free-free boundaries. A uniform adverse temperature gradient $\Delta T/d$ and concentration gradient $\Delta S/d$ is maintained between the surfaces. All these assumptions reported in Figure 2.1. Further the density variation is considered under Boussinesq approximation. The governing equations under above considerations are given by

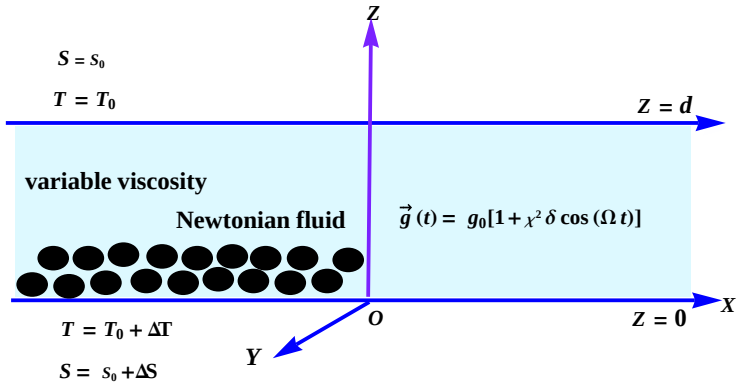

Figure 2.1: Physical configuration of the problem

$$\nabla.\mathbf{q} = 0, \tag{2.2.1}$$

$$\rho_0 \frac{\partial \mathbf{q}}{\partial t} = -\nabla p + \rho \mathbf{g}(t) - \mu K.\mathbf{q}, \tag{2.2.2}$$

$$\frac{\partial T}{\partial t} + (\mathbf{q}.\nabla)T = \kappa_T \nabla^2 T, \tag{2.2.3}$$

$$\frac{\partial S}{\partial t} + (\mathbf{q}.\nabla)S = \kappa_S \nabla^2 S, \tag{2.2.4}$$

$$\rho = \rho_0 \left[1 - \alpha_T \left(T - T_0\right) + \alpha_S \left(S - S_0\right)\right], \tag{2.2.5}$$

$$\mathbf{g}(t) = g_0 \left[1 + \chi^2 \delta \mathrm{Cos}(\Omega t)\right] \hat{k}, \tag{2.2.6}$$

$$\mu(T) = \frac{\mu_0}{1 + \chi^2 \delta_0 \left(T - T_0\right)}, \tag{2.2.7}$$

where $\mathbf{q}$ is velocity, p is the pressure, $\mathbf{g}$ is the acceleration due to gravity, μ is viscosity, ρ is density. T and S represents temperature and concentration respectively, K is the permeability of the porous media. ρ_0 is reference density, g_0 is mean gravity, δ is amplitude of gravity modulation, Ω is the frequency, χ is the quantity that indicates smallness in order of magnitude of modulation and t is time. Further more κ_T and κ_S are thermal and solutal diffusivity respectively, α_T is thermal volume expansion coefficient and α_S is density coefficient for salinity. Introducing the stream function ψ and eliminating the pressure term from Eq.(2.2.2), and then nondimensionalizing the resultant equations using the substitution

$$\begin{aligned} (x, y, z) = (x^*, y^*, z^*)\, d, t = t^* \left(d^2/\kappa_T\right), \\ \psi = (\kappa_T)\psi^*, T = (\Delta \mathrm{T})T^*, S = (\Delta \mathrm{S})S^*. \end{aligned} \tag{2.2.8}$$

The nondimensionlized Eqs.(2.2.2)-(2.2.4) obtained as follows:

$$\begin{aligned} \frac{1}{Va}\frac{\partial \left(\nabla^2 \psi\right)}{\partial t} = &- Ra \left(1 + \chi^2 \delta \mathrm{Cos}(\Omega t)\right) \frac{\partial T}{\partial x} + Ra_S \left(1 + \chi^2 \delta \mathrm{Cos}(\Omega t)\right) \frac{\partial S}{\partial x} \\ &- \bar{\mu}(T) \left(\frac{\partial^2}{\partial x^2} + \frac{\partial^2}{\partial z^2}\right) \psi - \left(\frac{\partial \bar{\mu}}{\partial x}\frac{\partial \psi}{\partial x} + \frac{\partial \bar{\mu}}{\partial z}\frac{\partial \psi}{\partial z}\right), \end{aligned} \tag{2.2.9}$$

$$\frac{\partial T}{\partial t} - \nabla^2 T = \frac{\partial(\psi, T)}{\partial(x, z)}, \tag{2.2.10}$$

$$\frac{\partial S}{\partial t} - \frac{1}{Le}\nabla^2 S = \frac{\partial(\psi, S)}{\partial(x, z)}, \tag{2.2.11}$$

where $Va = \frac{\nu d^2}{K\kappa_T}$ is the Vadász number, $Ra = \frac{\alpha_T g_0 \Delta T d K}{\nu \kappa_T}$ is the thermal Rayleigh number, $Ra_S = \frac{\alpha_S g_0 \Delta S d K}{\nu \kappa_T}$ is the solute Rayleigh number, $Le = \frac{\kappa_T}{\kappa_S}$ is the Lewis number, furthermore $\bar{\mu}(T) = \frac{1}{1+\chi^2 V(T-T_0)}$ and the appearance of χ^2 indicates that the viscosity variation is weak as χ is small quantity, $V = \delta_0 \Delta T$ thermo-rheological parameter.

The boundary condition for solving Eqs.(2.2.9)-(2.2.11) are

$$\psi = 0,\ T = 1 \text{ and } S = 1 \text{ at } z = 0, \tag{2.2.12}$$

$$\psi = 0,\ T = 0 \text{ and } S = 0 \text{ at } z = 1. \tag{2.2.13}$$

The conduction profile is given by

$$\psi_b = 0,\ T_b(z) = 1 - z \quad \text{and } S_b(z) = 1 - z. \tag{2.2.14}$$

Using $\bar{\mu} = \bar{\mu}\,(T_b)$ Eq.(2.2.9) reduces to

$$\begin{aligned} \frac{1}{Va}\frac{\partial\left(\nabla^2\psi\right)}{\partial t} = &- Ra\left(1 + \chi^2\delta\mathrm{Cos}(\Omega t)\right)\frac{\partial T}{\partial x} + Ra_S\left(1 + \chi^2\delta\mathrm{Cos}(\Omega t)\right)\frac{\partial S}{\partial x} \\ &- \bar{\mu}(T)\left(\frac{\partial^2}{\partial x^2} + \frac{\partial^2}{\partial z^2}\right)\psi - \frac{\partial\bar{\mu}}{\partial z}\frac{\partial\psi}{\partial z}, \end{aligned} \tag{2.2.15}$$

where $\bar{\mu}\,(T_b) = \frac{\mu'}{\mu_0} = \frac{1}{1+\chi^2 V(1-z)}$ and $\Omega^* = \frac{\Omega d^2}{\kappa_{Tz}}$.

Now imposing finite amplitude perturbations on the basic quiescent state given by Eq.(2.2.14) as

$$\psi = \Psi,\ T = 1 - z + \Theta \text{ and } S = 1 - z + \Phi \tag{2.2.16}$$

and substituting the above Eq.(2.2.16) in Eqs.(2.2.10), (2.2.11), (2.2.15), we have

$$\begin{aligned}\frac{1}{Va}\frac{\partial\left(\nabla^2\Psi\right)}{\partial t} =& -Ra\left(1+\chi^2\delta\mathrm{Cos}\left(\Omega_0^* t\right)\right)\frac{\partial\Theta}{\partial x}+Ra_S\left(1+\chi^2\delta\mathrm{Cos}\left(\Omega_0^* t\right)\right)\frac{\partial\Phi}{\partial x}\\ &-\frac{1}{1+\chi^2V(1-z)}\left(\frac{\partial^2}{\partial x^2}+\frac{\partial^2}{\partial z^2}\right)\Psi-\frac{\chi^2V}{\left[1+\chi^2V(1-z)\right]^2}\frac{\partial\Psi}{\partial z},\end{aligned} \tag{2.2.17}$$

$$\frac{\partial\Psi}{\partial x}+\frac{\partial\Theta}{\partial t}-\nabla^2\Theta = \frac{\partial(\Psi,\Theta)}{\partial(x,z)}, \tag{2.2.18}$$

$$\frac{\partial\Psi}{\partial x}+\frac{\partial\Phi}{\partial t}-\frac{1}{Le}\nabla^2\Phi = \frac{\partial(\Psi,\Phi)}{\partial(x,z)}. \tag{2.2.19}$$

Boundary conditions to solve Eqs.(2.2.17)-(2.2.19) are

$$\Psi=0\ ,\Theta=0 \text{ and } \Phi=0 \text{ at } z=0, \tag{2.2.20}$$

$$\Psi=0\ ,\Theta=0 \text{ and } \Phi=0 \text{ at } z=1. \tag{2.2.21}$$

We now introduce the following asymptotic expansion

$$Ra = R_0+\chi^2R_2+\chi^4R_4+\ldots, \tag{2.2.22}$$

$$\Psi = \chi\Psi_1+\chi^2\Psi_2+\chi^3\Psi_3+\ldots, \tag{2.2.23}$$

$$\Theta = \chi\Theta_1+\chi^2\Theta_2+\chi^3\Theta_3+\ldots, \tag{2.2.24}$$

$$\Phi = \chi\Phi_1+\chi^2\Phi_2+\chi^3\Phi_3+\ldots, \tag{2.2.25}$$

where R_0 is the critical value of the Rayleigh number at which the onset of convection takes place in the absence of gravity modulation.

We now assume the variation of time only at the slow time scale $\tau=\chi^2 t$ and arranging the systems at different order of χ.

At the **first order**, we have

$$\begin{pmatrix} \left(\frac{\partial^2}{\partial x^2}+\frac{\partial^2}{\partial z^2}\right) & R_0\frac{\partial}{\partial x} & -Ra_S\frac{\partial}{\partial x} \\ \frac{\partial}{\partial x} & -\nabla^2 & 0 \\ \frac{\partial}{\partial x} & 0 & -\frac{1}{Le}\nabla^2 \end{pmatrix} \begin{pmatrix} \Psi_1 \\ \Theta_1 \\ \Phi_1 \end{pmatrix} = 0, \tag{2.2.26}$$

solution at the lowest order is given by

$$\Psi_1 = A[\tau]\mathrm{Sin}\,(ax)\,\mathrm{Sin}(\pi z), \tag{2.2.27}$$

$$\Theta_1 = \frac{-a}{c}A[\tau]\ \mathrm{Cos}\,(ax)\,\mathrm{Sin}(\pi z), \tag{2.2.28}$$

$$\Phi_1 = \frac{-aLe}{c}A[\tau]\ \mathrm{Cos}\,(ax)\,\mathrm{Sin}(\pi z), \tag{2.2.29}$$

where $c = a^2 + \pi^2$. The critical value of the Rayleigh number and the corresponding wave number for the onset of stationary convection is calculated numerically and the expression for Rayleigh number is given by:

$$R_{0c} = \frac{(c^2 + Ra_S a^2 Le)}{a^2}. \tag{2.2.30}$$

2.3 Amplitude equation and heat and mass transport for stationary instability

At the **second order**, we have

$$\begin{pmatrix} \left(\frac{\partial^2}{\partial x^2}+\frac{\partial^2}{\partial z^2}\right) & R_0\frac{\partial}{\partial x} & -Ra_S\frac{\partial}{\partial x} \\ \frac{\partial}{\partial x} & -\nabla^2 & 0 \\ \frac{\partial}{\partial x} & 0 & -\frac{1}{Le}\nabla^2 \end{pmatrix} \begin{pmatrix} \Psi_2 \\ \Theta_2 \\ \Phi_2 \end{pmatrix} = \begin{pmatrix} R_{21} \\ R_{22} \\ R_{23} \end{pmatrix}, \tag{2.3.1}$$

where

$$R_{21} = 0, \tag{2.3.2}$$

$$R_{22} = \frac{-a^2\pi}{2c}A[\tau]^2\mathrm{Sin}(2\pi z), \tag{2.3.3}$$

$$R_{23} = \frac{-a^2 Le\pi}{2c} A[\tau]^2 \mathrm{Sin}(2\pi z). \tag{2.3.4}$$

The second order solution subject to the boundary conditions (2.2.20)-(2.2.21), are given by

$$\Psi_2 = 0, \tag{2.3.5}$$

$$\Theta_2 = \frac{-a^2}{8\pi c} A[\tau]^2 \mathrm{Sin}(2\pi z), \tag{2.3.6}$$

$$\Phi_2 = \frac{-a^2 Le^2}{8\pi c} A[\tau]^2 \mathrm{Sin}(2\pi z). \tag{2.3.7}$$

The horizontally averaged Nusselt number and Sherwood number, Nu and Sh, for stationary mode of convection (the mode considered in this problem) is given by:

$$Nu(\tau) = \frac{\left[\frac{a}{2\pi}\int_0^{\frac{2\pi}{a}} (1 - z + \Theta_2)_z \, dx\right]_{z=0}}{\left[\frac{a}{2\pi}\int_0^{\frac{2\pi}{a}} (1 - z)_z \, dx\right]_{z=0}}, \tag{2.3.8}$$

$$Sh(\tau) = \frac{\left[\frac{a}{2\pi}\int_0^{\frac{2\pi}{a}} (1 - z + \Phi_2)_z \, dx\right]_{z=0}}{\left[\frac{a}{2\pi}\int_0^{\frac{2\pi}{a}} (1 - z)_z \, dx\right]_{z=0}}. \tag{2.3.9}$$

One can notice here that the gravity modulation and variable viscosity parameter are effective at $O(\chi^2)$ and affects $Nu(\tau)$ and $Sh(\tau)$ through $A[\tau]$ is shown next. Substituting expressions of Θ_2 and Φ_2 in the above Eqs.(2.3.8)-(2.3.9) and simplifying, we get

$$Nu(\tau) = 1 + \frac{a^2}{4c}(A[\tau])^2, \tag{2.3.10}$$

$$Sh(\tau) = 1 + \frac{Le^2 a^2}{4c}(A[\tau])^2. \tag{2.3.11}$$

At the **third order**, we have

$$\begin{pmatrix} \left(\frac{\partial^2}{\partial x^2} + \frac{\partial^2}{\partial z^2}\right) & R_0 \frac{\partial}{\partial x} & -Ra_S \frac{\partial}{\partial x} \\ \frac{\partial}{\partial x} & -\nabla^2 & 0 \\ \frac{\partial}{\partial x} & 0 & -\frac{1}{Le}\nabla^2 \end{pmatrix} \begin{pmatrix} \Psi_3 \\ \Theta_3 \\ \Phi_3 \end{pmatrix} = \begin{pmatrix} R_{31} \\ R_{32} \\ R_{33} \end{pmatrix}, \tag{2.3.12}$$

where

$$R_{31} = -\frac{1}{Va}\frac{\partial}{\partial\tau}\left(\nabla^2\Psi_1\right) - V(1-z)\left(\frac{\partial^2}{\partial x^2}+\frac{\partial^2}{\partial z^2}\right)\Psi_1 - V\frac{\partial\Psi_1}{\partial z} \quad (2.3.13)$$
$$-\left(R_{0c}\left(2V(1-z)+\delta\mathrm{Cos}(\Omega\tau)\right)+R_2\right)\frac{\partial\Theta\delta}{\partial x} + Ra_S\left(2V(1-z)+\delta\mathrm{Cos}(\Omega\tau)\right)\frac{\partial\Phi_1}{\partial x}$$

$$R_{32} = \frac{\partial\Psi_1}{\partial x}\frac{\partial\Theta_2}{\partial z} - \frac{\partial\Theta_1}{\partial\tau}, \quad (2.3.14)$$

$$R_{33} = \frac{\partial\Psi_1}{\partial x}\frac{\partial\Phi_2}{\partial z} - \frac{\partial\Phi_1}{\partial\tau}, \quad (2.3.15)$$

and $\Omega = \frac{\Omega^*}{\chi^2} = \frac{\Omega d^2}{\chi^2\kappa_{Tz}}$.

Substituting the value of $\Psi_1, \Theta_1, \Theta_2, \Phi_1$ and Φ_2 in the above equations to get the expressions of R_{31}, R_{32}, R_{33}. Applying the solvability condition for the existence of third order solution, we get the non-autonomous Ginzburg-Landau equation with time periodic coefficients in the form

$$A_1A'[\tau] + A_2A[\tau] + A_3(A[\tau])^3 = 0, \quad (2.3.16)$$

where

$A_1 = \left(\frac{c}{Va} + \frac{a^2R_{0c}}{c^2} - \frac{a^2Le^2Ra_S}{c^2}\right)$,

$A_2 = \left(-\delta c\mathrm{Cos}(\Omega\tau) - R_2\frac{a^2}{c} - \frac{\delta^2V}{2}\right)$,

$A_3 = \left(\frac{a^4R_{0c}}{8c^2} - \frac{a^4Le^3Ra_S}{8c^2}\right)$.

The Ginzburg–Landau equation given by (2.3.16) is a Bernoulli equation and obtaining its analytical solution is difficult due to its non-autonomous nature. Therefore, it has been solved numerically by the in-built function NDSolve of Mathematica 7.0, subject to the initial condition $A[0] = a_0$, where a_0 is the chosen initial amplitude of convection. In our calculations, we may assume $R_2 = R_{0c}$ to keep the parameters to the minimum.

2.4 Results and Discussion

We perform weakly non-linear analysis of gravity modulation for temperature dependent viscosity fluid in closely packed anisotropic porous media, therefore the Darcy model is considered for the governing equation for linear momentum. The work of Nield(1996) has been used for the thermo-rheological relationship of temperature dependent viscosity of the fluid. We investigated the effect of gravity modulation and thermo-rheological parameter on heat and mass transport. We consider the effect of gravity modulation to be of order $O(\chi^2)$ and this will provide us only small amplitude vibrations. Such an assumption will help us in obtaining the amplitude equation of convection in a rather simple and elegant manner and is much easier to obtain than in the case of the Lorenz model.

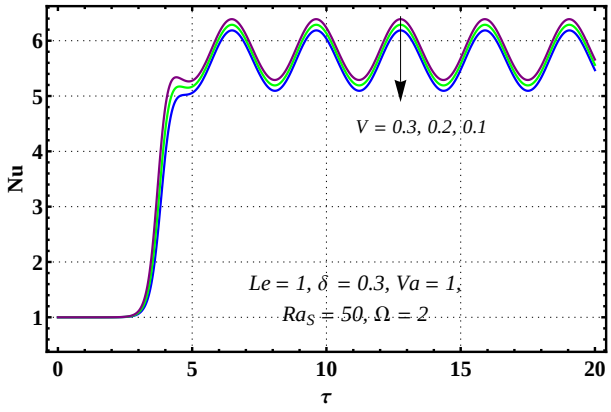

Figure 2.2: Variation of Nusselt number with time for different values of V

Before writing the discussion of the results, we enlighten some features of the following aspects of the problem:

1. The need for nonlinear stability analysis.

2. The relation of the problem to a real application.

3. The selection of all dimensionless parameters utilized in computations.

If one wants to quantify heat and mass transfer, which linear stability analysis is unable to do, this problem needs to perform the nonlinear analysis and hence the importance.

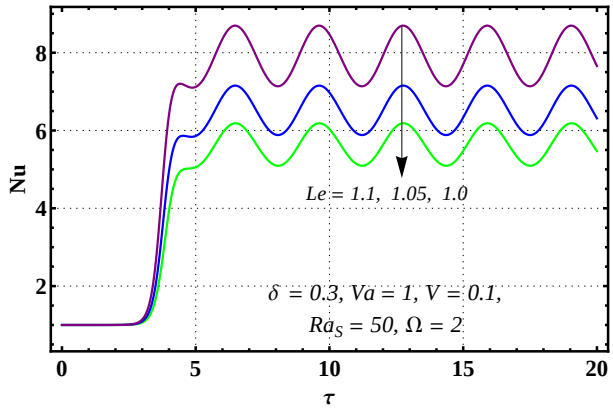

Figure 2.3: Variation of Nusselt number with time for different values of Le

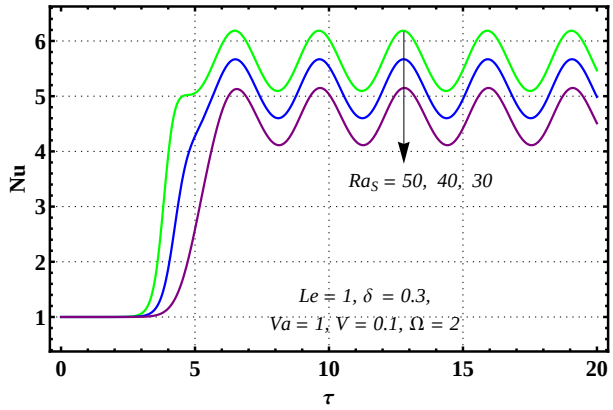

Figure 2.4: Variation of Nusselt number with time for different values of Ra_S

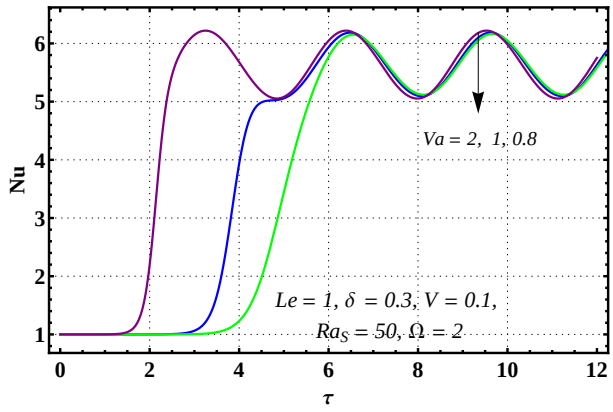

Figure 2.5: Variation of Nusselt number with time for different values Va

External regulation of convection is important in the study of double-diffusive convection in porous media. The objective of this study is to consider gravity modulation and temperature dependent viscosity variation for either enhancing or inhibiting convective heat transport as is required by a real application.

The parameters that appeared in this article and effect heat and mass transfer are V, Le, Ra_S, Va, δ, Ω. The first four parameters relate to the fluid and the structure of the porous medium, and the last two concern external mechanisms of controlling convection.

Some real world applications like fractured porous medium, sedimentation of rocks and the formation of mushy layer in the solidification of binary alloys where the value of Va may be considered to be of unity order Vadász(1998); therefore, we keep the time-derivative term in the present study, furthermore that is why we have kept the values of Va around one in our calculations, and retained the local acceleration term $\frac{1}{Va}\frac{\partial q}{\partial t}$.

The values of $Nu(\tau)$ and $Sh(\tau)$ are obtained numerically from the expressions of $Nu(\tau)$ and $Sh(\tau)$ by using the numerical value of amplitude obtained from the Ginzburg-Landau equation. We use the values to plot the curve for $Nu(\tau)$ and $Sh(\tau)$ versus τ and are presented in the Figures 2.2-2.13. Figures 2.2-2.7 correspond to heat transfer and 2.8-2.13 correspond to mass transfer. A close observation of Eq.(2.3.10)-(2.3.11) in conjunction with Eq.(2.3.16) reveals that $Nu(\tau)$ and $Sh(\tau)$ depends on Lewis number Le, solute Rayleigh number Ra_S, Vadász number Va, thermo-rheological parameter and amplitude of g-jitter. Initially the value of Nusselt number and Sherwood number is one which shows that, initially the heat transfer is by conduction alone and as time increases the value of Nusselt number and Sherwood number increases showing convection takes place and after reaching a certain value Nusselt number and Sherwood number starts oscillations sand remains oscillatory for the further elapses of time.

Following result has been found from Figures (2.2, 2.3, 2.4, 2.5, 2.6, 2.7) for heat transport

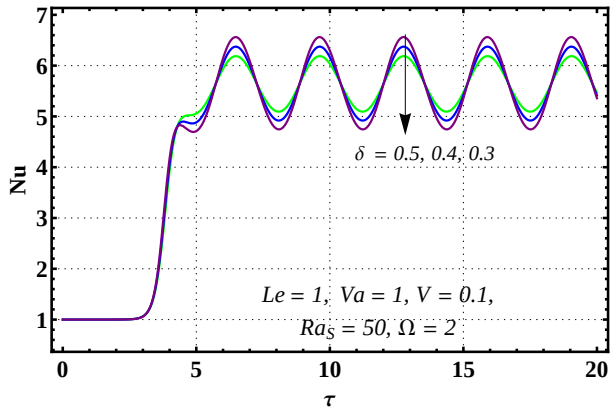

Figure 2.6: Variation of Nusselt number with time for different values δ

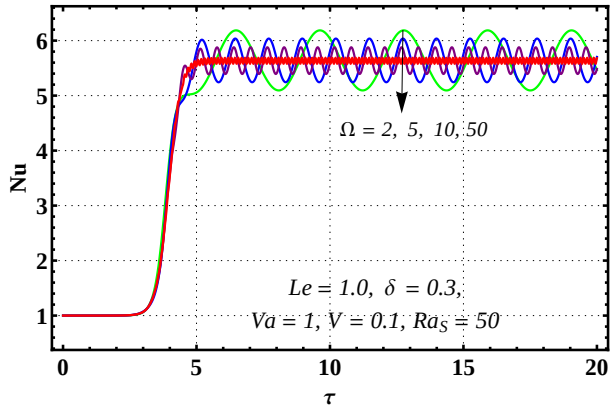

Figure 2.7: Variation of Nusselt number with time for different values Ω

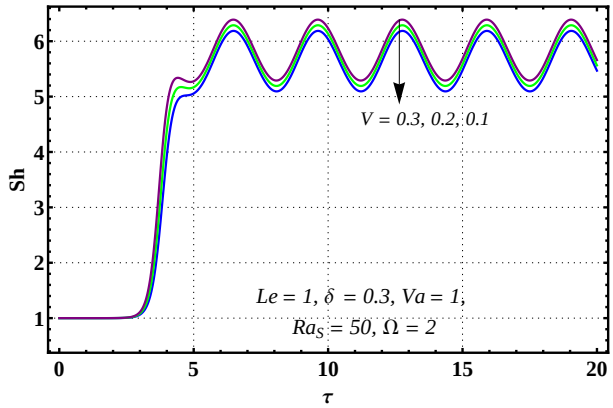

Figure 2.8: Variation of Sherwood number with time for different values of V

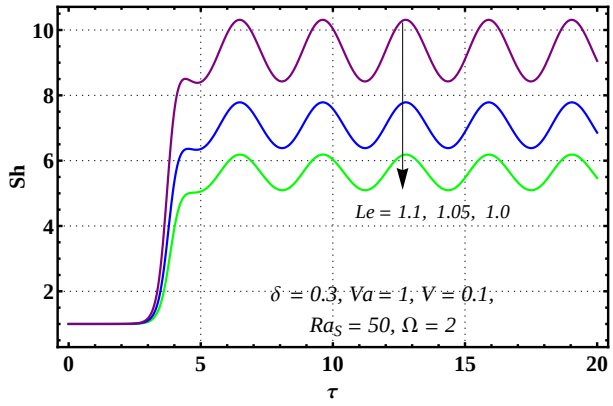

Figure 2.9: Variation of Sherwood number with time for different values of Le

1. $[Nu]_{V=0.1} < [Nu]_{V=0.2} < [Nu]_{V=0.3}$

2. $[Nu]_{Le=1.0} < [Nu]_{Le=1.05} < [Nu]_{Le=1.1}$

3. $[Nu]_{Ra_S=30} < [Nu]_{Ra_S=40} < [Nu]_{Ra_S=50}$

4. $[Nu]_{Va=0.8} < [Nu]_{Va=1} < [Nu]_{Va=2}$

5. $[Nu]_{\delta=0.3} < [Nu]_{\delta=0.4} < [Nu]_{\delta=0.5}$

6. $[Nu]_{\Omega=10} < [Nu]_{\Omega=5} < [Nu]_{\Omega=2}$

Following result has been found from Figures (2.8, 2.9, 2.10, 2.11, 2.12, 2.13) for mass transport

1. $[Sh]_{V=0.1} < [Sh]_{V=0.2} < [Sh]_{V=0.3}$

2. $[Sh]_{Le=1.0} < [Sh]_{Le=1.05} < [Sh]_{Le=1.1}$

3. $[Sh]_{Ra_S=30} < [Sh]_{Ra_S=40} < [Sh]_{Ra_S=50}$

4. $[Sh]_{Va=0.8} < [Sh]_{Va=1} < [Sh]_{Va=2}$

5. $[Sh]_{\delta=0.3} < [Sh]_{\delta=0.4} < [Sh]_{\delta=0.5}$

6. $[Sh]_{\Omega=10} < [Sh]_{\Omega=5} < [Sh]_{\Omega=2}$

From the Figure 2.2, we observe that for the increasing value of thermo-rheological parameter heat transfer increases, from the Figure 2.3, it is clear that when the value of Lewis

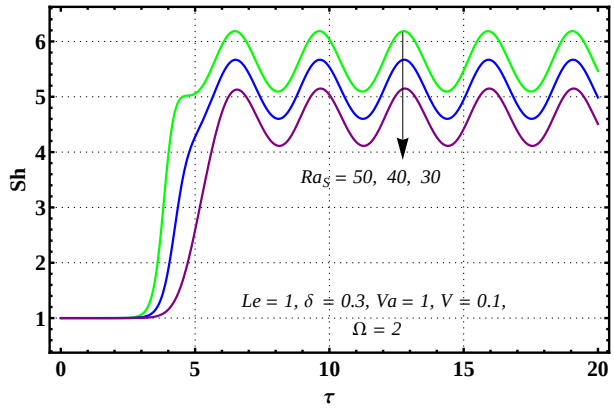

Figure 2.10: Variation of Sherwood number with time for different values of Ra_S

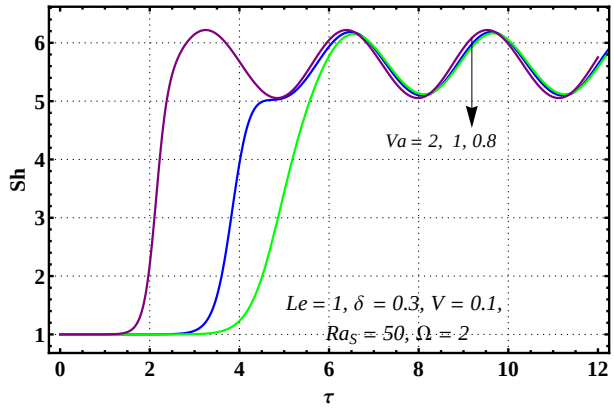

Figure 2.11: Variation of Sherwood number with time for different values Va

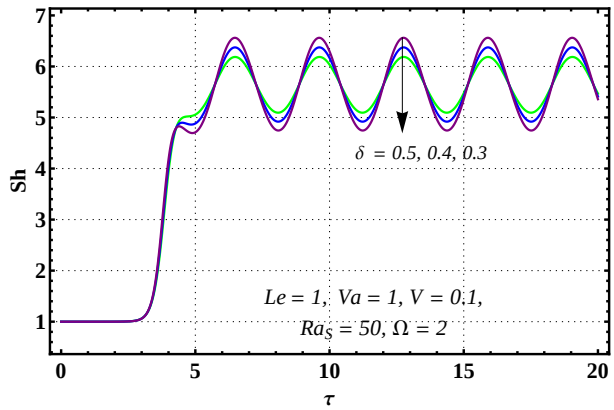

Figure 2.12: Variation of Sherwood number with time for different values δ

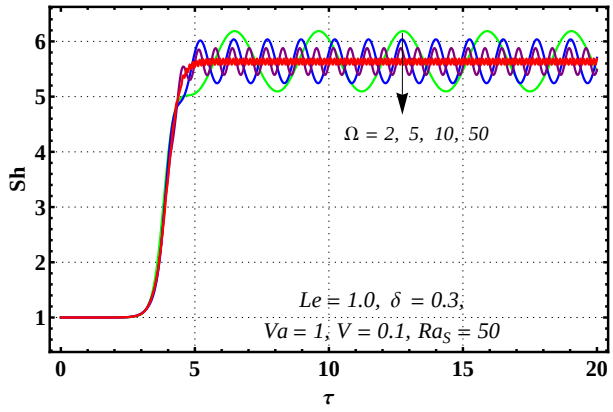

Figure 2.13: Variation of Sherwood number with time for different values Ω

number increases heat transfer increases, the variation of Nusselt number for the different values of solute Rayleigh number is shown in Figure 2.4 and is observed that from the graph that for the increasing value of solute Rayleigh number heat transfer increases, Figure 2.5 shows the variation of Nusselt number for the different values of Vadász number and it is observed that the heat transfer increases for the increasing value of Vadász number, from Figure 2.6 we see that for the increasing value of the amplitude of gravity modulation heat transfer increases, from Figure 2.7 we observe that the heat transfer decreases for the increasing value of Ω , furthermore for large values of frequency the effect of modulation is frail.

Figure 2.8 shows the variation Sherwood number for the different values of thermo-rheological parameter and it is found that for the increasing value of thermo-rheological parameter mass transfer increases, the variation of Sherwood number for the different values of Lewis number is shown in Figure 2.9 and from the graph we observe that for the increasing value Lewis number mass transfer increases, from the Figure 2.10, it is clear that for the increasing value of solute Rayleigh number mass transfer increases, the effect of Vadász number on the mass transfer is shown in Figure 2.11 and it is clear from the graph mass transfer increases for the increasing value of Vadász number, from Figure 2.12 we observe that the mass transfer increases to increase in the amplitude of gravity modulation, from Figure 2.13, it is clear that the mass transfer decreases for the increasing value of Ω, furthermore for large values of frequency, the effect of modulation is frail. We also found

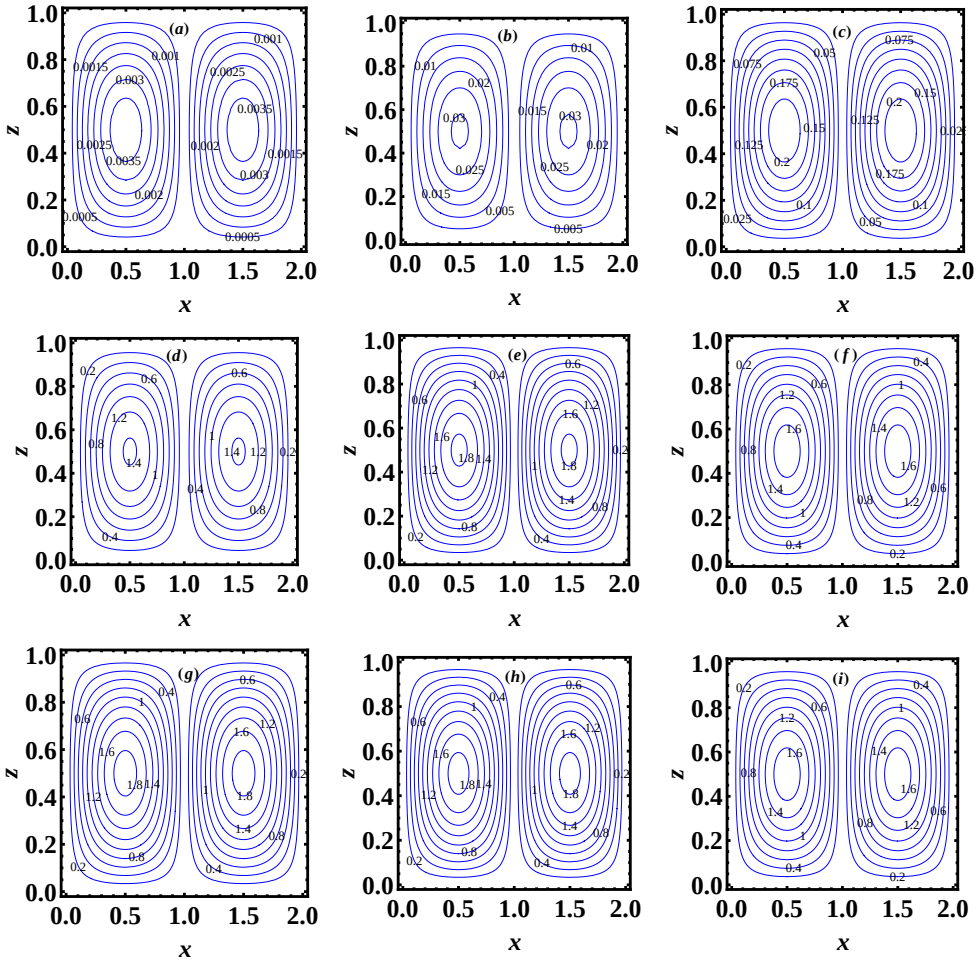

Figure 2.14: Streamlines at (a) $\tau = 0.1$, (b) $\tau = 1$, (c) $\tau = 2$, (d) $\tau = 3$, (e) $\tau = 4$, (f) $\tau = 5$, (g) $\tau = 6$, (h) $\tau = 7$, (i) $\tau = 8$

that the effect of Vadász number is not only on the heat transfer and mass transfer directly but also affects the heat and mass transfer through frequency of the modulation, we found that for some bigger value of Vadász number the effect of Vadász number is weak on the heat and mass transfer as well as the effect of frequency of modulation is not significant on the heat and mass transfer.

Variation of stream lines, isotherms, isohalines is shown graphically in Figures 2.14-2.16 at $\tau = 0.1, 1, 2, 3, 4, 5, 6, 7, 8$ for $V = 0.1, Va = 1, Le = 1, \Omega = 2, \delta = 0.5, Ra_s = 50, \chi = 0.3$. From Figures 2.14a-2.14i it is clear that the magnitudes of stream lines increases as time increases, Figures 2.15a-2.15i shows the variation of isotherms at the different instant of time and it is found that from the graph initially, isotherms are flat and parallel showing

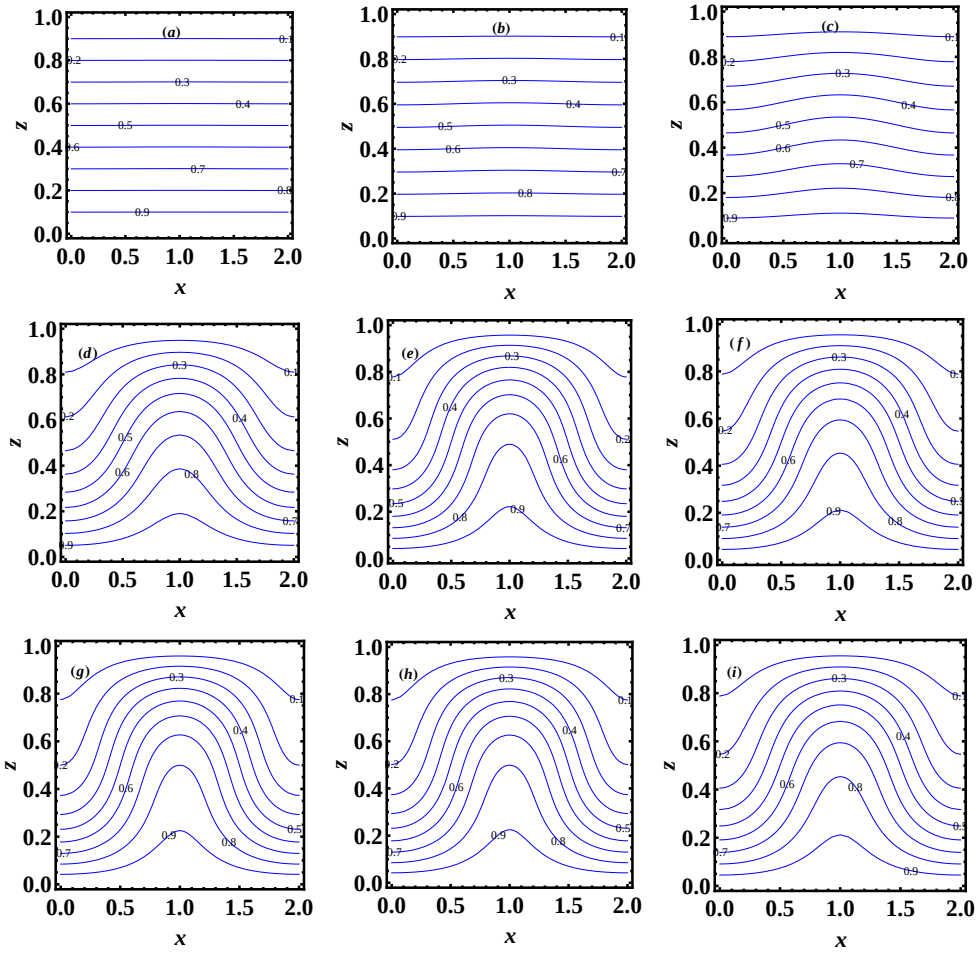

Figure 2.15: Isotherms at (a) $\tau = 0.1$, (b) $\tau = 1$, (c) $\tau = 2$, (d) $\tau = 3$, (e) $\tau = 4$, (f) $\tau = 5$, (g) $\tau = 6$, (h) $\tau = 7$, (i) $\tau = 8$

the heat transport is only by conduction and as time increases isotherms starts oscillating showing convective regime is in place and then forms contour showing that as time increases convection contributes in heat transport, similar behaviour is observed for isohalines in Figures 2.16a-2.16i, moreover, it is clear that from the Figures 2.14-2.16 after reaching at some instant stream lines, isotherms, isohalines oscillates for the further elapses of time.

2.5 Conclusions

We perform the weakly nonlinear analysis using the Ginzburg-Landau equation for double diffusive convection in an infinite horizontal anisotropic porous layer which is heated

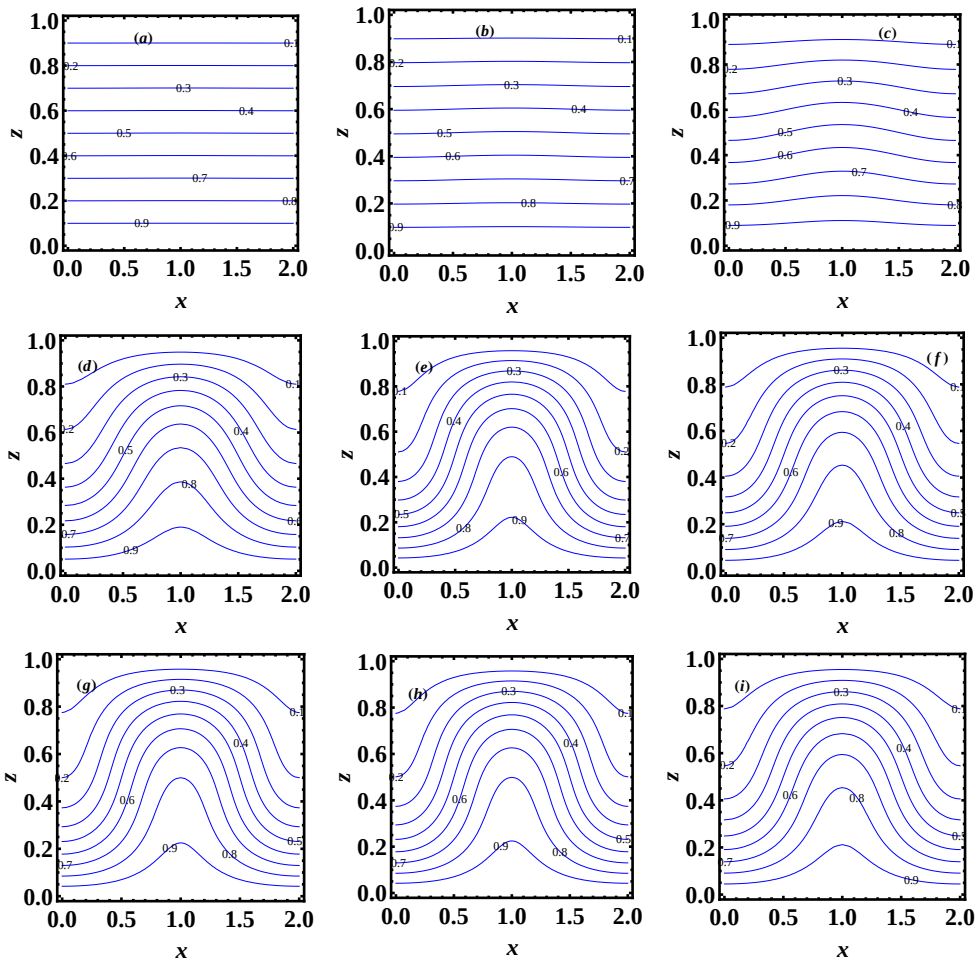

Figure 2.16: Isohalines at (a) $\tau = 0.1$, (b) $\tau = 1$, (c) $\tau = 2$, (d) $\tau = 3$, (e) $\tau = 4$, (f) $\tau = 5$, (g) $\tau = 6$, (h) $\tau = 7$, (i) $\tau = 8$

and salted from below saturated with temperature sensitive fluid in the presence of gravity modulation. We study the effect of gravity modulation and temperature dependent viscosity on the heat and mass transfer. We found that the Vadász number is effective for its value around unity and less and its effect is frail when we consider higher values. The following conclusions have been made from the present analysis, for the increasing values of parameters:

1. Thermo-rheological parameter V : heat transfer increases, mass transfer increases.

2. Lewis number Le : heat transfer increases, mass transfer increases.

3. Solute Rayleigh number Ra_S : heat transfer increases, mass transfer increases.

4. Vadász number Va : heat transfer increases, mass transfer increases.

5. Amplitude of modulation δ: heat transfer increases, mass transfer increases.

6. Frequency of modulation Ω: heat transfer decreases, mass transfer decreases.

Chapter 3

Stability analysis and internal heating effects on oscillatory convection in a viscoelastic fluid layer under gravity modulation

3.1 Introduction

In this chapter, we study internal heating effects for oscillatory convection in a viscoelastic fluid layer under gravity modulation. We also study the Hopf bifurcation and Pitchfork bifurcation on different parameters, which give the more control parameters to study the stability of the system.

Thermal convection in a horizontal fluid layer subject to constant but different temperature at the boundaries has been studied extensively due to its applications in various fields. The classical Rayleigh-Bénard convection is found to be an interesting phenomenon

This chapter is based on the research article: Stability analysis and internal heating effects on oscillatory convection in a viscoelastic fluid layer under gravity modulation, published in APJEST (2016).

introduced by Chandrasekhar(1961), due to bottom heating of a fluid layer. For more detailed analysis on thermal instability, refer some excellent books: Ingham and Pop(2005), Nield and Bejan(2012) and vafai(2000). From the applications point of view, the regulation of convection is very important. Thermo-gravitational vibration is known to be an effective technique for controlling the instability. The first idea of using mechanical vibration as a tool to enhance the heat transfer rate is presented by Gresho and Saini(1970). Further studies on gravity modulation are due to Malashetty and Padmavathi(1997), Malashetty and Swamy(2011), Bhadauria et al.(2005) and Siddhavaram and Hosmy(2006).

Industrial fluids are basically non-Newtonian fluids. In particular, viscoelastic fluids have found a wide range of industrial applications. The characteristics of heat transfer in viscoelastic fluid layer are also important in chemical processing industries. Therefore, proper understanding of convective motion and its behaviour is necessary for controlling many processes; such as, geothermal reservoirs, filtration, enhanced oil recovery, to name a few. In the literature, several articles are available in which different physical models with viscoelastic fluid layer have been used to study thermal instability. Green(1968) was the first to study the oscillatory convection in a viscoelastic fluid layer, the occurrence of overstability for typical Rayleigh-Bénard convection in a horizontal layer of homogeneous Maxwellian fluid, heated from below, is reported by Vest and Arpaci(1969). Convective instability in a rotating viscoelastic fluid layer was studied by Bhatia and Steiner(1972). Thermal instability in a viscoelastic fluid saturating a porous medium was studied by Kim et al.(2003). The Bénard-Marangoni thermal instability problem in a viscoelastic Jeffrey's fluid layer with internal heat generation was introduced by Comissiong et al.(2011); onset of oscillatory convection was studied using linear stability analysis and the dependence of critical Rayleigh number for oscillatory convection on internal heat generation, relaxation and retardation times was derived. Thermal instability using linear stability analysis was studied by Rajib and Layek(2012). Recently, Bhadauria and Kiran(2014b) investigated oscillatory convection in a viscoelastic fluid layer under gravity modulation by making a non-linear stability analysis.

Haajizadeh et al.(1984) have studied a uniform heat-generation term across an enclosure with isothermal vertical walls and adiabatic horizontal walls. Further, for more studies on internal heating we refer to Rao and wang(1991), Magyari and Pop(2007) and Bhadauria et al.(2013).

The qualitative analysis of a dynamical system provides much knowledge about the system. Bifurcations, the appearance of a topologically non-equivalent phase portrait under variation of parameters, are scientifically more important as they provide models of transitions and instabilities Strogatz(2007). In the present chapter, two types of bifurcation (1) Pitchfork bifurcation (common in physical problems that have a symmetry); (2) Hopf bifurcation (bifurcation corresponding to the presence of purely complex eigenvalue) are discussed, for details we refer to Kuznetsov(2004).

3.2 Mathematical structure

Consider an infinitely extended horizontal viscoelastic fluid layer of depth d, confined between two parallel planes, the lower plane at $z = 0$ while upper one is at $z = d$. A Cartesian frame of reference is adopted in such a way that the origin lies on the lower plane and z axis is vertically upward. The fluid layer is heated from below and cooled from above. The physical configuration of the model is depicted in Figure 3.1. The Oberbeck-Boussinesq approximation is adopted to solve the model equations. The governing equations of the flow and temperature fields as Bhadauria and Kiran(2014b) are given by

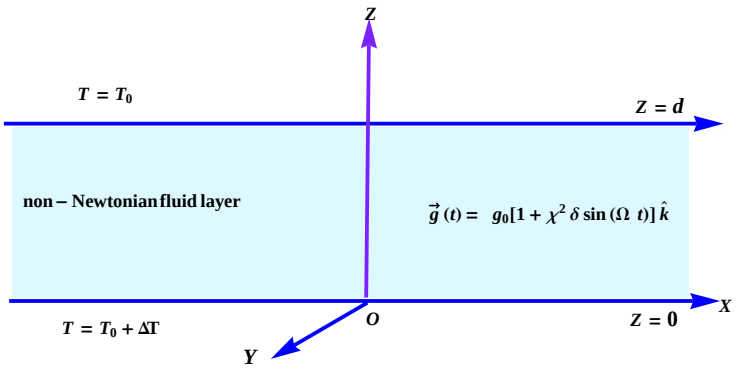

Figure 3.1: Physical configuration of the problem

$$\begin{cases} \nabla.\vec{q} = 0, \\ \\ \left(\overline{\lambda_1}\frac{\partial}{\partial t} + 1\right)\left(\frac{\partial \vec{q}}{\partial t} + (\vec{q}.\nabla)\vec{q} - \frac{1}{\rho_0}\nabla p + \frac{\rho}{\rho_0}\vec{g}\right) - \nu\left(\overline{\lambda_2}\frac{\partial}{\partial t} + 1\right)\nabla^2\vec{q} = 0, \\ \\ \frac{\partial T}{\partial t} + (\vec{q}.\nabla)T = \kappa_T\nabla^2 T + Q(T - T_0), \\ \\ \rho = \rho_0[1 - \alpha_T(T - T_0)], \end{cases} \tag{3.2.1}$$

where the physical meaning of the variables is as given in the nomenclature. The externally imposed gravitational field and the thermal boundary conditions are as follows

$$\vec{g} = g_0[1 + \chi^2\delta\cos(\Omega t)]\hat{k}, \tag{3.2.2}$$

$$\begin{cases} T = T_0 + \Delta T, & \text{at} \quad z = 0, \\ \\ = T_0, & \text{at} \quad z = d, \end{cases} \tag{3.2.3}$$

where g_0 is the mean gravity and $\vec{k}$ is the unit vector along the positive z-axis.

3.3 Basic state

The basic state is assumed to be quiescent, the quantities are taken as

$$\vec{q_b} = 0, p = p_b(z), T = T_b(z), \rho = \rho_b(z). \tag{3.3.1}$$

The following relations, which define basic state pressure and temperature mathematically, are obtained by putting Eq.(3.3.1) in Eq.(3.2.1):

$$\frac{dp_b}{dz} = -\rho_b g, \tag{3.3.2}$$

$$\kappa_T \frac{d^2(T_b - T_0)}{dz^2} + Q(T_b - T_0) = 0, \tag{3.3.3}$$

$$\rho_b = \rho_0[1 - \alpha_T(T_b - T_0)]. \tag{3.3.4}$$

The exact solution of Eq.(3.3.3) subject to the boundary conditions (3.2.3) is obtained as

$$T_b = T_0 + \Delta T \frac{\sin((\sqrt{\frac{Q}{\kappa_T}})(1 - \frac{z}{d}))}{\sin(\sqrt{\frac{Q}{\kappa_T}})}. \tag{3.3.5}$$

Now, we superimpose the finite amplitude perturbations on the basic state in the form:

$$\vec{q} = q_b + q', T = T_b + T', p = p_b + p', \rho = \rho_b + \rho', \tag{3.3.6}$$

where the primes represents the perturbation quantities. The dimensionless governing system as mentioned in Bhadauria and Kiran(2014b) is given as

$$\Big(\lambda_1 \frac{\partial}{\partial t} + 1\Big)\Big(\frac{1}{P_r}\frac{\partial}{\partial t}\nabla^2\psi - \frac{1}{P_r}\frac{\partial(\psi, \nabla^2\psi)}{\partial(x,z)} + g_m Ra \frac{\partial T}{\partial x}\Big) - \Big(\lambda_2 \frac{\partial}{\partial t} + 1\Big)\nabla^4\psi = 0, \tag{3.3.7}$$

$$-\frac{\partial\psi}{\partial x}\frac{\partial T_b}{\partial z} + \Big(\frac{\partial}{\partial t} - \nabla^2 - R_i\Big)T = \frac{\partial(\psi, T)}{\partial(x,z)}, \tag{3.3.8}$$

where $g_m = (1 + \chi^2 \delta cos(\Omega t))$, $Ra = \frac{\alpha_T g_0 \Delta T K d^3}{\nu \kappa_T}$ is the thermal Rayleigh number, $R_i = \frac{Qd^2}{\kappa_T}$ is the internal Rayleigh number, $\nu = \frac{\mu}{\rho_0}$ is the kinematic viscosity, and $P_r = \frac{\nu}{\kappa_T}$ is the Prandtl number. The above system will be solved by considering stress free and isothermal boundary conditions:

$$\psi = \frac{\partial^2\psi}{\partial z^2} = T = 0 \quad \text{on} \quad z = 0, z = 1. \tag{3.3.9}$$

The dimensionless steady temperature $T_b(z)$, appearing in Eq.(3.3.8) is

$$\frac{dT_b}{dz} = -\frac{\sqrt{R_i}\cos(\sqrt{R_i}(1 - z))}{\sin\sqrt{R_i}}. \tag{3.3.10}$$

On introducing a small perturbation parameter χ, which shows a deviation from the critical state of onset of convection, the variables for a weak non-linear state may be expanded in

power series of χ as Malkus and Veronis(1958); Venezian(1969)

$$Ra = R_0 + \chi^2 R_2 + \chi^4 R_4 + \cdots \tag{3.3.11}$$

$$\psi = \chi\psi_1 + \chi^2\psi_2 + \chi^3\psi_3 + \cdots \tag{3.3.12}$$

$$T = \chi T_1 + \chi^2 T_2 + \chi^3 T_3 + \cdots \tag{3.3.13}$$

where R_0 denotes the critical value of the Rayleigh number for the onset of convection in the absence of gravity modulation.

3.4 Analysis of the periodic solutions

In order to study the time periodic convective phenomenon, the slow and fast time scales are introduced by $\frac{\partial}{\partial t} = \frac{\partial}{\partial \tau} + \chi^2(\frac{\partial}{\partial s})$. The above system (3.3.7) and (3.3.8) is solved for each order of χ.

For the **first order**, the matrix operator is obtained similar to linear case as:

$$\begin{pmatrix} \frac{1}{P_r}(\lambda_1\frac{\partial}{\partial\tau}+1)\frac{\partial}{\partial\tau}\nabla^2 - (\lambda_2\frac{\partial}{\partial\tau}+1)\nabla^4 & R_0(\lambda_1\frac{\partial}{\partial\tau}+1)\frac{\partial}{\partial x} \\ -\frac{\partial}{\partial x}\frac{\partial T_b}{\partial z} & (\frac{\partial}{\partial\tau} - \nabla^2 - R_i) \end{pmatrix} \begin{pmatrix} \psi_1 \\ T_1 \end{pmatrix} = \begin{pmatrix} 0 \\ 0 \end{pmatrix}. \tag{3.4.1}$$

The solution of the first order system subject to the boundary conditions Eq.(3.3.9), is assumed to be

$$\psi_1 = (B(s)e^{i\omega\tau} + \overline{B}(s)e^{-i\omega\tau})\sin ax \ \sin \pi z, \tag{3.4.2}$$

$$T_1 = (A(s)e^{i\omega\tau} + \overline{A}(s)e^{-i\omega\tau})\cos ax \ \sin \pi z. \tag{3.4.3}$$

The unknown amplitudes are functions of slow time scale, and are related by the following expression:

$$B(s) = -\frac{(c + i\omega - R_i)(4\pi^2 - R_i)}{4\pi^2 a}A(s), \tag{3.4.4}$$

where $c = a^2 + \pi^2$. The values of the critical Rayleigh number and the corresponding wave

number of the system for a stationary mode of convection are as given below:

$$R_{0c}^{st} = \frac{c^2(c - R_i)(4\pi^2 - R_i)}{4\pi^2 a^2}, \tag{3.4.5}$$

$$a_c^2 = \frac{(R_i - \pi^2) \pm \sqrt{(\pi^2 - R_i)^2 + 8\pi^2(\pi^2 - R_i)}}{4}. \tag{3.4.6}$$

In particular, for $R_i = 0$ (without internal-heating), we have

$$R_{0c} = \frac{c^3}{a^2}, \tag{3.4.7}$$

$$a_c = \frac{\pi}{\sqrt{2}}, \tag{3.4.8}$$

which are the classical results as obtained by Chandrasekhar(1961). The critical Rayleigh number for the oscillatory mode of convection is computed as follows

$$R_{0c}^{osc} = \Big(\frac{c^3}{a^2} + \frac{(\lambda_1\omega^2 R_i c - P_r R_i c^2) - (\lambda_1 + \lambda_2 P_r)\omega^2 c(c+1)}{a^2 P_r}\Big)\frac{4\pi^2 - R_i}{4\pi^2}, \tag{3.4.9}$$

where ω is the oscillatory frequency as given below

$$\omega^2 = \frac{-1 + R_i/c + (\lambda_1 - \lambda_2)P_r c - P_r(1 - \lambda_2 R_i + \lambda_1 R_i)}{\lambda_1(\lambda_1 + \lambda_2 P_r) - \lambda_1^2 R_i/c}, \tag{3.4.10}$$

which is the same as computed by Rajib and Layek(2012) without internal-heating. Here, we compute the wave number, known as the critical wave number for which the Rayleigh number is minimum. It is to be noted that the critical Rayleigh number and the corresponding wave number do not depend on relaxation(λ_1) and retardation(λ_2) time in stationary mode of convection but it is not so in case of oscillatory mode of convection. Since ω_2 has to be positive and real, therefore from the relation (3.4.10), the necessary condition for oscillatory convection is obtained as

$$\lambda_1 > \lambda_2 + \frac{1 + P_r(1 + \lambda_1 R_i - \lambda_2 R_i) - R_i c}{c P_r}. \tag{3.4.11}$$

Now at **second order**, we have

$$\begin{pmatrix} \frac{1}{P_r}(\lambda_1\frac{\partial}{\partial\tau}+1)\frac{\partial}{\partial\tau}\nabla^2-(\lambda_2\frac{\partial}{\partial\tau}+1)\nabla^4 & R_0(\lambda_1\frac{\partial}{\partial\tau}+1)\frac{\partial}{\partial x} \\ -\frac{\partial}{\partial x}\frac{\partial T_b}{\partial z} & (\frac{\partial}{\partial\tau}-\nabla^2-R_i) \end{pmatrix} \begin{pmatrix} \psi_2 \\ T_2 \end{pmatrix} = \begin{pmatrix} R_{21} \\ R_{22} \end{pmatrix}, \quad (3.4.12)$$

where

$$R_{21} = 0, \quad (3.4.13)$$

$$R_{22} = \frac{\partial\psi_1}{\partial x}\frac{\partial T_1}{\partial z} - \frac{\partial\psi_1}{\partial z}\frac{\partial T_1}{\partial x}. \quad (3.4.14)$$

The second order solution subject to the boundary condition (3.3.9) is given by

$$\psi_2 = 0, \quad (3.4.15)$$

$$\Big(\frac{\partial}{\partial\tau}-\nabla^2-R_i\Big)T_2 = (R_{22}). \quad (3.4.16)$$

Now, we compute the temperature fields having the frequency 2ω, and independent of fast time scale. Thus, second order temperature terms can be expressed in the following form:

$$T_2 = \{T_{20} + T_{22}e^{2i\omega t} + \overline{T}_{22}e^{-2i\omega t}\}sin(2\pi z), \quad (3.4.17)$$

where T_{22} and T_{20} are temperature fields having the terms with the frequency 2ω and independent of fast time scale, respectively. The solutions of the second order problems are

$$T_{20} = \frac{\pi a}{8\pi^2 - 2R_i}\{A(s)\overline{B}(s) + \overline{A}(s)B(s)\}, \quad (3.4.18)$$

and

$$T_{22} = \frac{\pi a}{8\pi^2 + 4i\omega - 2R_i}A(s)B(s). \quad (3.4.19)$$

The horizontally averaged Nusselt number, $Nu(s)$, for the oscillatory mode of convection is given by

$$Nu(s) = 1 + \Big[\chi^2\Big(\frac{\partial T_2}{\partial z}\Big)_{z=0}/\Big(\frac{dT_b}{dz}\Big)_{z=0}\Big]. \quad (3.4.20)$$

By using Eqs.(3.3.10), (3.4.17), (3.4.18) and (3.4.19), we can simplify Eq.(3.4.20) as

$$Nu(s) = 1+\Big(\frac{(c-R_i)4\pi^2}{8\pi^2-2R_i}+\frac{2\pi^2\sqrt{(c-R_i)^2+\omega^2}}{\sqrt{(8\pi^2-2R_i)^2+16\omega^2}}\Big)\Big(\frac{4\pi^2-R_i}{4\pi^2}\Big)\frac{\tan\sqrt{R_i}}{\sqrt{R_i}}|A(s)|^2. \quad (3.4.21)$$

It is clear that the gravity modulation is effective at third order, and affects $Nu(s)$ through $A(s)$, which is evaluated at third order.

At the **third order**, we have

$$\begin{pmatrix} \frac{1}{P_r}(\lambda_1\frac{\partial}{\partial\tau}+1)\frac{\partial}{\partial\tau}\nabla^2-(\lambda_2\frac{\partial}{\partial\tau}+1)\nabla^4 & R_0(\lambda_1\frac{\partial}{\partial\tau}+1)\frac{\partial}{\partial x} \\ -\frac{\partial}{\partial x}\frac{\partial T_b}{\partial z} & (\frac{\partial}{\partial\tau}-\nabla^2-R_i) \end{pmatrix}\begin{pmatrix}\psi_3\\ T_3\end{pmatrix}=\begin{pmatrix}R_{31}\\ R_{32}\end{pmatrix}, \quad (3.4.22)$$

where

$$R_{31} = \lambda_2\frac{\partial}{\partial s}\nabla^4\psi_1 - R_0\lambda_1\frac{\partial}{\partial s}\frac{\partial T_1}{\partial x} - (R_2+R_0\delta\cos(\Omega s))(\lambda_1\frac{\partial}{\partial\tau}+1)\frac{\partial T_1}{\partial x} - \quad (3.4.23)$$

$$\frac{1}{P_r}(\lambda_1\frac{\partial}{\partial\tau}+1)\frac{\partial}{\partial s}(\nabla^2\psi_1) - \frac{1}{P_r}\lambda_1\frac{\partial}{\partial s}(\frac{\partial}{\partial\tau}\nabla^2\psi_1),$$

$$R_{32} = \frac{\partial\psi_1}{\partial x}\frac{\partial T_2}{\partial z} - \frac{\partial T_1}{\partial s}. \quad (3.4.24)$$

Using first and second order solutions, the expressions of R_{31} and R_{32} are determined. Now, under the solvability condition for the existence of third order solution, one may derive the complex Ginzburg-Landau equation for finite amplitude convection.

$$\frac{dA(s)}{ds} - \gamma^{-1}F(s)A(s) + \gamma^{-1}k|A(s)|^2A(s) = 0, \quad (3.4.25)$$

where

$$\gamma = \Big[1-a\Delta_1R_2\lambda_1+\frac{c^2\Delta_1\lambda_2(c+i\omega-R_i)(4\pi^2-R_i)}{a4\pi^2}+\frac{c\Delta_1(c+i\omega-R_i)(1+2\lambda_1i\omega)(4\pi^2-R_i)}{aP_r4\pi^2}\Big],$$

$$F(s) = [a\Delta_1R_2(1+i\omega\lambda_1)(1+\delta\cos(\Omega s))], \quad \Delta_1 = \Big[\frac{aP_r}{i\omega c(1+\lambda_1i\omega)+(1+\lambda_2i\omega)c^2P_r}\Big] \text{ and}$$

$$k = \Big[\frac{(c-R_i)(c+i\omega-R_i)(4\pi^2-R_i)\pi^2}{16\pi^4} + \frac{[(c-R_i)^2+\omega^2](4\pi^2-R_i)^2\pi^2}{(8\pi^2-2R_i+4i\omega)16\pi^4}\Big].$$

Writing A(s) in the phase-amplitude form, we get

$$A(s) = |A(s)|e^{i\phi}. \tag{3.4.26}$$

Now, substituting Eq.(3.4.26) in Eq.(3.4.25), we get the following expression for the amplitude $|A(s)|$ as

$$\frac{d|A(s)|^2}{ds} - 2p_r|A(s)|^2 + 2l_r|A(s)|^4 = 0, \tag{3.4.27}$$

$$\frac{d(ph(A(s)))}{ds} = pi - li|A(s)|^2, \tag{3.4.28}$$

where $\gamma^{-1}F(s) = p_r + ip_i$, $\gamma^{-1}k = l_r + il_i$ and ph(.) represents the phase shift. The Eq.(3.4.27) solved numerically using the function NDSolve of Mathematica, subject to the suitable initial condition $A(0) = a_0$, where a_0 is the chosen initial amplitude of convection. In our computation, we assume $R_2 = R_0$ to keep the parameters to a minimum.

3.5 Bifurcation analysis

In this section, a study of dynamical behaviour of the Complex Ginzburg−Landau equation (3.4.25) and amplitude equation (3.4.27) is done. It is shown that the Complex Ginzburg−Landau equation (3.4.25) undergoes subcritical Hopf bifurcation and amplitude equation (3.4.27) undergoes Pitchfork bifurcation.

3.5.1 Hopf bifurcation

The complex Ginzburg−Landau equation (3.4.25) can be written as

$$\begin{cases} \frac{dx}{ds} = p_r x - p_i y - (l_r x - l_i y)(x^2+y^2), \\ \\ \frac{dy}{ds} = p_i x + p_r - (l_i x + l_r y)(x^2+y^2), \end{cases} \tag{3.5.1}$$

where $A(s) = x(s) + iy(s), p_r = Re\left[\frac{F(s)}{\gamma}\right], p_i = Im\left[\frac{F(s)}{\gamma}\right], l_r = Re\left[\frac{k}{\gamma}\right], l_i = Im\left[\frac{k}{\gamma}\right]$.

Clearly the origin is the equilibrium point of the system (3.5.1). The Jacobian matrix of the system (3.5.1) at the origin is

$$J = \begin{bmatrix} p_r & -p_i \\ p_i & p_r \end{bmatrix}.$$

The trace and determinant of the Jacobian matrix J is $tr(J) = 2p_r$ and $det(J) = p_r^2 + p_i^2 > 0$ respectively.

If $p_r < 0$, both eigenvalues of the Jacobian matrix J have negative real parts, and hence the origin is asymptotically stable. If $p_r > 0$, both eigenvalues of the Jacobian matrix J have positive real parts, and hence the origin is unstable. If $p_r = 0$, the eigenvalues of the Jacobian matrix are purely imaginary, therefore, by implicit function theorem a Hopf bifurcation occurs and a periodic orbit arises as the stability of origin changes. Here, we assume λ_1 as bifurcation parameter. We shall sketch the phase portrait diagram for the system (3.5.1).

We consider $P_r = 1, R_i = 1, \lambda_2 = 0.1, \delta = 0.3$ and $\Omega = 50$. If $\lambda_1 = 0.4$, then $p_r < 0$, and from the above discussion, the origin is asymptotically stable. From Figure 3.11, we can see that the origin is a stable focus, surrounded by an unstable unique limit cycle. If $\lambda_1 = 0.47$, then $p_r = 0$, and the origin is unstable focus, Figure 3.12. If $\lambda_1 = 0.5$, then $p_r > 0$, and from the above discussion, the origin is unstable. From Figure 3.13, we can see that origin is a focus. This is the subcritical Hopf bifurcation.

3.5.2 Pitchfork bifurcation

The system (3.4.27) can be written as

$$\frac{d|A(s)|}{ds} - p_r|A(s)| + l_r|A(s)|^3 = 0 \tag{3.5.2}$$

It is clear that the system (3.5.2) has three equilibrium points, $|A(s)| = 0$ for all value of p_r, l_r, and $|A(s)| = \pm\sqrt{\frac{p_r}{l_r}}$ for $p_r > 0, l_r > 0$, and the solution of the differential equation (3.5.2) is given by

$$|A(s)|^2 = \frac{A_0^2}{\frac{l_r}{p_r}A_0^2 + (1 - \frac{l_r}{p_r}A_0^2)e^{-2p_r s}}, p_r > 0, l_r > 0 \tag{3.5.3}$$

where A_0 is the initial value of the amplitude. From equation (3.5.3), we see that solution trajectories approach $|A(s)| = 0$ as $s \to -\infty$, grow towards $\sqrt{p_r/l_r}$ when $0 < A_0 < \sqrt{p_r/l_r}$ as $s \to \infty$, decrease towards $\sqrt{p_r/l_r}$ when $A_0 > \sqrt{p_r/l_r}$ as $s \to \infty$. Thus, if $p_r < 0$ then $A(s) = 0$ is the only equilibrium point which is stable. If $p_r = 0$ then origin is again the only equilibrium point, which is still stable but much more weakly. So, if $p_r > 0$ and $l_r > 0$ then $|A(s)| = 0$ is still an equilibrium point but now it becomes unstable, and two new stable equilibrium points appear on either side of $|A(s)| = 0$, symmetrically located at $|A(s)| = \pm\sqrt{p_r/l_r}$, Figure 3.14. This is called the supercritical pitchfork bifurcation. The pitchfork bifurcation diagram is shown in the Figure 3.15.

3.6 Results and Discussion

This chapter deals with the combined effect of internal-heating and gravity modulation on oscillatory convection in a viscoelastic fluid layer. A weakly non-linear stability analysis is performed. The effect of gravity modulation on the Rayleigh-Bénard system has been assumed to be of order of (χ^2). The values of δ are assumed to be in the interval $(0, 0.5)$. It is observed that the relation (3.4.11) leads to an interesting result that the oscillatory type of instability exists only when the relaxation parameter λ_1 is greater than the retardation parameter λ_2. From the relation (3.4.21), it can be seen that the value of Nu starts with 1, thus showing the conduction state initially, that is heat transfer across the fluid layer is taking place through conduction only when s is small. The value of Nu increases for intermediate values of s thus showing that convection is in progress, and finally when s is very large, the oscillatory state is achieved. The numerical value of Nu is obtained from the expression (3.4.21) by solving the amplitude equation (3.4.27).

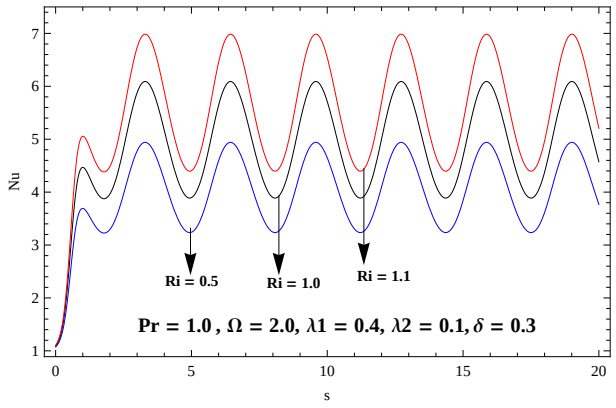

Figure 3.2: Effect of R_i on Nu for fixed other parameters

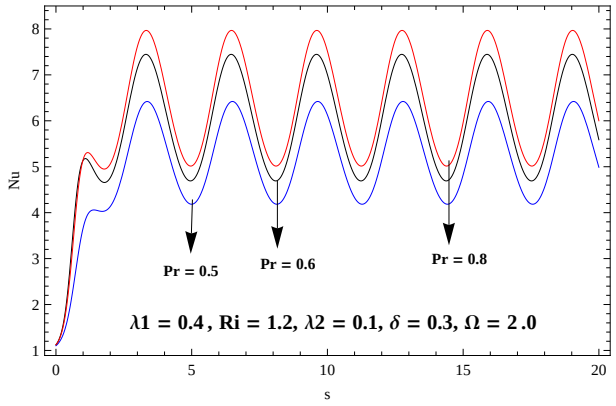

Figure 3.3: Effect of P_r on Nu for fixed other parameters

The combined effect of internal-heating and gravity modulation have been depicted in Figures 3.2-3.8, where Nu has been plotted with respect to the slow time s. From Figure 3.2, it can be see, that the effect of internal Rayleigh number on thermal instability is destabilizing, as Nu increases on increasing R_i, thus the heat transport is more for higher values of R_i. This confirms the results obtained by Bhadauria(2012). In Figure 3.3, it is found that as P_r increases, there is an increment in the heat transfer compatible with the results obtained by Bhadauria and kiran(2014b), thus the Prandtl number has a tendency to destabilize the system. Figure 3.4 indicates the effect of relaxation parameter λ_1 on oscillatory convection, and gives a destabilized system due to increasing heat transfer on

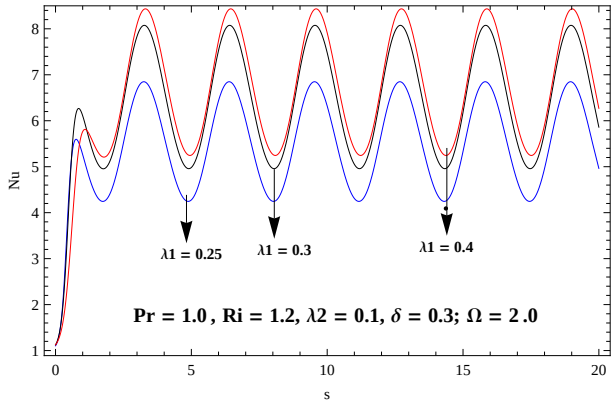

Figure 3.4: Effect of λ_1 on Nu for fixed other parameters

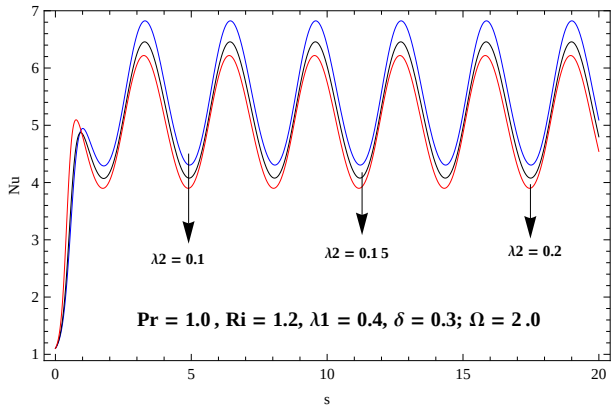

Figure 3.5: Effect of λ_2 on Nu for fixed other parameters

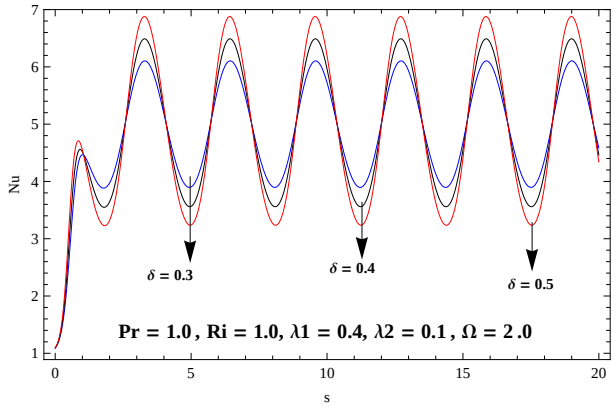

Figure 3.6: Effect of δ on Nu for fixed other parameters

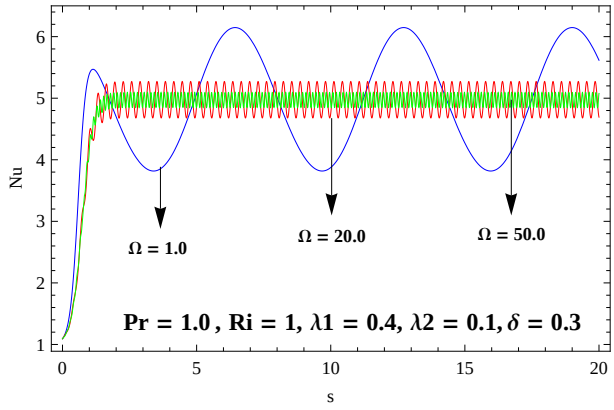

Figure 3.7: Effect of Ω on Nu for fixed other parameters

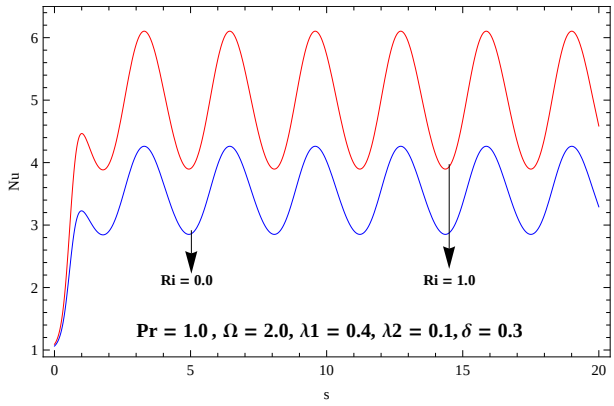

Figure 3.8: Comparison between internal and non-internal heating system

increasing λ_1. Further, the effect of retardation parameter, λ_2 is found to stabilize the system as the heat transfer decreases on increasing λ_2, given in Figure 3.5. The effects of the amplitude of modulation δ and frequency of modulation Ω on heat transport are given in Figures 3.6-3.7 respectively. In Figure 3.6, one can see that an increment in the amplitude of modulation increases the magnitude of Nu, thus enhances the heat transfer and advancing the onset of convection. An opposite effect is obtained in the case of frequency of modulation Ω as given in Figure 3.7. Hence, it is found that the effect of gravity modulation decreases as the frequency of modulation increases. The present result of internal heating has been compared with the results of non-internal heating in Figure 3.8. We observe that in the presence of internal heat source in the system, the value of Nu is more than that in the absence of internal-heating, i.e. the heat transport in the system is more

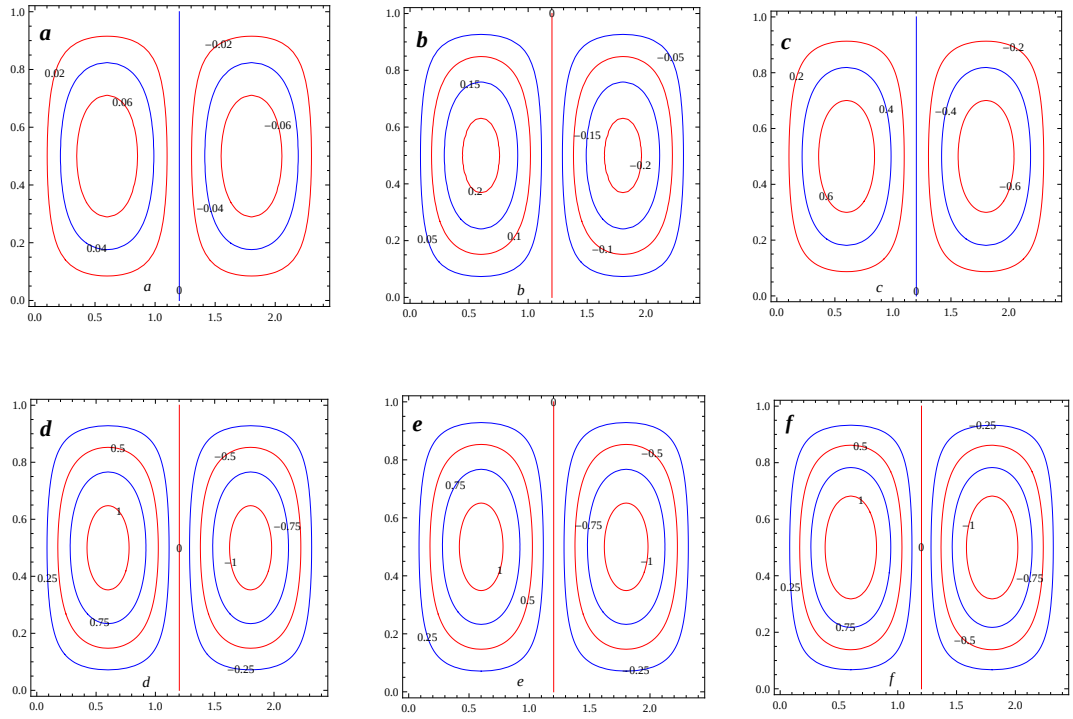

Figure 3.9: Streamlines at (a) $s = 0.0$, (b) $s = 0.4$, (c) $s = 0.8$, (d) $s = 1.0$, (e) $s = 1.2$, (f) $s = 1.5$

due to internal-heating. Thus, internal-heating advances the onset of convection, which is the same obtained by Bhadauria et al.(2013).

In Figures 3.9-3.10, the streamlines and corresponding isotherms are depicted respectively at $s = 0.0, 0.4, 0.8, 1.0, 1.2, 1.5$ for $\lambda_1 = 0.4, \lambda_2 = 0.1, \delta = 0.1, \Omega = 2, P_r = 1, \chi = 0.5$ and $R_i = 0.1$. From the figures, it is observed that initially when time is small, the magnitude of streamlines is also small, as given in Figure 3.9(a,b), and isotherms are straight, that is the system is in the conduction state, Figure 3.10(a,b). However, as time increases, the magnitude of streamlines increases and the isotherms lose their evenness Figures 3.9(c,d)-3.10(c,d). This shows that convection is taking place in the system. The system achieves the steady state beyond $s = 1.0$ as there is no further change in the streamlines and isotherms, Figures 3.9(e,f)-3.10(e,f).

It is also shown that the system represented by Landau equation (3.4.25) enters subcritical Hopf bifurcation as stress relaxation time λ_1 is taken as the bifurcation parameter.

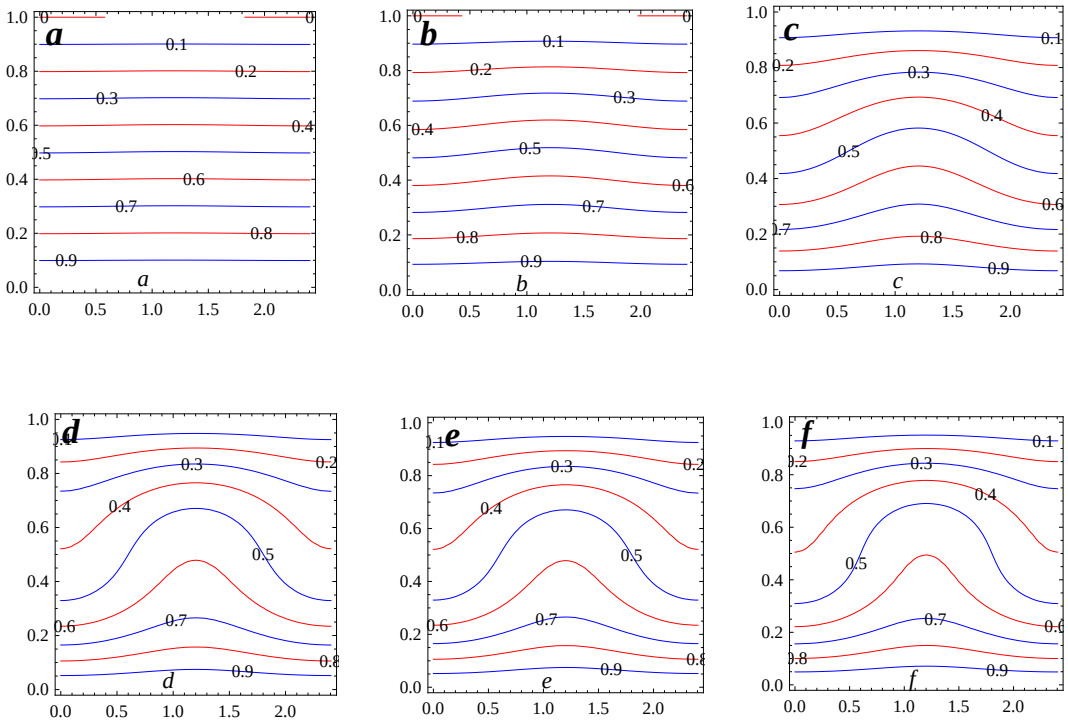

Figure 3.10: Isotherms at (a) $s = 0.0$, (b) $s = 0.4$, (c) $s = 0.8$, (d) $s = 1.0$, (e) $s = 1.2$, (f) $s = 1.5$

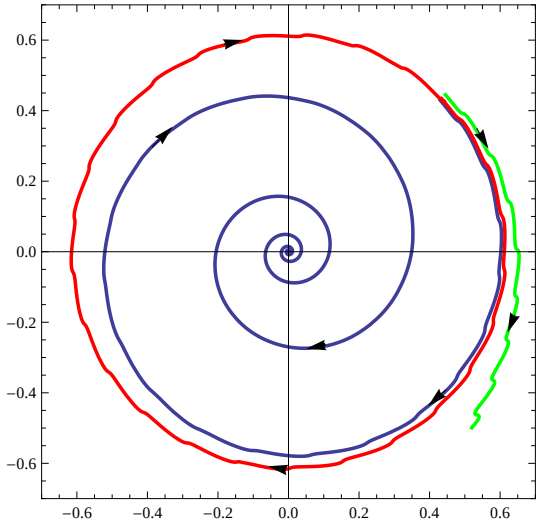

Figure 3.11: An unstable limit cycle (red) is created through Hopf bifurcation. The origin is asymptotically stable. $P_r = 1, R_i = 1, \lambda_1 = 0.4, \lambda_2 = 0.1, \delta = 0.3, \Omega = 50$

Thus, there exists a critical value of λ_1 such that if λ_1 is less than the critical value then the system is stable and if λ_1 is greater than the critical value then the system is unstable. The phase portrait diagrams for the subcritical Hopf bifurcation are shown in Figures

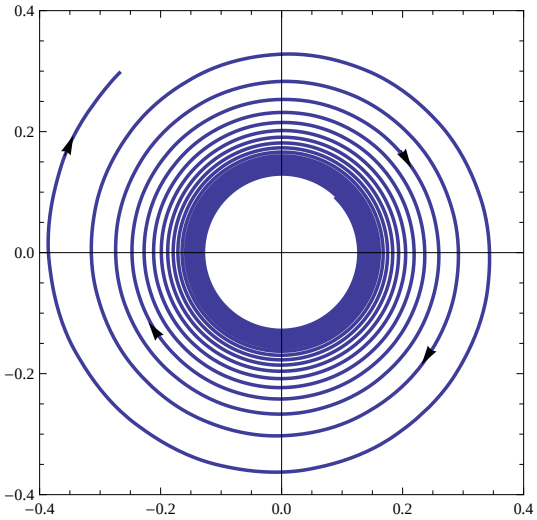

Figure 3.12: Hopf bifurcation diagram. $P_r = 1, R_i = 1, \lambda_1 = 0.47, \lambda_2 = 0.1, \delta = 0.3, \Omega = 50$

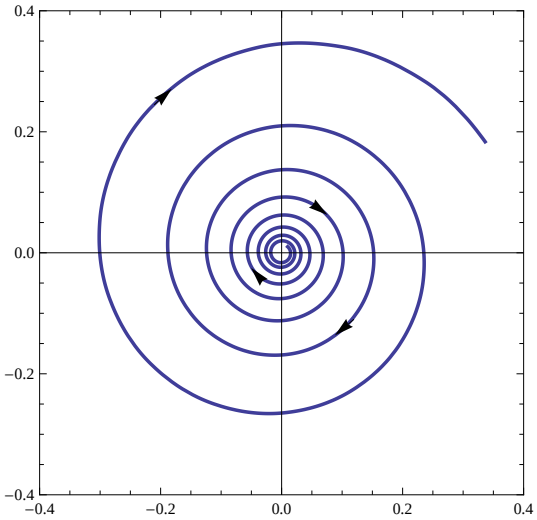

Figure 3.13: The origin is unstable. $P_r = 1, R_i = 1, \lambda_1 = 0.5, \lambda_2 = 0.1, \delta = 0.3, \Omega = 50$

3.11-3.13. The pitchfork bifurcation for the amplitude equation (3.4.27) on the parameter amplitude of gravity modulation δ is also discussed. The phase portrait diagram is shown in Figure 3.14. The supercritical Pitchfork bifurcation diagram in Figure 3.15 and subcritical Pitchfork bifurcation diagram in Figure 3.16 show that the system becomes unstable as δ increases.

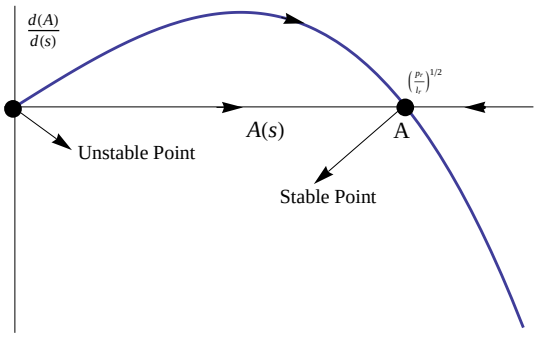

Figure 3.14: $P_r = 1, R_i = 1, \lambda_1 = 0.4, \lambda_2 = 0.1, a = 2.61411, \Omega = 1, s = 1000$

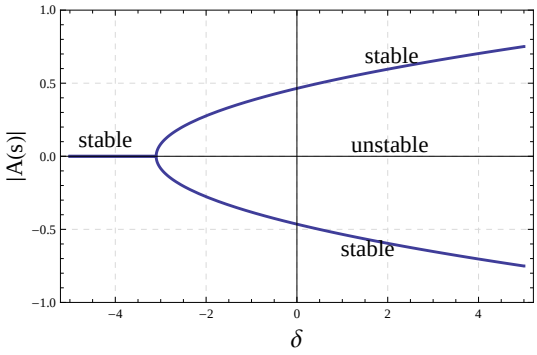

Figure 3.15: supercritical pitchfork bifurcation. $P_r = 1, R_i = 1, \lambda_1 = 0.5, \lambda_2 = 0.1, a = 2.61411, \Omega = 1, s = 2000$

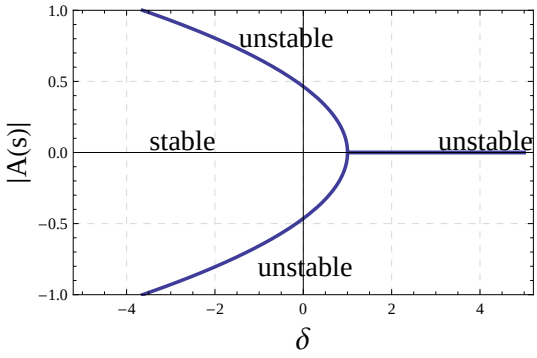

Figure 3.16: subcritical pitchfork bifurcation. $P_r = 1, R_i = 1, \lambda_1 = 0.5, \lambda_2 = 0.1, a = 2.61411, \Omega = 1, s = 2100$

3.7 Conclusions

Here, the combined effect of internal heating and gravity modulation on oscillatory convection in a viscoelastic fluid layer has been considered and a weakly non-linear stability analysis has been performed by using Ginzburg-Landau equation. The following conclusions are drawn:

a) Heat transport is more in the present case than in the absence of internal heating.

b) It is important that for the oscillatory convection the relaxation time λ_1 of fluid must be greater than the retardation time λ_2.

c) Effect of relaxation time λ_1 is to advance the onset of convection and hence enhances the heat transport.

d) Effect of retardation time λ_2 is to delay the onset of convection and hence decreases the heat transport.

e) An increment in the amplitude of modulation δ is to advance the onset of convection and thus increasing the heat transfer.

f) The frequency of modulation Ω is to decrease the heat transfer.

g) An increment in the value of Prandtl number P_r destabilizes the system, thus heat transfer increases.

h) The system is stable if relaxation time λ_1 is less than the critical point and becomes destabilized if the relaxation time λ_1 is greater than the critical point.

i) The system is destabilized as the amplitude of gravity modulation δ increases in bifurcation analysis.

Chapter 4

Throughflow and G-jitter effects on chaotic convection in an anisotropic porous medium

4.1 Introduction

In the previous chapters, the stationary and oscillatory convection has been studied using various physical models. In this chapter, we study convection in a porous medium system with chaotic analysis by employing trauncated Galerkin expansion method to obtained the Lorenz system.

The study of thermal instability in an anisotropic porous media plays very significant role in various fields, among them, in petroleum industry, chemical engineering, sedimentation and compaction. The problem with anisotropic porous medium has been studied in many researches, some of them are; Epherre(1977), Kvernvold and Tyvand(1979), Nisen and Storesletten(1990), Tyvand and Storesletten(1991). Alok et al.(2013), Bhadauria and

This chapter is based on the research article: Throughflow and G-jitter effects on chaotic convection in an anisotropic porous medium, published in AIN SHAMS J. (Elsevier-2017).

Kiran(2013) gave the model for anisotropic porous medium with variable viscosity.

Reza and Gupta(2012) investigated the effect of through flow on the onset of convection in a horizontal layer of electrically conducting fluid, confined between two rigid permeable boundaries, and heated from below, in the presence of a uniform vertical magnetic field. They found that magnetic field inhabits the onset of steady convection, and a positive throughflow is more stabilizing than negative throughflow. Nield and Kuznetsov(2010), Bhadauria and Kiran(2015) studied the effect of throughflow in porous medium for different models. The chaos model was proposed first of all by Poincaré(1890). In this model the author found that the dynamical system generated by the three body problem is quite sensitive to the initial conditions exhibiting chaotic behaviour. Later on, Edward Lorenz(1963) studied the system of three ordinary differential equations and developed the model for atmospheric convection. Vadász with his colleague Olek(1998-2000) presented a number of articles on the transition to chaotic behaviour in porous layer heated from below. Long et al.(2008) studied the chaotic convection of viscoelastic fluid in porous medium. Recently, Gupta and Singh(2013), Vadász(2014) and Bhadauria and Kiran(2015a, 2015b) studied chaotic convection in porous medium by using different physical model.

4.2 Mathematical structure of the problem

An infinitely extended horizontal anisotropic porous layer of depth d confined between two parallel planes is considered, the lower plane is at $z = 0$, while upper plane is at $z = d$. A Cartesian frame of reference is adopted in such a way that the origin lies on the lower plane and z axis is vertically upward. The porous layer is heated from below and cooled from the above. The physical configuration of the model is depicted in Figure 4.1. The Darcy law and Oberbeck-Boussinesq approximation is adopted to solve the model equations. The non-dimensionlized system of the model equations is obtain according as Alok et al.(2013), Gupta and Singh(2013)

$$\frac{1}{Va}\frac{\partial}{\partial t}(\nabla^2\psi) = -\nabla_\xi^2\psi - Ra(1+\delta sin(\Omega t))\frac{\partial T}{\partial x}, \tag{4.2.1}$$

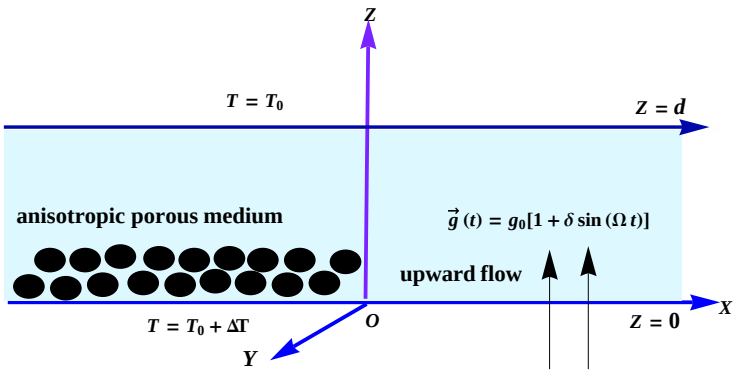

Figure 4.1: Physical configuration of the problem

$$-\frac{\partial\psi}{\partial x}\frac{\partial T_b}{\partial z}-\Big(\nabla_\eta^2-P_e\frac{\partial}{\partial z}\Big)T=-\frac{\partial T}{\partial t}+\frac{\partial(\psi,T)}{\partial(x,z)}, \tag{4.2.2}$$

where $Va=\frac{\phi\nu d^2}{K_z\kappa_{Tz}}$ Vadász number, $Ra=\frac{\alpha_T g_0\Delta T d K_z}{\nu\kappa_{Tz}}$ thermal Rayleigh number, $P_e=\frac{w_0 d}{\kappa_{Tz}}$ Péclet number, $(1+\delta sin(\Omega t))$ modulation term and other variables have their usual meanings as given in the nomenclature.

The externally imposed thermal boundary conditions are given by

$$T=\begin{cases} T_0+\Delta T, & \text{at} \quad z=0,\\ T_0, & \text{at} \quad z=d. \end{cases} \tag{4.2.3}$$

The basic state temperature (non-dimensionlized) present in Eq.(4.2.2) is obtained by using the above boundary condition Eq.(4.2.3) as Bhadauria and Kiran(2015)

$$T_b=\Big(\frac{e^{P_e z}-e^{P_e}}{1-e^{P_e}}\Big). \tag{4.2.4}$$

4.3 Method of solution

The solution of nonlinear Eqs.(4.2.1) and (4.2.2) are obtained by using truncated Galerkin expansion method. The stream function and temperature field are taken in the forms as

mentioned in Vadász(2014)

$$\psi = A_{11} \sin\left(\frac{\pi x}{L}\right) \sin(\pi z), \tag{4.3.1}$$

$$T = T_b + B_{11} \cos\left(\frac{\pi x}{L}\right) \sin(\pi z) + B_{02} \sin(2\pi z). \tag{4.3.2}$$

Using Eqs.(4.3.1) and (4.3.2) in to Eqs.(4.2.1) and (4.2.2), multiplying the equations by orthogonal eigenfunctions corresponding to Eqs.(4.3.1) and (4.3.2), and then integrating them over the spatial domain, yield a set of three differential equations for the time evolution of the amplitudes, in the form of

$$\frac{dA_{11}}{d\tau} = -\frac{V_a \gamma}{\pi^2}\left(\frac{Ra}{\pi\theta}(1 + \delta \sin(\Omega\tau))B_{11} + \zeta A_{11}\right), \tag{4.3.3}$$

$$\frac{dB_{11}}{d\tau} = -\frac{1}{\pi\theta}\left(\frac{4\pi^2}{P_e^2 + 4\pi^2}\right)A_{11} - \frac{1}{\theta}A_{11}B_{02} - \chi B_{11}, \tag{4.3.4}$$

$$\frac{dB_{02}}{d\tau} = \frac{1}{2\theta}A_{11}B_{11} - 4\gamma B_{02}, \tag{4.3.5}$$

where the time has been re-scaled and the following notations are introduce.

$$\tau = \frac{(L^2+1)\pi^2}{L^2}t, \theta = \frac{L^2+1}{L}, \gamma = \frac{L^2}{L^2+1}, \Omega = \frac{L^2}{(L^2+1)\pi^2}\Omega, \sigma = \frac{V_a\gamma}{\pi^2} \text{ and } R = \frac{Ra}{\pi^2\theta^2},$$
$$\chi_1 = \frac{\eta + L^2}{L^2}, \zeta = \frac{(L^2/\xi)+1}{L^2}.$$

Again re-scale the amplitude in the form of

$$X = -\frac{\sqrt{\zeta}A_{11}}{2\theta\sqrt{2\gamma(R-\zeta\chi_1)}}, Y = \frac{\pi R B_{11}}{2\sqrt{2\gamma\zeta(R-\zeta\chi_1)}} \text{ and } Z = -\frac{\pi R B_{02}}{(R-\zeta\chi_1)}.$$

The following set of equations is obtained

$$\begin{cases} \frac{dX}{d\tau} = \sigma\zeta((1+\delta\sin(\Omega\tau))Y - X), \\ \frac{dY}{d\tau} = \frac{1}{\zeta}\Big(R\big(\frac{4\pi^2}{P_e^2+4\pi^2}\big)X - \zeta\chi_1 Y - (R-\zeta\chi_1)XZ\Big), \\ \frac{dZ}{d\tau} = 4\gamma(XY - Z). \end{cases} \tag{4.3.6}$$

If the amplitude of gravity modulation $\delta = 0$ and $P_e = 0$, then the system (4.3.6) reduces into Gupta and Singh(2013) model as

$$\begin{cases} \frac{dX}{d\tau} = \sigma\zeta(Y - X), \\ \frac{dY}{d\tau} = \frac{1}{\zeta}(RX - \zeta\chi_1 Y - (R-\zeta\chi_1)XZ), \\ \frac{dZ}{d\tau} = 4\gamma(XY - Z). \end{cases} \tag{4.3.7}$$

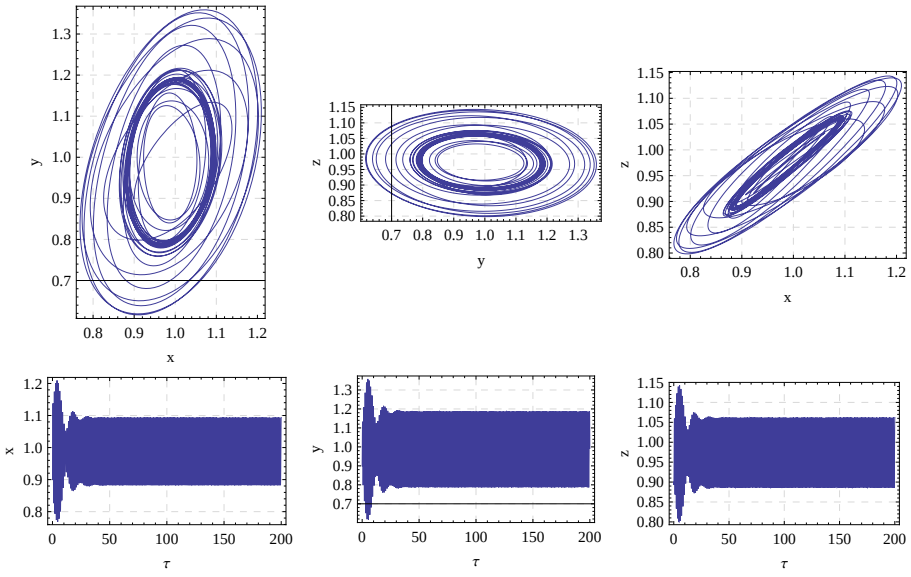

Figure 4.2: Phase portrait and time domain diagrams for the system (4.3.6) with parameters $R = 5$ and $\zeta = 0.4$, $\chi_1 = 0.4$, $P_e = 1.0$, $\delta = 0.1$, $\Omega = 5$

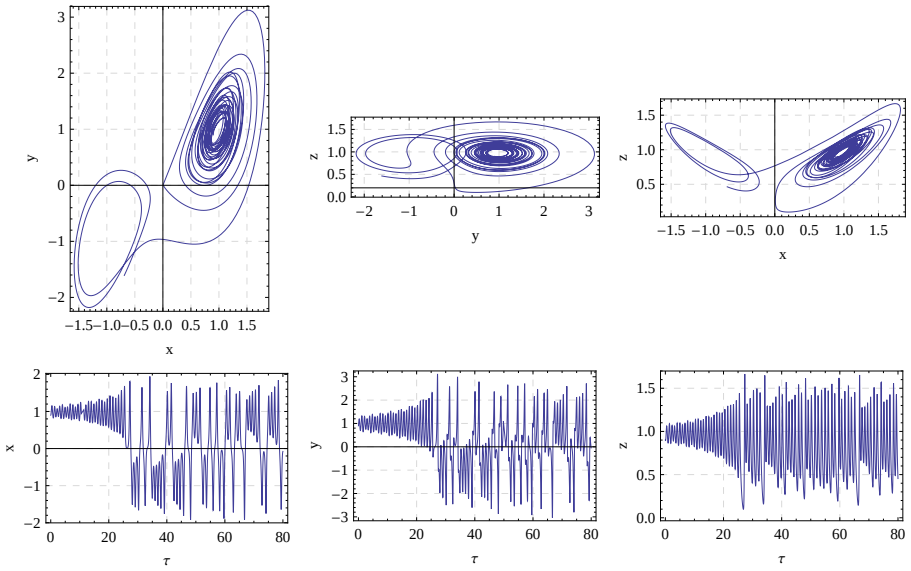

Figure 4.3: Phase portrait and time domain diagrams for the system (4.3.6) with parameters $R = 8.5$ and $\zeta = 0.4$, $\chi_1 = 0.4$, $P_e = 1.0$, $\delta = 0.1$, $\Omega = 5$

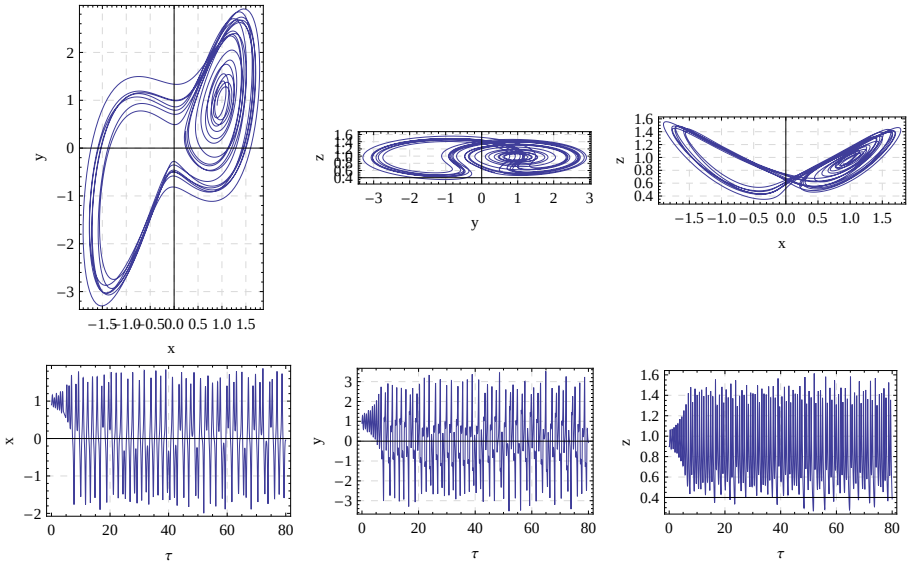

Figure 4.4: Phase portrait and time domain diagrams for the system (4.3.6) with parameters $R = 15$ and $\zeta = 0.4$, $\chi_1 = 0.4$, $P_e = 1.0$, $\delta = 0.1$, $\Omega = 5$

4.4 Results and Discussion

MATHEMATICA 7.0 has been used for the numerical simulation of the Lorenz system (4.3.6). In this simulation, we considered the initial conditions $\tau = 0 : X = Y = Z = 0.9$ and fixed the parameters $\sigma = 10, \gamma = 0.5$. The parameters $R, P_e, \delta, \Omega, \chi_1, \zeta$ are considered

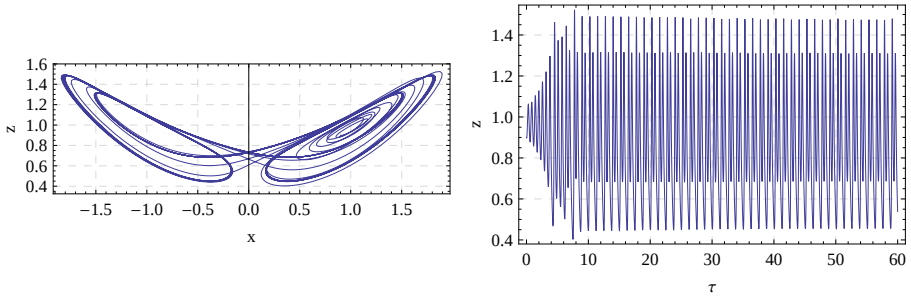

Figure 4.5: Phase portrait and time domain diagrams for the system (4.3.6) with parameters $R = 23$ and $\zeta = 0.4$, $\chi_1 = 0.4$, $P_e = 1.0$, $\delta = 0.1$, $\Omega = 5$

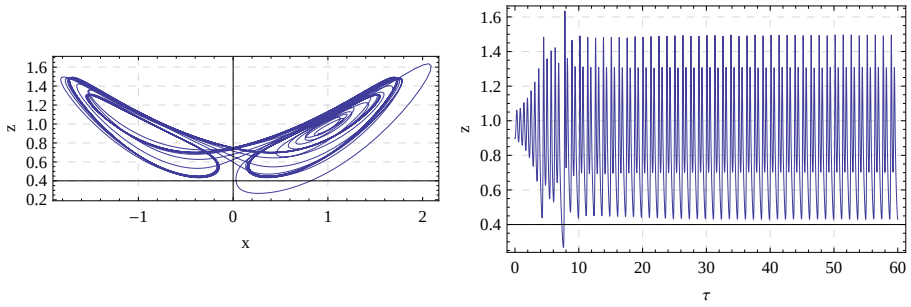

Figure 4.6: Phase portrait and time domain diagrams for the system (4.3.6) with parameters $R = 24$ and $\zeta = 0.4$, $\chi_1 = 0.4$, $P_e = 1.0$, $\delta = 0.1$, $\Omega = 5$

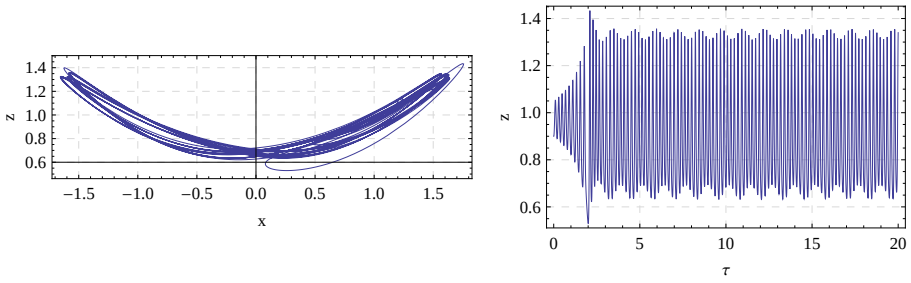

Figure 4.7: Phase portrait and time domain diagrams for the system (4.3.6) with parameters $R = 200$ and $\zeta = 0.4$, $\chi_1 = 0.4$, $P_e = 1.0$, $\delta = 0.1$, $\Omega = 5$

as variables to examine the behaviour of modulated chaotic system. The phase-portrait diagrams depict how modulation term affects the dynamics of the thermal convection for a combination of varied parameters. The results are further depicted in Figures 4.2-4.26 to analyse the Lorenz model by using phase-portrait and time domain diagrams.

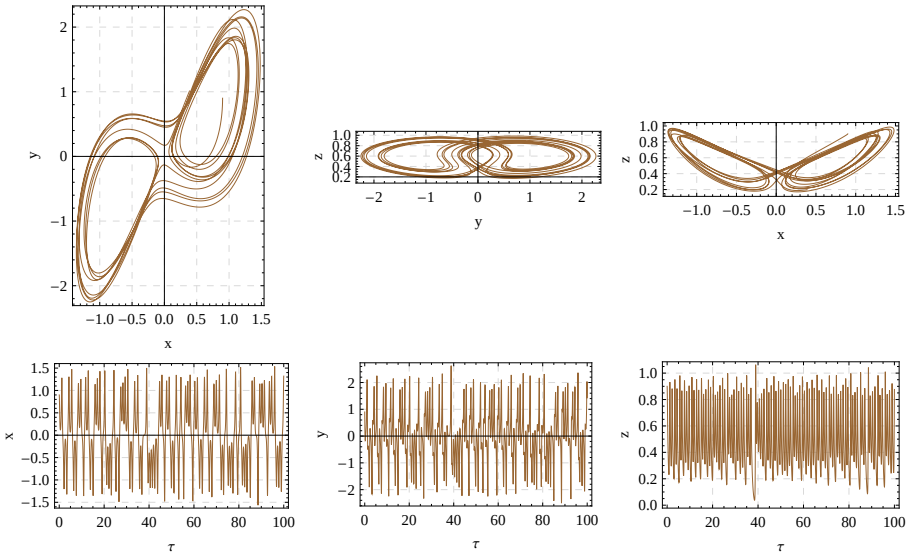

Figure 4.8: Phase portrait and time domain diagrams for the system (4.3.6) with parameters P_e =5 and ζ= 0.4, χ_1 = 0.4, R=15, δ = 0.1, Ω = 5

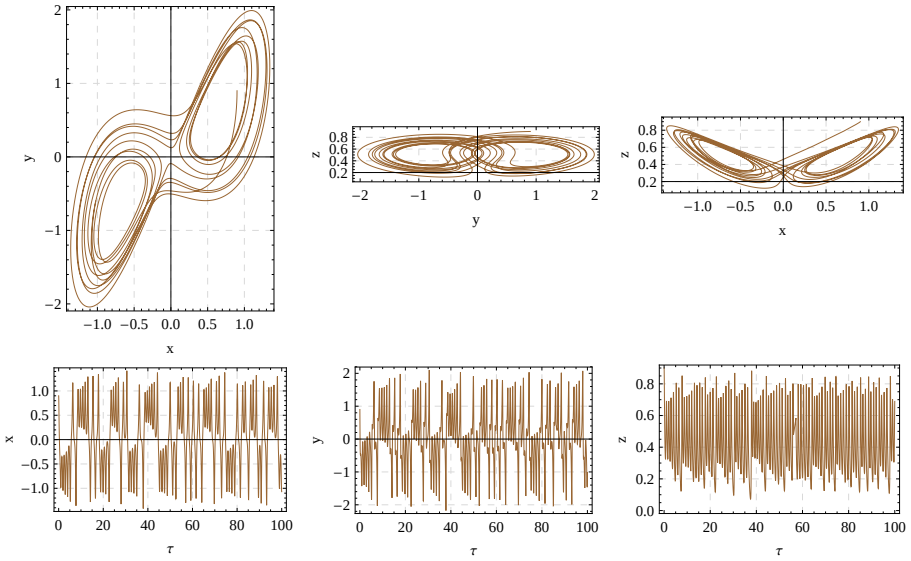

Figure 4.9: Phase portrait and time domain diagrams for the system (4.3.6) with parameters P_e =6 and ζ= 0.4, χ_1 = 0.4, R=15, δ = 0.1, Ω = 5

The effects of scaled Rayleigh number R on the system are depicted in Figures 4.2-4.7, keeping fixed the other parameters. Figure 4.2 shows a periodic solution (R = 5) and for (R = 8.5) system moves from periodic to weak chaotic solution in Figure 4.3. Figure 4.4 (R = 15) depicts a chaotic behaviour or aperiodic solution of the Lorenz system which shows that heat transfer is more in this case in comparison to previous two case. Further in Figures

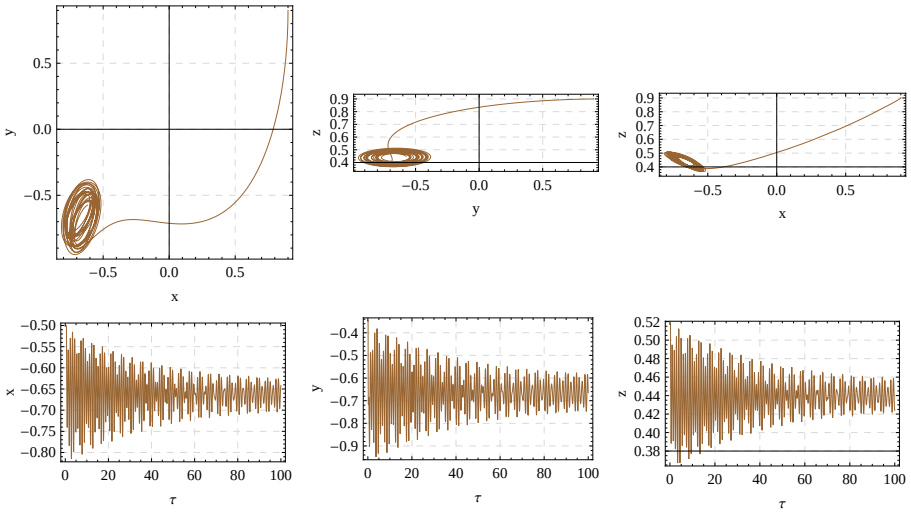

Figure 4.10: Phase portrait and time domain diagrams for the system (4.3.6) with parameters P_e =7 and ζ= 0.4, $\chi_1 = 0.4$, R=15, $\delta = 0.1$, $\Omega = 5$

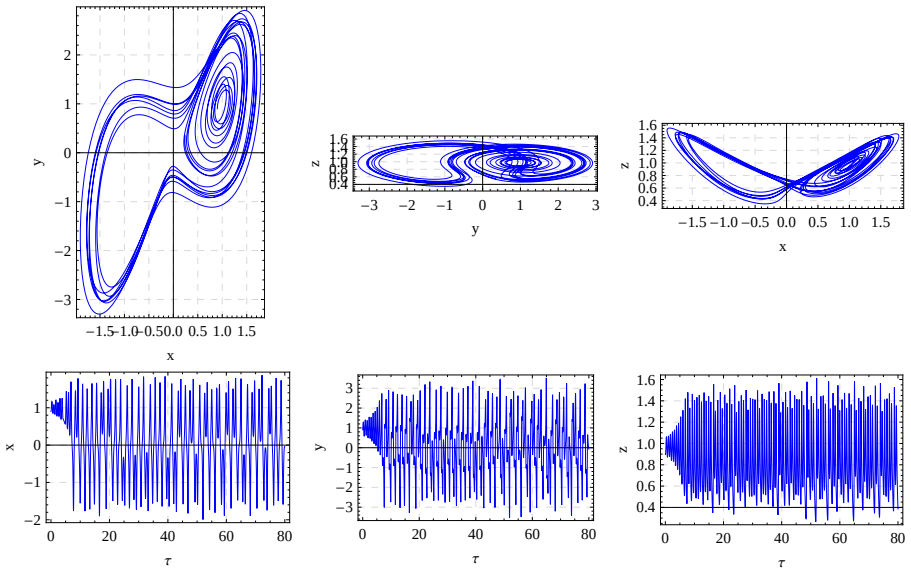

Figure 4.11: Phase portrait and time domain diagrams for the system (4.3.6) with parameters ζ= 0.4 and P_e =1, $\chi_1 = 0.4$, R=15, $\delta = 0.1$, $\Omega = 5$

(4.5, 4.6) system shows periodic solution for $(R = 23, R = 24)$ respectively. On increasing the higher value of $R > 100$ system always shows periodic solution depicts in Figure 4.7. Hence, we conclude that the system has either periodic or chaotic behaviour depending upon the value of scaled Rayleigh number which agrees with the results obtained by Long et al.(2008). The impact of Péclet number P_e on the system, for different parametric values $P_e = 5, 6, 7$, keeping fixed the other parameters, is depicted in Figures (4.8, 4.9, 4.10),

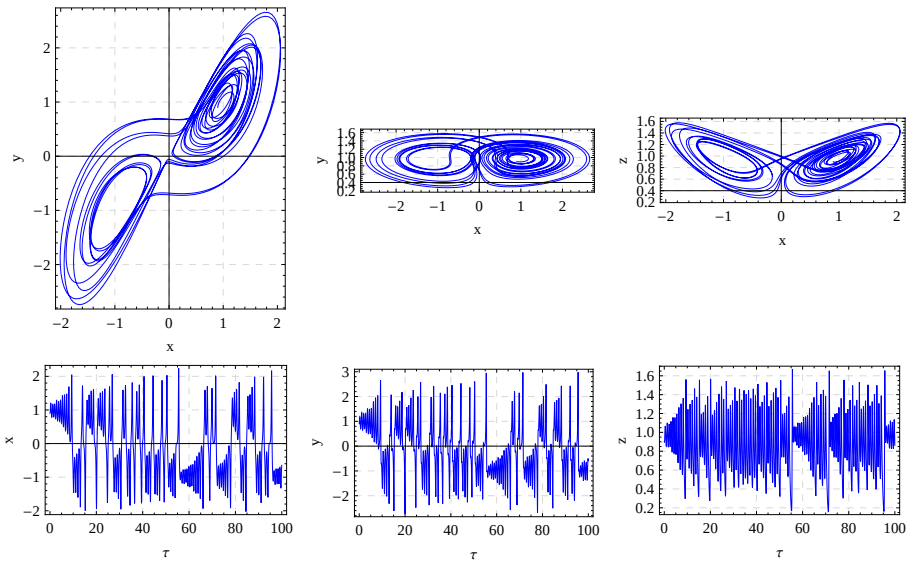

Figure 4.12: Phase portrait and time domain diagrams for the system (4.3.6) with parameters ζ= 0.7 and P_e =1, $\chi_1 = 0.4$, R=15, $\delta = 0.1$, $\Omega = 5$

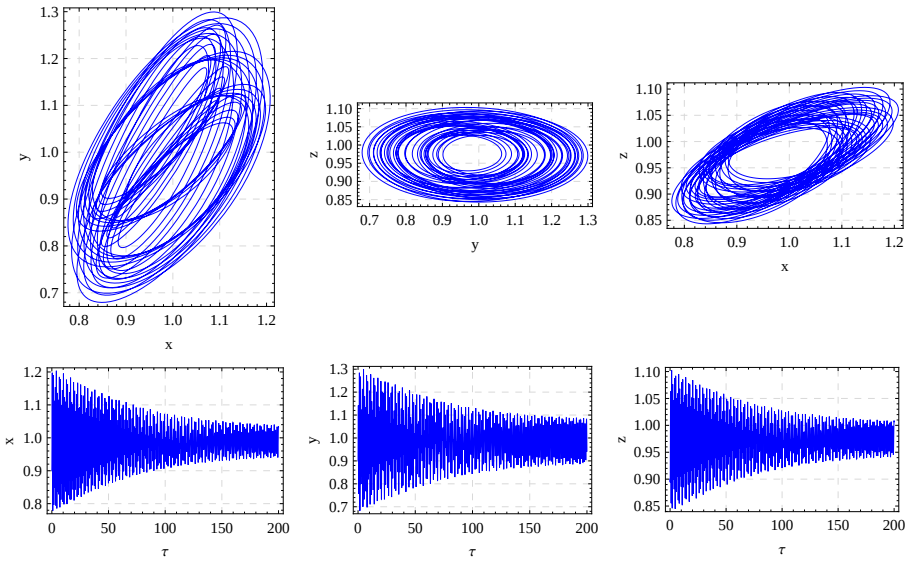

Figure 4.13: Phase portrait and time domain diagrams for the system (4.3.6) with parameters ζ= 0.9 and P_e =1, $\chi_1 = 0.4$, R=15, $\delta = 0.1$, $\Omega = 5$

respectively. From these Figs. it is observed that system transition from chaos to periodic i.e. heat transfer level down on increasing the value P_e, clear from the diagrams.

Figures (4.11, 4.12, 4.13) depict the effects of different values of scaled mechanical anisotropic parameter $\zeta = 0.4, 0.7, 0.9$, keeping fixed the other parameters. The phase-

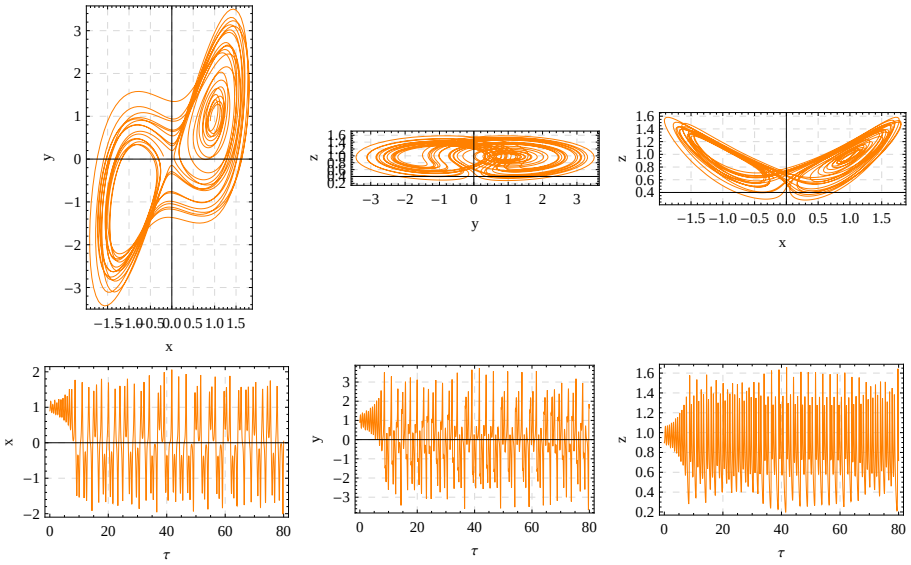

Figure 4.14: Phase portrait and time domain diagrams for the system (4.3.6) with parameters $\chi_1 = 0.5$ and P_e =1, ζ= 0.4, R=15, $\delta = 0.1$, $\Omega = 5$

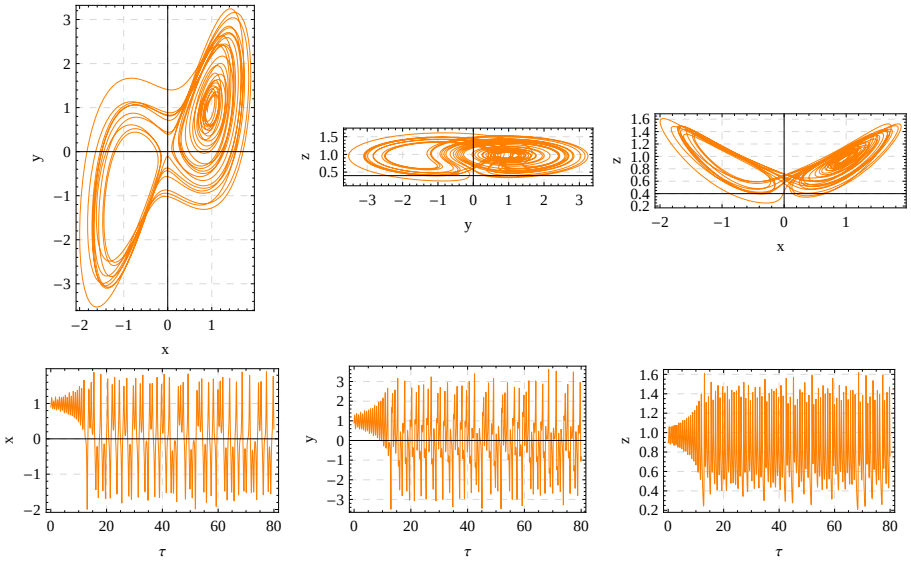

Figure 4.15: Phase portrait and time domain diagrams for the system (4.3.6) with parameters $\chi_1 = 0.7$ and P_e =1, ζ= 0.4, R=15, $\delta = 0.1$, $\Omega = 5$

portrait diagrams and time domain solutions show that the system has chaotic nature for $\zeta = 0.4$ and $= 0.7$, while the system shows a periodic nature for $\zeta = 0.9$. Thus, the system returns to periodic solution from the chaotic solution as ζ increases, and so, mechanical anisotropic parameter ζ delays the heat transfer. Effects of another anisotropic parameter χ_1 on the system are depicted in Figures (4.14, 4.15, 4.16) for $\chi_1 = 0.5, 0.7, 0.9$ respectively.

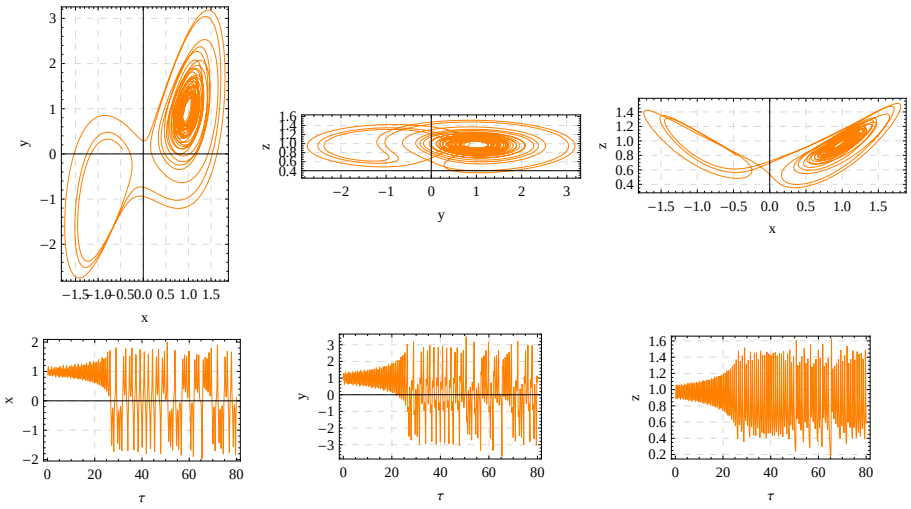

Figure 4.16: Phase portrait and time domain diagrams for the system (4.3.6) with parameters $\chi_1 = 0.9$ and P_e =1, ζ= 0.4, R=15, $\delta = 0.1$, $\Omega = 5$

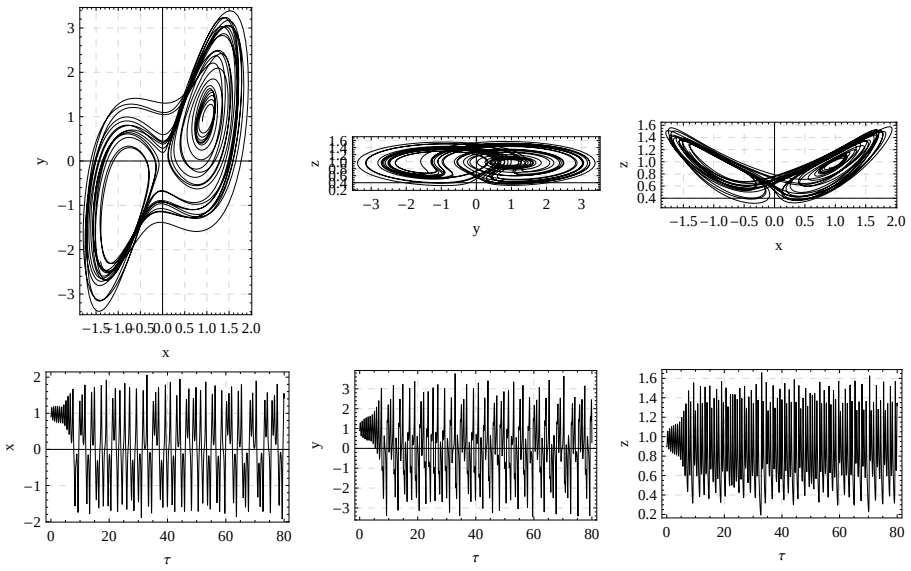

Figure 4.17: Phase portrait and time domain diagrams for the system (4.3.6) with parameters $\Omega = 10$ and P_e =1, ζ= 0.4, R=15, $\delta = 0.1$, $\chi_1 = 0.4$

It is evident from the time domain solution, heat transfer decreases, finally system tends to periodic behaviour on increasing χ_1 compatible with the result of Gupta and Singh(2013).

The effect of frequency of gravity modulation, Ω, is depicted in Figures (4.17, 4.18, 4.19)

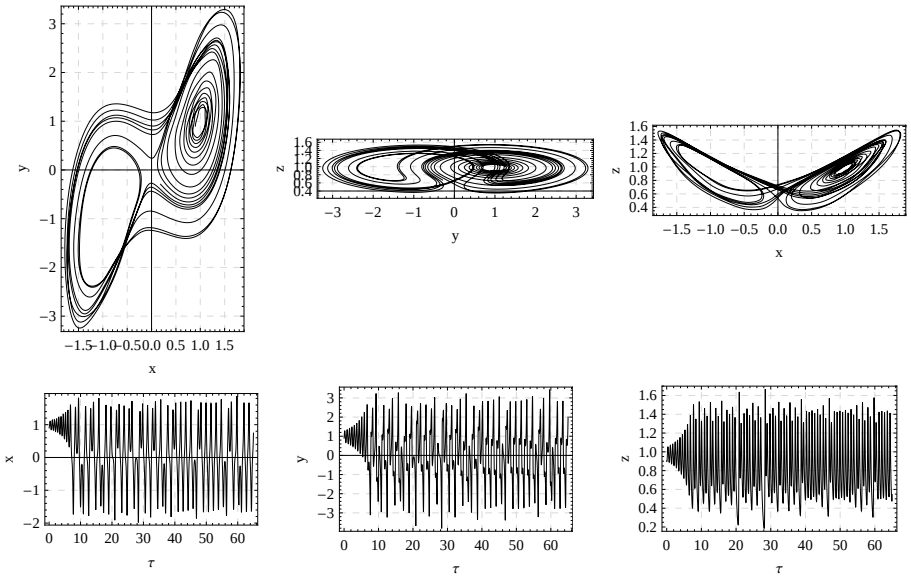

Figure 4.18: Phase portrait and time domain diagrams for the system (4.3.6) with parameters $\Omega = 40$ and P_e =1, ζ= 0.4, R=15, $\delta = 0.1$, $\chi_1 = 0.4$

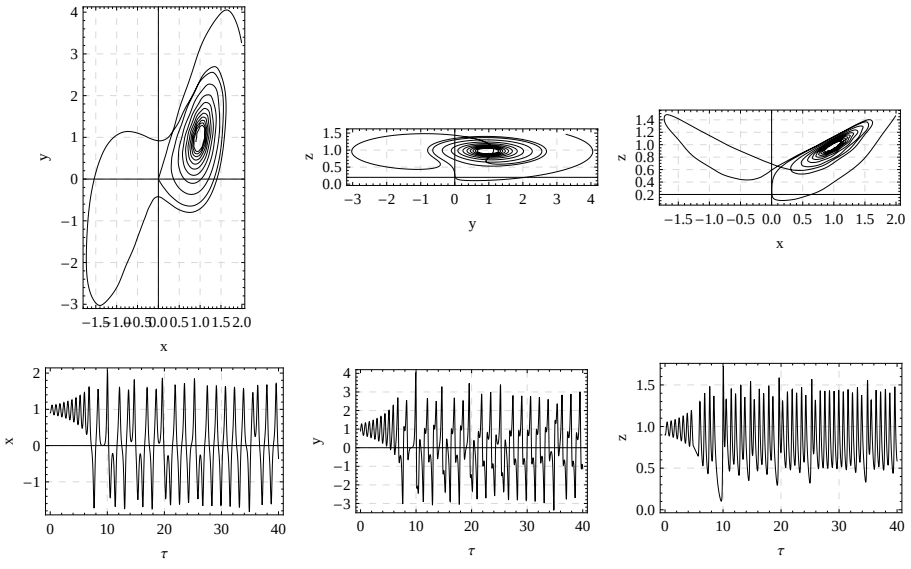

Figure 4.19: Phase portrait and time domain diagrams for the system (4.3.6) with parameters $\Omega = 80$ and P_e =1, ζ= 0.4, R=15, $\delta = 0.1$, $\chi_1 = 0.4$

for $\Omega = 10, 40, 80$, keeping fixed other parameters. In this case, the system looses its chaotic behaviour and shifts into periodic behaviour, and so, heat transfer delays the convection. The impact of amplitude of gravity modulation δ on the system for different parametric

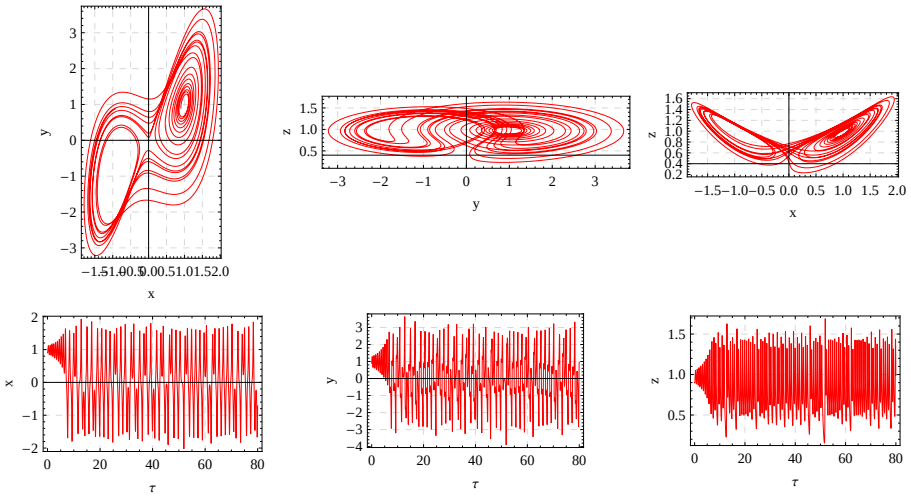

Figure 4.20: Phase portrait and time domain diagrams for the system (4.3.6) with parameters $\delta = 0.01$ and P_e =1, ζ= 0.4, R=15, $\Omega = 5$, $\chi_1 = 0.4$

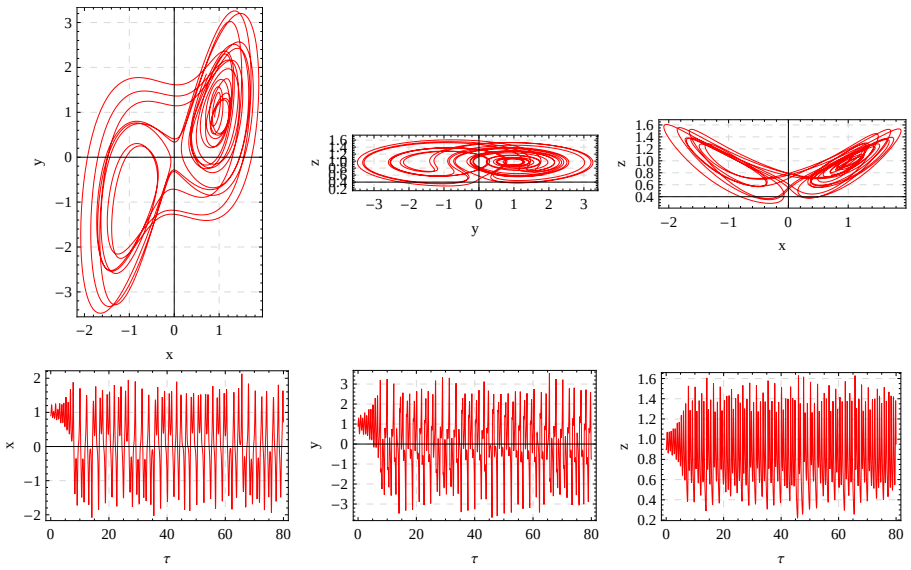

Figure 4.21: Phase portrait and time domain diagrams for the system (4.3.6) with parameters $\delta = 0.2$ and P_e =1, ζ= 0.4, R=15, $\Omega = 5$, $\chi_1 = 0.4$

values $\delta = 0.01, 0.2, 0.4$ keeping fixed the other parameters, is depicted in Figures (4.20, 4.21, 4.22), respectively. These figures depict that the trajectories are much disturbed on increasing δ. Therefore, the chaotic behaviour advances, that is, the heat transfer is increases gradually.

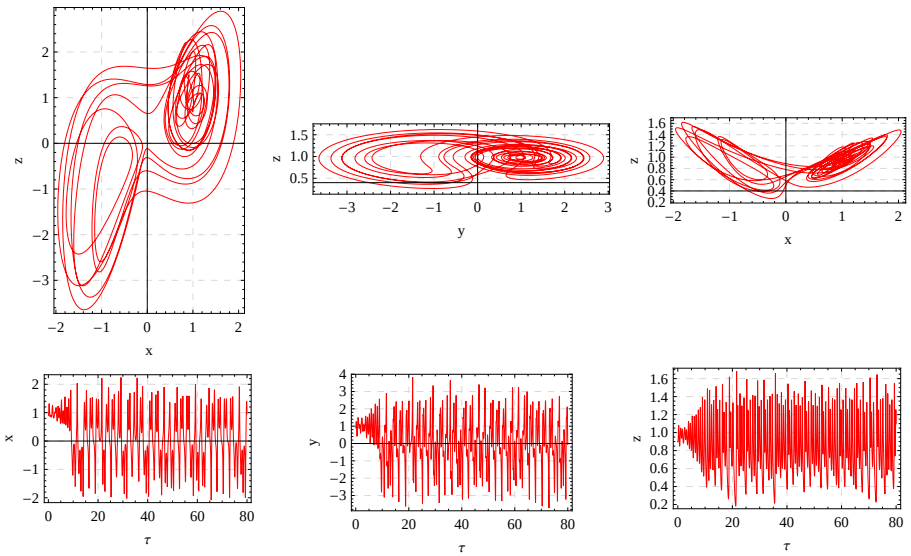

Figure 4.22: Phase portrait and time domain diagrams for the system (4.3.6) with parameters $\delta = 0.4$ and P_e =1, ζ= 0.4, R=15, $\Omega = 5$, $\chi_1 = 0.4$

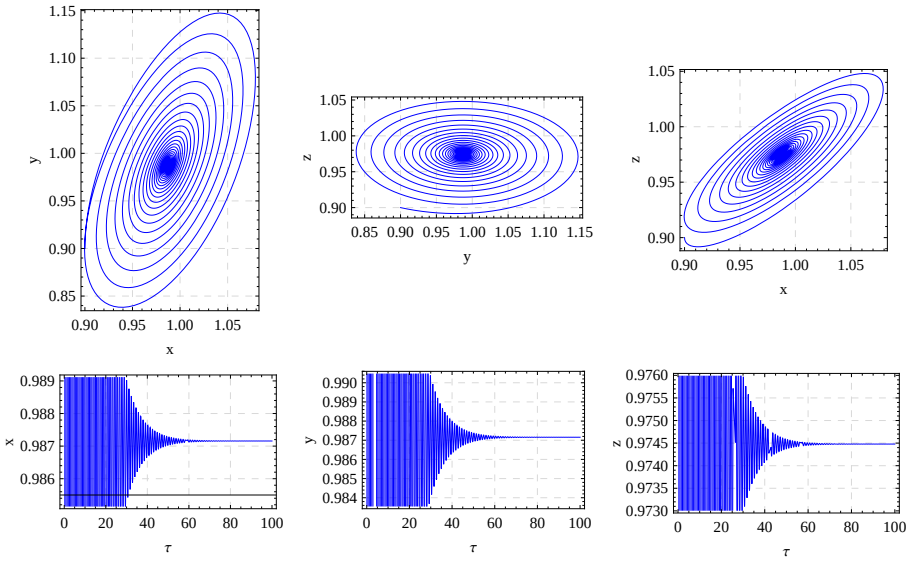

Figure 4.23: Phase portrait and time domain diagrams for the system (4.3.6) with parameters $\delta = 0.0$ and P_e =1, ζ= 0.4, R=5, $\Omega = 5$, $\chi_1 = 0.4$

Further, we compare the result of gravity modulated and unmodulated systems. For $\delta = 0, R = 5$ and fixed the other parameters, the Figure 4.23 shows a stable solution, while for $\delta = 0.1, R = 5$, the system has periodic solution, as depicted in Figure 4.24. It is noticed

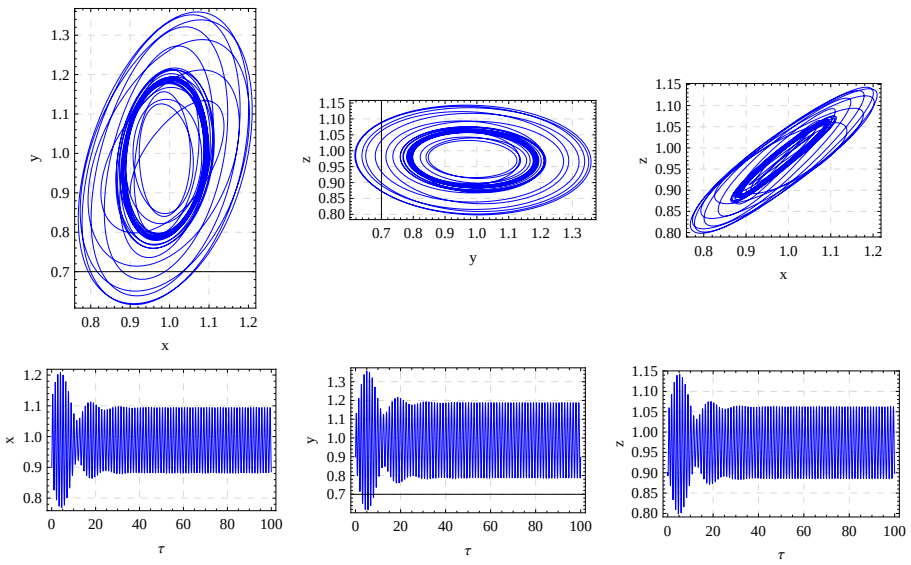

Figure 4.24: Phase portrait and time domain diagrams for the system (4.3.6) with parameters $\delta = 0.1$ and P_e =1, ζ= 0.4, R=5, $\Omega = 5$, $\chi_1 = 0.4$

that in gravity modulated system heat transfer is more in comparison to unmodulated system. Lastly, a comparison between the present results and the results already obtained by Gupta and Singh(2013) is depicted in Figure 4.25. In Figure 4.25, all the trajectories are moving into fixed point and time domain solution shows a stable solution for given parametric values. On the other hand, all the trajectories are much disturbed in Figure 4.26 due to presence of the modulation term δ, and time domain solution depicted a periodic system, hence the heat transfer is more in modulated system.

4.5 Conclusions

In this chapter, throughflow and G-jitter effects on chaotic convection in an anisotropic porous medium are studied. The adopted model is first reduced into Lorenz system by employing trauncated Galerkin expansion method. By using phase portrait and time domain diagrams the following findings are made

a) The effect of scaled Rayleigh number R is to either increase(chaotic) or de-

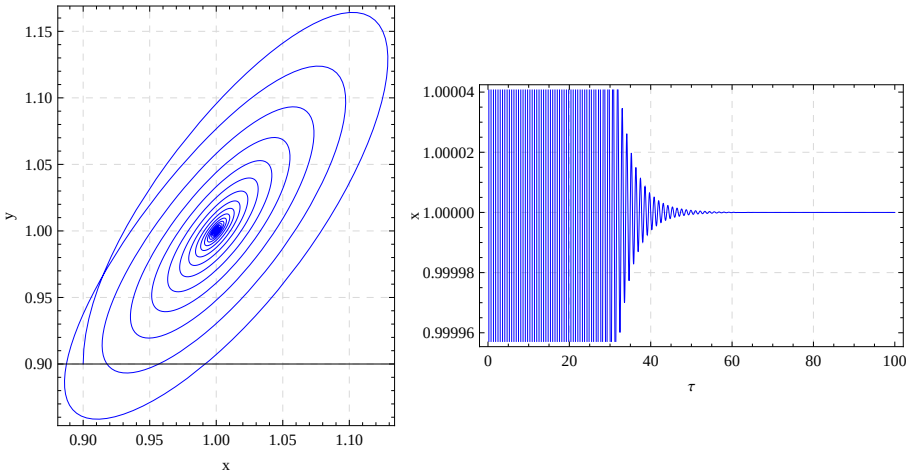

Figure 4.25: Phase portrait and time domain diagrams for the system (4.3.6) with parameters $\delta = 0.0$ and ζ= 1.5, R=16, $\chi_1 = 0.6$, $\sigma = 5$

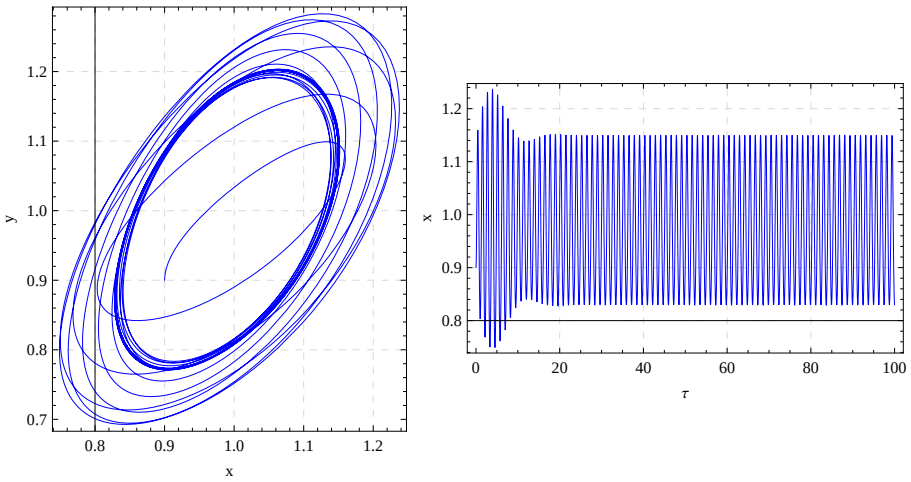

Figure 4.26: Phase portrait and time domain diagrams for the system (4.3.6) with parameters $\delta = 0.1$ and P_e =1, ζ= 1.5, R=16, $\Omega = 5$, $\chi_1 = 0.6$, $\sigma = 5$

crease(periodic) the heat transport in the Lorenz system.

b) The throughflow parameter P_e is to delay the chaotic convection i.e. heat transfer decreases in the system.

c) The amplitude δ (frequency Ω) of modulation is to advance (delay) the heat transfer in the Lorenz system.

d) The anisotropic parameters χ_1 and ζ has tendency to delay the chaotic behaviour in the system.

e) Finally, it is found that heat transfer is more in modulated system in comparison to the unmodulated system.

Chapter 5

Oscillatory and chaotic convection in a couple-stress fluid saturated rotating porous medium under temperature modulation

5.1 Introduction

In the previous chapters, onset of convection and heat transfer has been studied under gravity modulation considering various models. Therefore, in this chapter a study has been done under thermal modulation.

Some studies on the onset of convection in a rotating porous medium have been done by-Friedrich(1983), Palm and Tyvand(1984), Straughan(2001), Govender(2003) and Bhadauria(2007). Stability analysis under temperature/gravity-modulated for stationary Rayleigh-Bénard convection in a rotating porous medium is done by Bhadauria and Kumar(2012).

This chapter is based on the research article: Oscillatory and chaotic convection in a couple-stress fluid saturated rotating porous medium under temperature modulation, communicated.

Recently Bhadauria and Kiran(2016) studied oscillatory convection in a rotating fluid layer under temperature modulation and shown the effect of each convective parameters on the system by computing the Nusselt number.

Couple-stress fluid is a kind of non-Newtonian fluid having polar effects. The applications of couple-stress fluid is in the study of mechanisms of lubrication of synovial joints. The synovial fluid has been modelled as a couple-stress fluid in human joints by Walicki and Walicki(1999). Moreover, applications of couple-stress fluids in various fields named some as, industrial sciences, solidification of liquid crystals, cooling of metallic plate in a bath etc. Firstly, Stokes(1966) proposed the model for couple-stress fluid and found that the rotational field is defined in terms of velocity field itself and the stress tensor is no longer symmetric. In the literature, many study are available on couple-stress fluid, some of them are Sunil et al.(2004), Malashetty et al.(2005, 2006), Shivakumara et al.(2011). Recently, Gupta et al.(2016a) studied heat and mass transport in a couple-stress liquid under G-jitter. The stability of a convective system can be controlled by adjusting the modulation parameter like amplitude and frequency. Thus, in the present model, temperature modulation is considered as an external regulation. The effect of temperature modulation has been studied by many authors some of them are; Venezian(1969) was the first who considered temperature modulation in a viscous fluid layer, Caltagirone(1976) studied thermal instability in a horizontal porous layer with temperature modulation, Chhuon and Caltagirone(1979), Malashetty and Wadi(1999), Bhadauria and kiran(2013, 2014a) found that amplitude of modulation destabilizes the system whereas frequency of modulation stabilizes the system.

The study of chaotic convection has numerous applications in different areas such as production of crystals, weather sciences, signals and industrial systems. Firstly, the study of chaos model was given by Poincaré(1890) and found that the dynamical system generated by the three body problem is quite sensitive to the initial conditions, exhibiting chaotic behaviour. Long et al.(2008) studied the chaotic convection of viscoelastic fluid in porous medium and discuss the stability of chaotic system. The effect of magnetic field on

chaotic convection in fluid layer is studied by Mahmud and Hasim(2011). They found that the system looses its stability via a subcritical Hopf bifurcation producing a homoclinic explosion.

The motive of this chapter is to study oscillatory and chaotic convection in a couple-stress fluid saturated rotating porous medium under temperature modulation. The heat transfer rate is examined by computing the Nusselt number in terms of the amplitude of convection by solving the complex Ginzburg-Landau equation. The effect of all oscillatory convection parameters on the system has been shown through the diagrams, plotted as Nusselt number versus slow time scale. Further, for chaotic convection the problem has been converted into (non-autonomous) Lorenz system by employing truncated Galerkin expansion method and all findings are obtained by using phase portrait and time domain diagrams analysis numerically.

5.2 Mathematical formulation of the problem

We consider an infinitely extended horizontal incompressible couple-stress fluid saturated porous medium of depth d, confined between two parallel planes, the lower plane at $z = 0$ while upper one is at $z = d$, which is heated from below and cooled from above. A cartesian frame of reference is adopted in such a way that the origin lies on the lower plane and z axis is vertically upward. In this model, we suppose that porous layer is rotating about the z-axis with a constant angular velocity Ω_1. Darcy model and couple-stress parameter has been employed in the momentum equation. The physical sketch of the problem is depicted in Figure 5.1. The non-dimensionlized system of the model equations is obtain according as Bhadauria and Kumar(2012), Gupta et al.(2016a)

$$\left(\frac{1}{Va}\frac{\partial}{\partial t} + 1 - C_1\nabla^2\right)(\nabla^2\psi) - \sqrt{Ta}\frac{\partial V}{\partial z} = -Ra\frac{\partial T}{\partial x}, \tag{5.2.1}$$

$$-\frac{\partial\psi}{\partial x}\frac{\partial T_b}{\partial z} - \nabla^2 T = -\frac{\partial T}{\partial t} + \frac{\partial(\psi, T)}{\partial(x, z)}, \tag{5.2.2}$$

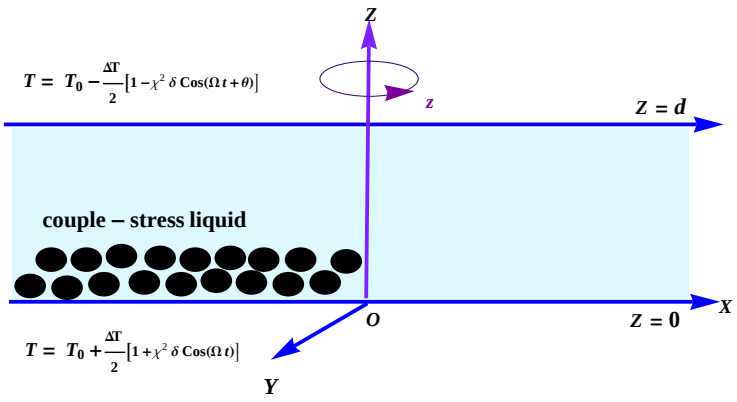

Figure 5.1: Physical configuration of the problem

$$\left(\frac{1}{Va}\frac{\partial}{\partial t}+1-C_1\nabla^2\right)V=-\sqrt{Ta}\frac{\partial\psi}{\partial z}, \tag{5.2.3}$$

where $Va=\frac{\phi\nu d^2}{K\kappa_T}$ Vadász number, $Ra=\frac{\alpha_T g\Delta T dK}{\nu\kappa_T}$ thermal Rayleigh number, $Ta=(\frac{2\Omega_1 d}{\nu})^2$ Taylor number, $C_1=\frac{\mu_c}{\mu d^2}$ couple-stress parameter and remaining variables have their usual meanings as given in the nomenclature. The externally imposed temperature field is given by as Venezian(1969)

$$T=\begin{cases} T_0+\frac{\Delta T}{2}[1+\chi^2\delta cos(\Omega t)] & \text{at} \quad z=0, \\ \\ T_0-\frac{\Delta T}{2}[1-\chi^2\delta cos(\Omega t+\theta)] & \text{at} \quad z=d. \end{cases} \tag{5.2.4}$$

The above system will be solved using stress free and isothermal boundary conditions as given below:

$$\psi=\frac{\partial^2\psi}{\partial z^2}=T=0 \ \text{ on } \ z=0, z=1. \tag{5.2.5}$$

The dimensionless basic temperature term $T_b(z)$, appearing in Eq.(5.2.2), is defined mathematically as

$$\frac{\partial T_b}{\partial z}=-1+\chi^2\delta(f_2(z,t)), \tag{5.2.6}$$

where

$$f_2(z,t) = R_e[f(z)e^{-i\Omega t}],$$

$$f(z) = [A(\lambda)e^{\lambda z} + A(-\lambda)e^{-\lambda z}], \quad A(\lambda) = \frac{\lambda}{2}\Big(\frac{e^{-i\theta} - e^{-\lambda}}{e^{\lambda} - e^{-\lambda}}\Big) \text{ and } \lambda = (1-i)\sqrt{\frac{\Omega}{2}}.$$

A small perturbation parameter χ which shows a deviation from the critical state of onset of convection has been introduced. The variables for a weak non-linear state may be expanded in power series of χ as Venezian(1969), Malkus(1958)

$$Ra = R_0 + \chi^2 R_2 + \chi^4 R_4 + \cdots, \tag{5.2.7}$$

$$\psi = \chi\psi_1 + \chi^2\psi_2 + \chi^3\psi_3 + \cdots, \tag{5.2.8}$$

$$T = \chi T_1 + \chi^2 T_2 + \chi^3 T_3 + \cdots, \tag{5.2.9}$$

where R_0 denotes the critical value of the Rayleigh number for the onset of convection in the absence of temperature modulation.

5.3 Formulation of Ginzburg-Landau (amplitude) equation

For further study of the time periodic convective phenomenon, we rescale the time as ($\frac{\partial}{\partial t} = \frac{\partial}{\partial \tau} + \chi^2\frac{\partial}{\partial s}$). The above system (5.2.1), (5.2.2) and (5.2.3) is computed for each order (up to third order) of χ.

At the **first order**, the matrix operator is obtained similar to linear case as:

$$\begin{pmatrix} [\frac{1}{Va}\frac{\partial}{\partial\tau} + (1 - C_1\nabla^2)]\nabla^2 & R_0\frac{\partial}{\partial x} & -\sqrt{Ta}\frac{\partial}{\partial z} \\ \frac{\partial}{\partial x} & (\frac{\partial}{\partial\tau} - \nabla^2) & 0 \\ \sqrt{Ta}\frac{\partial}{\partial z} & 0 & [\frac{1}{Va}\frac{\partial}{\partial\tau} + (1 - C_1\nabla^2)] \end{pmatrix} \begin{pmatrix} \psi_1 \\ T_1 \\ V_1 \end{pmatrix} = \begin{pmatrix} 0 \\ 0 \\ 0 \end{pmatrix}. \tag{5.3.1}$$

The solution of the first order system subject to the boundary condition Eq.(5.2.5), is assumed to be

$$\psi_1 = (A(s)e^{i\omega\tau} + \overline{A}(s)e^{-i\omega\tau}) \sin ax \ \sin \pi z, \tag{5.3.2}$$

$$T_1 = (B(s)e^{i\omega\tau} + \overline{B}(s)e^{-i\omega\tau}) \cos ax \ \sin \pi z, \tag{5.3.3}$$

$$V_1 = (C(s)e^{i\omega\tau} + \overline{C}(s)e^{-i\omega\tau}) \sin ax \ \cos \pi z. \tag{5.3.4}$$

The unknown amplitudes are functions of rescale time (s), and are related by the following expression:

$$B(s) = -\frac{a}{(c + i\omega)}A(s), \tag{5.3.5}$$

$$C(s) = -\frac{\pi\sqrt{T_a}}{(\frac{i\omega}{Va}) + (1 + C_1 c)}A(s), \tag{5.3.6}$$

where $c = a^2 + \pi^2$. The values of the critical Rayleigh number for stationary and oscillatory mode of convection are as given below respectively:

$$R_{0c}^{st} = \frac{1}{a^2}\Big(c^2 + c^3C_1 + \frac{c\pi^2 Ta}{(1 + C_1c)^2} + \frac{c^2C_1\pi^2 Ta}{(1 + C_1c)^2}\Big), \tag{5.3.7}$$

$$R_{0c}^{ost} = \frac{1}{a^2}\left(c^2 + c^3C_1 - \frac{c\omega^2}{Va} + \frac{c\pi^2 Ta}{(1 + C_1c)^2 + \frac{\omega^2}{Va^2}} + \frac{c^2C_1\pi^2 Ta}{(1 + C_1c)^2 + \frac{\omega^2}{Va^2}} + \frac{\pi^2 Ta\omega^2}{Va((1 + C_1c)^2 + \frac{\omega^2}{Va^2})}\right), \tag{5.3.8}$$

where ω is the oscillatory frequency given by

$$\begin{aligned}\omega^2 &= \frac{-cVa^2(c+Va) - 2c^3C_1Va^2 - c^4C_1^2Va^2(1+C_1Va) + \pi^2TaVa^2(c-Va)}{c^2+cVa+C_1c^2Va} \\ &+\frac{-3c^2C_1Va^3(1+C_1c) - C_1c\pi^2TaVa^3}{c^2+cVa+C_1c^2Va}.\end{aligned} \tag{5.3.9}$$

Now, the critical wave number a_c is computed for which the Rayleigh number is minimum with respect to a^2. Since ω^2 has to be positive and real, therefore from the relation (5.3.9), the necessary parametric relation for the existence of oscillatory convection in the system is given by

$$T_a > \frac{-c(c+Va) - 2c^3C_1 - c^4C_1^2(1+C_1Va) - 3C_1c^2Va(1+C_1c)}{-c\pi^2+\pi^2Va+C_1c\pi^2Va}. \tag{5.3.10}$$

For particular case, we take $(C_1 = 0, \omega = 0)$, the Rayleigh number reduces as

$$R_{0c} = \frac{1}{a^2}(c^2 + c\pi^2Ta). \tag{5.3.11}$$

The above result presented in Eq.(5.3.11) for stationary mode is obtained by Bhadauria and Kumar(2012).

Now, at **second order**, we have

$$\begin{pmatrix} [\frac{1}{Va}\frac{\partial}{\partial\tau} + (1-C_1\nabla^2)]\nabla^2 & R_0\frac{\partial}{\partial x} & -\sqrt{Ta}\frac{\partial}{\partial z} \\ \frac{\partial}{\partial x} & (\frac{\partial}{\partial\tau} - \nabla^2) & 0 \\ \sqrt{Ta}\frac{\partial}{\partial z} & 0 & [\frac{1}{Va}\frac{\partial}{\partial\tau} + (1-C_1\nabla^2)] \end{pmatrix} \begin{pmatrix} \psi_2 \\ T_2 \\ V_2 \end{pmatrix} = \begin{pmatrix} R_{21} \\ R_{22} \\ R_{23} \end{pmatrix}, \tag{5.3.12}$$

where

$$R_{21} = 0, \tag{5.3.13}$$

$$R_{22} = \frac{\partial\psi_1}{\partial x}\frac{\partial T_1}{\partial z} - \frac{\partial\psi_1}{\partial z}\frac{\partial T_1}{\partial x}, \tag{5.3.14}$$

$$R_{23} = 0. \tag{5.3.15}$$

The second order solution subject to the boundary condition (5.2.5) is given by

$$\psi_2 = 0, \tag{5.3.16}$$

$$\Big(\frac{\partial}{\partial\tau} - \nabla^2\Big)T_2 = R_{22}, \tag{5.3.17}$$

$$V_2 = 0. \tag{5.3.18}$$

Now, we compute the temperature fields having the frequency 2ω and free from the rescale time τ. Thus, second order temperature terms can be expressed in the following form:

$$T_2 = \{T_{20} + T_{22}e^{2i\omega t} + \overline{T}_{22}e^{-2i\omega t}\}sin(2\pi z), \tag{5.3.19}$$

where T_{22} and T_{20} are temperature fields having the terms with the frequency 2ω and free from the rescale time τ, respectively. The solutions of the second order temperature field are as

$$T_{20} = \frac{a}{8\pi}\{A(s)\overline{B}(s) + \overline{A}(s)B(s)\}, \tag{5.3.20}$$

and

$$T_{22} = \frac{\pi a}{8\pi^2 + 4i\omega}A(s)B(s). \tag{5.3.21}$$

The horizontally averaged Nusselt number, $Nu(s)$, for the oscillatory mode of convection is given by

$$Nu(s) = 1 + \Big[\chi^2\Big(\frac{\partial T_2}{\partial z}\Big)_{z=0}/\Big(\frac{dT_b}{dz}\Big)_{z=0}\Big]. \tag{5.3.22}$$

By using Eqs.(5.2.6), (5.3.19), (5.3.20) and (5.3.21), the Eq.(5.3.22) is simplified as

$$Nu(s) = 1 + \Big(\frac{ca^2}{2(c^2+\omega^2)} + \frac{\pi^2a^2}{\sqrt{c^2+\omega^2}\sqrt{16\pi^4+4\omega^2}}\Big)|A(s)|^2. \tag{5.3.23}$$

It is clear that the temperature modulation is effective at third order and affects $Nu(s)$ through $A(s)$ which is evaluated at next order.

At the **third order**, we have

$$\begin{pmatrix} [\frac{1}{Va}\frac{\partial}{\partial\tau}+(1-C_1\nabla^2)]\nabla^2 & R_0\frac{\partial}{\partial x} & -\sqrt{Ta}\frac{\partial}{\partial z} \\ \frac{\partial}{\partial x} & (\frac{\partial}{\partial\tau}-\nabla^2) & 0 \\ \sqrt{Ta}\frac{\partial}{\partial z} & 0 & [\frac{1}{Va}\frac{\partial}{\partial\tau}+(1-C_1\nabla^2)] \end{pmatrix} \begin{pmatrix} \psi_3 \\ T_3 \\ V_3 \end{pmatrix} = \begin{pmatrix} R_{31} \\ R_{32} \\ R_{33} \end{pmatrix}, \tag{5.3.24}$$

where

$$R_{31} = -\frac{1}{Va}\frac{\partial}{\partial s}(\nabla^2\psi_1) - R_2\frac{\partial T_1}{\partial x}, \tag{5.3.25}$$

$$R_{32} = \frac{\partial\psi_1}{\partial x}\frac{\partial T_2}{\partial z} - \frac{\partial T_1}{\partial s} + \delta f_2(z,s)\frac{\partial\psi_1}{\partial x}, \tag{5.3.26}$$

$$R_{33} = -\frac{1}{Va}\frac{\partial V_1}{\partial s}. \tag{5.3.27}$$

Using first/second order solutions, the expressions of R_{31}, R_{32} and R_{33} are computed. Applying solvability condition for the existence of third order solution, one may derive the complex Ginzburg-Landau equation.

$$\frac{dA(s)}{ds} - L^{-1}G(s)A(s) + L^{-1}M|A(s)|^2A(s) = 0, \tag{5.3.28}$$

where

$$L = \left(\frac{c}{Va} + \frac{a^2R_0}{(c+i\omega)^2} - \frac{\pi^2Ta}{Va(\frac{i\omega}{Va}+(1+C_1c)^2)}\right),$$

$$G(s) = \left(\frac{a^2R_2}{c+i\omega} - \frac{2a^2R_0\delta I_1}{c+i\omega}\right), I_1 = \int_0^1 f_2(z,s)\sin^2(\pi z)dz,$$

$$M = \left(\frac{a^4cR_0}{4(c^2+\omega^2)(c+i\omega)} + \frac{a^4\pi^2R_0}{(8\pi^2+4i\omega)(c+i\omega)^2}\right).$$

Writing $A(s)$ in the phase-amplitude form, we get

$$A(s) = |A(s)|e^{i\phi}. \tag{5.3.29}$$

Now, substituting Eq.(5.3.29) in Eq.(5.3.28), the following expression for the amplitude $|A(s)|$ has been obtained

$$\frac{d|A(s)|^2}{ds} - 2p_r|A(s)|^2 + 2l_r|A(s)|^4 = 0, \tag{5.3.30}$$

$$\frac{d(ph(A(s)))}{ds} = pi - li|A(s)|^2, \tag{5.3.31}$$

where $L^{-1}G(s) = p_r + ip_i$, $L^{-1}M = l_r + il_i$ and ph(.) represents the phase shift. The Eq.(5.3.30) solved numerically using the function NDSolve of Mathematica, subject to the suitable initial condition $A(0) = a_0$, where a_0 is the chosen initial amplitude of oscillatory convection.

5.4 Formulation of the Lorenz system

To obtain chaotic system we reconstruct the model equations of Bhadauria and Kumar(2012) analogous to Gupta et al.(2015) as well as leaving the perturbation parameter χ from the modulation term and couple-stress parameter C_1 to reduce the complexity for further study. The new non-dimensionlized system equations are obtained as

$$\left(\left(\frac{1}{Va}\frac{\partial}{\partial t} + 1\right)^2 \nabla^2 + Ta\frac{\partial^2}{\partial z^2}\right)\psi = Ra\frac{\partial T}{\partial x}\left(\frac{1}{Va}\frac{\partial}{\partial t} + 1\right), \tag{5.4.1}$$

$$\frac{\partial T}{\partial t} - \frac{\partial \psi}{\partial z}\frac{\partial T}{\partial x} + \frac{\partial \psi}{\partial x}\frac{\partial T}{\partial z} = \nabla^2 T. \tag{5.4.2}$$

The solution of nonlinear Eqs.(5.4.1) and (5.4.2) are obtained by using truncated Galerkin expansion method. The stream function and temperature field are taken in the forms as mentioned in Gupta et al.(2015).

$$\psi = A_{11}\sin(ax)\sin(\pi z), \tag{5.4.3}$$

$$T = T_b + B_{11}\cos(ax)\sin(\pi z) + B_{02}\sin(2\pi z). \tag{5.4.4}$$

Using Eqs.(5.4.3) and (5.4.4) in to Eqs.(5.4.1) and (5.4.2), multiplying the equations by orthogonal eigenfunctions corresponding to Eqs.(5.4.3) and (5.4.4), and then integrating them over the spatial domain, yield a set of three differential equations for the time evolution of the amplitudes, in the form of

$$\frac{d^2A_{11}}{d\tau^2} = -\frac{2Va}{c}\frac{dA_{11}}{d\tau} - \frac{Va^2}{c^2}\Big(\frac{\pi^2 T_a}{c} + 1\Big)A_{11} + \frac{aR_aV_a}{c^2}\Big(\frac{Va}{c} + \frac{\partial}{\partial\tau}\Big)B_{11}, \tag{5.4.5}$$

$$\frac{dB_{11}}{d\tau} = \frac{a}{c}(1 - 2\delta I_1)A_{11} + \frac{a\pi}{c}A_{11}B_{02} - B_{11}, \tag{5.4.6}$$

$$\frac{dB_{02}}{d\tau} = -\frac{a\pi}{2c}A_{11}B_{11} - \frac{4\pi^2}{c}B_{02}, \tag{5.4.7}$$

where $c = a^2+\pi^2$, time has been re-scaled ($\tau = ct$) and the following notations are introduce.

$$\Omega = \frac{\Omega}{c}, \sigma = \frac{Va}{c}, R = \frac{a^2Ra}{c^2}, T_A = \frac{\pi^2 Ta}{c} \text{ and } \gamma = -\frac{4\pi^2}{c}.$$

Again re-scale the amplitude in the form of

$$X = \frac{\pi a A_{11}}{c\sqrt{2}}, Y = \frac{\pi R B_{11}}{\sqrt{2}} \text{ and } Z = -\pi R B_{02}$$

which provide the following set of equations

$$\begin{cases} \frac{dX}{d\tau} = W, \\ \frac{dY}{d\tau} = R(1 - 2\delta I_1)X - Y - XZ, \\ \frac{dZ}{d\tau} = \gamma Z + XY, \\ \frac{dW}{d\tau} = -2\sigma W + \sigma(R(1 - 2\delta I_1) - \sigma(T_A + 1))X + \sigma(\sigma - 1)Y - \sigma XZ. \end{cases} \tag{5.4.8}$$

5.5 Results and discussion

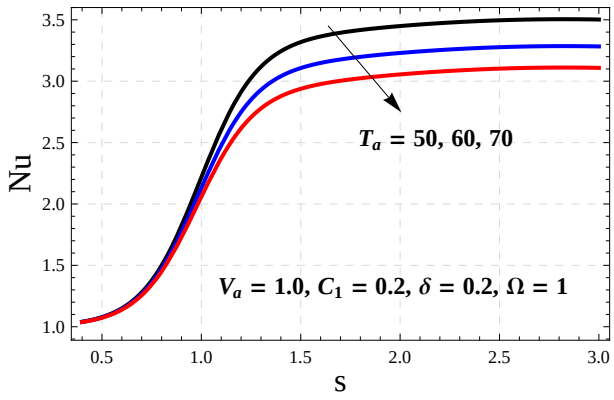

Figure 5.2: Effect of Ta on Nu for IPM case ($\theta = 0$)

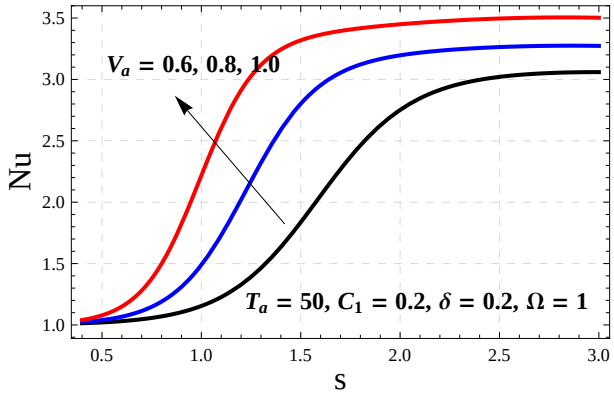

Figure 5.3: Effect of Va on Nu for IPM case ($\theta = 0$)

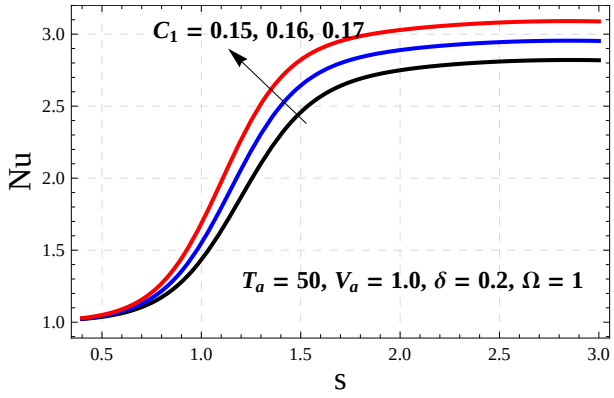

Figure 5.4: Effect of C_1 on Nu for IPM case ($\theta = 0$)

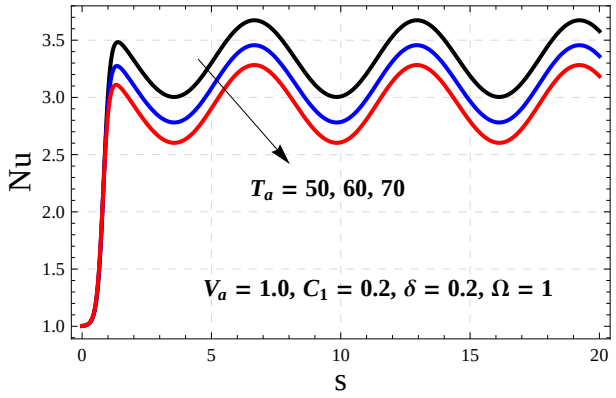

Figure 5.5: Effect of Ta on Nu for OPM case ($\theta = \pi$)

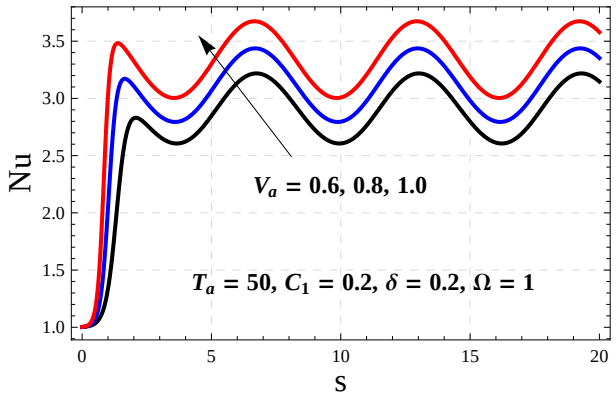

Figure 5.6: Effect of Va on Nu for OPM case ($\theta = \pi$)

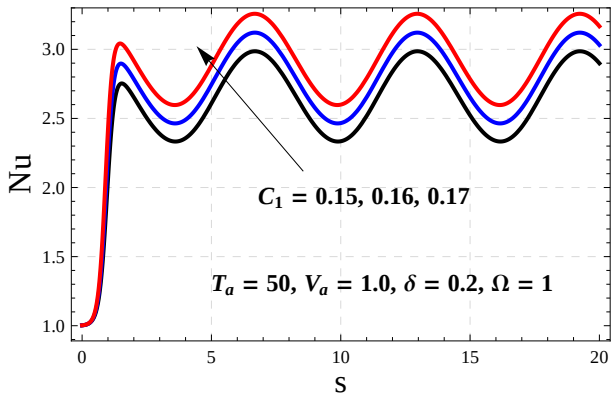

Figure 5.7: Effect of C_1 on Nu for OPM case ($\theta = \pi$)

In this chapter, the effect of oscillatory and chaotic convection in a couple-stress fluid saturated rotating porous medium under temperature modulation has been studied. A weakly non-linear stability analysis has been performed by adopting power series expansion in terms of the amplitude of temperature modulation. Here three cases arise due to temperature modulation as

1. In-phase modulation (IPM, $\theta = 0$)
2. Out-phase modulation (OPM, $\theta = \pi$)
3. Lower-boundary modulation (LBMO, $\theta = -i\infty$)

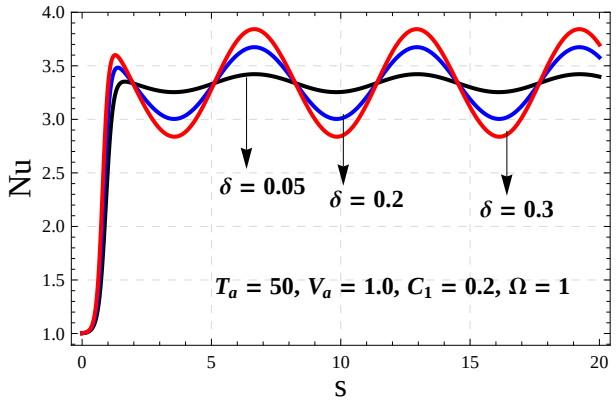

Figure 5.8: Effect of δ on Nu for OPM case ($\theta = \pi$)

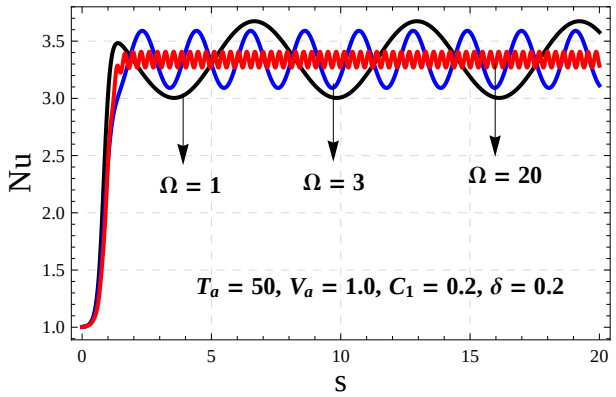

Figure 5.9: Effect of Ω on Nu for OPM case ($\theta = \pi$)

It is evident that the value of Nu begins with 1, thus showing the conduction state (IPM) initially, the value of Nu increases as time increases thus showing the convection state, becomes oscillatory (OPM or LBMO), thus showing the modulation effect. For the

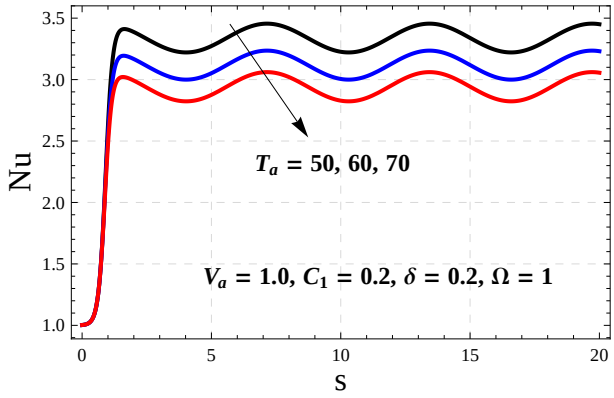

Figure 5.10: Effect of Ta on Nu for LBMO case ($\theta = -i\infty$)

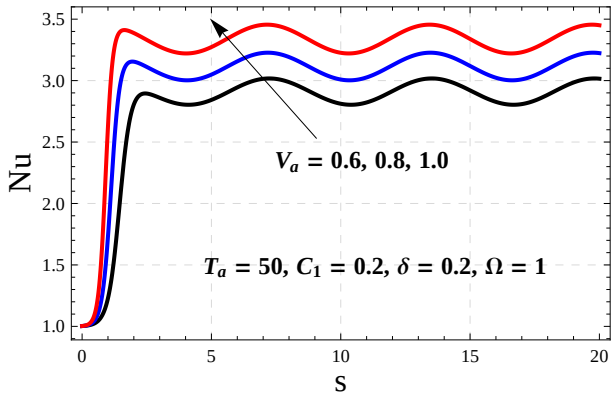

Figure 5.11: Effect of Va on Nu for LBMO case ($\theta = -i\infty$)

existence of oscillatory mode, the parametric relation of Eq.(5.3.10) must hold. The numerical values of Nu have been obtained from the expression (5.3.23) by solving the amplitude Eq.(5.3.30). Heat transfer analyses of the system is done in terms of the Nusselt number by taking different convective parameters, and depicting in Figures 5.2-5.15 graphically (Nu versus s) for each cases of modulation.

From Figures 5.2-5.4, one can see the effect of IPM ($\theta = 0$) on the system. At the initial state (very small time) the modulation effect about to negligible because the numeric value of Nu is not affected by amplitude and frequency of modulation on increasing time, so the system shows constant behaviour for both parameters. In Figure 5.2, the effect of Taylor number Ta on the system is depicted where it is noticed that on increasing the value of Ta heat transport decreases, since the value of Nu decreases in the system. Consequently, the

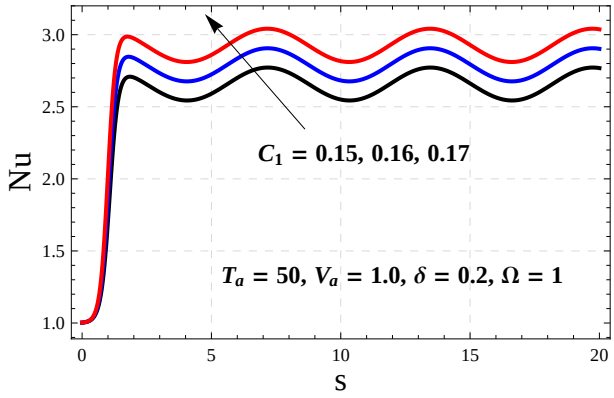

Figure 5.12: Effect of C_1 on Nu for LBMO case ($\theta = -i\infty$)

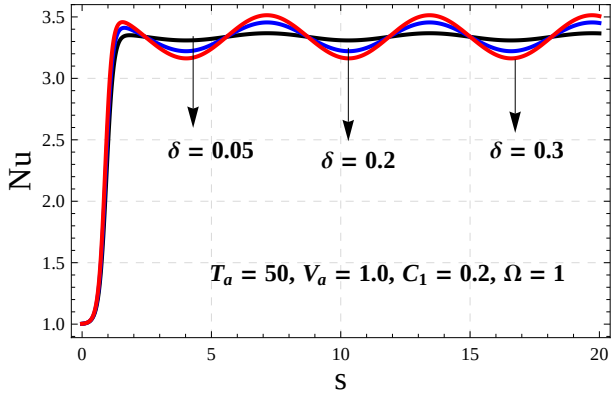

Figure 5.13: Effect of δ on Nu for LBMO case ($\theta = -i\infty$)

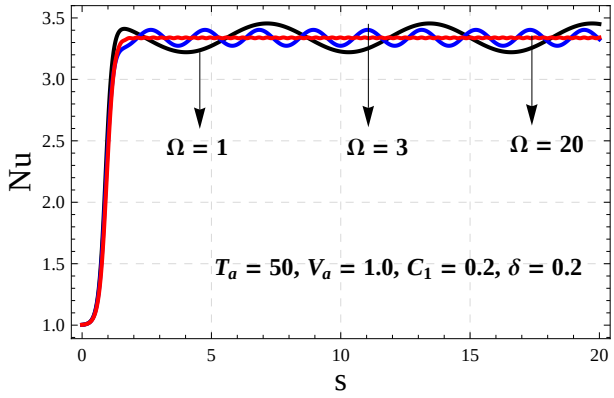

Figure 5.14: Effect of Ω on Nu for LBMO case ($\theta = -i\infty$)

system is stabilized, which is similar to results obtained by Bhadauria and Kumar(2012). In Figure 5.3, as Va increases the value of Nu increases, therefore heat transfer rate advances in the system compatible with the results obtained by Bhadauria and Kumar(2012), thus

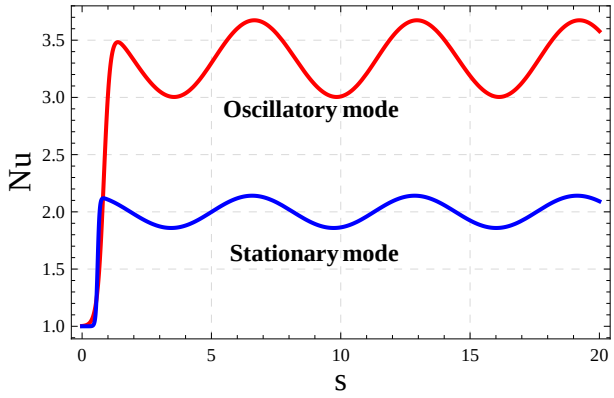

Figure 5.15: Comparison of stationary and oscillatory systems

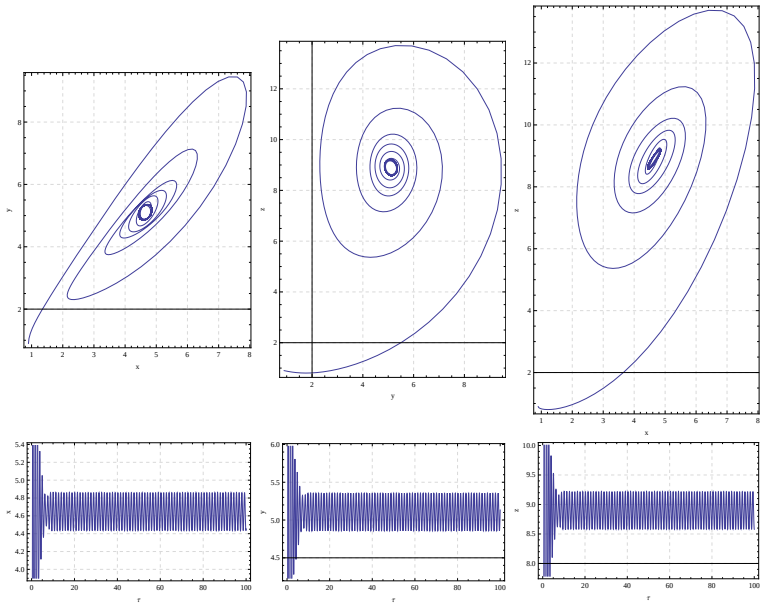

Figure 5.16: Phase portrait diagrams and time domain for the system (5.4.8) with parameters $R = 10, T_A = 0.1, \delta = 0.1$

the Vadász number has a tendency to destabilize the system. In Figure 5.4, the effect of couple-stress parameter C_1 on the system is depicted where it is found that on increasing the value of C_1 heat transport increases, consequently, the system is destabilized, similar to the results obtained by Gupta et al.(2016a).

From Figures 5.5-5.9, one can see the effect of all convective parameters for the case OPM ($\theta = \pi$) on the system. The effect of Taylor number Ta on the system is depicted in Figure 5.5, where it is observed that on increasing the value of Ta, heat transport is

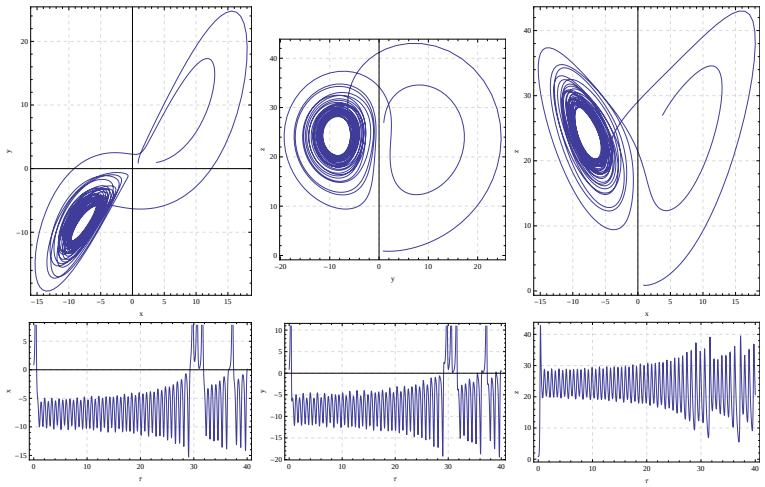

Figure 5.17: Phase portrait diagrams and time domain for the system (5.4.8) with parameters $R = 25.5, T_A = 0.1, \delta = 0.1$

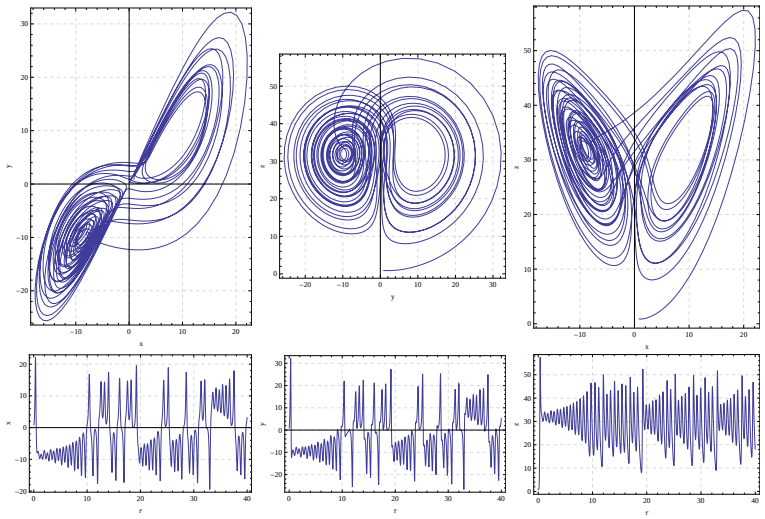

Figure 5.18: Phase portrait diagrams and time domain for the system (5.4.8) with parameters $R = 33, T_A = 0.1, \delta = 0.1$

suppressed in the system, therefore the system is stabilized. In Figure 5.6, as Va increases the value of Nu increases, thus heat transfer gradually increases in the system on increasing Va, thus the Vadász number has a destabilizing effect. The effect of couple-stress parameter C_1 on the system is depicted in Figure 5.7, here it is found that on increasing the value of C_1, heat transport increases as Nu increases, and so the system is destabilized. The effects of the amplitude of modulation δ and frequency of modulation Ω on the system are given in Figures 5.8-5.9 respectively. Figure 5.8 shows that an increment in the amplitude

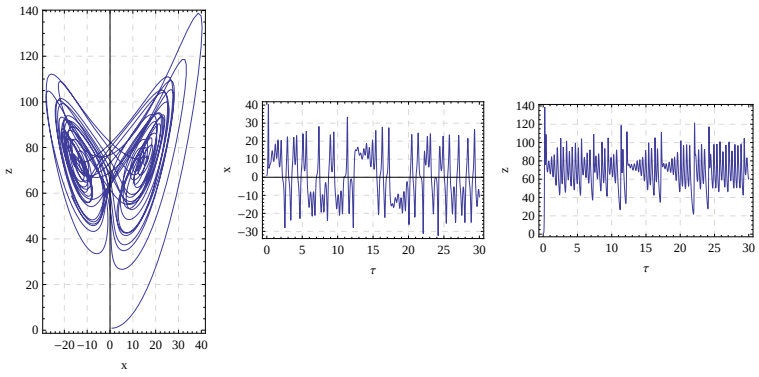

Figure 5.19: Phase portrait diagrams and time domain for the system (5.4.8) with parameters $R = 75, T_A = 0.1, \delta = 0.1$

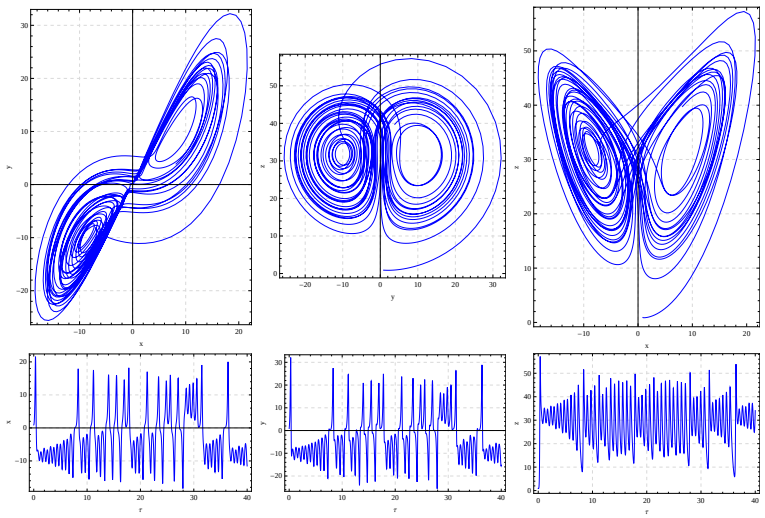

Figure 5.20: Phase portrait diagrams and time domain for the system (5.4.8) with parameters $R = 33, T_A = 0.2, \delta = 0.1$

of modulation increases the magnitude of Nu, thus enhances the heat transfer and so advancing the onset of convection. An opposite effect is obtained in the case of frequency of modulation Ω as given in Figure 5.9. Hence, it is found that the effect of temperature modulation decreases as the frequency of modulation increases, both results are analogous to Bhadauria and Kiran(2016) for fluid layer. The results for LBMO ($\theta = -i\infty$) are depicted in Figures 5.10-5.14. From the figures, it is found that the results are similar as obtained for OPM case in Figures 5.5-5.9. In Figure 5.15, we compare the stationary and oscillatory system and found that heat transfer is more in oscillatory system than in stationary system.

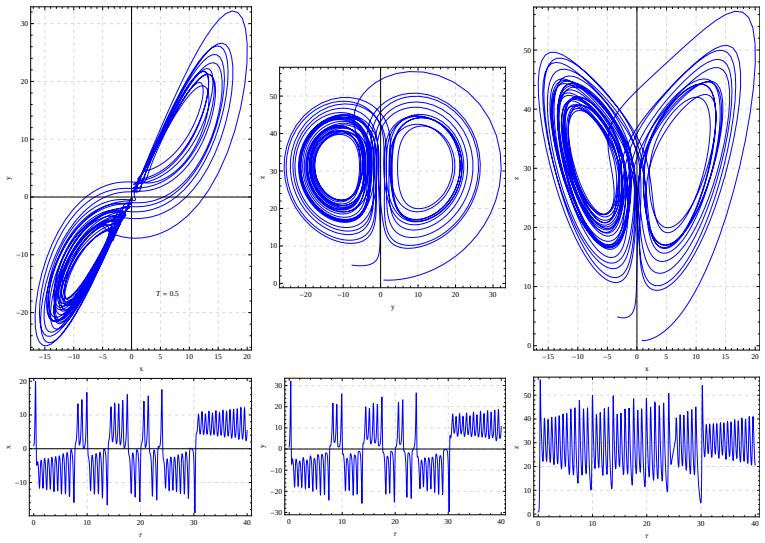

Figure 5.21: Phase portrait diagrams and time domain for the system (5.4.8) with parameters $R = 33, T_A = 0.5, \delta = 0.1$

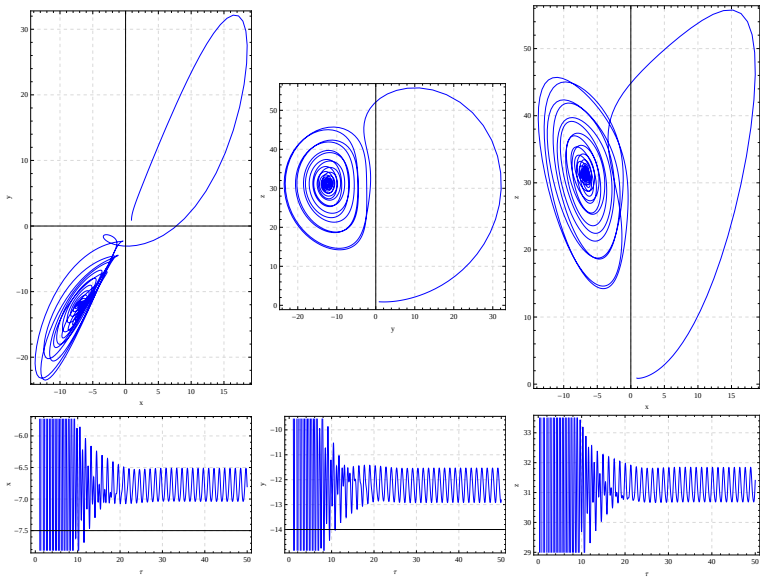

Figure 5.22: Phase portrait diagrams and time domain for the system (5.4.8) with parameters $R = 33, T_A = 0.8, \delta = 0.1$

The numerical simulation of the **Lorenz system** (5.4.8) is done by **Mathematica** 7.0. In this simulation, the initial conditions $\tau = 0 : X = Y = Z = 0.9, W = 0.1$ are considered and the parameter values are fixed as $\sigma = 10, \gamma = -8/3$, $\Omega = 5$ and $\theta = \pi$. The parameters R, T_A, δ are considered as variable to examine the behaviour of modulated chaotic system. The phase-portrait and time domain diagrams depict how modulation term affect the dy-

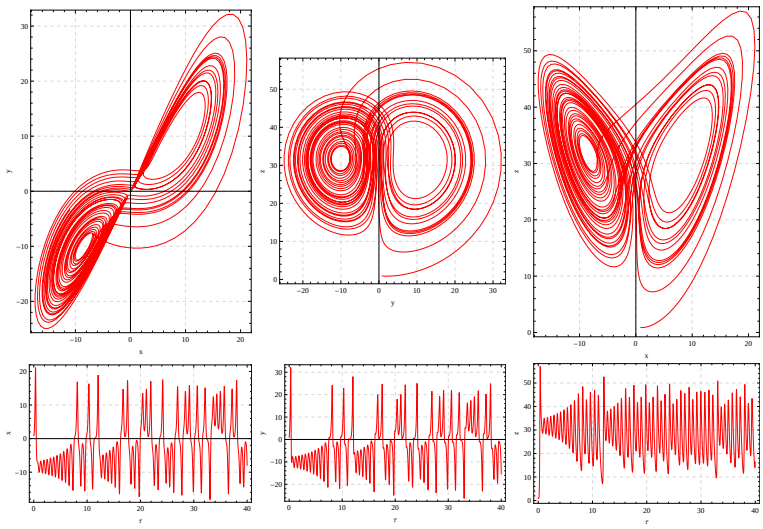

Figure 5.23: Phase portrait diagrams and time domain for the system (5.4.8) with parameters $R = 33, T_A = 0.2, \delta = 0.01$

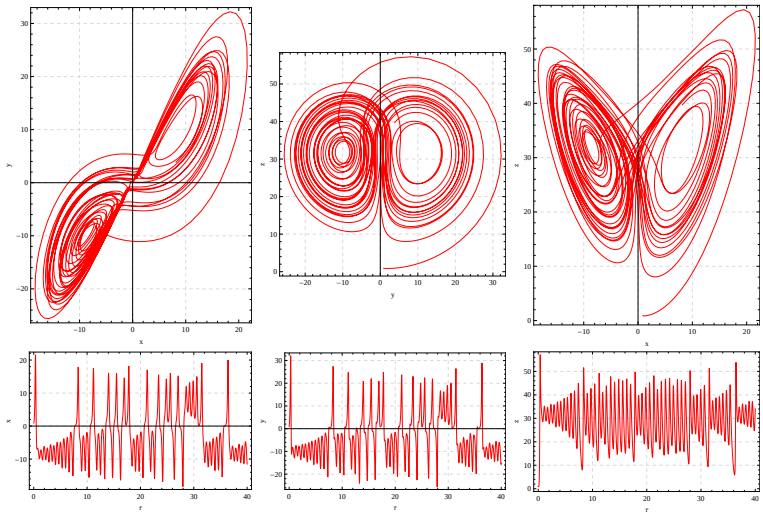

Figure 5.24: Phase portrait diagrams and time domain for the system (5.4.8) with parameters $R = 33, T_A = 0.2, \delta = 0.1$

namics of the thermal convection for a combination of varied parameters. The results are further depicted in Figures 5.16-5.27 to analyse the Lorenz system by using phase-portrait and time domain diagrams.

The effect of scaled Rayleigh number R on the chaotic system is depicted in Figures 5.16-5.19, keeping fixed the other parameters. Figure 5.16 shows a periodic solution for

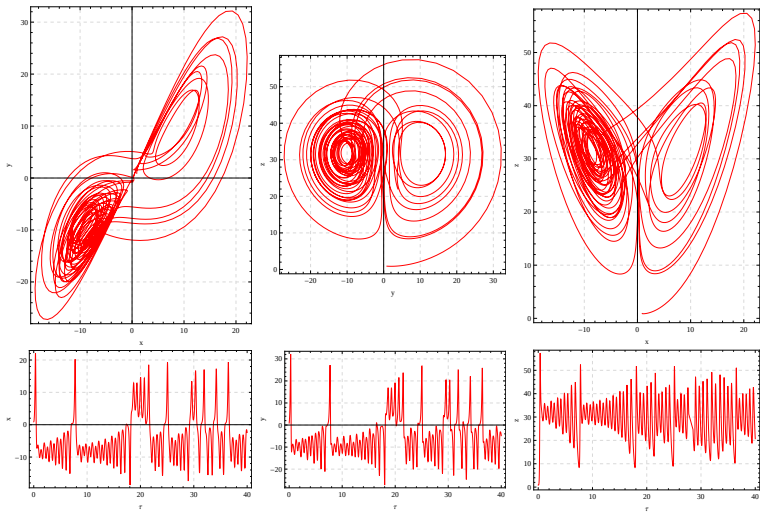

Figure 5.25: Phase portrait diagrams and time domain for the system (5.4.8) with parameters $R = 33, T_A = 0.2, \delta = 0.2$

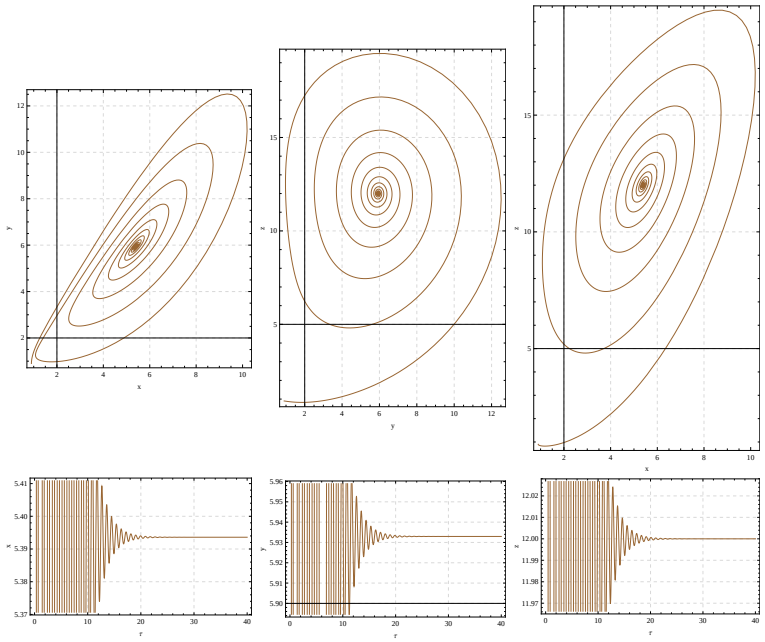

Figure 5.26: Phase portrait diagrams and time domain for the system (5.4.8) with parameters $R = 13.1, T_A = 0.1, \delta = 0.0$

$R = 10$ and for $R = 25.5$, system transition from periodic to weak chaotic solution in Figure 5.17. Figure 5.18 ($R = 33$) depicts a initially chaotic behaviour or aperiodic solution of the Lorenz system, which shows that heat transfer is more in this case in comparison to earlier two cases. Moreover, on increasing the values of R, system always shows chaotic

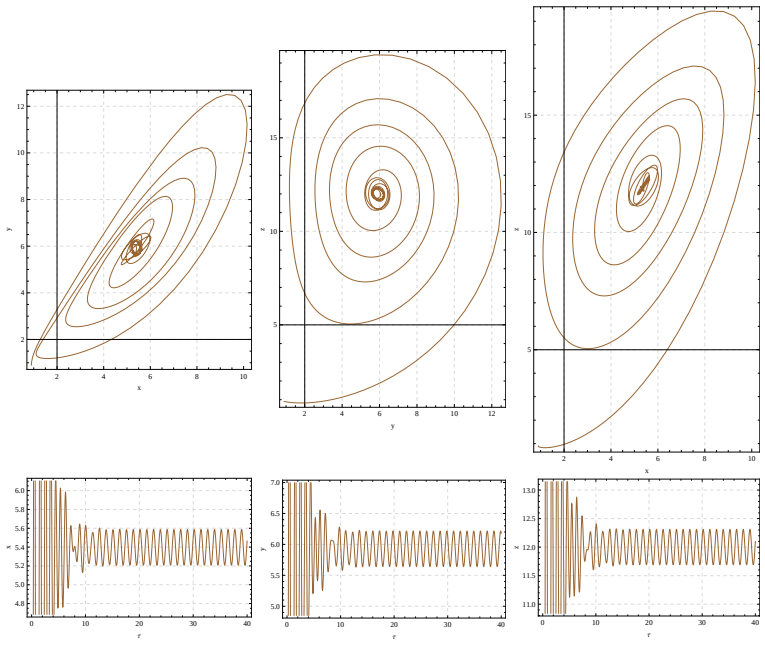

Figure 5.27: Phase portrait diagrams and time domain for the system (5.4.8) with parameters $R = 13.1, T_A = 0.1, \delta = 0.1$

solution in Figure 5.19. Hence it is concluded that the system has either periodic or chaotic nature depending upon the suitable value of scaled Rayleigh number, which is same as obtained by Long et al.(2008). Figures 5.20-5.22 depict the effect of different values of scaled Taylor number $T_A = 0.2, 0.5, 0.8$, keeping fixed the other parameters. The phase-portrait diagrams and time domain solutions show that the system has chaotic nature for $T_A = 0.2$, for $T_A = 0.5$ system looses its chaotic nature very slowly while the system shows a periodic nature for $T_A = 0.8$. Therefore, on increasing the value of T_A system always has periodic nature, compatible with the results obtained by Gupta et al.(2015). The impact of amplitude of temperature modulation δ on the chaotic system for different parametric values $\delta = 0.01, 0.1, 0.2$ keeping fixed the other parameters, is depicted in Figures 5.23-5.25, respectively. These figures depict that the trajectories are much disturbed on increasing δ. Therefore, the chaotic behaviour advances slightly in the system, that is, the heat transfer increases gradually which confirms the results obtained by Bhadauria and kiran(2015a). Further, the present results are compared with the result already obtained by Gupta et al.(2015) and depicted in Figure 5.26. In Figure 5.26 all the trajectories are moving in to fixed point and time domain solution shows a stable solution for given parametric values.

On the other hand all the trajectories are much disturbed and moving around a fixed point as presented in Figure 5.27 which is due to the presence of modulation term δ, and time domain solution depicts a periodic system, therefore we analyse that heat transfer is more in modulated system.

5.6 Conclusions

Oscillatory and chaotic convection in a couple-stress fluid saturated rotating porous medium under temperature modulation has been studied. The findings are as follow:

a) $Nu^{IPM} < Nu^{LBMO} < Nu^{OPM}$ exists for temperature modulation.

b) The Taylor number Ta has stablize effect on oscillatory system for each type of modulation.

c) Vadász number Va has destabilizing effect on the system.

d) Couple-stress parameter C_1 destabilizes the oscillatory system for all case.

e) The amplitude δ and frequency Ω of temperature modulation either advance or delay the convection for OPM and LBMO.

f) The heat transfer is more in oscillatory mode than in stationary mode of convection.

g) The effect of scaled Rayleigh number R is to either increase(chaotic) or decrease(periodic) the heat transport for suitable value of R in the Lorenz system.

h) The scaled Taylor number T_A reduces the chaotic level in the Lorenz system.

i) The amplitude δ of modulation is to advance the heat transfer in the Lorenz system.

j) Heat transfer is more in present study than in the unmodulation case.

Chapter 6

Numerical study on chaotic convection in a viscoelastic fluid saturated porous medium under temperature modulation

6.1 Introduction

In this chapter, we study chaotic convection in a viscoelastic fluid saturated porous medium under temperature modulation and by doing numerical simulation. Study in porous media has attracted the researchers during the last three decades due to its wide range of applications in various fields such as petroleum industry, chemical engineering and geophysics, etc. First of all Venezian(1969) investigated the effect of temperature modulation in a viscous fluid layer. A lot of work has been done by many researchers to study the convective event in a viscoelastic fluid saturated porous medium. At first, Green(1968) studied the oscillatory convection in a viscoelastic fluid layer. The occurrence of overstability for typi-

This chapter is based on the research article: Numerical study on chaotic convection in a viscoelastic fluid saturated porous medium under temperature modulation, published as proceeding in NCRAMA (2015).

cal Rayleigh-Bénard convection of a horizontal homogeneous Maxwellian fluid layer heated from below, was reported by Vest and Arpaci(1969).

Now-a-days many researchers have taken interest in the study of chaotic convection. Such type of convection is applicable in various fields, for instance, in the production of crystals and weather sciences, etc. The chaos model was proposed first of all by Poincaré(1890). In this model the author found that the dynamical system generated by the three body problem is quite sensitive to the initial conditions exhibiting chaotic behaviour. Later on, Edward Lorenz(1963) studied the system of three ordinary differential equations and developed the model for atmospheric convection. A similar work has been done in Sparrow(1982).

6.2 Mathematical structure of the problem

In this section, we consider an infinitely extended horizontal viscoelatic fluid saturated porous medium of depth d, confined between two parallel planes at $z = 0$ (lower plane) and $z = d$ (upper plane), heated from below as depicted in Figure 6.1. The Darcy law and Boussinesq approximation are used to solve the model equations. The governing equations of this model are as Bhadauria and Kiran(2014a)

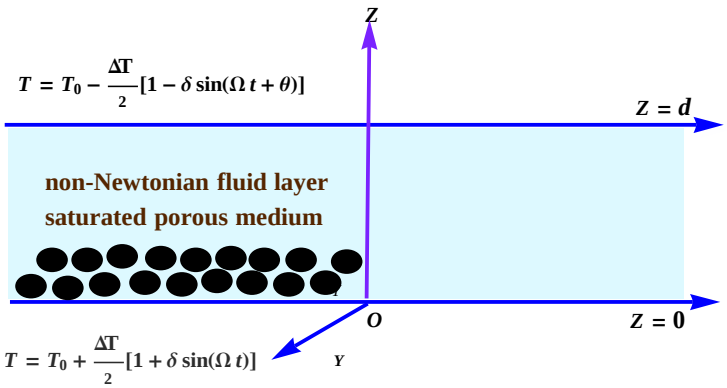

Figure 6.1: Physical configuration of the problem

$$\begin{cases} \nabla.\vec{q} = 0, \\ \\ \left(\overline{\lambda_1}\frac{\partial}{\partial t} + 1\right)\left(\frac{\rho_0}{\phi}\frac{\partial q}{\partial t} + \nabla p - \rho\vec{g}\right) + \frac{\mu}{K}\left(\overline{\lambda_2}\frac{\partial}{\partial t} + 1\right)\vec{q} = 0, \\ \\ \frac{\partial T}{\partial t} + (\vec{q}.\nabla)T = \kappa_T\nabla^2 T, \\ \\ \rho = \rho_0[1 - \alpha_T(T - T_0)], \end{cases} \tag{6.2.1}$$

where the physical variables have their usual meanings as given in nomenclature. The externally imposed thermal boundary conditions are given by

$$T = \begin{cases} T_0 + \frac{\Delta T}{2}[1 + \delta\sin(\Omega t)] & \text{at} \quad z = 0, \\ \\ T_0 - \frac{\Delta T}{2}[1 - \delta\sin(\Omega t + \theta)] & \text{at} \quad z = d. \end{cases} \tag{6.2.2}$$

6.3 Basic state

In basic state, the velocity and temperature profiles are given by

$$\vec{q_b} = 0, p = p_b(z), T = T_b(z), \rho = \rho_b(z). \tag{6.3.1}$$

Using Eq.(6.3.1) in Eq.(6.2.1), the following relations are obtained

$$\frac{\partial p_b}{\partial z} = -\rho_b g, \tag{6.3.2}$$

$$\kappa_T\frac{d^2T_b}{dz^2} = \frac{\partial T}{\partial t}, \tag{6.3.3}$$

$$\rho_b = \rho_0[1 - \alpha_T(T_b - T_0)]. \tag{6.3.4}$$

Now, we superimpose finite amplitude perturbations, on the basic state in the form

$$\vec{q} = q_b + q', T = T_b + T', p = p_b + p', \rho = \rho_b + \rho', \tag{6.3.5}$$

where the primes represent the perturbed quantities. According to Long et al.(2008) and Bhadauria and Kiran(2015a), the dimensionless governing system is given by

$$\Big[\frac{1}{P_{rD}}\Big(\lambda_1\frac{\partial}{\partial t}+1\Big)\frac{\partial}{\partial t}+\Big(\lambda_2\frac{\partial}{\partial t}+1\Big)\Big]\nabla^2\psi = Ra\Big(\lambda_1\frac{\partial}{\partial t}+1\Big)\frac{\partial T}{\partial x}, \tag{6.3.6}$$

$$-\frac{\partial\psi}{\partial x}\frac{\partial T_b}{\partial z}-\nabla^2 T = -\frac{\partial T}{\partial t}+\frac{\partial(\psi,T)}{\partial(x,z)}, \tag{6.3.7}$$

where $P_{rD}=\frac{\phi P_r}{D_a}$ is the Darcy-Prandtl number, $D_a=\frac{K}{d^2}$ is the Darcy number, $P_r=\frac{\nu}{k_T}$ is the Prandtl number, $Ra=\frac{g_0\alpha_T\triangle TKd}{\nu k_T}$ is the DarcyRayleigh number, $\nu=\frac{\mu}{\rho_0}$ is kinematic viscosity.

The above system will be solved by considering stress free and isothermal boundary conditions as given below:

$$\psi=\frac{\partial^2\psi}{\partial z^2}=T=0 \quad \text{on} \quad z=0, z=1. \tag{6.3.8}$$

The dimensionless basic temperature term $T_b(z)$, appearing in Eq.(6.3.7) defined mathematically as

$$\frac{\partial T_b}{\partial z}=-1+\delta(f_2(z,t)), \tag{6.3.9}$$

where

$$f_2(z,t)=R_e[f(z)e^{-i\Omega t}],$$

$$f(z)=[A(\lambda)e^{\lambda z}+A(-\lambda)e^{-\lambda z}], \quad A(\lambda)=\frac{\lambda}{2}\Big(\frac{e^{-i\theta}-e^{-\lambda}}{e^{\lambda}-e^{-\lambda}}\Big) \quad \textit{and} \quad \lambda=(1-i)\sqrt{\frac{\Omega}{2}}.$$

6.4 Method of solution

The solution of nonlinear Eqs.(6.3.6) and (6.3.7) subject to the boundary condition (6.3.8) are obtained by using truncated Galerkin expansion method. The stream function and temperature field are taken in the forms as mentioned in Vadász(2014).

$$\psi=A_{11}\sin\Big(\frac{\pi x}{L}\Big)\sin(\pi z), \tag{6.4.1}$$

$$T = T_b + B_{11}\cos\left(\frac{\pi x}{L}\right)\sin(\pi z) + B_{02}\sin(2\pi z). \tag{6.4.2}$$

Using Eqs.(6.4.1) and (6.4.2) into Eqs.(6.3.6) and (6.3.7), multiplying the equations by orthogonal eigenfunctions corresponding to Eqs.(6.4.1) and (6.4.2), and then integrating them over the spatial domain, yield a set of three differential equations for the time evolution of the amplitudes, in the form of

$$\left[\left(1+\Gamma\frac{d}{d\tau}\right)\frac{d}{d\tau} + \frac{P_{rD}\gamma}{\pi^2}\left(1+\Gamma\Lambda'\frac{d}{d\tau}\right)\right]A_{11} = \frac{P_{rD}\gamma Ra}{\chi'\pi^3}\left(1+\Gamma\frac{d}{d\tau}\right)B_{11}, \tag{6.4.3}$$

$$\frac{dB_{11}}{d\tau} = -B_{11} + \frac{1}{\pi\chi'}(1-2\delta I_1)A_{11} + \frac{1}{\chi'}A_{11}B_{02}, \tag{6.4.4}$$

$$\frac{dB_{02}}{d\tau} = -\frac{1}{2\chi'}A_{11}B_{11} - 4\gamma B_{02}, \tag{6.4.5}$$

where the time has been re-scaled and the following notations are introduced:

$\tau = \frac{(L^2+1)\pi^2}{L^2}t$, $\chi' = \frac{L^2+1}{L}$, $\gamma = \frac{L^2}{L^2+1}$, $\Omega = \frac{L^2}{(L^2+1)\pi^2}\Omega$,

$\sigma = \frac{P_{rD}\gamma}{\pi^2}$, $R = \frac{Ra}{\pi^2\chi'^2}$ and $I_1 = \int_0^1 f_2(z,t)\sin^2(\pi z)dz$.

Again rescaling the amplitudes in the form of

$$X = \frac{A_{11}}{2\chi'\sqrt{2\gamma(R-1)}}, Y = \frac{\pi R B_{11}}{2\sqrt{2\gamma(R-1)}} \text{ and } Z = -\frac{\pi R B_{02}}{(R-1)}.$$

This provides the following set of equations

$$\begin{cases} \frac{dX}{d\tau} = W, \\ \\ \frac{dY}{d\tau} = R(1-2\delta I_1)X - Y - (R-1)XZ, \\ \\ \frac{dZ}{d\tau} = 4\gamma(XY - Z) \\ \\ \frac{dW}{d\tau} = \sigma[(R(1-2\delta I_1) - \frac{1}{\Gamma})X + (\frac{1}{\Gamma} - 1)Y - (R-1)XZ - (\Lambda' + \frac{1}{\sigma\Gamma})W]. \end{cases} \tag{6.4.6}$$

If the amplitude of temperature modulation $\delta = 0$, then the system (6.4.6) reduces into the model of Long et al.(2008).

6.5 Results and Discussion

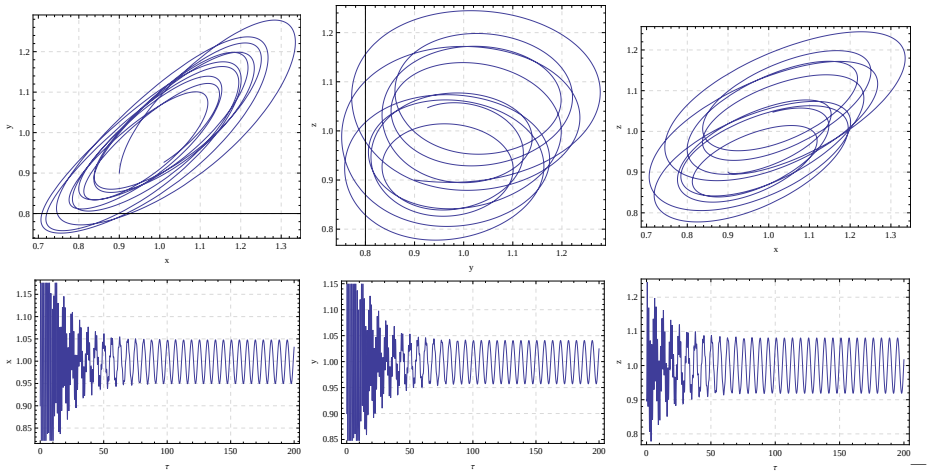

Figure 6.2: Phase portrait and time domain diagrams for the system (6.4.6) with parameters $R = 10$ and $\Gamma = 1$, $\Lambda' = 0.7$, $\delta = 0.1$

MATHEMATICA 7.0 has been used for the numerical simulation of the Lorenz system (6.4.6). Here out of phase modulation (OPM) has been considered throughout the study to see the effect of temperature modulation on the convective system. It was found in previous chapter that heat transport is more in out of phase modulation than in the other two cases. In this simulation, the initial conditions are $\tau = 0 : X = Y = Z = 0.9, W = 0.1$ and the

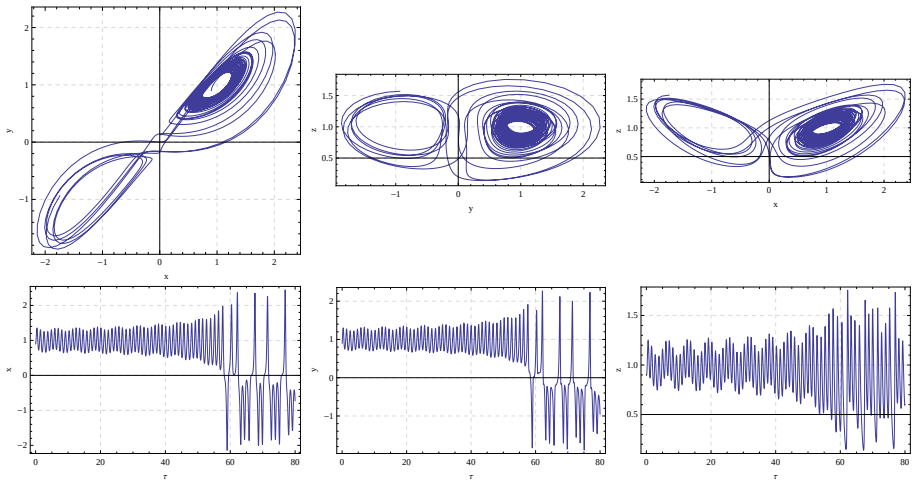

Figure 6.3: Phase portrait and time domain diagrams for the system (6.4.6) with parameters $R = 11$ and $\Gamma = 1$, $\Lambda' = 0.7$, $\delta = 0.1$

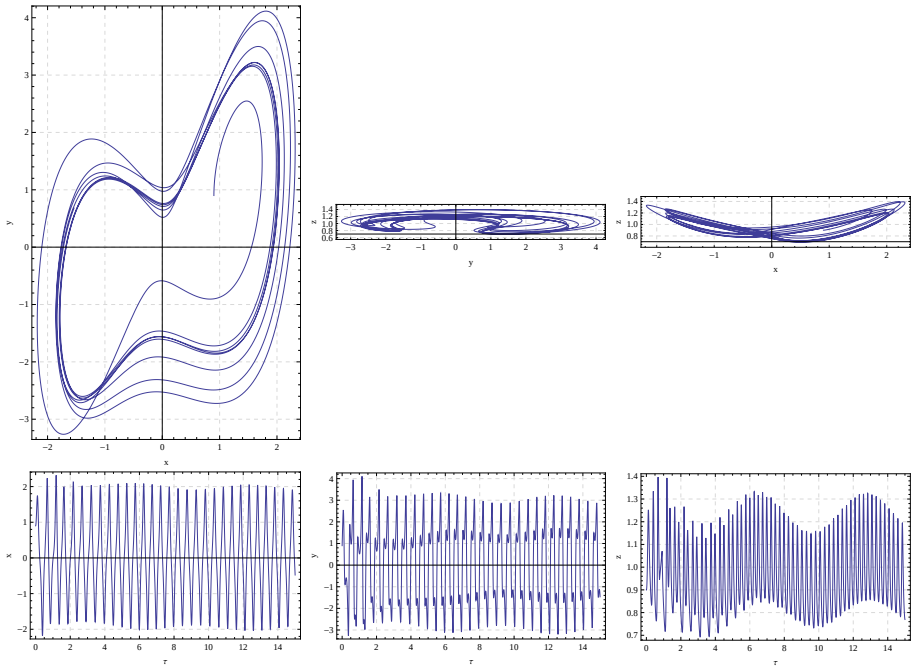

Figure 6.4: Phase portrait and time domain diagrams for the system (6.4.6) with parameters $R = 200$ and $\Gamma = 1$, $\Lambda' = 0.7$, $\delta = 0.1$

values of parameters are fixed as $\sigma = 10, \gamma = 0.5, \Omega = 1, \theta = \pi$. The parameters $R, \Gamma, \delta, \Lambda'$ are considered as variables to examine the effect of temperature modulation on the chaotic system. The phase-portrait diagrams depict how modulation term affects the dynamics of the thermal convection for a combination of varied parameters. The results are further depicted in Figures 6.2-6.15 to analyse the Lorenz model by using phase-portrait and time

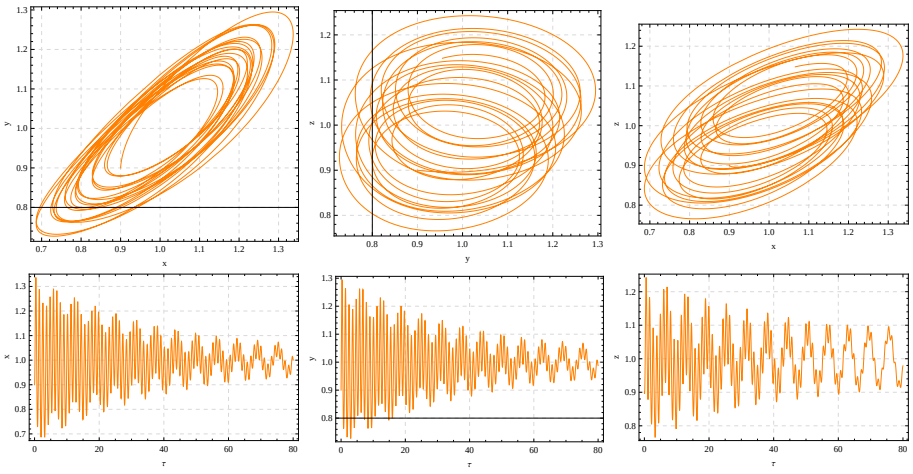

Figure 6.5: Phase portrait and time domain diagrams for the system (6.4.6) with parameters $\Gamma = 0.6$ and $R = 11$, $\Lambda' = 0.7$, $\delta = 0.1$

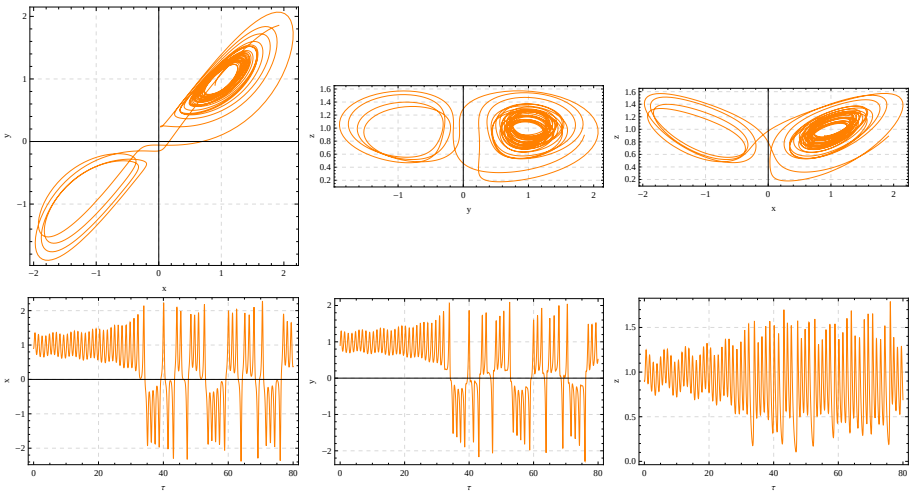

Figure 6.6: Phase portrait and time domain diagrams for the system (6.4.6) with parameters $\Gamma = 1.5$ and $R = 11$, $\Lambda' = 0.7$, $\delta = 0.1$

domain diagrams.

The effect of scaled Rayleigh number R on the system is depicted in Figures 6.2-6.4, keeping fixed the other parameters. Figure 6.2 ($R = 10$) shows a periodic solution but this periodicity of the system is not long lasting. Figure 6.3 ($R = 11$) depicts a transition from periodic to chaotic behaviour or aperiodic solution of the Lorenz system, which shows clearly that heat transfer is more on increasing R. Further, for higher values of $R = 200$, one can see that the system again represents a periodic behaviour, due to the decrease

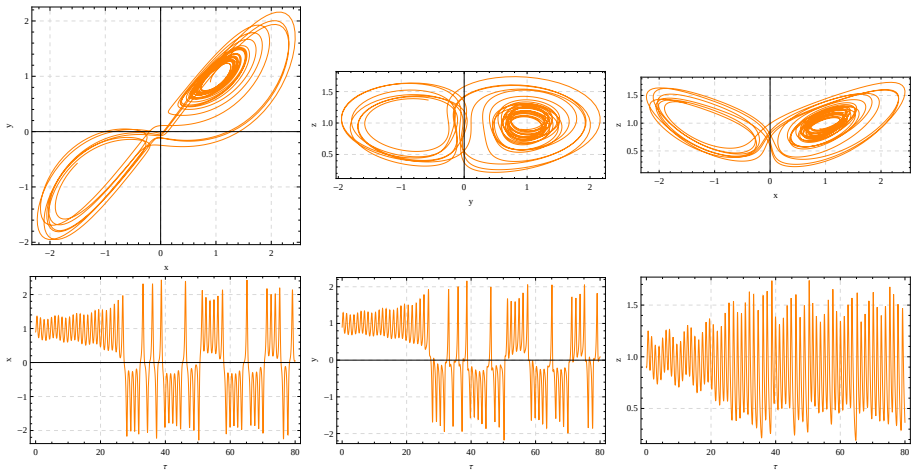

Figure 6.7: Phase portrait and time domain diagrams for the system (6.4.6) with parameters $\Gamma = 3$ and $R = 11$, $\Lambda' = 0.7$, $\delta = 0.1$

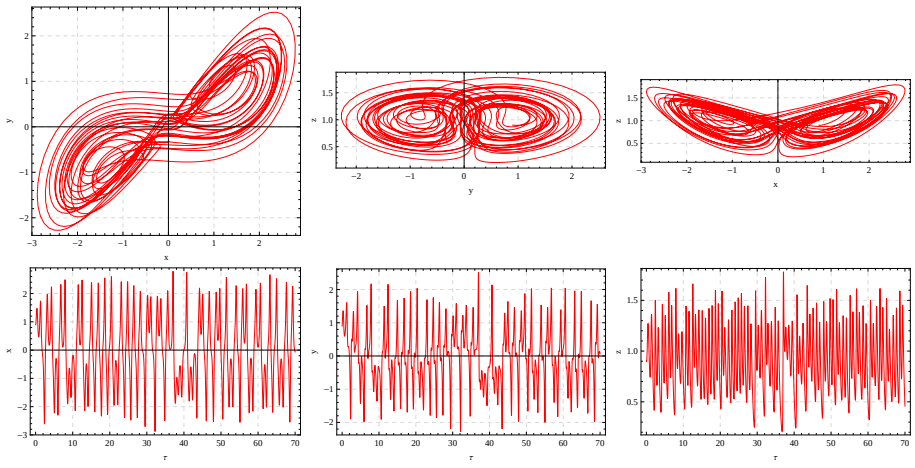

Figure 6.8: Phase portrait and time domain diagrams for the system (6.4.6) with parameters $\Lambda' = 0.5$ and $\Gamma = 1$, $R = 15$, $\delta = 0.1$

of the disturbances i.e. heat transfer. Thus, whenever R increases the heat transfer first increases and then decreases.

The effect of scaled relaxation parameter Γ can be seen in Figures 6.5-6.7 for its different values $\Gamma = 0.6, 1.5, 3$ respectively, keeping fixed the other parameters. It is evident that on increasing Γ the disturbance in solution increases, which is depicted by phase-portrait and time domain diagrams. The system looses its periodicity and transfers into chaotic solution, and so, heat transfer advances the convection. The scaled retardation parameter

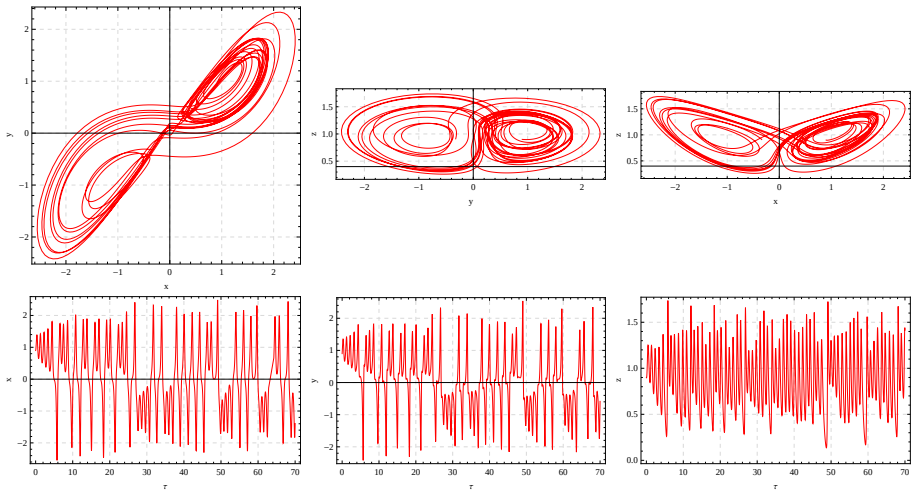

Figure 6.9: Phase portrait and time domain diagrams for the system (6.4.6) with parameters $\Lambda' = 0.7$ and $\Gamma = 1$, $R = 15$, $\delta = 0.1$

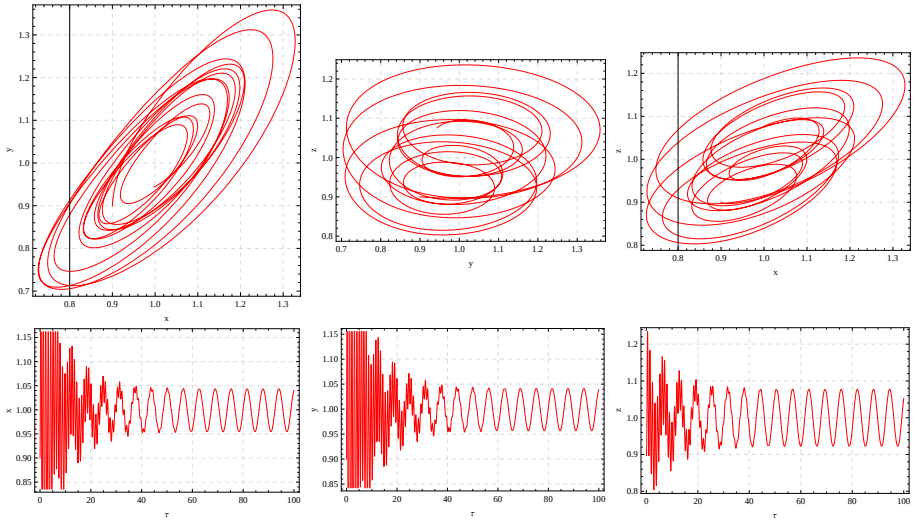

Figure 6.10: Phase portrait and time domain diagrams for the system (6.4.6) with parameters $\Lambda' = 0.9$ and $\Gamma = 1$, $R = 15$, $\delta = 0.1$

Λ' shows an opposite effect of the scaled relaxation parameter Γ, and is depicted in Figures 6.8-6.10 for $\Lambda' = 0.5, 0.7, 0.9$, keeping fixed other parameters. In this case, the system looses its chaotic behaviour and shows periodic behaviour. Heat transfer decreases which delays the convection, similar as Bhadauria and Kiran(2015b). The impact of amplitude of temperature modulation δ on the system for different parametric values $\delta = 0.01, 0.1, 0.3$ is depicted in Figures 6.11-6.13, respectively. These figures depict that the trajectories are much disturbed on increasing δ. Therefore, the chaotic behaviour advances, that is, the

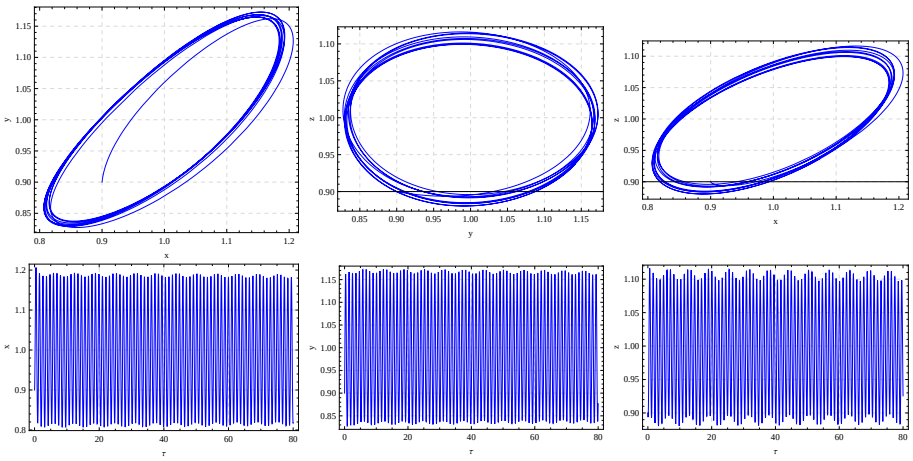

Figure 6.11: Phase portrait and time domain diagrams for the system (6.4.6) with parameters $\delta = 0.01$ and $\Gamma = 1$, $R = 11$, $\Lambda' = 0.7$

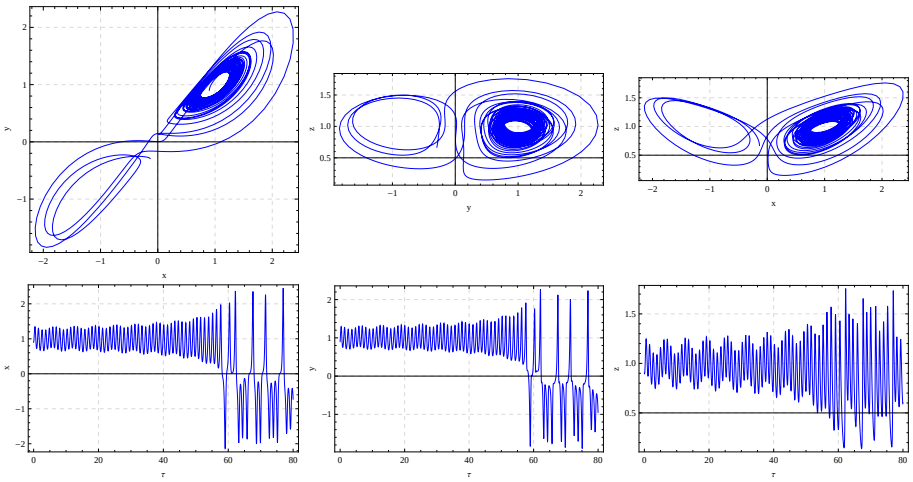

Figure 6.12: Phase portrait and time domain diagrams for the system (6.4.6) with parameters $\delta = 0.1$ and $\Gamma = 1$, $R = 11$, $\Lambda' = 0.7$

heat transfer increases gradually, which is same as Bhadauria and Kiran(2015a).

Finally, the results of temperature modulated and unmodulated systems are we compared. For $\delta = 0, R = 1.1$, the Figure 6.14 shows a stable solution as Long et al.(2008), clear from the plots, while for $\delta = 0.1, R = 1.1$, the system has periodic solution, as depicted in Figure 6.15. Overall, it is noticed from the diagrams that in temperature modulated system heat transfer is more in comparison to unmodulated system.

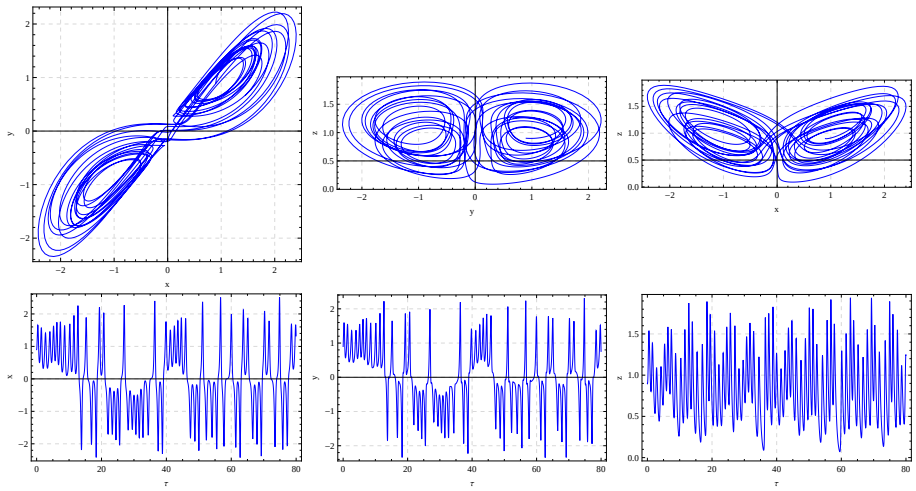

Figure 6.13: Phase portrait and time domain diagrams for the system (6.4.6) with parameters $\delta = 0.3$ and $\Gamma = 1$, $R = 11$, $\Lambda' = 0.7$

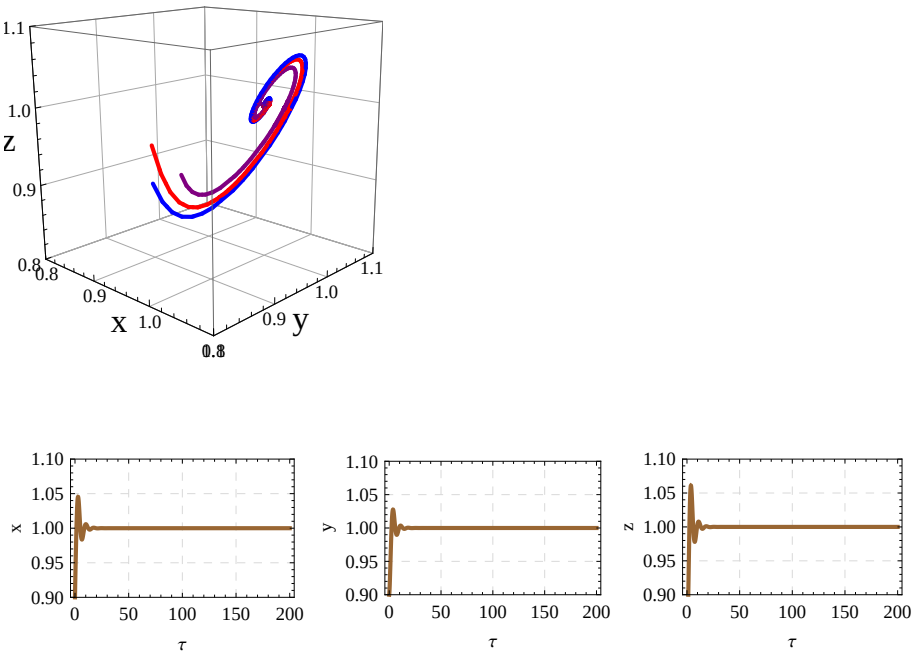

Figure 6.14: Phase portrait and time domain diagrams for the system (6.4.6) with parameters $\delta = 0.0$ and $\Gamma = 1$, $R = 1.1$, $\Lambda' = 0.1$

6.6 Conclusions

In this chapter, the chaotic convection of viscoelastic fluid saturated porous medium under temperature modulation is studied. The adopted model is first reduced into Lorentz

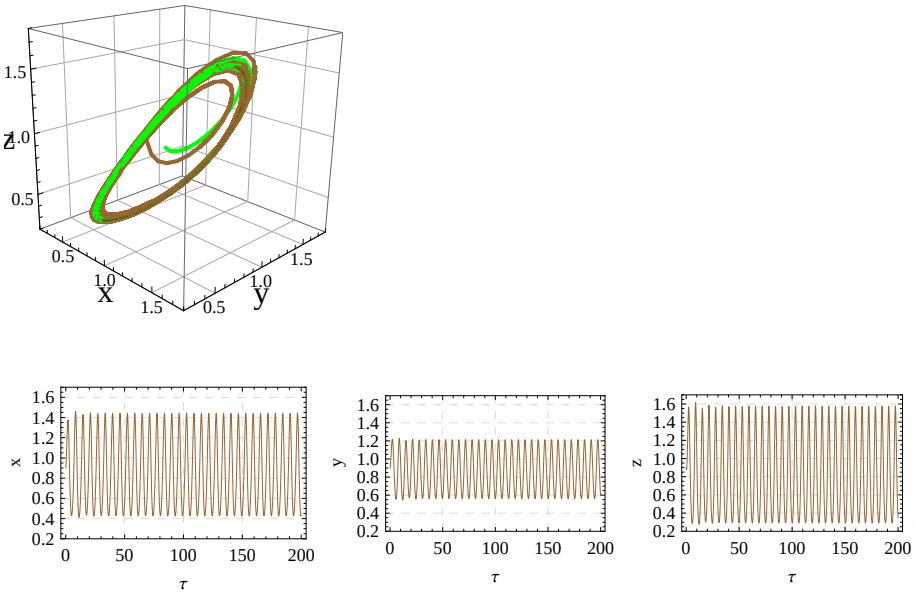

Figure 6.15: Phase portrait and time domain diagrams for the system (6.4.6) with parameters $\delta = 0.1$ and $\Gamma = 1$, $R = 1.1$, $\Lambda' = 0.1$

system by employing trauncated Galerkin expansion method. By using phase portrait and time domain diagrams, the following findings are obtained:

a) The effect of scaled Rayleigh number R is to increase or decease the heat transport in the Lorenz system.

b) The amplitude δ is to advance the heat transfer in the Lorenz system.

c) The scaled relaxation parameter Γ has tendency to advance the chaotic behaviour whereas the scaled retardation parameter Λ' delays the chaotic behaviour in the system.

d) Finally, it is obtained that heat transfer is more in the modulated system than in unmodulated system.

Chapter 7

Nonlinear g-jitter thermal instability in nanofluid in the presence of throughflow and heat source

7.1 Introduction

Due to their enhanced abilities over ordinary fluids as heat exchangers and transporters, nanofluids are being used as heat transfer media from the last few years. Few small quantity of nanoparticles in base fluid produces a significant enhancement in the heat transfer characteristics. This characteristic of nanofluids depends on the thermo-physical properties of the base fluid and the suspended nanoparticles. The nanofluids found a wide range of applications in industrial, commercial, residential and transportation sectors. The main feature of nanofluids is the thermal conductivity enhancement, which was first given by Masuda et al.(1993). The term nanofluid was introduced by Choi(1995). Buongiorno(2006) was the first, to develop a model for convective transport in nanofluids. An extension to the porous medium of this model was studied by Nield and Kuznetsov(2009). Two-dimensional non-

This chapter is based on the research article: Nonlinear g-jitter thermal instability in nanofluid in the presence of throughflow and heat source, communicated.

linear convection in nanofluid saturated porous medium have been studied by Bhadauria and Agarwal(2011a).

Throughflow during convection is an effective mechanism to control the convective flow in engineering sciences, industries, geophysics etc. The basic state temperature profile of throughflow changes from linear state to nonlinear state with layer of height, which affects the stability of the system. There are many studied available on throughflow mechanism, some of them are, Wooding(1960), Sutton(1970), Gershuni(1976), Nield(1987), Shivakumara(1999), Barletta et al.(2010), Nield and Kuznetsov(2011). Nield and Kuznetsov(2015) has done a study with throughflow under the revised boundary conditions, where they considered that the total nanoparticle flux is the sum of diffusive, convective and thermophoretic terms. Convective heat transfer in porous media has received much attention during the past few decades because of its wide range of applications in many engineering and natural systems of practical interest; for instance, in geothermal energy utilization, in thermal energy storage and recovery systems, in petroleum reservoirs, in industrial and agricultural water distribution. There are several articles in which the effect of internal heating on convective flow has been investigated, some of them are; Roberts(1967), Tveitereid(1976), Yu and Shih(1980), Bhattacharya and Jena(1984), Takashima(1989), Joshi et al.(2006).

Therefore, in this chapter a nonlinear g-jitter thermal instability in nanofluid in the presence of throughflow and internal heat source has been studied. A weakly nonlinear stability analysis has been carried out to obtain the Nusselt number to check the heat and mass transport in the system. Effect of each parameter has been depicted graphically in terms of the Nusselt number as function of t.

7.2 Mathematical structure of the problem

An infinitely extended horizontal nanofluid layer of depth d, confined between two parallel planes, the lower plane at $z = 0$ while the upper plane at $z = d$ is considered. A Cartesian

frame of reference is adopted in such a way that the origin lies on the lower plane and z axis is vertically upward. The nanofluid layer is heated from below and cooled from above. The physical configuration of the model is depicted in Figure 7.1. Darcy law and Oberbeck-Boussinesq approximation are adopted to model the physical problem. The governing equations to study the thermal instability in a nanofluid layer are [Buongiorno(2006), Nield and Kuznetsov (2013)]

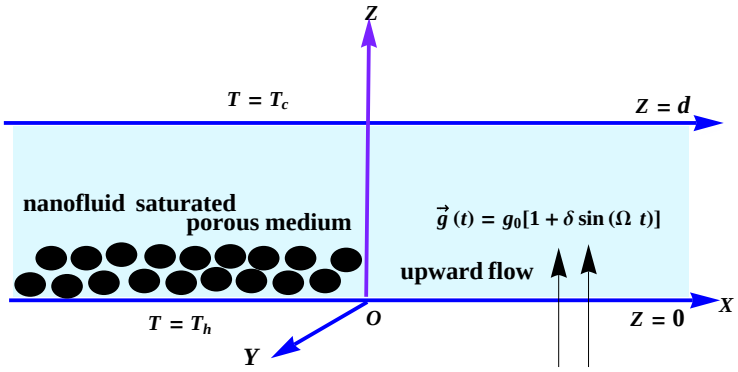

Figure 7.1: Physical configuration of the problem

$$\begin{cases} \nabla.\vec{q} = 0, \\ \rho_f \frac{\partial \mathbf{q}}{\partial t} + \frac{\mu}{K}\mathbf{q} + \nabla p = \big(\phi\rho_p + (1-\phi)[\rho_f(1-\beta(T-T_c))]\big)\mathbf{g}, \\ (\rho c)_f \left(\frac{\partial T}{\partial t} + \mathbf{q}.\nabla T\right) = k_{nf}\nabla^2 T + (\rho c)_p \left(D_B \nabla\phi + \frac{D_T}{T_c}\nabla T\right).\nabla T + Q(T-T_c), \\ \frac{\partial \phi}{\partial t} + \frac{1}{\epsilon}\mathbf{q}.\nabla\phi = D_B\nabla^2\phi + \frac{D_T}{T_c}\nabla^2 T, \\ g(\vec{t}) = g_0(1+\delta\sin(\Omega t)), \end{cases} \tag{7.2.1}$$

where ρ_f, ρ_p are density of fluid and nanoparticle respectively. k_{nf} is thermal diffusivity of nanofluid. T_h and T_c are the temperatures at the lower and upper walls such that $T_h > T_c$. The constants and variables used in the above equations have their usual meanings, and

are given in the nomenclature. The boundary conditions are taken as

$$\begin{cases} \mathbf{q} = 0, T = T_h, \phi = \phi_0 \ \text{ at } \ z = 0, \\ \\ \mathbf{q} = 0, T = T_c, \phi = \phi_1 \ \text{ at } \ z = d, \end{cases} \tag{7.2.2}$$

where $\phi_1 > \phi_0$.

The non-dimensionalized governing equations are as Bhadauria and Kiran(2014)

$$\begin{cases} \nabla.\vec{q} = 0, \\ \\ \frac{1}{Pr}\frac{\partial \mathbf{q}}{\partial t} + \mathbf{q} = -\nabla p - g_m(Rm - RaT + Rn\phi), \\ \\ \frac{\partial T}{\partial t} + \mathbf{q}.\nabla T = \nabla^2 T + \frac{N_B}{Le}\nabla\phi.\nabla T + \frac{N_A N_B}{Le}\nabla T.\nabla T + R_i T, \\ \\ \frac{\partial \phi}{\partial t} + \frac{1}{\epsilon}\mathbf{q}.\nabla\phi = \frac{1}{Le}\nabla^2\phi + \frac{N_A}{Le}\nabla^2 T, \\ \\ g_m = (1 + \delta\sin(\Omega t)), \end{cases} \tag{7.2.3}$$

with the boundary conditions

$$\begin{cases} \mathbf{q} = 0, T = 1, \phi = 0 \ \text{ at } \ z = 0, \\ \\ \mathbf{q} = 0, T = 0, \phi = 1 \ \text{ at } \ z = d. \end{cases} \tag{7.2.4}$$

The non-dimensionlized parameters in the above equations are as given below

$$P_e = \frac{w_0}{k_T z}, \qquad R_i = \frac{Qd^2}{k_T}, \qquad P_r = \frac{\mu(\rho c)_f}{\rho_f k_f},$$

$$Ra = \frac{\rho_f g_0 \beta d(T_h - T_c)}{\mu\alpha_f}, \quad Rn = \frac{(\rho_p - \rho_f)\phi_0 g_0 d}{\mu\alpha_f}, \quad Rm = \frac{\big(\rho_p\phi_0 + \rho_f(1-\phi_0)\big)g_0 d}{\mu\alpha_f}, \tag{7.2.5}$$

$$N_A = \frac{D_T(T_h - T_c)}{D_B T_c \phi_0}, \qquad N_B = \frac{(\rho c)_p}{(\rho c)_f}\phi_0, \qquad Le = \frac{\alpha_f}{D_B}.$$

7.3 Basic state

At the basic state, the nanofluid layer is at rest, so it is assumed that

$$\vec{q_b} = (0, 0, P_e), \quad p = p_b(z), \quad T = T_b(z), \quad \phi = \phi_b(z). \tag{7.3.1}$$

After putting Eq.(7.3.1) in Eq.(7.2.3) the following basic state equations are obtained

$$\frac{d^2T_b}{dz^2} - P_e\frac{dT_b}{dz} + R_iT_b = 0,$$

$$\frac{d^2\phi_b}{dz^2} + N_A\frac{d^2T_b}{dz^2} - \frac{P_eLe}{\epsilon}\frac{d\phi_b}{dz} = 0.$$

7.4 Perturbed state

Basic state of the system is perturbed by superimposing the finite amplitude disturbances as

$$\vec{q} = q_b + q', T = T_b + T', p = p_b + p', \phi = \phi_b + \phi'. \tag{7.4.1}$$

7.5 Non-linear stability analysis

Using Eq.(7.3.1) and Eq.(7.4.1) in system of Eqs.(7.2.3), eliminating the pressure and introducing the stream function, the obtained system is

$$\begin{cases} \left(\frac{1}{P_r}\frac{\partial\nabla^2}{\partial t} + \nabla^2\right)\psi = \left(-Ra\frac{\partial T}{\partial x} + Rn\frac{\partial\phi}{\partial x}\right)g_m, \\ \frac{\partial T}{\partial t} - \frac{\partial T_b}{\partial z}\frac{\partial\psi}{\partial x} = \nabla^2T + \frac{\partial(\psi,T)}{\partial(x,z)} + R_iT - P_e\frac{\partial T}{\partial z}, \\ \frac{\partial\phi}{\partial t} - \frac{1}{\epsilon}\frac{\partial\phi_b}{\partial z}\frac{\partial\psi}{\partial x} = \frac{1}{Le}\nabla^2\phi + \frac{N_A}{Le}\nabla^2T + \frac{1}{\epsilon}\frac{\partial(\psi,\phi)}{\partial(x,z)}. \end{cases} \tag{7.5.1}$$

The basic state temperature field and basic state nanoparticle volume fraction, involved in

system of Eq.(7.5.1) are obtained by using basic state equations, given by

$$\begin{cases} T_b = \frac{e^{d_1+\frac{1}{2}(P_e-d_1)z}-e^{\frac{1}{2}(P_e+d_1)z}}{-1+e^{d_1}}, \\ \\ \phi_b = \frac{1}{4}\left(\frac{4e^{\frac{1}{2}(P_e-d_1)z}N_A\left(\frac{e^{d_1 z(P_e+d_1)}}{d_1+P_e-2\Lambda}+\frac{e^{d_1(-d_1+P_e)}}{d_1-P_e+2\Lambda}\right)}{-1+e^{d_1}}\right), \end{cases} \tag{7.5.2}$$

where $d_1 = \sqrt{P_e^2 - 4R_i}$, $\quad \Lambda = \frac{P_e Le}{\epsilon}$.

A local nonlinear stability analysis is performed by taking the following Fourier expressions:

$$\begin{cases} \psi = A_{11}(t)\sin(ax)\sin(\pi z), \\ \\ T = B_{11}(t)\cos(ax)\sin(\pi z) + B_{02}(t)\sin(2\pi z), \\ \\ \phi = C_{11}(t)\cos(ax)\sin(\pi z) + C_{02}(t)\sin(2\pi z). \end{cases} \tag{7.5.3}$$

Substituting the Eq.(7.5.3) in Eq.(7.5.1) and using the orthogonality condition the following system is obtained

$$\begin{cases} \frac{dA_{11}(t)}{dt} = \frac{P_r}{c}\left(ag_m(RnC_{11} - RaB_{11}) - cA_{11}\right), \\ \\ \frac{dB_{11}(t)}{dt} = \frac{\pi a}{k_1}k_2 A_{11} - (c - R_i)B_{11} - \pi a A_{11}B_{02}, \\ \\ \frac{dB_{02}(t)}{dt} = \frac{1}{2}(-8\pi^2 B_{02} + 2R_i B_{02} + \pi a A_{11}B_{11}), \\ \\ \frac{dC_{11}(t)}{dt} = \frac{4a}{\pi}\left(-k_3 A_{11} - \frac{3N_A(-8\pi^2+(-2+P_e)R_i)}{96\pi\epsilon}A_{11} - \frac{\pi^2}{4\epsilon}A_{11}C_{02}\right) - \frac{\pi c}{4Lea}(N_A B_{11} + C_{11}), \\ \\ \frac{dC_{02}(t)}{dt} = \frac{-8\pi^2 N_A \epsilon B_{02} - 8\pi^2 \epsilon C_{02} + \pi Lea A_{11}C_{11}}{2Le\epsilon}, \end{cases} \tag{7.5.4}$$

where

$$c = \pi^2 + a^2, \quad k_1 = (-1 + e^{d_1})(16\pi^4 + 4\pi^2(P_e^2 - 2R_i) + R_i^2),$$

$$k_2 = (-1 + e^{d_1})(16\pi^3 + 2\pi P_e^2) - 2\pi(-1 + 2e^{\frac{P_e + d_1}{2}} - e^{d_1})P_e d_1 - 4\pi R_i(-1 + e^{d_1}),$$

$$k_3 = \frac{1}{96\pi\epsilon^2} P_e Le(-12N_A\pi^2 + N_A(3 + \pi^2)R_i).$$

The above system of simultaneous autonomous ordinary differential equations can be subsequently solved numerically using Mathematica NDSolve.

7.6 Nusselt number for heat and mass transport

The horizontally averaged thermal Nusselt number, is defined as:

$$Nu(t) = \frac{\text{heat transport by (conduction+convection)}}{\text{heat transport by conduction}},$$

$$Nu(t) = 1 + \left(\int_0^{2\pi/a} \left(\frac{\partial T}{\partial z} \right)_{z=0} dx \Big/ \int_0^{2\pi/a} \left(\frac{\partial T_b}{\partial z} \right)_{z=0} dx \right).$$

The nanoparticle concentration Nusselt number $Nu_\phi(t)$ is defined similar to the thermal Nusselt number $Nu(t)$ as

$$Nu_\phi(t) = \frac{\text{mass transport by (molecular diffusion+advection)}}{\text{mass transport by molecular diffusion}}.$$

The numerical values of both types of Nusselt numbers are obtained by using Eq.(7.5.2), Eq.(7.5.3) and are given by

$$\begin{cases} Nu(t) = 1 + \frac{2\pi B_{02}}{k_4}, \\ \\ Nu_\phi(t) = 1 + \frac{2\pi C_{02}}{k_5} + N_A(1 - 2\pi B_{02}), \end{cases} \tag{7.6.1}$$

where k_4 and k_5 are given by

$$k_4 = \frac{(-P_e-d_1)+e^{d_1}(P_e-d_1)}{2(-1+e^{d_1})}, \qquad k_5 = \frac{d_1 N_A(P_e+d_1)}{(-1+e^{d_1})(d_1+P_e-2\Lambda)} + \frac{N_A(P_e-d_1)\left(\frac{P_e+d_1}{d_1+P_e-2\Lambda}+\frac{e^{d_1}(P_e-d_1)}{d_1-P_e+2\Lambda}\right)}{2(-1+e^{d_1})}.$$

7.7 Results and Discussion

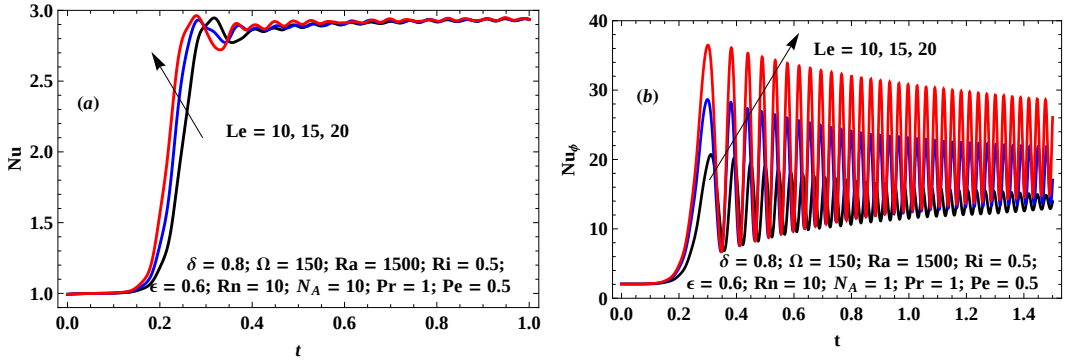

Figure 7.2: Effect of Le on heat and mass transfer

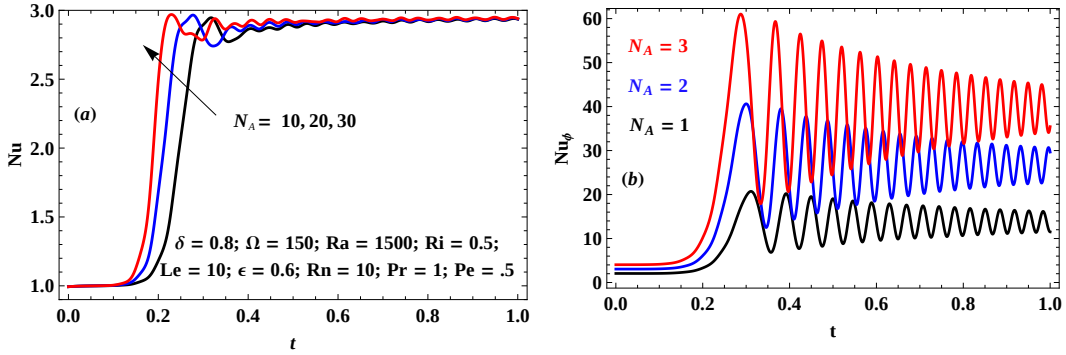

Figure 7.3: Effect of N_A on heat and mass transfer

This chapter investigates the effect of nonlinear g-jitter thermal instability in nanofluid in the presence of throughflow and internal heating effects, considering gravity modulation. A weakly nonlinear stability analysis has been performed. It is to be noticed that according to Buongiorno(2006), for most nanofluids investigated so far Le is large, but in the present case $Le = 10$ has been considered as per Bhadauria and Agarwal(2011b). The effect of all convective parameters on heat and mass transport is depicted in terms of Nusselt number, in Figures 7.2-7.10. In all Figures parts **(a)** show heat transfer while parts **(b)** show mass transfer in the system.

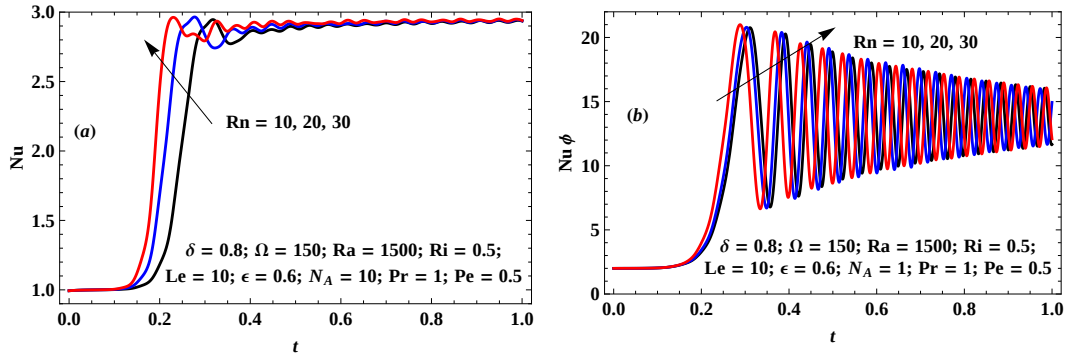

Figure 7.4: Effect of Rn on heat and mass transfer

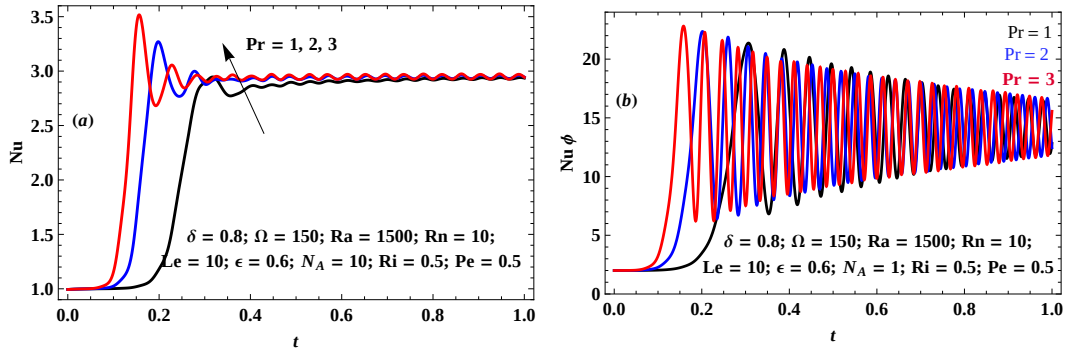

Figure 7.5: Effect of P_r on heat and mass transfer

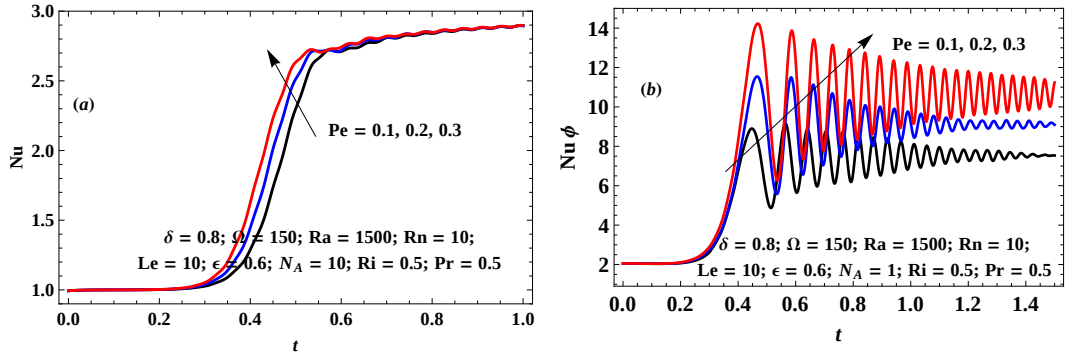

Figure 7.6: Effect of P_e on heat and mass transfer

The influence of nanofluid parameters like Le, N_A and Rn is depicted in Figures 7.2-7.4. It is noticed from these figures that Lewis number Le, modified diffusivity ratio N_A and the concentration Rayleigh number Rn have a destabilizing effect on the system. An increment in the value of any of these parameters increases heat and mass transfer in the system, same as the results of Bhadauria and Kiran (2014). Figures 7.5-7.7 show a destabilizing

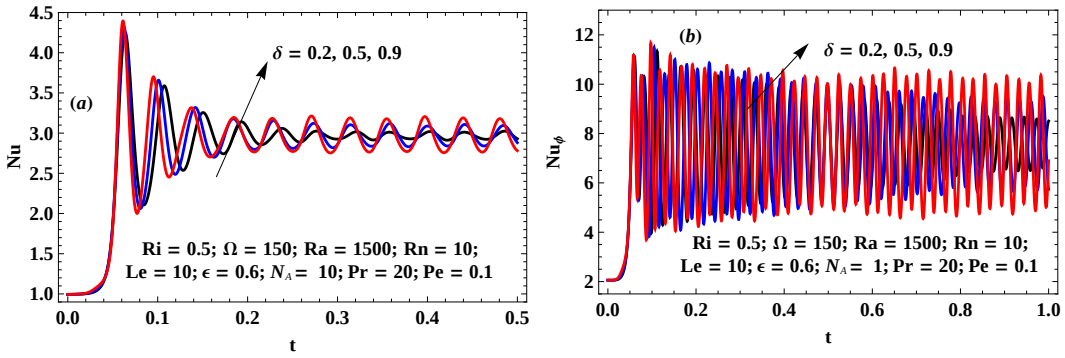

Figure 7.7: Effect of δ on heat and mass transfer

effect of each parameters P_r, P_e and δ respectively, as convection advances on increasing the values of these parameters. Figures 7.8-7.9 show the effect of frequency of modulation Ω and internal Rayleigh number R_i. It is clear from the graphs that for higher values of Ω, system represents a stable behaviour due to delay in convection while for increasing values of R_i, the system has an opposite (destabilize) effect. In the last, the results of modulated and unmodulated systems are compared. It is found that heat and mass transport is more in modulated case as presented in the Figure 7.10.

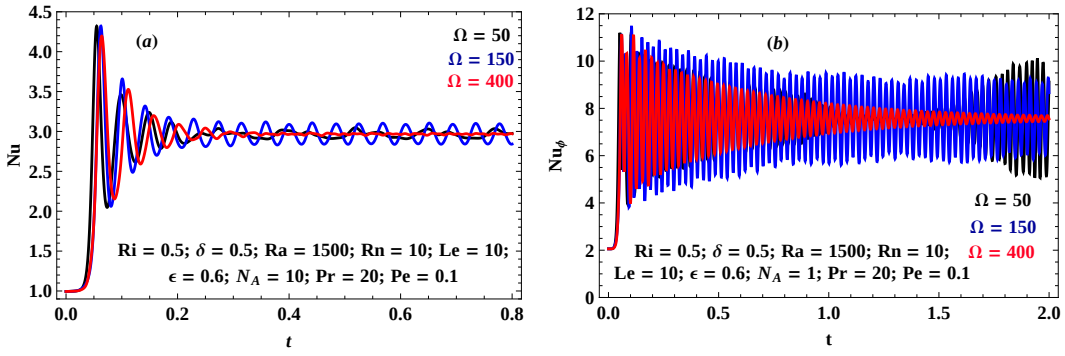

Figure 7.8: Effect of Ω on heat and mass transfer

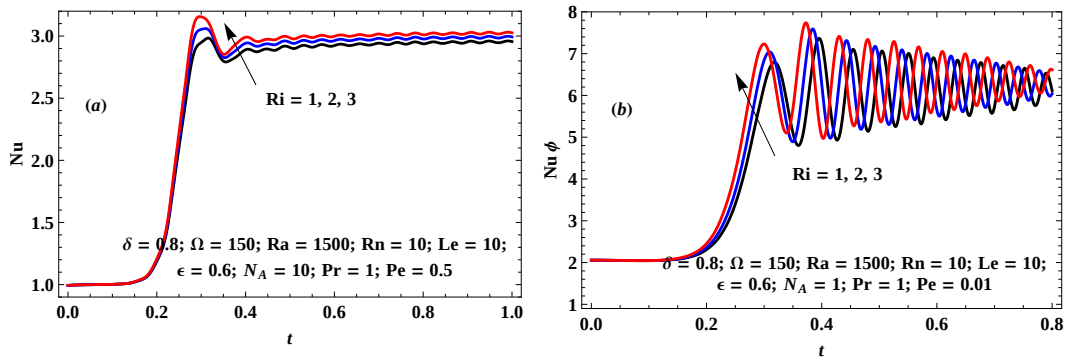

Figure 7.9: Effect of R_i on heat and mass transfer

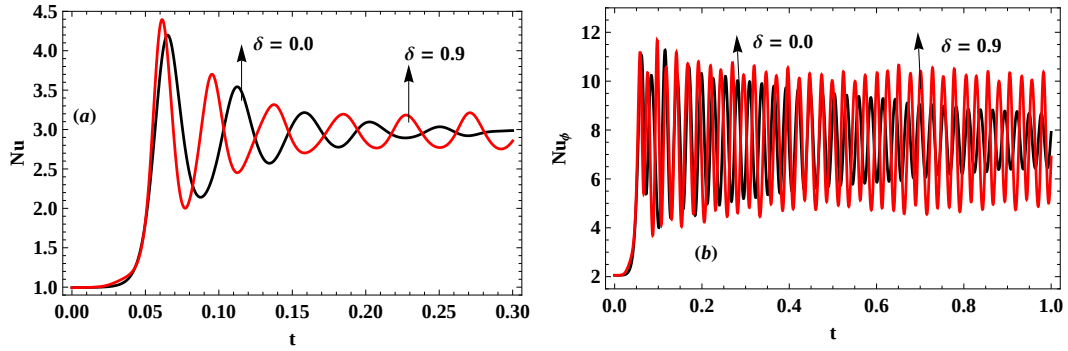

Figure 7.10: Comparison between modulated and unmodulated system

7.8 Conclusions

The findings of the physical problem are as follows:

a) The nanofluid parameters Le, N_A and Rn have destabilizing effect.

b) The Prandtl number P_r, Péclet number P_e, and amplitude of modulation δ have destabilizing effects on the system.

c) The frequency of modulation Ω diminishes the heat transfer rate and shows stabilizing effect on heat and mass transport.

d) The system shows destabilizing effect for internal Rayleigh number R_i.

e) Finally, it is obtained that heat transfer is more in the modulated system in comparison to the unmodulated system.

Bibliography

[1] Alok et al. (2013); Heat Transport in an anisotropic porous medium saturated with variable viscosity liquid under G-jitter and internal heating effects. Transp. Porous Med. 99(2), 359-376.

[2] Altawallbeh AA, Bhadauria BS, Hashim I (2013); Linear and nonlinear double-diffusive convection in a saturated anisotropic porous layer with Soret effect and internal heat source. Int J Heat Mass Trans. 59, 103-111.

[3] Barletta A, di Schio ER, Storesletten L(2010); Convective roll instabilities of vertical throughflow with viscous dissipation in a horizontal porous layer. Transp. Porous Med. 81, 461-77.

[4] Bénard H (1900); Les Tourbillons cellularies dans une nappe liquide, Revue generale des sciences pures et appliques. 11, 1261-1271 and 1309-1328.

[5] Bhadauria BS (2006a); Time-periodic heating of Rayleigh-Bénard convection in a vertical magnetic field. Phys. Scr. 73(3), 296.

[6] Bhadauria BS (2006b); Gravitational modulation of Rayleigh-Bénard convection. Proc Natl Acad Sci India 76(A), 61-67.

[7] Bhadauria BS (2007); Fluid convection in a rotating porous layer under modulated temperature on the boundaries. Transp. Porous Med. 67, 297-315.

[8] Bhadauria BS (2012); Double diffusive convection in a saturated anisotropic porous layer with internal heat source. Transport in Porous Med. 92, 299-320.

[9] Bhadauria BS, Agarwal S, Kumar A (2011a); Non-linear two-dimensional convection in a nanofluid saturated porous medium. Transp. Porous Med. 90(2), 605-625.

[10] Bhadauria BS, Agarwal S (2011b); Natural convection in a nanofluid saturated rotating porous layer. Transp. Porous Med. 87, 585-602.

[11] Bhadauria BS, Anoj K, Jogendra K, Sacheti NC, Chandran P (2011); Natural convection in a rotating anisotropic porous layer with internal heat generation. Transp. Porous Med. 90(2), 687-705.

[12] Bhadauria BS, Bhatia PK (2002); Time periodic heating of Rayleigh-Bénard convection. Physica Scripta. 66, 59-65.

[13] Bhadauria BS, Bhatia PK, Debnath L (2005); Convection in Hele-Shaw cell with parametric excitation. Int. J. Non-Linear Mech. 40, 475-484.

[14] Bhadauria BS, Bhatia PK, Debnath L (2009); Weakly nonlinear analysis of Rayleigh-Bénard convection with time periodic heating. Int. J. of Non-Linear Mech. 44(1), 58-65.

[15] Bhadauria BS, Hashim I, Siddheshwar PG (2013); Effect of internal-heating on weakly non-linear stability analysis of Rayleigh-Benard convection under G-jitter. Int. J. Non-Linear Mech. 54, 35-42.

[16] Bhadauria BS, Hashim I, Siddheshwar PG (2013); Study of heat transport in a porous medium under G-jitter and internal heating effects. Transp. Porous Med. 96, 21-37.

[17] Bhadauria BS, Kiran P (2013); Heat transport in an anisotropic porous medium saturated with variable viscosity liquid under temperature modulation. Transp. Porous Med. 100(2), 279-295.

[18] Bhadauria BS, Kiran P (2014); Non-linear thermal Darcy convection in a nanofluid saturated porous medium under gravity modualtion. Advanced Science Letters. 20, 903-910.

[19] Bhadauria BS, Kiran P (2014a); Weakly non-linear oscillatory convection in a viscoelastic fluid saturating porous medium under temperature modulation. Int. J. Heat Mass Transf. 77, 843-851.

[20] Bhadauria BS, Kiran P (2014b); Weakly non-linear oscillatory convection in a viscoelastic fluid layer under gravity modulation. Int. J. Non-Linear Mech. 65, 133-140.

[21] Bhadauria BS, Kiran P (2014c); Weakly non-linear double diffusive magneto-convection in a Newtonian liquid under temperature modulation. Int. J. Engg. Mathe. Hindawi, 1-14.

[22] Bhadauria BS, Kiran P (2014d); Heat and mass transfer for oscillatory convection in a binary viscoelastic fluid layer subject to temperature modulation by using complex Ginzburg-Landau equation. Int. Communi. Heat and mass Transf. 58, 166-175.

[23] Bhadauria BS, Kiran P (2015); Nonlinear throughflow effects on thermally modulated porous medium (in press). doi:10.1016/j.asej.03.010

[24] Bhadauria BS, Kiran P (2015a); Chaotic convection in a porous medium under temperature modulation. Transp. Porous med. 107, 745-763.

[25] Bhadauria BS, Kiran P (2015b); Chaotic and oscillatory magneto-convection in a binary viscoelastic fluid under G-jitter. Int. J. Heat Mass Transf. 84, 610-624.

[26] Bhadauria BS, Kiran P (2016); Weakly non-linear oscillatory convection in a rotating fluid layer under temperature modulation. ASME DOI- 10.1115/1.4032329.

[27] Bhadauria BS, Kumar J (2012); Stability analysis of Temperature/Gravity-Modulated stationary Rayleigh-Bénard convection in a rotating porous medium, Transp Porous Med. 92, 633-647.

[28] Bhatia PK, Steiner JM (1972); Convective instability in a rotating viscoelastic fluid layer. ZAMM. 52, 321-327.

[29] Bhattacharya SP, Jena SK (1984); Thermal instability of a horizontal layer of micropolar fluid with heat source. Proceedings of the Indian Academy of Sciences (Mathematical Sciences) 93(1), 13-26.

[30] Biringen S, Peltier LJ (1990); Numerical simulation of 3D Bénard convection with gravitational modulation. Physics of Fluids(A). 2, 754-764.

[31] Brevdo L (2009); Three-dimensional absolute and convective instabilities at the onset of convection in a porous medium with inclined temperature gradient and vertical throughflow. J. Fluid Mech. 641, 475-87.

[32] Buongiorno J (2006); Convective transport in nanofluids. ASME J. Heat Transf. 128, 240-250.

[33] Caltaoirone JP (1976); Stability of a horizontal porous layer under periodical boundary conditions. Int. J. Heat Mass Transf. 19, 815-820.

[34] Capone F, Gentile M, Hill AA (2011); Double-diffusive penetrative convection simulated via internal heating in an anisotropic porous layer with throughflow. Int. J. Heat Mass Transf. 54, 1622-1626.

[35] Chandrasekhar S (1961); Hydrodynamic and Hydromagnetic Stability. Oxford University Press, Oxford, UK.

[36] Chen WY, Chen CF (1999); Effect of gravity modulation on the stability of convection in a vertical slot. J. Fluid. Mech. 395, 327-344.

[37] Chhuon B, Caltagirone JP (1979); Stability of a horizontal porous layer with time wise periodic boundary conditions. ASME J. Heat Transf. 101, 244-248.

[38] Choi S (1995); Enhancing thermal conductivity of fluids with nanoparticles, In: Siginer DA, Wang HP (eds) Development and applications of Non-Newtonian Flows. ASME FED 231/MD. 66, 99-105.

[39] Clever R, Schubert G, Busse FH (1993); Two dimensional oscillatory convection in a gravitationally modulated fluid layer. J. of Fluid Mech. 253, 663-680.

[40] Comissiong Donna MG, Dass TD, Ramkissoon H, Sankar AR (2011); On thermal instabilities in a viscoelastic fluid subject to internal heat generation. World Acad. Sci.Eng.Tech. 56, 08-24.

[41] Degan G, Vasseur P, Bilgen E (1995); Convective heat transfer in a vertical anisotropic porous layer. Heat Mass Transf. 38(11), 1975-1987.

[42] Epherre JF (1977); Crit'ere d'apparition de la convection naturalle dans une couche poreuse anisotrope. Rev. Gn. Thermique, 1975 168 949-950 English translation Int Chem. Eng. 17, 615-616.

[43] Finucane RG, Kelly RE (1976); Onset of instability in a fluid layer heated sinusoidally from below. Int J Heat Mass Transf. 19, 71-85.

[44] Friedrich R (1983); Einfluss der Prandtl-Zahl auf die Zellularkonvektion in einem rotieren-den, mil Fluid gesattigten porosen Medium. Z. Angew. Math. Mech. 63, T246-T249.

[45] Gershuni GZ, Zhukhovitskii EM (1963); On parametric excitation of convective instability. J. Appl. Math. Mech. 27, 1197-1204.

[46] Gershuni GZ, Zhukhovitskii EM (1976); Convective stability in incompressible fluids. Jerusalem Keter Publishing House.

[47] Govender S (2003); Oscillatory convection induced by gravity and centrifugal forces in a rotating porous layer distant from the axis of rotation. Int. J. Eng. Sci. 41(6), 539-545.

[48] Govender S (2004); Three dimensional convection in an inclined porous layer heated from below and subjected to gravity and coriolis effects. Transp Porous Med. 55, 103-112.

[49] Govender S (2005); Weak non-linear analysis of convection in a gravity modulated porous layer. Transp. Porous Med. 60, 33-42.

[50] Govender S (2005a); Linear stability and convection in a gravity modulated porous layer heated from below:transition from synchronous to subharmonic solutions. Trans. Porous Med. 59, 227-238.

[51] Govender S (2006); On line effect of anisotropy on the stability of convection in a rotating porous media. Transp. Porous Med. 64, 413-422.

[52] Govender S (2007); Coriolise effect on the stability of centrifugally driven convection in a rotating anisotropic porous layer subject to gravity. Transp. Porous Med. 69, 55-66.

[53] Green T (1968); Oscillating convection in an elasticoviscous liquid. Phys. Fluids. 111410.

[54] Gresho PM, Sani R (1970); The effects of gravity modulation on the stability of a heated fluid layer. J. Fluid Mech. 40, 783-806.

[55] Griffith RW (1981); Layered double-diffusive convection in porous media. J. Fluid Mech. 102, 221-248.

[56] Gupta et al. (2015); Chaotic convection in a rotating fluid layer. Alexandria Engineering Journal. In Press.

[57] Gupta et al. (2016); Chaotic convection in couple stress liquid saturated porous layer. Int. J. Industrial Mathematics. 8(2), 00675.

[58] Gupta VK, Bhadauria BS, Siddheshwar PG, Singh AK (2016); A local nonlinear stability analysis of modulated double diffusive stationary convection in a couple stress liquid. JAFM. 9, 1255-1264.

[59] Gupta VK, Kumar A, Vanita (2016a); Study of heat and mass transport in couple-stress liquid under G-jitter effect. Ain Shams Engineering J. Article in Press.

[60] Gupta VK, Singh AK (2013); A study of chaos in an anisotropic porous cavity. Int. J. of Energy and Technology. 5(27), 1-12.

[61] Haajizadeh M, Ozguc AF, Tien CL(1984); Natural convection in a vertical porous enclosure with internal heat generation. Int. J. Heat Mass Transf. 27, 1893-1902.

[62] Holzbecher E (1998); The influence of variable viscosity on thermal convection in porous media. International conference on advanced computational methods in heat transfer. 115-124, Cracow, 17-19 June.

[63] Homsy GM, Sherwood AE (1976); Convective instabilities in porous media with throughflow. AICHE J. 22, 168-74.

[64] Horton CW, Rogers FT (1945); Convection currents in a porous medium. J. Appl. Phys. 16, 367-370.

[65] Ingham DB, Pop I (2005); Transport Phenomena in Porous Media. vol. III, 1st ed. Elsevier, Oxford.

[66] Jones MC, Persichetti JM (1986); Convective instability in packed beds with throughflow. AIChE J. 32, 1555-557.

[67] Joshi MV, Gaitonde UN, Mitra SK (2006); Analytical study of natural convection in a cavity with volumetric heat generation. ASME J. Heat Transf. 128, 176-182.

[68] Khalili A, Shivakumara IS (1998); Onset of convection in a porous layer with net throughflow and internal heat generation. Phys of Fluids. 10, 315.

[69] Kim MC, Lee SB, Kim S, Chung BJ (2003); Thermal instability of viscoelastic fluids in porous media. Int. J. Heat Mass Transf. 46, 5065-5072.

[70] Kiran P, Bhadauria BS, Kumar V (2016); Thermal convection in a nanofluid saturated porous medium with internal heating and gravity modulation. J. Nanofluids. 5(3), 328-339.

[71] Kiran P, Narasimhulu Y (2017); Weakly nonlinear oscillatory convection in an electrically conduction fluid layer under gravity modulation. Int. J. App. Compu. Math. 3(3), 1969-1983.

[72] Kvernvold O, Tyvand PA (1979); Nonlinear thermal convection in anisotropic porous media. J. Fluid Mech. 90, 609-624.

[73] Kuznetsov YA (2004); Elements of Applied Bifurcation Theory. Appl. Math. Sci. Springer-Verlag, New York.

[74] Kuznetsov AV (2005); The onset of bioconvection in a suspension of negatively geotactic microorganisms with high-frequency vertical vibration. Int. Comm. Heat Mass Transf. 1119-1127.

[75] Kuznetsov AV (2006a); Linear stability analysis of the effect of vertical vibration on bioconvection in a horizontal porous layer of finite depth. J. Porous Media 9, 597-608.

[76] Kuznetsov AV (2006b); Investigation of the onset of bioconvection in a suspension of oxytactic microorganisms subjected to high frequency vertical vibration. Theor. Comput. Fluid Dynam. 20, 73-87.

[77] Kuznetsov AV, Nield DA (2008); The effects of combined horizontal and vertical heterogeneity on the onset of convection in a porous medium: double diffusive case. Trans. Porous Med. 72, 157-170.

[78] Kuznetsov AV, Nield DA (2010); The onset of double-diffusive nanofluid convection in a layer of a saturated porous medium. Trans. Porous Med. 85, 941-951.

[79] Kuznetsov AV, Nield DA (2011); Double-diffusive natural convective boundary-layer flow of a nanofluid past a vertical plate. Int. J. Th. Sci. 50, 712-717.

[80] Lapwood ER (1948); Convection of a fluid in a porous medium. Proc. Camb. Phil. Soc. 44, 508-521.

[81] Long et al. (2008); Chaotic convection of viscoelastic fluid in porous media. Chaos. Solitons and Fractals. 37, 113-124.

[82] Lorenz EN (1963); Deterministic non-periodic flow. J Atmos Sci. 20, 130-141.

[83] Magyari E, Pop I, Postelnicu A (2007); Effect of the source term on steady free convection boundary layer flows over a vertical plate in a porous medium. Part I. Transp. Porous Med. 67, 49-67.

[84] Mahmud MN, Hasim I (2011); Effect of magnetic field on chaotic convection in fluid layer heated from below. Int. Commun. Heat Mass Trans. 38, 481-486.

[85] Malashetty MS, Basavaraja D (2002); Rayleigh-Bénard convection subject to time dependent wall temperature/ gravity in a fluid saturated anisotropic porous medium. Int. J. Heat Mass Transf. 38, 551-563.

[86] Malashetty MS, Basavaraja D (2005); Effect of thermal/gravity modulation on the onset of Rayleigh-Bénard convection in a couple stress fluid. Int. J. Trans. Phenom. 7, 31-44.

[87] Malashetty MS, Begum I (2011); Effect of thermal/gravity modulation on the onset of convection in a maxwell fluid saturated porous layer. Tranap. Porous Med. 90, 889-909.

[88] Malashetty MS, Gaikwad SN, Swamy M (2006); An analytical study of linear and non-linear double diffusive convection with Soret effect in couple stress liquids. Int. J. Therm. Sci. 9, 897-907.

[89] Malashetty MS, Heera R (2006); The effect of rotation on the onset of double diffusive convection in a horizontal anisotropic porous layer. Numer. Heat Transf. 49, 69-94.

[90] Malashetty MS, Padmavathi V (1997); Effect of gravity modulation on the onset of convection in a fluid and porous layer. Int J Engg Science. 35, 829-83.

[91] Malashetty MS, Swamy M (2007); The effect of rotation on the onset of convection in a horizontal anisotropic porous layer. Int J Therm. Sci. 46, 1023-1032.

[92] Malashetty MS, Swamy M (2011); Effect of gravity modulation on the onset of thermal convection in rotating fluid and porous layer. Phys Fluids. 23(6), 064108.

[93] Malashetty MS, Wadi VS (1999); Rayleigh-Bénard convection subject to time dependent wall temperature in a fluid saturated porous layer. Fluid Dyn. Res. 24, 293-308.

[94] Malkus WVR, Veronis G (1958); Finite amplitude cellular convection. J. Fluid Mech. 4, 225-260.

[95] Masuda H, Ebata A, Teramae K, Hishinuma N (1993); Alteration of thermal conductivity and viscosity of liquid by dispersing ultra fine particles. Netsu Bussei. 7, 227-233.

[96] Matta A, PA, Lakshmi Narayana (2016); Effect of variable gravity on linear and nonlinear stability of double diffusive hadley flow in porous media. Journal of Porous Med. 19(4), 287-301.

[97] Mulone G, Straughan B (2006); An operative method to obtain necessary and sufficient stability conditions for double diffusive convection in porous media. ZAMM. 86, 507-520.

[98] Nield DA (1968); Onset of thermohaline convection in a porous medium. WaterResour. Res. 4, 553 DOI:10.1029/WR004i003p00553.

[99] Nield DA (1987); Convective instability in porous media with throughflow. AICHE J. 33, 1222-224.

[100] Nield DA (1996); The effect of temperature-dependent viscosity on the onset of convection in a saturated porous medium. ASME J. Heat Transf. 118, 803-805.

[101] Nield DA, Bejan A (2012); Convection in Porous Media. 4th edn. Springer New York.

[102] Nield DA, Kuznetsov AV (2003); Effects of gross heterogeneity and anisotropy in forced convection in a porous medium. layered medium analysis J. Porous Med. 6, 51-57.

[103] Nield DA, Kuznetsov AV (2007); The effects of combined horizontal and vertical heterogeneity and anisotropy on the onset of convection in a porous medium. Int J Therm. Sci. 46, 1211-1218.

[104] Nield DA, Kuznetsov AV (2009); Thermal instability in a porous medium layer saturated by nanofluid. Int. J. Heat Mass Transf. 52, 5796-5801.

[105] Nield DA, Kuznetsov AV (2010); The effects of combined horizontal and vertical heterogeneity on the onset of convection in a porous medium with horizontal throughflow. Int J Heat and Mass Transf. 54, 5595-601.

[106] Nield DA, Kuznetsov AV (2011); The effect of vertical throughflow on thermal instability in a porous medium layer saturated by a nanofluid, Transp. Porous Med. 87, 765-775.

[107] Nield DA, Kuznetsov AV (2011a); The Cheng-Minkowycz problem for the double-diffusive natural convective boundary layer flow in a porous medium saturated by a nanofluid. Int. J. Heat Mass Transfer 54, 374-378.

[108] Nield DA, Kuznetsov AV (2015); The effect of vertical throughflow on thermal instability in a porous medium layer saturated by a nanofluid, A revised model. ASME j. 137, 052601-052605.

[109] Nisen T, Storesletten L (1990); An analytical study of natural convection in isotropic and anisotropic porous channels. Trans. ASME J Heat Transf. 112, 369-401.

[110] Palm E, Tyvand A (1984); Thermal convection in rotating porous layer. Z. Angew. Math. Phys. 35, 122-123.

[111] Parthiban C, Patil PR (1997); Thermal instability in an anisotropic porous medium with internal heat source and inclined temperature gradient. Int. Comm. Heat Mass Transf. 24(7), 1049-1058.

[112] Payne LE, Song JC, Straughan B (1999); Continuous dependence and convergence for Brinkman and Forchheimer models with variable viscosity. Proc. R. Soc. Lond. 452, 2173-2190.

[113] Poincaré JH (1890); Sur le probléme des trois corps et les équations de la dynamique. Acta Mathematica. 13, 01-279.

[114] Poulikakos D (1986); Double diffusive convection in a horizontally sparsely packed porous layer. Int. Commun. Heat Mass Transfer. 13, 587.

[115] Qin Y, Chadam J (1996); Non-linear convective stability in a porous medium with temperature-dependent viscosity and inertial drag. Stud. Appl. Math. 96, 273-288.

[116] Rajib B, Layek GC (2012); The onset of thermo-convection in a horizontal viscoelastic fluid layer heated underneath. Thermal Energy Power.Eng. 1(1), 1-9.

[117] Raju VRK, Bhattacharya SN (2010); Onset of thermal instability in a horizontal layer of fluid with modulated boundary temperatures. J. Engg Math. 66, 343-351.

[118] Rao YF, Wang BX (1991); Natural convection in vertical porous enclosures with internal heat generation. Int. J. Heat Mass Transf. 34, 247-252.

[119] Rayleigh L (1916); On Convective currents in a horizontal layer of fluid when the higher temperature is on the under side. Phil. Mag. 32, 529-546.

[120] Razi YP, Mojtabi I, Charrier-Mojtabi MC (2009); A summary of new predictive high frequency thermo-vibrational modes in porous media. Trans. Porous Med. 77, 207-208.

[121] Rees DAS, Hossain MA, Kabir S(2002); Natural convection of fluid with variable viscosity from a heated vertical wavy surface. ZAMP. 53, 48-57.

[122] Rees DAS, Pop I (2000); The effect of G-jitter on vertical free convection boundary-layer flow in porous media. Int Comm. Heat Mass Transf. 27(3), 415-424.

[123] Rees DAS, Pop I (2001); The effect of G-jitter on free convection near a stagnation point in a porous medium. Int.J. Heat Mass Transf. 44, 877-883.

[124] Rees DAS, Pop I (2003); The effect of large-amplitude G-jitter vertical free convection boundary-layer flow in porous media. Int. J. Heat Mass Transf. 46, 1097-1102.

[125] Reza M, Gupta AS (2012); Magnetohydrodynamics thermal instability in a conducting fluid layer with through flow. Int J Non-Linear Mech. 47, 616-25.

[126] Richardson L, Straughan B (1993); Convection with temperature dependent viscosity in a porous medium: non-linear stability and the Brinkman effect. Atti. Accad. Naz. Lincei-Ci-Sci-Fis. Mat. 4, 223-232.

[127] Roberts PH (1967); Convection in horizontal layers with internal heat generation. Theory, J. Fluid Mech. 30, 33-49.

[128] Rosenblat S, Herbert DM (1970); Low frequency modulation of thermal instability. J. Fluid Mech. 43, 385-398.

[129] Rosenblat S, Tanaka GA (1971); Modulation of thermal convection instability. Phys Fluids. 14, 1319-1322.

[130] Rudraiah N, Malashetty MS (1990); Effect of modulation on the onset of convection in a sparsely packed porous layer. ASME J Heat Transf. 112, 685-689.

[131] Rudraiah N, Siddheshwar PG (1998); A weak nonlinear stability analysis of double diffusive convection with cross-diffusion in a fluid-saturated porous medium. Heat Mass Transfer. 33, 287-293.

[132] Rudraiah N, Srimani PK, Friedrich R (1982); Finite amplitude convection in a two-component fluid saturated porous layer. Heat Mass Transfer. 25, 715-722.

[133] Saravanan S, Arunkumar A (2010); Convective instability in a gravity modulated anisotropic thermally stable porous medium. Int. J. Eng. Sci. 48, 742-750.

[134] Saravanan S, Purusothaman A (2009); Floquent instability of a modulated Rayleigh-Bénard problem in an anisotropic porous medium. Int. J. Therm. Sci. 48, 2085-2091.

[135] Saravanan S, Sivakumar T (2010); Onset of filteration convection in a vibrating medium: The Brinkman model. Phys. Fluids. 22, 034104.

[136] Saravanan S, Sivakumar T (2011); Thermo vibrational instability in a fluid saturated anisotropic porous medium. ASME, J. Heat Transf. 133(5), 051601; doi:10.1115/1.4003013.

[137] Shivakumara IS (1997); Effects of throughflow on convection in porous media. Proc. 7th Asian Congr. Fluid Mech. 2, 557-60.

[138] Shivakumara IS (1999); Boundary and inertia effects on convection in a porous media with throughflow. Acta Mech. 137, 151-65.

[139] Shivakumara IS, Jinho Lee, Malashetty MS, Sureshkumar S (2011); Effect of thermal modulation on the onset of convection in walters B viscoelastic fluid saturated porous medium. Transp. Porous Med. 87, 291-307.

[140] Shivakumara IS, Nanjundappa CE (2006); Effects of quadratic drag and throughflow on double diffusive convection in a porous layer. Int Communi Heat and Mass Transf. 33, 357-63.

[141] Shivakumara IS, Sureshkumar S (2007); Convective instabilities in a viscoelastic-fluid-saturated porous medium with throughflow. J. Geophys. Eng. 4, 104-15.

[142] Shivakumara JS, Sureshkumar S, Devaraju N (2011); Coriolis effect on thermal convection in a couple-stress fluid-saturated rotating rigid porous layer. Arch. Appl. Math. 81, 513-530.

[143] Shu Y, Li BQ, Ramaprian BR (2005); Convection in modulated thermal gradients and gravity: experimental measurements and numerical simulations. Int. J. Heat. Mass. Transf. 48, 145-160.

[144] Siddhavaram VK, Homsy GM (2006); The effects of gravity modulation on fluid mixing Part 1 Harmonic modulation. J. Fluid Mech. 562, 445-475.

[145] Siddheshwar PG, Bhadauria BS, Mishra P, Srivastava AK (2012a); Study of heat transport by stationary magneto convection in a Newtonian liquid under temperature or gravity modulation using Ginzburg-Landau model. Int J Non-Linear Mech. 47, 418-425.

[146] Siddheshwar PG, Bhadauria BS, Srivastava A (2012); An analytical study of nonlinear double diffusive convection in a porous medium under temperature/gravity modulation. Transp. Porous Med. 91, 585-604.

[147] Siddheshwar PG, Bhadauria BS, Suthar OMP (2013); Synchronous and asynchronous boundary temperature modulations of Bénard Darcy convection. Int. J. Non-Linear Mech. 49, 84-89.

[148] Siddheshwar PG, Chan AT (2004); Thermorheological effect on Bénard and Marangoni convections in anisotropic porous media. In: Cheng L, Yeow K (eds.) Hydrodynamics VI Theory and Applications. 471-476. Taylor and Francis, London.

[149] Siddheshwar PG, Revathi BR (2013); Effect of gravity modulation on weakly nonlinear stability of stationary convection in a dielectric liquid. World Academy of Science, Engg. and Tech. 7(1), 119-124.

[150] Siddheshwar PG, Vanishree RK (2012); Study of heat transport in Bénard-Darcy convection with G-Jitter and thermo-mechanical anisotropy in variable viscosity liquids. Transp. Porous Med. 92, 277-288.

[151] Simmons CT, Kuznetsov AV, Nield DA (2010); Effect of strong heterogeneity on the onset of convection in a porous medium: importance of spatial dimensionality and geologic controls. Water Resour. Res. 46, W09539 . doi:10.1029/2009WR008606

[152] Sparrow C (1982); The Lorenz Equations: Bifurcations, Chaos, and Strange Attractors. Springer-Verlag, New York.

[153] Srivastava A, Bhadauria BS, Siddheshwar PG, Hashim I (2013); Heat transport in an anisotropic porous medium saturated with variable viscosity liquid under G-jitter and internal heating effects. Transp. Porous Med. 99, 359-376.

[154] Stokes VK (1966); Couple-Stresses in fluids. Phys. Fluids. 9, 1709-1715.

[155] Stokes VK (1984); Theories of Fluids with Microstructure. Springer-Verleg, New-York.

[156] Straughan B (2001); A sharp non-linear stability threshold in rotating porous convection. Proc. R. Soc. Lond. A 457, 87-93.

[157] Strogatz SH (2007); Non-linear Dynamics and Chaos. Levant Books, Edition-I Kolkata India.

[158] Strong N (2008a); Effect of vertical modulation on the onset of filtration convection. J. Math. Fluid Mech. 10, 488-502.

[159] Strong N (2008b); Double-diffusive convection in a porous layer in the presence of vibration. SIAM J. Appl. Math. 69, 1263-1276.

[160] Sunil, Sharma RC, Chandel RS (2004); Effect of suspended particles on couple-stress fluid heated and soluted from below in porous medium. J. Porous Med. 7, 9-18.

[161] Suthar OMP, Siddheshwar PG, Bhadauria BS (2016); A study on the onset of thermally modulated Darcy Bénard convection. J. Engg. mathematics. 101 (1), 175-188.

[162] Sutton FM (1970); Onset of convection in a porous channel with net throughflow. Phys of Fluids. 13, 1931.

[163] Swamy M (2014); Effect of G-jitter on the onset of double diffusive convection in fluid/porous layer. Journal of Porous Med. 17(2), 117-128.

[164] Takashima M (1989); The stability of natural convection in an inclined fluid layer with internal heat generation, J. Phys. Soc. Japan. 58, 4431-4440.

[165] Taunton JW, Lightfoot EN, Green T (1972); Thermohaline instability and salt fingers in a porous medium. Phys. Fluids. 15, 748-753.

[166] Tveitereid M (1976); Thermal convection in a horizontal fluid layer with internal heat sources. Int. J. Heat Mass Transf. 21, 335-339.

[167] Tyvand PA, Storesletten L (1991); Onset of convection in an anisotropic porous medium with oblique principal axes. J Fluid Mech. 226, 371-382.

[168] Vadász P (1998); Coriolis effect on gravity-driven convection in a rotating porous layer heated from below. J. Fluid Mech. 376, 351-375.

[169] Vadász P(2008); Emerging Topics in Heat and Mass Transfer in Porous Media. Springer, New York.

[170] Vadász et al. (2014); Chaotic and Periodic natural convection for moderate and high Prandtl numbers in a porous layer subject to vibrations. Transp. Porous Med. 103, 279-294.

[171] Vadász P, Olek S (1998); Transition and chaos for free convection in a rotating porous layer. Int. J. Heat Mass Transfer. 41(11), 1417-1435.

[172] Vadász P, Olek S (1999); Weak turbulence and chaos for low Prandtl number gravity driven convection in porous media. Transp. Porous Med. 37(1), 69-91.

[173] Vadász P, Olek S (1999); Computational recovery of the homoclinic orbit in porous media convection. Int. J. Non-Linear Mech. 34(6), 89-93.

[174] Vadász P, Olek S (2000); Route to chaos for moderate Prandtl number convection in a porous layer heated from below. Transp. Porous Med. 41(2) 211-239.

[175] Vadász P, Olek S (2000); Convergence and accuracy of Adomian's decomposition method for the solution of Lorenz equations. Int. J. Heat Mass Transfer. 43(10), 1715-1734.

[176] Vafai K (2000); Handbook of Porous Media. Marcel Dekker, New York.

[177] Vafai K (2010); Porous Media: Applications in Biological Systems and Biotechnology. CRC Press.

[178] Vanishree RK, Siddheshwar PG (2010); Effect of rotation on thermal convection in an anisotropic porous medium with temperature-dependent viscosity. Transp. Porous Med. 81, 73-87.

[179] Venezian G (1969); Effect of modulation on the onset of thermal convection. J. Fluid Mech. 35, 243-254.

[180] Vest CM, Arpaci VS (1969); Overstability of a viscoelastic fluid layer heated from below. J. Fluid Mech. 36, 613-623.

[181] Walicki E, Walicka A (1999); Interia effect in the squeeze film of a couple-stress fluidsin biological bearings. Int. J. Appl. Mech. Engg. 4, 363-373.

[182] Wang S, Tan W (2011); Stability analysis of soret-driven double-diffusive convection of Maxwell fluid in a porous medium. Int. J. Heat Fluid Flow. 32(1), 88-94.

[183] Wooding RA (1960); Rayleigh instability of a thermal boundary layer in flow through a porous medium. J Fluid Mech. 9, 183-92.

[184] Yu CP, Shih YD (1980); Thermal instability of an internally heated fluid layer in a magnetic field. Phys. Fluids. 23, 411.

List of Publications

Accepted

1. B.S. Bhadauria, **Ajay Singh**, M. K. Singh, B. K. Singh, Stability analysis and internal heating effects on oscillatory convection in a viscoelastic fluid layer under gravity modulation. Asia Pacific Journal of Engineering Science and Technology. 2(1), 26-47 (2016).

2. B.S. Bhadauria, **Ajay Singh**, Throughflow and G-jitter effects on chaotic convection in an anisotropic porous medium. Ain Shams Engineering Journal (Elsevier), http://dx.doi.org/10.1016/j. asej. 2016. 08. 024.

3. Alok Srivastava, B.S. Bhadauria, **Ajay Singh**, An analytical study of heat and mass transport in Bénard-Darcy convection with G-jitter and variable viscosity liquids in porous media. Special Topics and Reviews in Porous Media (Begell House-2017).

4. B.S. Bhadauria, **Ajay Singh**, M. K. Singh, B. K. Singh, Numerical study on chaotic convection in a viscoelastic fluid saturated porous medium under temperature modulation. Published as a book chapter in "Recent advances in mathematical and computational science" (2015).

Communicated

1. B.S. Bhadauria, **Ajay Singh**, Vineet Kumar, Nonlinear g-jitter thermal instability in nanofluid in the presence of throughflow and heat source.

2. B.S. Bhadauria, **Ajay Singh**, Oscillatory and chaotic convection in a couple-stress fluid saturated rotating porous medium under temperature modulation.

Papers presented in International / National Conferences

International conferences

1. Oscillatory convection in viscoelastic porous layer in the presence of throughflow and internal heating under gravity modulation. International conference on **Fluid Dynamics and Its Applications**, BNMIT, Bengaluru. July 12-14, 2017.

2. Nonlinear G-jitter thermal instability in nanofluid presence of throughflow and heat source. International conference on **Nanoscience and Nanotechnology**, BBAU, Lucknow. September 22-24, 2017.

National conferences

1. Internal heating effects on oscillatory convection in a viscoelastic fluid layer under gravity modulation. National conference on **Recent Advances in Mathematics and Applications**, BBAU, Lucknow. October 30-31, 2014.

2. Weakly non-linear analysis of internal heating effect on oscillatory convection in viscoelastic fluid layer under gravity modulation. National conference on **Mathematical Analysis and Application**, BHU, Varanasi. January 30-31, 2015.

3. Numerical study on chaotic convection in a viscoelastic fluid saturated porous medium under temperature modulation. National conference on **Science For Society: An Interdisciplinary Approach**, BBAU, Lucknow. October 31- November 2, 2015.

4. Effect of throughflow and variable viscosity in an anisotropic porous medium under gravity modulation. National conference on **Mathematical Techniques in Engineering and Technology**, BBAU, Lucknow. March 30-31, 2016.

5. Feedback control and G-jitter effects on chaos in porous medium. National conference on **Science Technology and Innovations for Sustainable Development**, BBAU, Lucknow. March 3-4, 2017.

6. Throughflow and internal heating effects on oscillatory convection in viscoelatic porous layer under G-jitter. National conference on **Mathematical Modelling-Modern Approaches**, DITU, Dehradun. October 13-14, 2017.

Workshop

1. A Mini workshop on **Biomathematics**, BHU, Varanasi. March 28-30, 2015.

Conferences Attended

1. International conference on **Emerging Trends in Computational and Applied Mathematics**, ITM University, Gurgaon. June 2-4, 2014.

2. International conference on **Modelling and Computing**, BBAU, Lucknow. July 10-11, 2014.

Asia Pacific Journal of Engineering Science and Technology

journal homepage: www.apjest.com

Full length article

Stability analysis and internal heating effects on oscillatory convection in a viscoelastic fluid layer under gravity modulation

B. S. Bhadauria[a], Ajay Singh[b]*, Manoj K. Singh[c], Brajesh K. Singh[d]

[a]*Department of Mathematics, Faculty of Sciences, Banaras Hindu University, Varanasi-221605, India*
[b,c,d]*Department of Applied Mathematics, School for Physical Sciences, Babasaheb Bhimrao Ambedkar University, Lucknow-226025, India.*

(Received 13 January 2016; accepted 11 February 2016; published online 29 February 2016)

ABSTRACT

In this paper, we study the combined effect of internal heating and time periodic gravity modulation on thermal instability in a viscoelastic fluid layer, using complex non-autonomous Ginzburg-Landau equation. The influence of relaxation and retardation time of viscoelastic fluid on heat transfer has been discussed. A weak non-linear stability analysis has been performed by using power series expansion in terms of the amplitude of gravity modulation, which is assumed to be small. The Nusselt number has been obtained in terms of the amplitude for oscillatory mode of convection. It is found that modulation has a destabilizing effect at low frequencies and stabilizing effect at high frequencies. Further, it is also found that overstability advances the onset of convection more with internal heating, hence increases heat transfer. We have also studied the subcritical Hopf bifurcation and pitchfork bifurcation. The phase portrait diagrams are also shown for these bifurcations.

Keywords: Non-linear stability analysis; Complex Ginzburg-Landau equation; Gravity modulation; Internal heating; Bifurcation

1. Introduction

Thermal convection in a horizontal fluid layer subject to constant but different temperatures at the boundaries has been studied extensively due to its applications in various fields. The classical Rayleigh-Benard convection is found to be an interesting phenomenon introduced by Chandrasekhar [1], due to bottom heating of a fluid layer. For analysis on thermal instability in detail, one may refer excellent books due to Ingham and Pop [2], Nield and Bejan [3] and vafai

*E-mail address: ajaysingh0044@gmail.com

[4]. From the applications point of view, the regulation of convection is very important. Thermo-gravitational vibration is known to be an effective technique for controlling the instability. The first idea of using mechanical vibration as a tool to enhance the heat transfer rate is presented by Gresho and Saini [5]. Further studies on gravity modulation are due to Malashetty and Padmavathi [6], Malashetty and Swamy [7], Bhadauria et al. [8] and Siddhavaram and Hosmy [9].

Basically, industrial fluids are non-Newtonian fluids. Specially, viscoelastic fluids have been found a wide range of industrial applications. The characteristics of heat transfer in viscoelastic fluid layer are also important in chemical processing industries, and so, the proper understanding of convective motion and its behaviour is necessary for controlling many processes such as geothermal reservoirs, filtration, enhanced oil recovery etc. In the recent years, several articles are available in which different physical models with viscoelastic fluid layer have been used to study thermal instability. First of all Green [10] study the oscillatory convection in a viscoelastic fluid layer, the occurrence of over stability for typical Rayleigh-Benard convection in a horizontal layer of homogeneous Maxwellian fluid, heated from below, is reported by Vest and Arpaci [11]. Convective instability in a rotating viscoelastic fluid layer was studied by Bhatia and Steiner [12]. Thermal instability in a viscoelastic fluid saturating a porous medium was studied by Kim et al. [13]. The Benard-Marangoni thermal instability problem in a viscoelastic Jeffrey's fluid layer with internal heat generation was introduced by Comissiong et al. [14]; onset of oscillatory convection was studied using linear stability analysis and the dependence of critical Rayleigh number for oscillatory convection on internal heat generation, relaxation and retardation times was derived. Thermal instability using linear stability analysis was studied by Rajib and Layek [15]. Recently, Bhadauria and Kiran [16] investigated oscillatory convection in a viscoelastic fluid layer under gravity modulation by making a non-linear stability analysis.

Internal heat is one of the main sources of energy for celestial bodies, caused by nuclear fusion and decaying of radioactive materials. It is due to the internal heating of the earth that there exists a thermal gradient between the interior and exterior of the earth's crust, saturated by multi-components fluids, which helps convective flow, thereby transferring the thermal energy toward the surface of the earth, and so internal heat generation plays a very significant role in several applications which include geophysics, reactor safety analyses, metal waste form development for spent nuclear fuel, fire and combustion studies, and storage of radioactive materials. Convective heat transfer in porous media has received much attention during the past few decades because of its wide range of applications in many engineering and natural systems of practical interest; for instance, geothermal energy utilization, thermal energy storage and recovery systems, petroleum reservoirs, industrial and agricultural water distribution. Haajizadeh et al. [17] have studied a uniform heat generation term across an enclosure with isothermal vertical walls and adiabatic horizontal walls. Further, for more studies on internal heating we refer to [18- 26].

The qualitative analysis of a dynamical system provides much knowledge about the system. Bifurcations, the appearance of a topologically non-equivalent phase portrait under variation of

parameters, are scientifically more important as they provide models of transitions and instabilities [27]. In the present paper, two types of bifurcation (1) Pitchfork bifurcation (common in physical problems that have a symmetry); (2) Hopf bifurcation (bifurcation corresponding to the presence of purely complex eigenvalue) are discussed, for details we refer to [28].

In the existing literature, no work is available on internal heating system for oscillatory mode of convection with viscoelastic fluid layer and bifurcation analysis of the system. Therefore, in this paper, we study internal heating effects for a weak non-linear oscillatory convection in a viscoelastic fluid layer under gravity modulation. The heat transfer rate is examined by computing the Nusselt number in terms of the amplitude of convection by solving the complex Ginzburg-Landau equation. We also study the Hopf bifurcation and Pitchfork bifurcation on different parameters, which gives the more control parameters to study the stability of the system.

2. Mathematical Structure

We consider an infinitely extended horizontal viscoelastic fluid layer of depth d, confined between two parallel planes, the lower plane at $z=0$ while upper one is at $z=d$. A Cartesian frame of reference is adopted in such a way that the origin lies on the lower plane and z axis is vertically upward. The fluid layer is heated from below and cooled from the above. The physical configuration of the model is depicted in Fig. 1. The Oberbeck Boussinesq approximation is adopted to solve the model equations. The governing equations of the flow and temperature fields [16] are given by

$$\begin{cases} \nabla.\vec{q}=0, \\ \left(\bar{\lambda}_1\dfrac{\partial}{\partial t}+1\right)\left(\dfrac{\partial\vec{q}}{\partial t}+(\vec{q}.\nabla)\vec{q}-\dfrac{1}{\rho_0}\nabla p+\dfrac{\rho\vec{g}}{\rho_0}\right)-\nu\left(\bar{\lambda}_2\dfrac{\partial}{\partial t}+1\right)\nabla^2\vec{q}=0, \\ \dfrac{\partial T}{\partial t}+(\vec{q}.\nabla)\mathrm{T}=\kappa_T\nabla^2 T+Q(\mathrm{T}-\mathrm{T}_0), \\ \rho=\rho_0\{1-\alpha_T(\mathrm{T}-\mathrm{T}_0)\}, \end{cases} \tag{1}$$

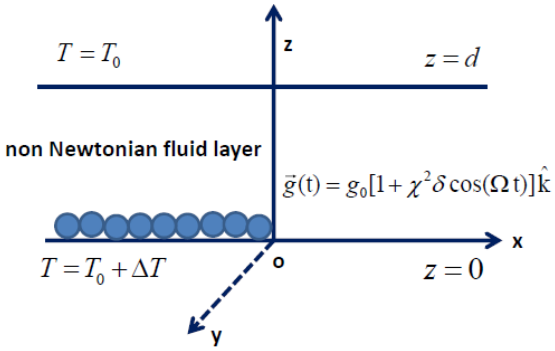

Fig.1. Physical configuration of the problem

where the physical meaning of the variables is as given in the nomenclature. The externally imposed gravitational field and the thermal boundary conditions are as follows

$$\vec{g} = g_0\{1+\chi^2\delta\cos(\Omega t)\}\hat{k}, \tag{2}$$

$$\begin{cases} T = T_0 + \Delta T, & \text{at } z=0, \\ T_0, & \text{at } z=d, \end{cases} \tag{3}$$

where g_0 is the mean gravity and $\hat{k}$ is the unit vector along the positive z axis.

3. Basic state

The basic state is assumed to be quiescent, the quantities are taken as

$$\vec{q}_b = 0, \quad p=p_b(z), \quad T=T_b(z), \quad \rho=\rho_b(z). \tag{4}$$

The following relations, which define basic state pressure and temperature mathematically, are obtained by putting Eq. (4) in Eq. (1):

$$\frac{\partial p_b}{\partial z} = -\rho_b\,\vec{g}, \tag{5}$$

$$\kappa_T\frac{d^2(T_b-T_0)}{dz^2} + Q(T_b-T_0) = 0, \tag{6}$$

$$\rho_b = \rho_0\{1-\alpha_T(T_b-T_0)\}. \tag{7}$$

The exact solution of Eq. (6) together with the boundary conditions (3) is given by

$$T_b = T_0 + \Delta T\frac{\sin\left(\left(\sqrt{\frac{Q}{\kappa_T}}\right)\left(1-\frac{z}{d}\right)\right)}{\sin\left(\sqrt{\frac{Q}{\kappa_T}}\right)}. \tag{8}$$

Now, we superimpose the finite amplitude perturbations on the basic state in the form:

$$\vec{q} = q_b + q', \quad T=T_b+T', \quad p=p_b+p', \quad \rho=\rho_b+\rho', \tag{9}$$

the primes denote the perturbed quantities. The dimensionless governing system as mentioned in [16] is reduces to

$$\left(\lambda_1\frac{\partial}{\partial t}+1\right)\left(\frac{1}{P_r}\frac{\partial}{\partial t}\nabla^2\psi - \frac{1}{P_r}\frac{\partial(\psi,\nabla^2\psi)}{\partial(x,z)} + g_m R_a\frac{\partial T}{\partial x}\right) - \left(\lambda_2\frac{\partial}{\partial t}+1\right)\nabla^4\psi = 0, \tag{10}$$

$$-\frac{\partial\psi}{\partial x}\frac{\partial T_b}{\partial z} + \left(\frac{\partial}{\partial t} - \nabla^2 - R_i\right)T = \frac{\partial(\psi,T)}{\partial(x,z)}, \tag{11}$$

where $g_m = (1+\chi^2\delta\cos(\Omega t))$, $R_a = \dfrac{\alpha_T g_0 \Delta T K d^3}{\nu\kappa_T}$ is the thermal Rayleigh number, $R_i = \dfrac{Qd^2}{\kappa_T}$ is the internal Rayleigh number, $\nu = \dfrac{\mu}{\rho_0}$ is the kinematic viscosity and $P_r = \dfrac{\nu}{\kappa_T}$ is the Prandtl

number. The above system will be solved by considering stress free and isothermal boundary conditions:

$$\psi = \frac{\partial^2 \psi}{\partial z^2} = T = 0 \quad \text{on} \quad z=0,\ z=1. \tag{12}$$

The dimensionless steady temperature $T_b(z)$, appearing in Eq. (11) is

$$\frac{dT_b}{dz} = -\frac{\sqrt{R_i}\cos\left(\sqrt{R_i}(1-z)\right)}{\sin\left(\sqrt{R_i}\right)}. \tag{13}$$

On introducing a small perturbation parameter χ : a deviation from the critical state of onset of convection, the variables for a weak non-linear state may be expanded in power series of χ [29, 30] a

$$R_a = R_0 + \chi^2 R_2 + \chi^4 R_4 + \cdots \tag{14}$$

$$\psi = \chi\psi_1 + \chi^2\psi_2 + \chi^3\psi_3 + ... \tag{15}$$

$$T = \chi T_1 + \chi^2 T_2 + \chi^3 T_3 + ... \tag{16}$$

where R_0 denotes the critical value of the Rayleigh number for the onset of convection in the absence of gravity modulation.

4. Analysis of the periodic solutions

In order to study the time periodic convective phenomenon, the slow and fast time scales are introduced $\left(\frac{\partial}{\partial t} = \frac{\partial}{\partial \tau} + \chi^2 \frac{\partial}{\partial s}\right)$ by [13, 16]. The above system (10) and (11) is solved for each order of χ.

For the first order, the matrix operator is obtained similar to linear case as:

$$\begin{bmatrix} \frac{1}{P_r}\left(\lambda_1 \frac{\partial}{\partial \tau}+1\right)\frac{\partial}{\partial \tau}\nabla^2 - \left(\lambda_2 \frac{\partial}{\partial \tau}+1\right)\nabla^4 & \mathrm{R}_0\left(\lambda_1 \frac{\partial}{\partial \tau}+1\right)\frac{\partial}{\partial x} \\ -\frac{\partial}{\partial x}\frac{\partial T_b}{\partial z} & \left(\frac{\partial}{\partial \tau} - \nabla^2 - R_i\right) \end{bmatrix} \begin{bmatrix} \psi_1 \\ T_1 \end{bmatrix} = \begin{bmatrix} 0 \\ 0 \end{bmatrix}. \tag{17}$$

The solution of the first order system subject to the boundary conditions Eq. (12), is assumed to be

$$\psi_1 = (\mathrm{B(s)}\,e^{i\omega\tau} + \bar{\mathrm{B}}(\mathrm{s})\,e^{-i\omega\tau})\sin ax\ \sin \pi z, \tag{18}$$

$$T_1 = (\mathrm{A(s)}\,e^{i\omega\tau} + \bar{A}(\mathrm{s})\,e^{-i\omega\tau})\cos ax\ \sin \pi z, \tag{19}$$

where the unknown amplitudes are functions of slow time scale, and are related by the following expression:

$$B(\mathrm{s}) = -\frac{(c + i\omega - R_i)(4\pi^2 - R_i)}{4\pi^2 a} A(\mathrm{s}), \quad c = a^2 + \pi^2. \tag{20}$$

The values of the critical Rayleigh number and the corresponding wave number of the system for a stationary mode of convection are as given below:

$$R_0^{st} = \frac{c^2(\mathrm{c} - R_i)(4\pi^2 - R_i)}{4\pi^2 a^2}, \tag{21}$$

$$a_c^2 = \frac{(\mathrm{R}_i - \pi^2) \pm \sqrt{(\pi^2 - \mathrm{R}_i)^2 + 8\pi^2(\pi^2 - \mathrm{R}_i)}}{4}. \tag{22}$$

In particular, for $R_i = 0$ (without internal-heating), we have

$$R_0 = \frac{c^3}{a^2}, \tag{23}$$

$$a_c = \frac{\pi}{\sqrt{2}}, \tag{24}$$

which are the classical results as obtained by Chandrasekhar [1]. The critical Rayleigh number for the oscillatory mode of convection is computed as follows

$$R_0^{osc} = \left(\frac{c^3}{a^2} + \frac{(\lambda_1\omega^2 \mathrm{R}_i \mathrm{c} - \mathrm{P}_r \mathrm{R}_i c^2) - (\lambda_1 + \lambda_2 \mathrm{P}_r)\omega^2 c(\mathrm{c}+1)}{a^2 \mathrm{P}_r} \right) \frac{4\pi^2 - R_i}{4\pi^2}, \tag{25}$$

where ω is the oscillatory frequency as given below

$$\omega^2 = \frac{-1 + \frac{R_i}{c} + (\lambda_1 - \lambda_2)\mathrm{P}_r c - \mathrm{P}_r(1 - \lambda_2 R_i + \lambda_1 R_i)}{\lambda_1(\lambda_1 + \lambda_2 \mathrm{P}_r) - \lambda_1^2 \frac{R_i}{c}}, \tag{26}$$

The similar result is computed by Rajib and Layek [15] without internal-heating. We compute the wave number (i.e., the critical wave number for which the Rayleigh number is minimum). It is to be noted that the critical Rayleigh number and the corresponding wave number do not depend on relaxation (λ_1) and retardation (λ_2) time in stationary mode of convection but it is not so in case of oscillatory mode of convection. Since ω has to be positive and real, and so, from the relation (26), the necessary condition for oscillatory convection is obtained as

$$\lambda_1 > \lambda_2 + \frac{1 + P_r(1 + \lambda_1 \mathrm{R}_i - \lambda_2 \mathrm{R}_i) - \mathrm{R}_i c}{cP_r}. \tag{27}$$

Now at second order, we have

$$\begin{bmatrix} \frac{1}{P_r}\left(\lambda_1 \frac{\partial}{\partial\tau} + 1\right)\frac{\partial}{\partial\tau}\nabla^2 - \left(\lambda_2 \frac{\partial}{\partial\tau} + 1\right)\nabla^4 & \mathrm{R}_0\left(\lambda_1 \frac{\partial}{\partial\tau} + 1\right)\frac{\partial}{\partial x} \\ -\frac{\partial}{\partial x}\frac{\partial T_b}{\partial z} & \left(\frac{\partial}{\partial\tau} - \nabla^2 - R_i\right) \end{bmatrix} \begin{bmatrix} \psi_2 \\ T_2 \end{bmatrix} = \begin{bmatrix} R_{21} \\ R_{22} \end{bmatrix}, \tag{28}$$

where

$$R_{21} = 0, \tag{29}$$

$$R_{22} = \frac{\partial \psi_1}{\partial x}\frac{\partial T_1}{\partial z} - \frac{\partial \psi_1}{\partial z}\frac{\partial T_1}{\partial x}. \tag{30}$$

The second order solution subject to the boundary condition (12) is given by

$$\psi_2 = 0, \tag{31}$$

$$\left(\frac{\partial}{\partial \tau} - \nabla^2 - R_i\right) T_2 = R_{22}. \tag{32}$$

Next, we compute the temperature fields having the frequency 2ω, and independent of fast time scale [13, 16]. Thus, second order temperature terms can be expressed in the following form:

$$T_2 = \{T_{20} + T_{22}\, e^{2i\omega\tau} + \bar{T}_{22}\, e^{-2i\omega\tau}\}\sin(2\pi z), \tag{33}$$

where T_{22} and T_{20} are temperature fields having the terms with the frequency 2ω and independent of fast time scale, respectively. The solutions of the second order problems are

$$T_{20} = \frac{\pi a}{8\pi^2 - 2R_i}\{A(s)\bar{B}(s) + \bar{A}(s)B(s)\}, \tag{34}$$

and

$$T_{22} = \frac{\pi a}{8\pi^2 + 4i\omega - 2R_i} A(s)B(s). \tag{35}$$

Horizontally averaged Nusselt number, $N_u(s)$ for the oscillatory mode of convection is given by

$$N_u(s) = 1 + \left[\chi^2 \left(\frac{\partial T_2}{\partial z}\right)_{z=0} / \left(\frac{\partial T_b}{\partial z}\right)_{z=0}\right]. \tag{36}$$

By using Eq. (13), (33), (34) and (35), we can simplify Eq. (36)

$$N_u(s) = 1 + \left[\frac{(c - R_i)4\pi^2}{8\pi^2 - 2R_i} + \frac{2\pi^2\sqrt{(c - R_i)^2 + \omega^2}}{\sqrt{(8\pi^2 - 2R_i)^2 + 16\omega^2}}\right]\left(\frac{4\pi^2 - R_i}{4\pi^2}\right)\frac{\tan\sqrt{R_i}}{\sqrt{R_i}}|A(s)|^2. \tag{37}$$

It is clear that the gravity modulation is effective at third order, and affects $N_u(s)$ through A(s), which is evaluated at third order. At the third order, we have

$$\begin{bmatrix} \frac{1}{P_r}\left(\lambda_1\frac{\partial}{\partial\tau}+1\right)\frac{\partial}{\partial\tau}\nabla^2 - \left(\lambda_2\frac{\partial}{\partial\tau}+1\right)\nabla^4 & R_0\left(\lambda_1\frac{\partial}{\partial\tau}+1\right)\frac{\partial}{\partial x} \\ -\frac{\partial}{\partial x}\frac{\partial T_b}{\partial z} & \left(\frac{\partial}{\partial\tau} - \nabla^2 - R_i\right) \end{bmatrix} \begin{bmatrix} \psi_3 \\ T_3 \end{bmatrix} = \begin{bmatrix} R_{31} \\ R_{32} \end{bmatrix}, \tag{38}$$

where

$$R_{31}=\lambda_2\frac{\partial}{\partial s}\nabla^4\psi_1-R_0\lambda_1\frac{\partial}{\partial s}\frac{\partial T_1}{\partial x}-(R_2+R_0\delta\cos(\Omega s))\left(\lambda_1\frac{\partial}{\partial\tau}+1\right)\frac{\partial T_1}{\partial x}$$
$$-\frac{1}{P_r}\left(\lambda_1\frac{\partial}{\partial\tau}+1\right)\frac{\partial}{\partial s}\nabla^2\psi_1-\frac{1}{P_r}\lambda_1\frac{\partial}{\partial s}\left(\frac{\partial}{\partial\tau}\nabla^2\psi_1\right), \tag{39}$$

$$R_{32}=\frac{\partial\psi_1}{\partial x}\frac{\partial T_2}{\partial z}-\frac{\partial T_1}{\partial s}. \tag{40}$$

Using first and second order solutions, the expressions of R_{31} and R_{32} are determined. Now, under the solvability condition for the existence of third order solution, one may derive the complex Ginzburg-Landau equation for finite amplitude convection.

$$\frac{dA(\mathrm{s})}{ds}-\gamma^{-1}F(\mathrm{s})\,\mathrm{A}(\mathrm{s})+\gamma^{-1}k\left|A(\mathrm{s})\right|^2A(\mathrm{s})=0, \tag{41}$$

Where

$$\gamma=\left(1-a\Delta_1R_2\lambda_1+\frac{c^2\Delta_1\lambda_2(\mathrm{c}+\mathrm{i}\,\omega-\mathrm{R}_i)(4\pi^2-\mathrm{R}_i)}{4\pi^2a}+\frac{c\Delta_1(\mathrm{c}+\mathrm{i}\,\omega-\mathrm{R}_i)(1+2\lambda_1\,\mathrm{i}\,\omega)(4\pi^2-\mathrm{R}_i)}{4\pi^2aP_r}\right),$$

$$F(\mathrm{s})=\left\{a\Delta_1R_2(1+\mathrm{i}\,\omega\lambda_1)(1+\delta\cos(\Omega\mathrm{s}))\right\},\ \Delta_1=\left\{\frac{aP_r}{i\omega c(1+\mathrm{i}\,\omega\lambda_1)+(1+\mathrm{i}\,\omega\lambda_2)\,\mathrm{c}^2\,P_r}\right\}$$

$$k=\left\{\frac{(\mathrm{c}-\mathrm{R}_i)(\mathrm{c}+\mathrm{i}\,\omega-\mathrm{R}_i)(4\pi^2-\mathrm{R}_i)\pi^2}{16\pi^4}+\frac{\{(\mathrm{c}-\mathrm{R}_i)^2+\omega^2\}(4\pi^2-\mathrm{R}_i)^2\pi^2}{(8\pi^2-2\,\mathrm{R}_i+4\mathrm{i}\,\omega)16\pi^4}\right\}.$$

Writing A(s) in the phase-amplitude form, we get

$$A(\mathrm{s})=\left|A(\mathrm{s})\right|e^{i\varphi}. \tag{42}$$

On substituting Eq. (42) in Eq. (41), we get the following expression for the amplitude $\left|A(\mathrm{s})\right|$ as

$$\frac{d\left|A(\mathrm{s})\right|^2}{ds}-2p_r\left|A(\mathrm{s})\right|^2+2l_r\left|A(\mathrm{s})\right|^4=0, \tag{43}$$

$$\frac{d(\mathrm{ph}(\mathrm{A}(\mathrm{s})))}{ds}=p_i-l_i\left|A(\mathrm{s})\right|^2, \tag{44}$$

where $\gamma^{-1}F(\mathrm{s})=p_r+ip_i$, $\gamma^{-1}k=l_r+il_i$ and ph(.) represents the phase shift. The Eq. (43) solved numerically using the function NDSolve of Mathematica, subject to the suitable initial condition $A(0)=\mathrm{a}_0$, where a_0 is the chosen initial amplitude of convection. In our computation, we assume $R_2=R_0$ to keep the parameters to a minimum.

5. Bifurcation Analysis

In this section we are interested in the study of dynamical behaviour of the Complex Ginzburg-Landau Eq. (41) and amplitude Eq. (43). We show that the Complex Ginzburg-Landau

Eq. (41) undergoes subcritical Hopf bifurcation whereas amplitude Eq. (43) undergoes pitchfork bifurcation.

5.1 Hopf bifurcation

The complex Ginzburg-Landau equation (41) can be written as

$$\begin{aligned}\frac{dx}{ds} &= p_r x - p_i y - (\mathrm{l}_r \mathrm{x} - \mathrm{l}_i \mathrm{y})(\mathrm{x}^2 + \mathrm{y}^2),\\ \frac{dy}{ds} &= p_i x + p_r y - (\mathrm{l}_i \mathrm{x} + \mathrm{l}_r \mathrm{y})(\mathrm{x}^2 + \mathrm{y}^2),\end{aligned} \tag{45}$$

where

$$A(\mathrm{s}) = \mathrm{x}(\mathrm{s}) + \mathrm{iy}(\mathrm{s}),\ \mathrm{p}_r = R_e\left[\frac{F(\mathrm{s})}{\gamma}\right],\ \mathrm{p}_i = \mathrm{I}_m\left[\frac{F(\mathrm{s})}{\gamma}\right],\ \mathrm{l}_r = R_e\left[\frac{k}{\gamma}\right],\ \mathrm{l}_i = \mathrm{I}_m\left[\frac{k}{\gamma}\right].$$

Clearly the origin is the equilibrium point of the system (45). The Jacobian matrix of the system (45) at the origin is

$$J = \begin{bmatrix} p_r & -p_i \\ p_i & p_r \end{bmatrix}.$$

The trace and determinant of the Jacobian matrix J is $tr(\mathrm{J}) = 2\mathrm{p}_r$ and $\det(\mathrm{J}) = \mathrm{p}_r^2 + \mathrm{p}_i^2 > 0$ respectively.

If $p_r < 0,$ both eigenvalues of the Jacobian matrix J have negative real parts, and hence the origin is asymptotically stable. If $p_r > 0,$ then real parts of both eigenvalues of J are positive, which confirms that the origin is unstable. For $p_r = 0,$ the eigenvalues of J are purely imaginary, and so, from implicit function theorem a Hopf bifurcation occurs and a periodic orbit arises as the stability of origin changes. Here, we assume λ_1 as bifurcation parameter, and sketch the phase portrait diagram for the system (45).

We consider $P_r = 1,\ R_i = 1,\ \lambda_2 = 0.1,\ \delta$=0.3, and Ω=50. If $\lambda_1 = 0.4,$ then $p_r < 0,$ and from the above discussion, the origin is asymptotically stable. From Fig. 11, we can see that the origin is a stable focus, surrounded by an unstable unique limit cycle. If $\lambda_1 = 0.47,$ then $p_r = 0,$ and the origin is unstable focus, Fig 12. If $\lambda_1 = 0.5,$ then $p_r > 0,$ and from the above discussion, the origin is unstable. Fig. 13 confirms that the origin is a focus. Such type bifurcation is the subcritical Hopf bifurcation.

5.2 Pitchfork bifurcation

The system (43) can be written as

$$\frac{d|A(\mathrm{s})|}{ds} - p_r|A(\mathrm{s})| + l_r|A(\mathrm{s})|^3 = 0. \tag{46}$$

It is clear that the system (46) has three equilibrium points $|A(s)|=0$ for all value of p_r, l_r and $|A(s)|=\pm\sqrt{\frac{p_r}{l_r}}$ for $p_r>0,\ l_r>0,$ and the solution of the differential equation (46) is given by

$$|A(s)|^2=\frac{A_0^2}{\frac{l_r}{p_r}A_0^2+\left(1-\frac{l_r}{p_r}A_0^2\right)e^{-2p_r s}},\ p_r>0,\ l_r>0, \tag{47}$$

where A_0 is the initial value of the amplitude. From Eq. (47), we see that solution trajectories approach $|A(s)|=0$ as $s\to-\infty$, grow towards $\sqrt{\frac{p_r}{l_r}}$ when $0<A_0<\sqrt{\frac{p_r}{l_r}}$ as $s\to\infty$, decrease towards $\sqrt{\frac{p_r}{lr}}$ when $A_0>\sqrt{\frac{p_r}{l_r}}$ as $s\to\infty$. Thus, if $p_r<0$ then $A(s)=0$ is the only equilibrium point which is stable. If $P_r=0$ then origin again the only equilibrium point, which is still stable but much more weakly. So, if $P_r>0$ and $l_r>0$ then $|A(s)|=0$ is still an equilibrium point but now it becomes unstable, and two new stable equilibrium points appear on either side of $|A(s)|=0,$ symmetrically located at $|A(s)|=\pm\sqrt{\frac{p_r}{l_r}}$, Fig. 14. This is called the supercritical pitchfork bifurcation. The pitchfork bifurcation diagram is depicted in Fig. 15.

6. Results and Discussion

In present paper, the combined effect of internal-heating and gravity modulation on oscillatory convection in a viscoelastic fluid layer has been studied by performing a weak non-linear stability analysis. The effect of gravity modulation on the Rayleigh-Benard system has been assumed to be of order of (χ^2). The values of δ are assumed to be in the interval $(0,0.5)$. It is observed that Eq. (27) leads to an interesting result that the oscillatory type of instability exists only when the relaxation parameter λ_1 is greater than the retardation parameter λ_2. From Eq. (37), it can be seen that the value of N_u starts with 1, thus showing the conduction state initially, that is heat transfer across the fluid layer is taking place through conduction only when s is small. The value of N_u increases for intermediate values of s thus showing that convection is in progress, and finally when s is very large, the oscillatory state is achieved. The numerical value of N_u is obtained from Eq. (37) by solving the amplitude equation (43).

The combined effect of internal-heating and gravity modulation has been depicted in Figs. 2-8, where we have plotted N_u with respect to the slow time s. It is evident from Fig. 2 that the effect of internal Rayleigh number on thermal instability is destabilizing as N_u increases on

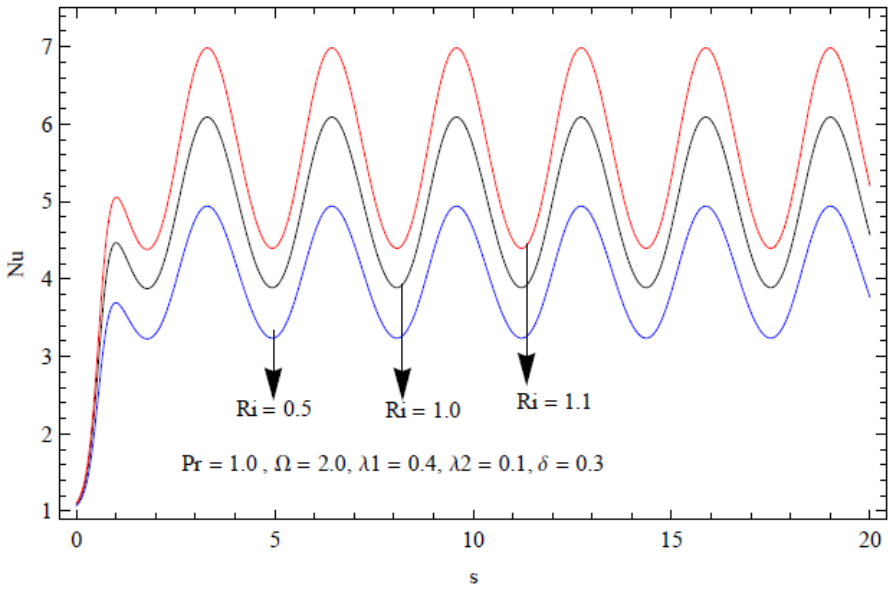

Fig .2. Effect of Ri on Nu For fixed values of the other parameters

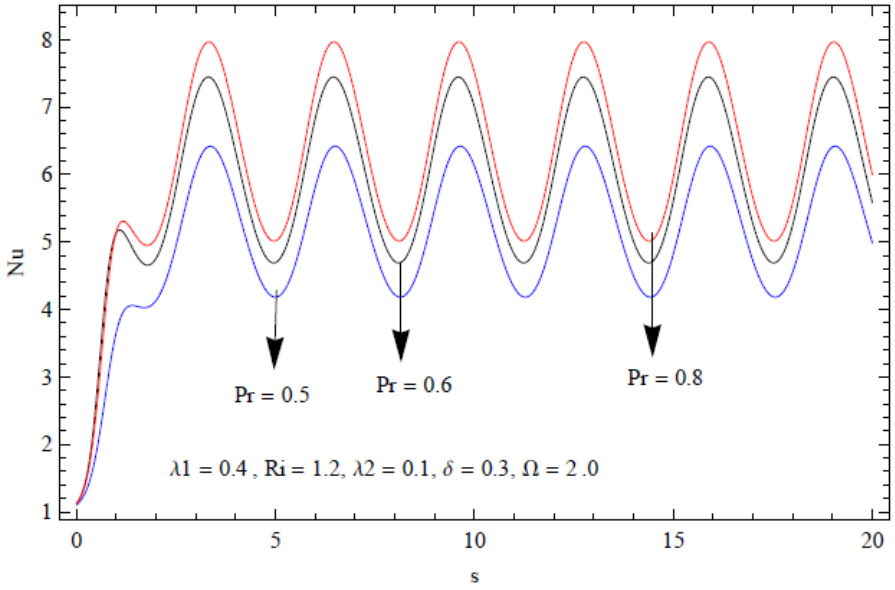

Fig .3. Effect of Pr on Nu For fixed values of the other parameters

increasing R_i, thus the heat transport is more for higher values of R_i. This agreed the results obtained by Bhadauria et al. [25]. Fig. 3 confirms that as P_r increases there is an increment in the heat transfer compatible with the results obtained by Bhadauria and kiran [16], thus the Prandtl number has a tendency to destabilize the system. Fig. 4 indicates the effect of relaxation parameter λ_1 on oscillatory convection, and gives a destabilized system due to increasing heat transfer on increasing λ_1. Further, the effect of retardation parameter λ_2 is found to stabilize the

system as the heat transfer decreases on increasing λ_2, given in Fig. 5. The effects of the amplitude of modulation δ and frequency of modulation Ω on heat transport are given in Fig. 6-7 respectively. In Fig. 6, one can see that an increment in the amplitude of modulation increases the magnitude of N_u, thus enhances the heat transfer and advancing the onset of convection. An opposite effect is obtained in the case of frequency of modulation Ω as given in Fig. 7. Hence, we found that the effect of gravity modulation decreases as the frequency of modulation increases.

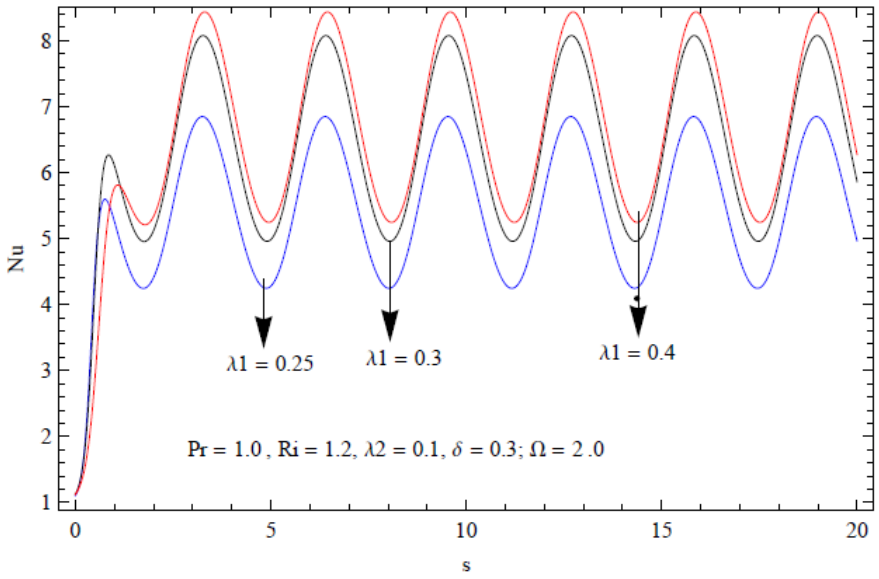

Fig .4. Effect of λ1 on Nu For fixed values of the other parameters

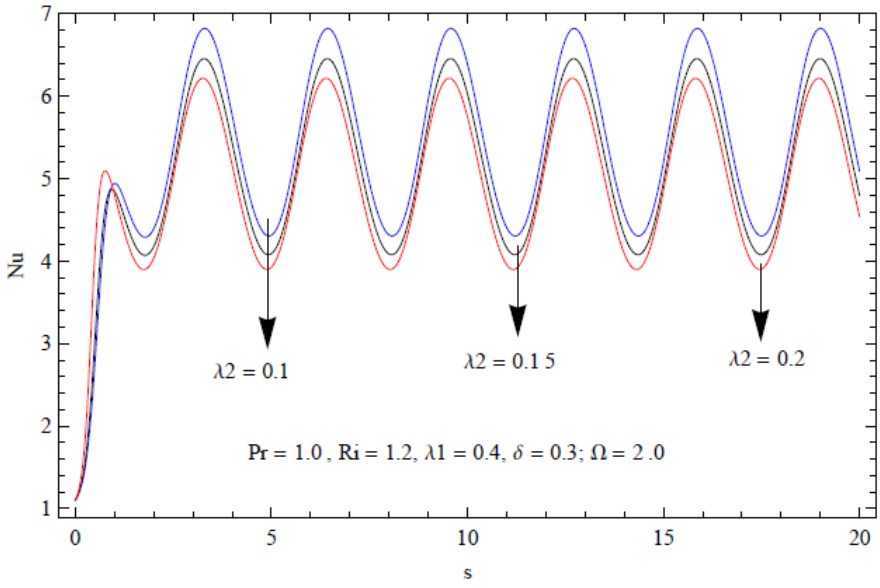

Fig .5. Effect of λ2 on Nu For fixed values of the other parameters

The present result of internal heating has been compared with the results of non-internal heating in Fig. 8. We observe that in the presence of internal heat source in the system, the value of N_u is more than that in the absence of internal-heating, i.e. the heat transport in the system is more due to internal-heating. Thus, internal-heating advances the onset of convection, which is the same as the result obtained by Bhadauria et al. [26].

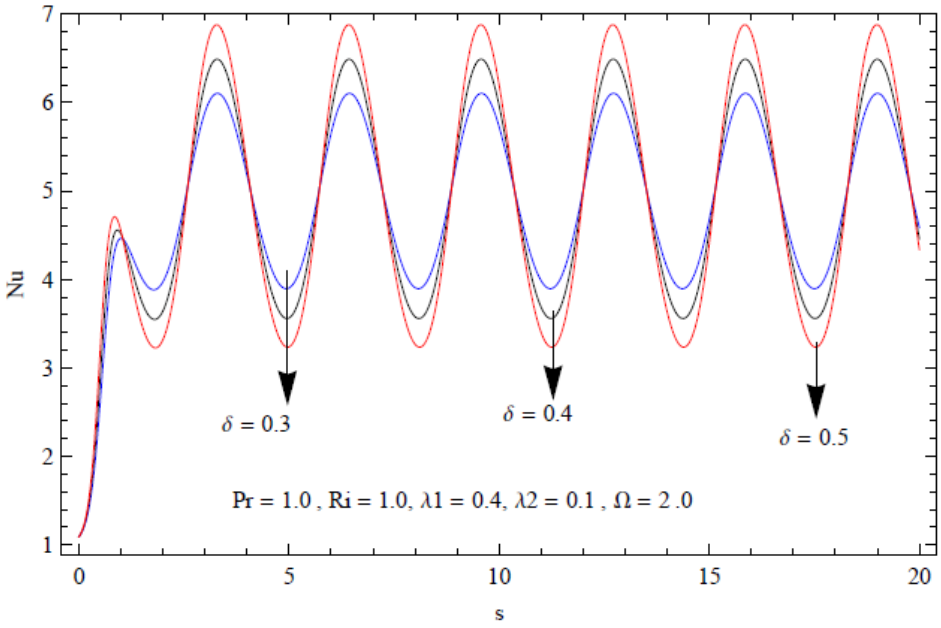

Fig .6. Effect of δ on Nu For fixed values of the other parameters

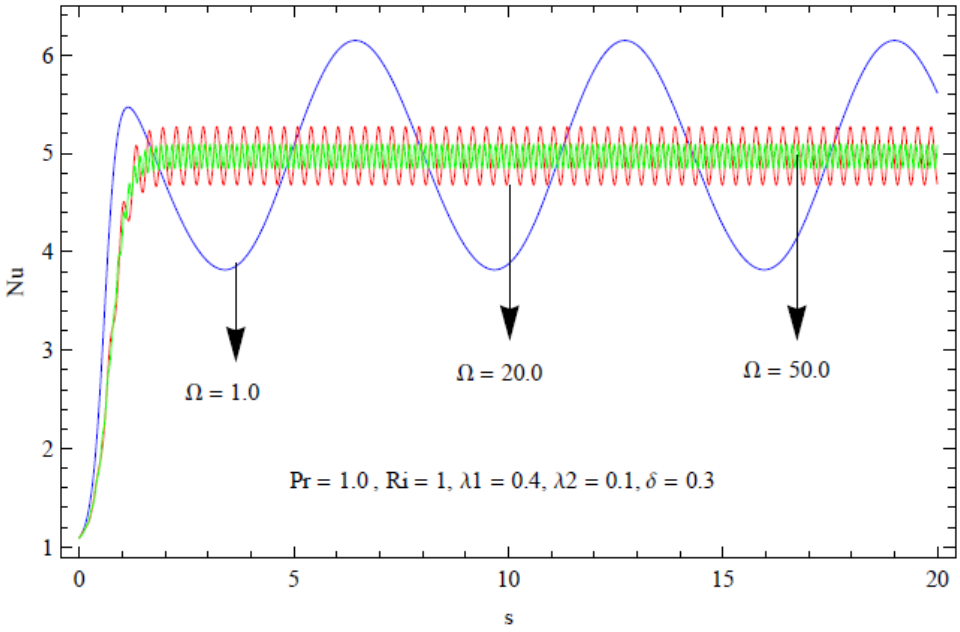

Fig .7. Effect of Ω on Nu For fixed values of the other parameters

In Fig. 9-10, the streamlines and corresponding isotherms are depicted respectively for different values of $s = 0.0,\ 0.4,\ 0.8,\ 1.0,\ 1.2,\ 1.5$ with $\lambda_1 = 0.4,\ \lambda_2 = 0.1,\ \delta = 0.1,\ \Omega = 2,$ $P_r = 1,\ \chi = 0.5$ and $R_i = 0.1$. From these figures, we observed that initially when time is small, the magnitude of streamlines is also small, as given in Fig. 9 (a, b), and isotherms are straight, that is the system is in the conduction state, Fig. 10 (a, b). However, as time increases, the magnitude of streamlines increases and the isotherms lose their evenness Fig. 9 (c, d)-10 (c, d). This shows that convection is taking place in the system. The system achieves the steady state beyond $s = 1.0$ as there is no further change in the streamlines and isotherms Fig. 9 (e, f) - 10 (e, f).

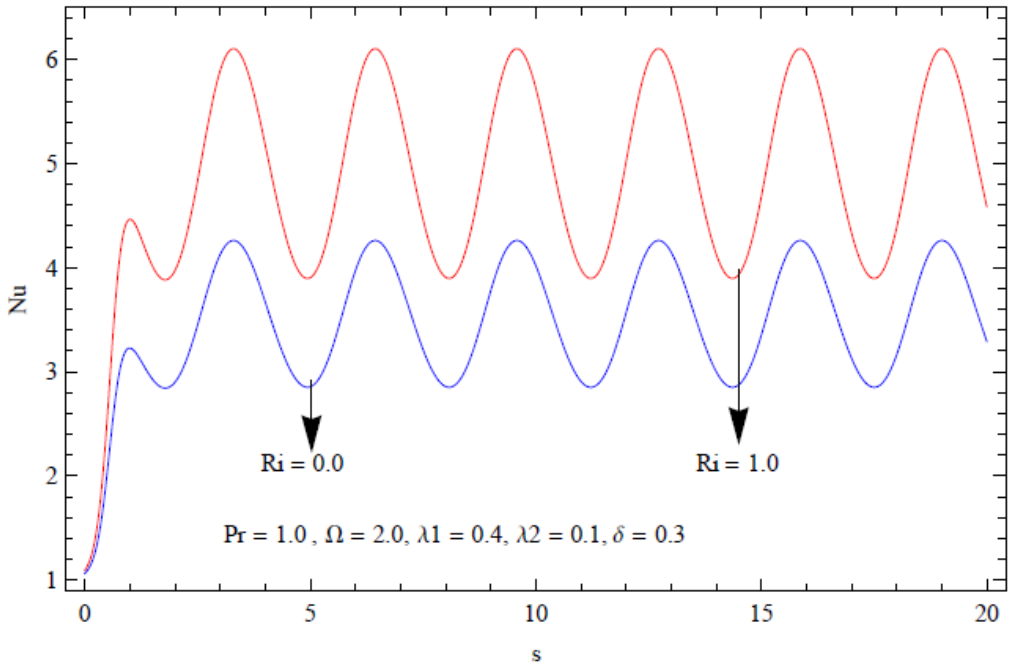

Fig .8. Comparison between internal and non internal - heating system

It is also shown that the system represented by Landau equation (41) enters subcritical Hopf bifurcation as stress relaxation time λ_1 is taken as the bifurcation parameter. Thus there exist critical value of λ_1 such that if λ_1 is less than the critical value then the system is stable and if λ_1 is greater than the critical value then the system is unstable. The phase portrait diagrams for the subcritical Hopf bifurcation are shown in Figs. 11-13. We have also discussed the pitchfork bifurcation for the amplitude equation (43) on the parameter amplitude of gravity modulation δ. The phase portrait diagram is shown in Fig. (14). The supercritical Pitchfork bifurcation diagram in Fig. (15) and subcritical Pitchfork bifurcation diagram in Fig. (16) show that the system becomes unstable as δ increases.

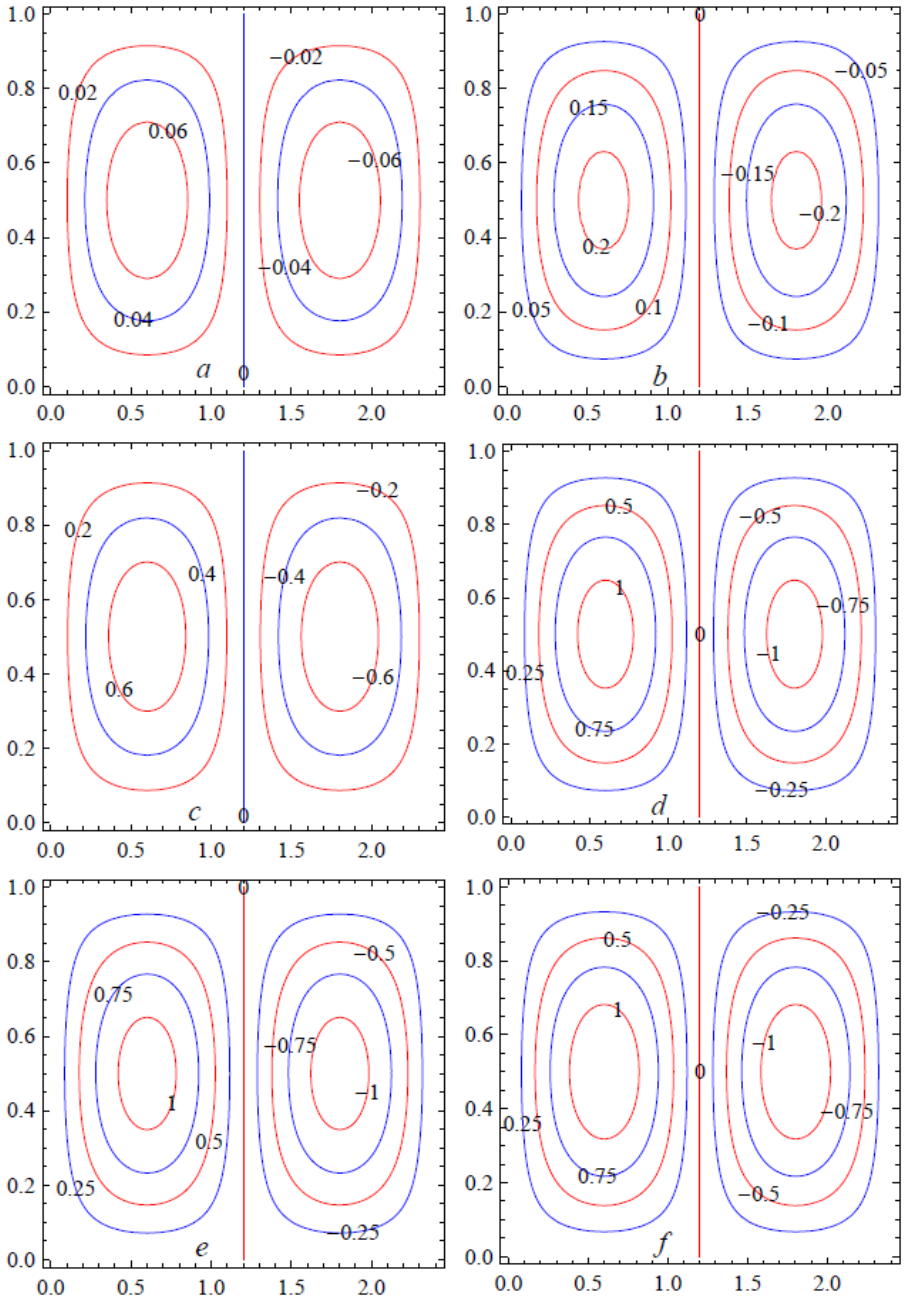

Fig .9 Stremlines at
(a) s = 0.0, (b) s = 0.4, (c) s = 0.8,
(d) s = 1.0, (e) s = 1.2, (f) s = 1.5

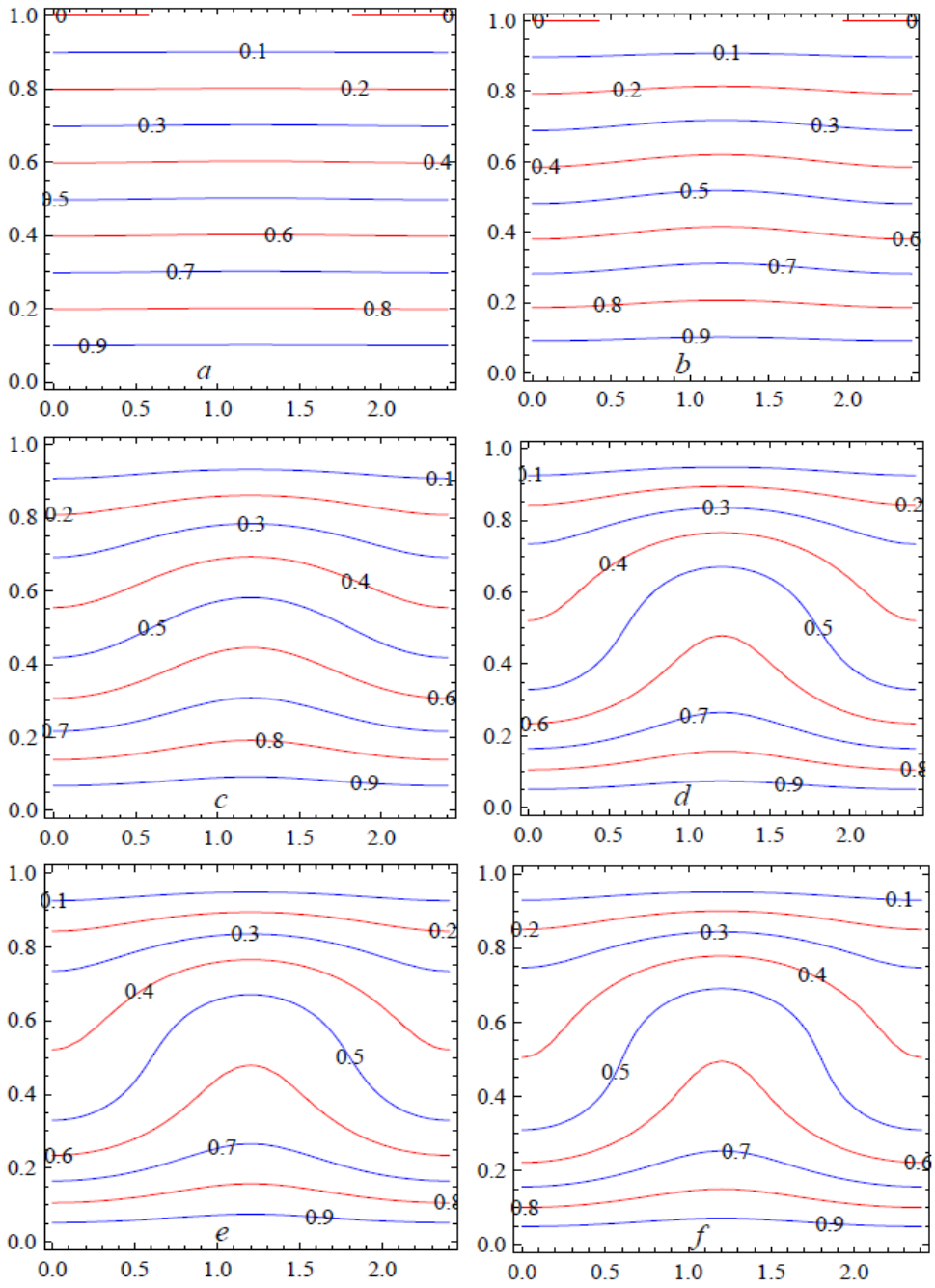

Fig .10 Isotherms at
(a) s = 0.0, (b) s = 0.4, (c) s = 0.8,
(d) s = 1.0, (e) s = 1.2, (f) s = 1.5

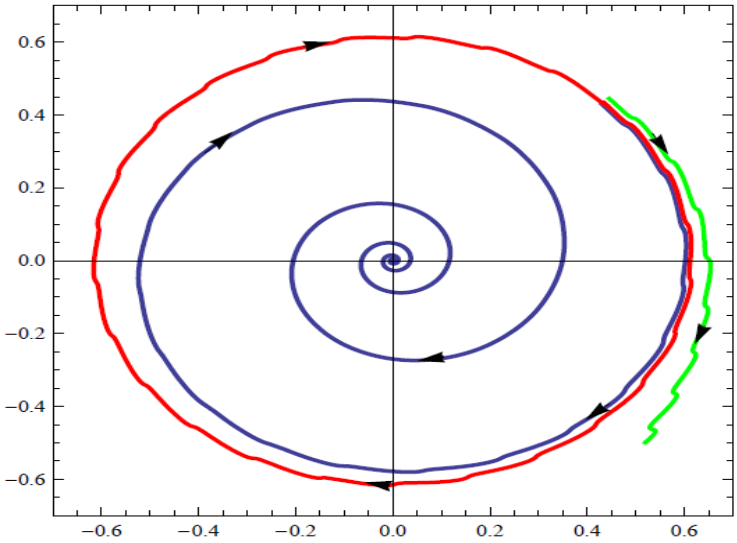

Pr = 1, Ri = 1, $\lambda 1$ = 0.4, $\lambda 2$ = 0.1, δ = 0.3, Ω = 50.

Fig. 11 An unstable limt cycle (red) is created thrugh Hopf bifurcation. The origin is asymptotically stable.

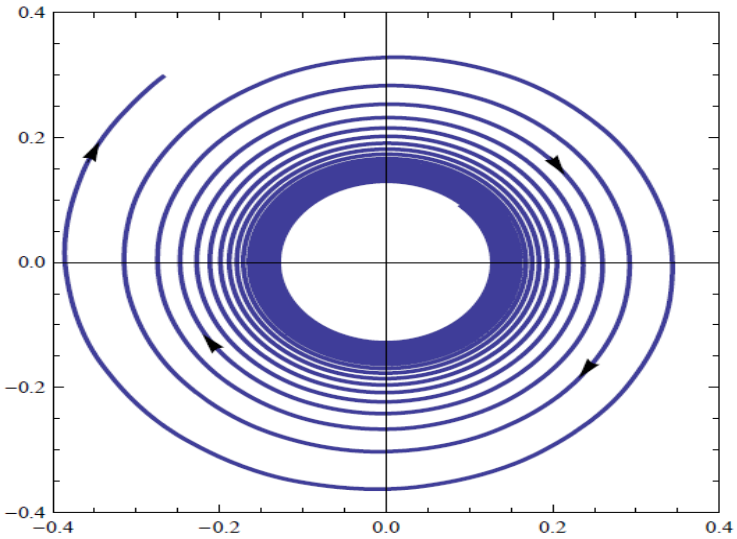

Pr = 1, Ri = 1, $\lambda 1$ = 0.47, $\lambda 2$ = 0.1, δ = 0.3, Ω = 50.

Fig. 12 Hopf bifurcation diagram.

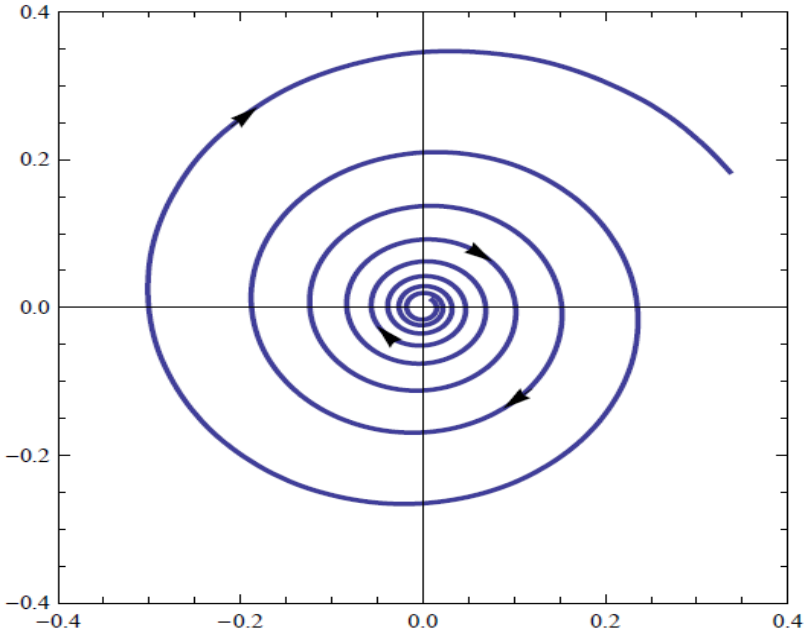

Pr = 1, Ri = 1, λ1 = 0.5,
λ2 = 0.1, δ = 0.3, Ω = 50.

Fig .13 The origin is unstable.

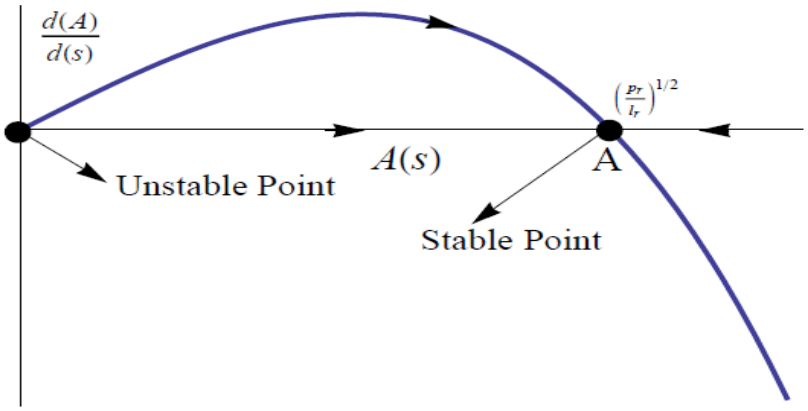

Fig. 14 Pr = 1, Ri = 1, λ1 = 0.4 , λ2 = .1, a = 2.61411, δ = 0.3, Ω = 1, s = 1000.

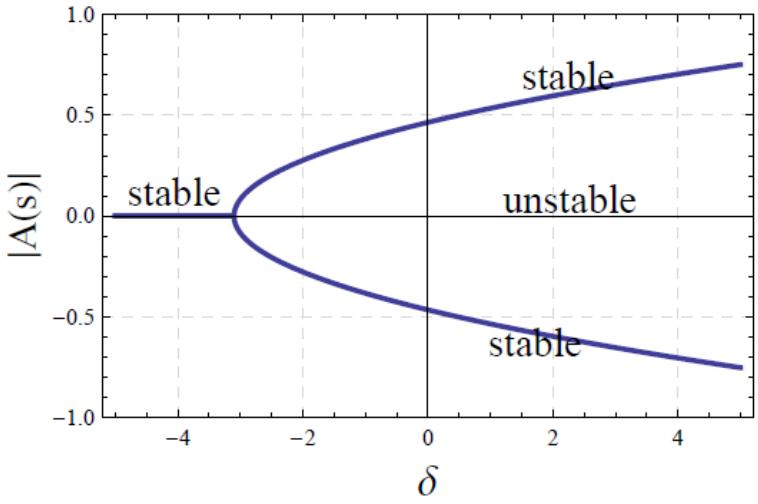

$P_r = 1,\ R_i = 1,\ \lambda_1 = 0.4,\ \lambda_2 = .1,\ a = 2.61411,\ \Omega = 1,\ s = 2000.$

Fig. 15 Supercritical Pitchfork Bifurcation.

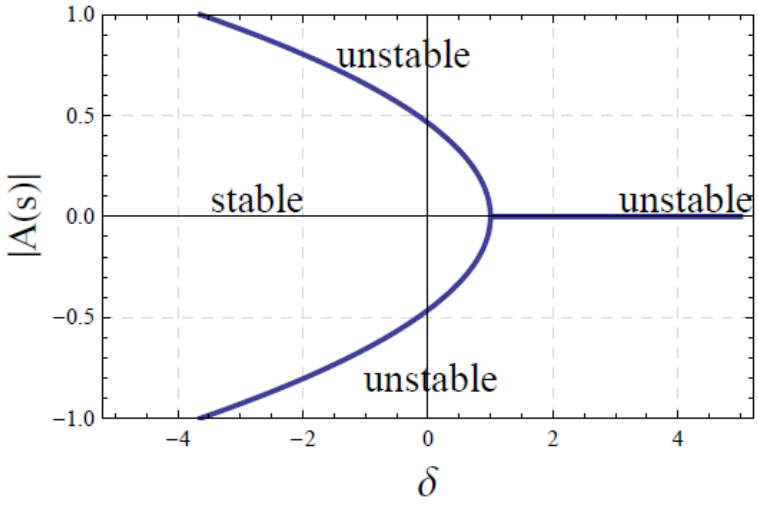

$P_r = 1,\ R_i = 1,\ \lambda_1 = 0.4,\ \lambda_2 = 0.1,\ a = 2.61411,\ \Omega = 1,\ s = 2100.$

Fig .16 Subcritical Pitchfork bifurcation.

7. Conclusions

In the present paper, we consider the combined effect of internal heating and gravity modulation on oscillatory convection in a viscoelastic fluid layer, and perform a weak non-linear stability analysis by using the Ginzburg-Landau equation.

The following conclusions are drawn:

a) Heat transport is more in this case than in the absence of internal heating.

b) It is important that for the oscillatory convection the relaxation time λ_1 of fluid must be greater than the retardation time λ_2.
c) Effect of relaxation time λ_1 is to advance the onset of convection and hence enhances the heat transport.
d) Effect of retardation time λ_2 is to delay the onset of convection and hence decreases the heat transport.
e) An increment in the amplitude of modulation δ is to advance the onset of convection and thus increasing the heat transfer.
f) The frequency of modulation Ω is to decrease the heat transfer.
g) An increment in the value of prandtl number P_r destabilizes the system, thus heat transfer increases.
h) The system is stable if relaxation time λ_1 is less than the critical point and becomes destabilized if the relaxation time λ_1 is greater than the critical point.
i) The system is destabilized as the amplitude of gravity modulation δ increases in bifurcation analysis.

Acknowledgment

The authors are grateful to the anonymous referees for the time, effort, and extensive comments which improve the quality of the presentation of the paper. Ajay Singh and Manoj K. Singh gratefully acknowledge the financial assistance from Babasaheb Bhimrao Ambedkar University, Lucknow, India as a research fellowship.

Nomenclature

Nomenclature			
Latin symbols		μ	dynamic viscosity of fluid
A(s)	amplitude of convection	ν	kinematic viscosity
a	wave number	ρ	fluid density
δ	amplitude of gravity modulation	ψ	stream function
d	depth of fluid layer	s	slow time scale
g	acceleration due to gravity	χ	perturbation parameter
N_u	Nusselt number	τ	fast time scale
p	reduced pressure	Ω	frequency of modulation
R_a	thermal Rayleigh number	ω	oscillatory frequency
T	temperature		
ΔT	temperature difference	**Superscripts**	
t	time	,	perturbed quantity

$\vec{q}$ fluid velocity (u, v, w)
Q internal heat source
R_i internal Rayleigh number
(x, z) horizontal and vertical co-ordinates

Greek symbols

α_T coefficient of thermal expansion
K permeability
k_T effective thermal diffusivity
$\bar{\lambda}_1$ stress relaxation time
$\bar{\lambda}_2$ strain retardation time

* dimensionless quantity

Subscripts

b basic state
c critical
0 reference value

Other symbols

$$\nabla^2 = \frac{\partial^2}{\partial x^2} + \frac{\partial^2}{\partial y^2} + \frac{\partial^2}{\partial z^2}$$

References

[1] S. Chandrasekhar, Hydrodynamic and Hydromagnetic Stability, Oxford University Press, Oxford, UK (1961).
[2] D.B. Ingham, I. Pop, Transport Phenomena in Porous Media, vol. III, 1st ed. Elsevier, Oxford (2005).
[3] D.A. Nield, A. Bejan, Convection in Porous Media, 3rd ed. Springer, New York (2006).
[4] K. Vafai, Handbook of Porous Media, Marcel Dekker, New York (2000).
[5] P.M. Gresho, R. Sani, The effects of gravity modulation on the stability of a heated fluid layer, J. Fluid Mech., 40 (1970) 783-806.
[6] M.S. Malashetty, V. Padmavathi, Effect of gravity modulation on the onset of convection in a fluid and porous layer, International Journal of Engineering Science, 35 (1997) 829-839.
[7] M.S. Malashetty, M. Swamy, Effect of gravity modulation on the onset of thermal convection in rotating fluid and porous layer, Phys. Fluids, 23 (6) (2011) 064108.
[8] B.S. Bhadauria, P.K. Bhatia, L. Debnath, Convection in Hele-Shaw cell with parametric excitation, Int. J. Non-Linear Mech., 40 (2005) 475-484.
[9] V.K.Siddhavaram, G.M. Homsy, The effects of gravity modulation on fluid mixing Part 1 Harmonic modulation, J. Fluid Mech., 562 (2006) 445-475.
[10] T. Green III, Oscillating convection in an elasticoviscous liquid, Phys. Fluids, (1968) 111410.
[11] C.M. Vest, V.S. Arpaci, Overstability of a viscoelastic fluid layer heated from below, J. Fluid Mech., 36 (1969) 613-623.
[12] P.K. Bhatia, J.M. Steiner, Convective instability in a rotating viscoelastic fluid layer, ZAMM, 52 (1972) 321-327.
[13] M.C. Kim, S.B. Lee, S. Kim, B.J. Chung, Thermal instability of viscoelastic fluids in porous media, Int. J. Heat Mass Transf., 46 (2003) 5065-5072.
[14] Donna M.G. Comissiong, Tyrone D. Dass, Harold Ramkissoon, Alana R. Sankar, On thermal instabilities in a viscoelastic fluid subject to internal heat generation, World Acad. Sci.Eng.Tech., 56 (2011) 08-24.
[15] B. Rajib, G.C. Layek, The onset of thermo-convection in a horizontal viscoelastic fluid layer heated underneath, Thermal Energy Power.Eng., 1 (1) (2012) 1-9.
[16] B.S. Bhadauria, P.kiran, Weak non-linear oscillatory convection in a viscoelastic fluid layer under gravity modulation, Int. J. Non-Linear Mech., 65 (2014) 133-140.

[17] M. Haajizadeh, A.F. Ozguc, C.L. Tien, Natural convection in a vertical porous enclosure with internal heat generation, Int. J. Heat Mass Transf., 27 (1984) 1893-1902.
[18] S.P. Bhattacharya, S.K.Jena, Thermal instability of a horizontal layer of micropolar fluid with heat source, Proceedings of the Indian Academy of Sciences (Mathematical Sciences), 93 (1) (1984) 13-26.
[19] Y.F. Rao, B.X. Wang, Natural convection in vertical porous enclosures with internal heat generation, Int. J. Heat Mass Transf., 34 (1991) 247-252.
[20] C. Parthiban, P.R. Patil, Thermal instability in an anisotropic porous medium with internal heat source and inclined temperature gradient, Int. Comm. Heat Mass Transf., 24 (7) (1997) 1049-1058.
[21] M.V. Joshi, U.N. Gaitonde, S.K. Mitra, Analytical study of natural convection in a cavity with volumetric heat generation, ASME J. Heat Transf., 128 (2006) 176-182.
[22] E. Magyari, I. Pop, A. Postelnicu, Effect of the source term on steady free convection boundary layer flows over a vertical plate in a porous medium, Part I. Transp. Porous Media, 67 (2007) 49-67.
[23] F. Capone, M. Gentile, A.A. Hill, Double-diffusive penetrative convection simulated via internal heating in an anisotropic porous layer with throughflow, Int. J. Heat Mass Transf., 54 (2011) 1622-1626.
[24] B.S. Bhadauria, K. Anoj, K. Jogendra, N.C. Sacheti, P. Chandran, Natural convection in a rotating anisotropic porous layer with internal heat generation, Transp. Porous Media, 90 (2) (2011) 687-705.
[25] B.S. Bhadauria, Double diffusive convection in a saturated anisotropic porous layer with internal heat source, Transport in Porous Media, 92 (2012) 299-320.
[26] B.S. Bhadauria, I. Hashim, P.G. Siddheshwar, Effect of internal-heating on weakly non-linear stability analysis of Rayleigh-B´enard convection under g-jitter, Int. J. Non-Linear Mech., 54 (2013) 35-42.
[27] S.H. Strogatz, Non-linear Dynamics and Chaos, Levant Books, Edition-I Kolkata India (2007).
[28] Yuri A. Kuznetsov, Elements of Applied Bifurcation Theory. Edition-II, Springer.
[29] W.V.R. Malkus, G. Veronis, Finite amplitude cellular convection, J. Fluid Mech, 4 (1958) 225-260.
[30] G. Venezian, Effect of modulation on the onset of thermal convection, J. Fluid Mech., 35 (1969) 243-254.

Ain Shams Engineering Journal xxx (2017) xxx–xxx

Contents lists available at ScienceDirect

Ain Shams Engineering Journal

journal homepage: www.sciencedirect.com

Engineering Physics and Mathematics

Throughflow and G-jitter effects on chaotic convection in an anisotropic porous medium

B.S. Bhadauria *, Ajay Singh

Department of Applied Mathematics, School for Physical Sciences, Babasaheb Bhimrao Ambedkar University, Lucknow 226025, India

ARTICLE INFO

Article history:
Received 9 June 2016
Revised 26 July 2016
Accepted 21 August 2016
Available online xxxx

Keywords:
Non-linear theory
Gravity modulation
Chaos theory
Throughflow

ABSTRACT

The present article is to investigate the effect of various parameters on chaotic convection in an anisotropic porous medium under gravity modulation. For this, the problem is reduced into Lorenz system (non-autonomous) by employing truncated Galerkin expansion method. It is found that the system shows either chaotic or periodic nature for suitable values of scaled Rayleigh number. The influence of amplitude of modulation is to advance the chaotic nature in the system while that of frequency of modulation has tendency to delay the chaotic behaviour. The effects of Péclet number and anisotropic parameters on the chaotic system are also studied and found these are delay the chaotic nature. The phase portrait and time domain diagrams of the Lorenz system for suitable parametric values has been used to analysed the system. Finally, we conclude that the system has either chaotic or periodic solution depending upon the values of the parameters.

1. Introduction

The stability of the convective system depends upon the temperature difference. When this temperature difference between fluid layer is large enough, instability occurs in the system due to buoyant force. This instability makes the system unstable which generates an interesting phenomenon known as convection. The Rayleigh-Bénard convection in porous medium is called as Darcy Bénard convection or Horton-Rogers problem. Study in porous media has attracted the attention of many researchers during the last three decades due to its applications in various fields such as petroleum industry, chemical engineering and geophysics. For more details, we can refer the most excellent books due to Ingham and Pop [1], Nield and Bejan [2] and Vafai [3], etc. An anisotropy in porous medium comes from asymmetric geometry of porous matrix or fibres. The studies of thermal instability in an anisotropic porous media plays very significant roles in many research fields such as in petroleum industry, chemical engineering, sedimentation and compaction. Some of the studies related to the anisotropic porous medium are due to Epherre [4], Kvernvold and Tyvand [5], Nisen and Storesletten [6], Tyvand and Storesletten [7], Degan et al. [8], Nield and Kuznetsov [9,10], Govender [11,12], Malashetty and Heera [13], Malashetty and Swamy [14], Simmons et al. [15] and Altawallbeh et al. [16]. Recently Alok et al. [17] Bhadauria and Kiran [18].

In this article, we consider gravity as a function of time (t) known as gravity modulation or G-jitter, in literature. This gives two parameters to understand the dynamics of the system. It is very useful to control many engineering thermal sciences process. Therefore, modulation (thermal, gravity, magnetic field) is the much interesting area for research due to its controlling nature of convective system. Gresho and Sani [19] were the first to propose the gravity modulation of the system as a technique to control the convective flow. They observed that the gravity modulation enable the system to get control on its instability either by suitable adjusting the values of frequency or the amplitude of modulation. For more details on gravity modulation, we refer [20–25].

Further, the concept of throughflow is used to control the convective mechanism in engineering sciences, industries, geophysics, etc. The basic state temperature profile of throughflow changes from linear to non-linear with layer height, which affects the stability of the system. The effect of throughflow on the onset of convection in a horizontal porous layer has been studied by Wooding [26], Sutton [27], Homsy and Sherwood [28], Jones and Persichetti [29]. Nield [30] and Shivakumara [31] showed that a small amount of throughflow can have a destabilizing effect on the system. Khalili and Shivakumara [32] have investigated the effect of

Peer review under responsibility of Ain Shams University.

* Corresponding author at: Department of Applied Mathematics, School for Physical Sciences, Babasaheb Bhimrao Ambedkar University, Lucknow 226025, India.

E-mail addresses: mathsbsb@yahoo.com (B.S. Bhadauria), ajaysingh0044@gmail.com (A. Singh).

http://dx.doi.org/10.1016/j.asej.2016.08.024
2090-4479/

Please cite this article in press as: Bhadauria BS, Singh A. Throughflow and G-jitter effects on chaotic convection in an anisotropic porous medium. Ain Shams Eng J (2017), http://dx.doi.org/10.1016/j.asej.2016.08.024

Nomenclature

Latin symbols

δ	amplitude of gravity modulation
d	depth of fluid layer
L	length of porous layer
$\vec{g}$	acceleration due to gravity
p	reduced pressure
Ra_D	thermal Darcy-Rayleigh number
R	scaled Rayleigh number
T	temperature
P_e	Péclet number
ΔT	temperature difference across the porous layer
t	time
$\mathbf{q}$	fluid velocity(u,v,w)
(x,z)	horizontal and vertical co-ordinates

Greek symbols

α_T	coefficient of thermal expansion
κ_T	effective thermal diffusivity $\kappa_{Tx}(\hat{i}\hat{i}+\hat{j}\hat{j})+\kappa_{Tz}(\hat{k}\hat{k})$
K	permeability $K_x(\hat{i}\hat{i}+\hat{j}\hat{j})+K_z(\hat{k}\hat{k})$
K_x	permeability in x direction
K_z	permeability z direction
η	thermal anisotropic parameter κ_{Tx}/κ_{Tz}
ξ	mechanical anisotropic parameter K_x/K_z
χ	scaled thermal anisotropic parameter
ζ	scaled mechanical anisotropic parameter
Ω	frequency of modulation
μ	dynamic viscosity of the fluid
ϕ	porosity
γ	heat capacity ratio
ν	kinematic viscosity
ρ	fluid density
ψ	stream function
τ	rescaled time
X	rescaled amplitude
Y	rescaled amplitude
Z	rescaled amplitude

Other symbols

∇^2	$\frac{\partial^2}{\partial x^2}+\frac{\partial^2}{\partial y^2}+\frac{\partial^2}{\partial z^2}$

Subscripts

b	basic state
0	reference value

Superscripts

$'$	perturbed quantity
$*$	dimensionless quantity

throughflow and internal heat generation on the onset of convection in a porous medium. The non-Darcian effects on convective instability in a porous medium with throughflow has been studied by Shivakumara [33]. Shivakumara and Nanjundappa [34] investigated analytically, the effects of quadratic drag and vertical throughflow on double diffusive convection in a horizontal porous medium using the Forchheimer extended Darcy equation. It is found that irrespective of the nature of boundaries, a small amount of throughflow in either of its direction destabilizes the system. Shivakumara and Sureshkumar [35] have studied convective instability in non-newtonian fluid saturated porous medium in the presence of vertical throughflow and found that throughflow has stabilizing or destabilizing effect depending on the boundaries and the directions of the flow. Brevdo [36] investigated three-dimensional absolute and convective instabilities at the onset of convection in a porous medium with inclined temperature gradient and vertical throughflow. Barletta et al. [37] analyzed the convective roll instabilities of vertical throughflow with viscous dissipation in a horizontal porous medium. Reza and Gupta [38] investigated the effect of through flow on the onset of convection in a horizontal layer of electrically conducting fluid, confined between two rigid permeable boundaries, heated from below, in the presence of a uniform vertical magnetic field. They found that magnetic field inhabits the onset of steady convection, and a positive throughflow is more stabilizing than negative throughflow. Recently, Nield and Kuznetsov [39], Bhaduria and kiran [40] studied the effect of throughflow in porous medium for different model.

Many researchers have studied the chaotic convection due to its great importance in daily life. Such type of convection is applicable in various kind of fields, for instance, in the production of crystals and weather sciences, etc. The chaos model was firstly proposed by Poincaré [41]. In this model the author found that the dynamical system generated by the three body problem is quite sensitive to the initial conditions exhibiting chaotic behaviour. Later on, Edward Lorenz [42] studied the system of three ordinary differential equations and developed the model for atmospheric convection, similar work has been done in [43]. Vadasz with their colleague presented a number of articles on the transition to chaotic behaviour in porous layer heated from below [44–48]. Long et al. [49] studied the chaotic convection of viscoelastic fluid in porous medium. Recently, Vadasz [50], Bhadauria and Kiran [51,52] and Gupta and Singh [53] have studied chaotic convection in porous medium by using different physical models.

In the present article, the combined effect of throughflow and gravity modulation on chaotic convection in an anisotropic porous medium is studied. Firstly the adopted model is reduced into Lorenz system by employing the truncated Galerkin expansion method. The influence of amplitude of modulation is to advance the chaotic nature in the system while that of frequency of modulation has tendency to delay the chaotic behaviour. The effects of Péclet number and anisotropic parameters on the chaotic system are also discussed. The proposed Lorenz system has been analysed by using phase portrait and time domain diagrams.

2. Mathematical structure of the problem

An infinitely extended horizontal anisotropic porous layer of depth d confined between two parallel planes: the lower plane is at $z=0$ while the upper plane is at $z=d$. A Cartesian frame of reference is adopted in such a way that the origin lies on the lower plane and z-axis is vertically upward. The porous layer is heated from below and cooled from above. The physical configuration of the model is depicted in Fig. 1. The Darcy law and Oberbeck-Boussinesq approximation is adopted to solve the model equations. The non-dimensionalized system of the governing equations is obtain according to [17,53]

$$\frac{1}{V_a}\frac{\partial}{\partial t}(\nabla^2\psi) = -\nabla_\xi^2\psi - R_a(1+\delta\sin(\Omega t))\frac{\partial T}{\partial x}, \tag{1}$$

$$-\frac{\partial\psi}{\partial x}\frac{\partial T_b}{\partial z} - \left(\nabla_\eta^2 - P_e\frac{\partial}{\partial z}\right)T = -\frac{\partial T}{\partial t} + \frac{\partial(\psi,T)}{\partial(x,z)}, \tag{2}$$

Please cite this article in press as: Bhadauria BS, Singh A. Throughflow and G-jitter effects on chaotic convection in an anisotropic porous medium. Ain Shams Eng J (2017), http://dx.doi.org/10.1016/j.asej.2016.08.024

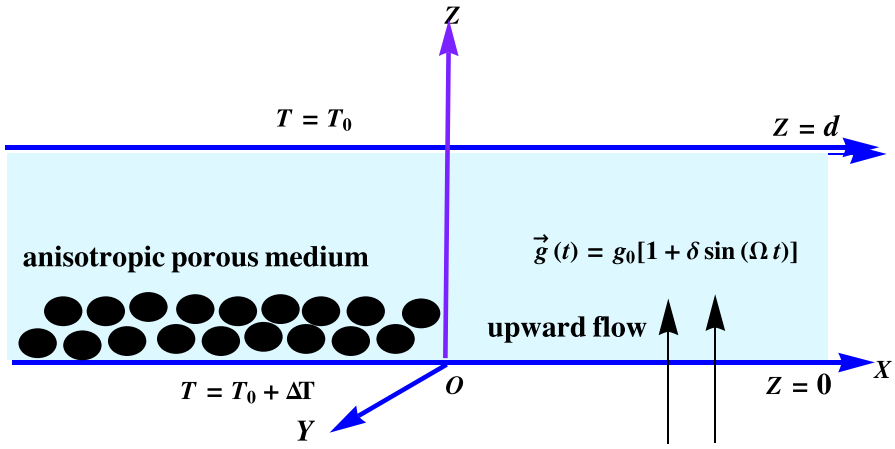

Fig. 1. Physical configuration of the problem.

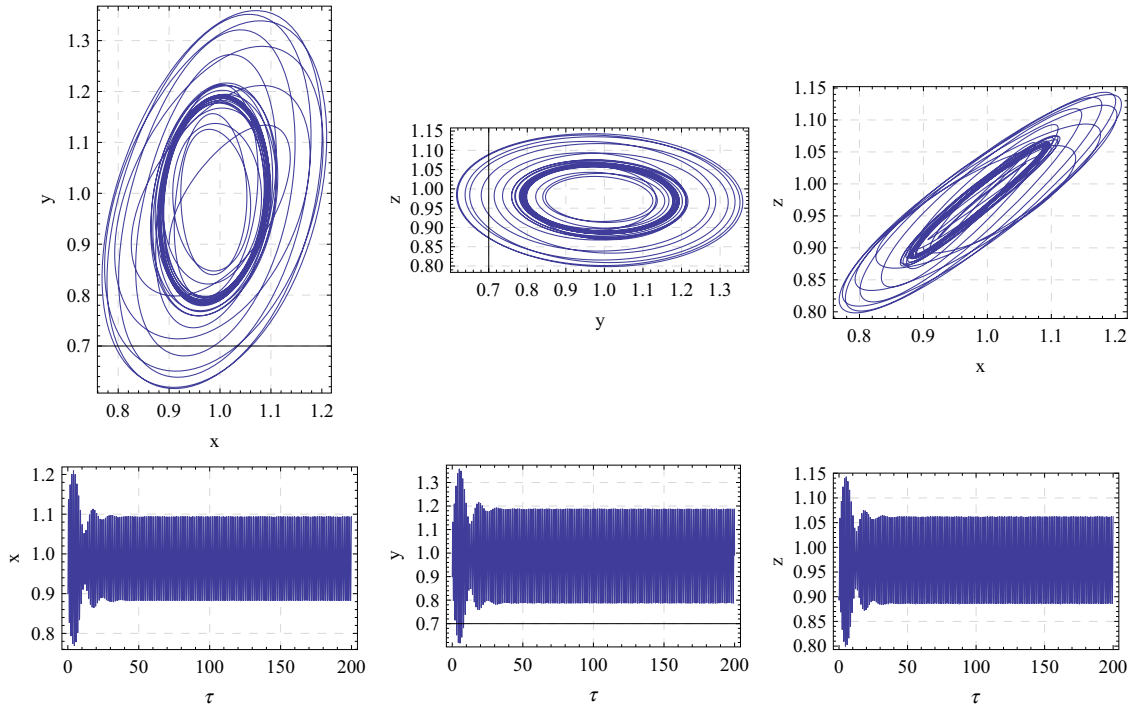

Fig. 2. Phase Portrait and time domain diagrams For the System (10) with parameters $R = 5$ and $\zeta = 0.4$, $\chi = 0.4$, $P_e = 1.0$, $\delta = 0.1$, $\Omega = 5$.

where $V_a = \frac{\phi v d^2}{K_z \kappa_{Tz}}$ is Vadasz number, $R_a = \frac{\alpha_T g_0 \Delta T d K_z}{\nu \kappa_{Tz}}$ is thermal Rayleigh number, $P_e = \frac{w_0 d}{\kappa_{Tz}}$ is Péclet number, $(1 + \delta \sin(\Omega t))$ is modulation term and the other variables have their usual meanings as given in the nomenclature.

The externally imposed thermal boundary conditions are given by

$$T = \begin{cases} T_0 + \Delta T, & \text{at } z = 0, \\ T_0, & \text{at } z = d. \end{cases} \tag{3}$$

The basic state temperature present in Eq. (2) is obtained by using the above boundary condition (3) as in [40]

$$T_b = \frac{e^{P_e z} - e^{P_e}}{1 - e^{P_e}}. \tag{4}$$

3. Method of solution

The solution of nonlinear Eqs. (1) and (2) are obtained by using truncated Galerkin expansion method. The stream function and temperature field are taken in the forms as mentioned in [50].

$$\psi = A_{11} \sin\left(\frac{\pi x}{L}\right) \sin(\pi z), \tag{5}$$

$$T = T_b + B_{11} \cos\left(\frac{\pi x}{L}\right) \sin(\pi z) + B_{02} \sin(2\pi z). \tag{6}$$

Using Eqs. (5) and (6) into Eqs. (1) and (2), multiplying the equations by orthogonal eigenfunctions corresponding to Eqs. (5) and (6), and then integrating them over the spatial domain, we get a set of three differential equations for the time evolution of the amplitudes, in the form of

$$\frac{dA_{11}}{d\tau} = -\frac{V_a \gamma}{\pi^2}\left(\frac{R_a}{\pi\theta}(1 + \delta \sin(\Omega\tau))B_{11} + \zeta A_{11}\right), \tag{7}$$

$$\frac{dB_{11}}{d\tau} = -\frac{1}{\pi\theta}\left(\frac{4\pi^2}{P_e^2 + 4\pi^2}\right)A_{11} - \frac{1}{\theta}A_{11}B_{02} - \chi B_{11}, \tag{8}$$

Please cite this article in press as: Bhadauria BS, Singh A. Throughflow and G-jitter effects on chaotic convection in an anisotropic porous medium. Ain Shams Eng J (2017), http://dx.doi.org/10.1016/j.asej.2016.08.024

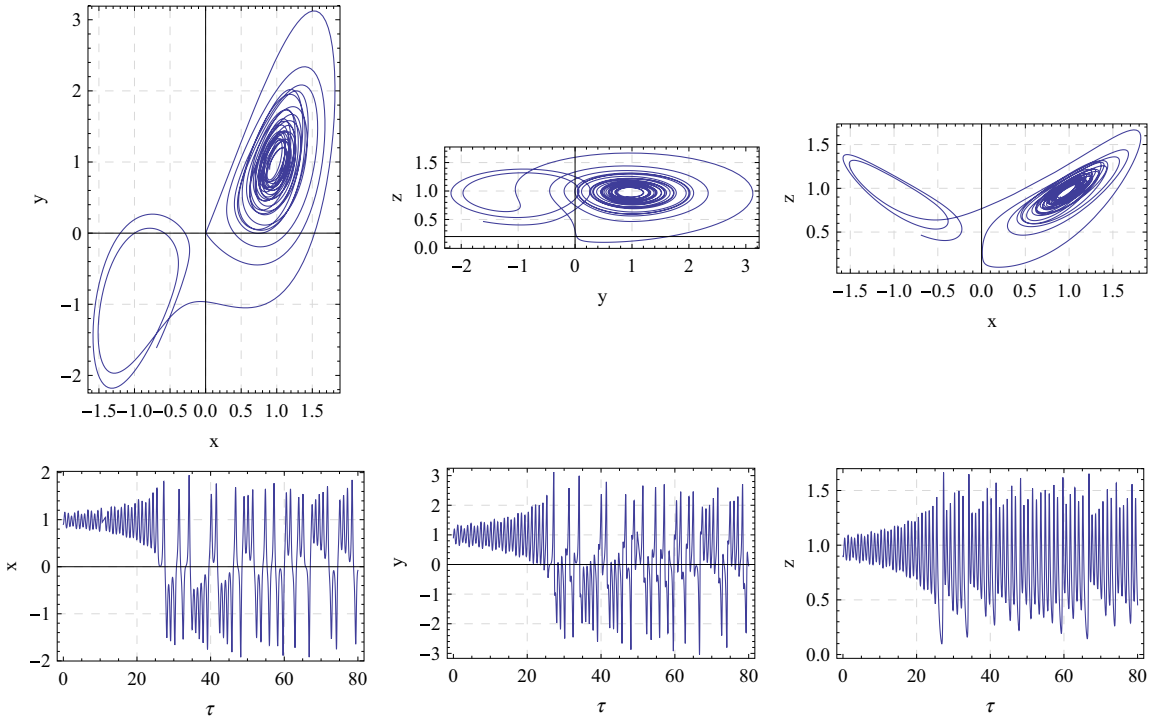

Fig. 3. Phase Portrait and time domain diagrams For the System (10) with parameters $R = 8.5$ and $\zeta = 0.4$, $\chi = 0.4$, $P_e = 1.0$, $\delta = 0.1$, $\Omega = 5$.

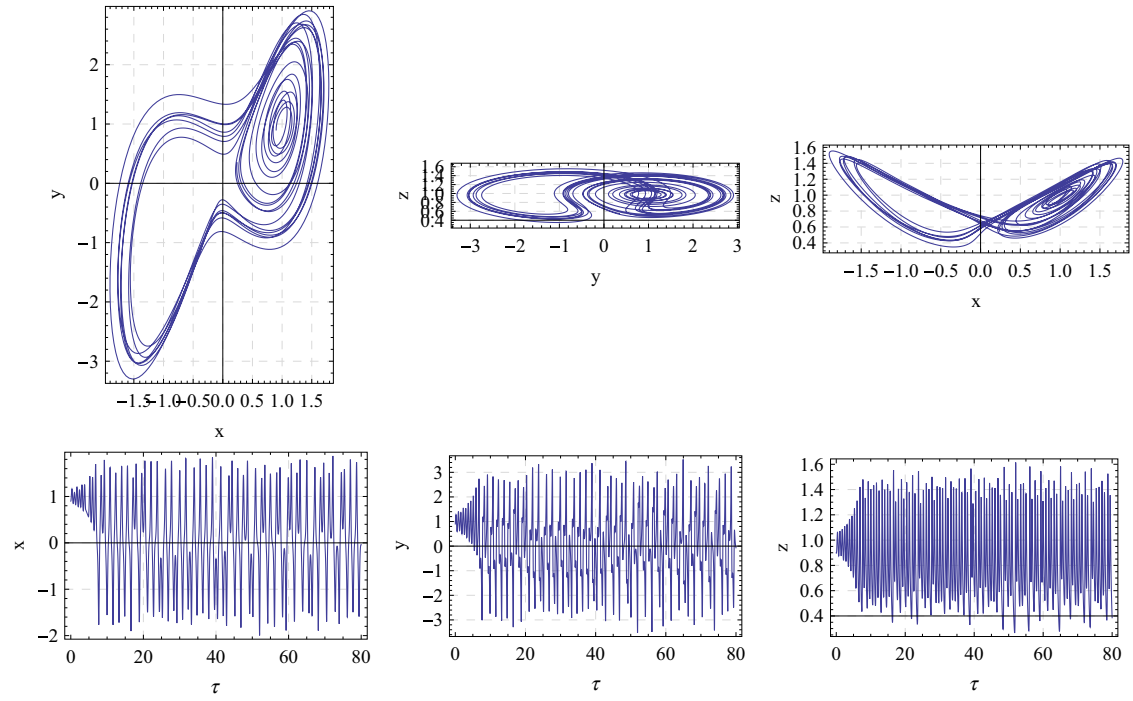

Fig. 4. Phase Portrait and time domain diagrams For the System (10) with parameters $R = 15$ and $\zeta = 0.4$, $\chi = 0.4$, $P_e = 1.0$, $\delta = 0.1$, $\Omega = 5$.

$$\frac{dB_{02}}{d\tau} = \frac{1}{2\theta}A_{11}B_{11} - 4\gamma B_{02}, \tag{9}$$

where the time has been re-scaled and the following notations are introduced

$$\tau = \frac{(L^2+1)\pi^2}{L^2}t,\ \theta = \frac{L^2+1}{L^2},\ \gamma = \frac{L^2}{L^2+1},\ \Omega = \frac{L^2}{(L^2+1)\pi^2}\Omega,\ \sigma = \frac{V_a\gamma}{\pi^2},\ R = \frac{R_a}{\pi^2\theta^2},\ \chi = \frac{\eta+L^2}{L^2}\ \text{and}\ \zeta = \frac{(L^2/\xi)+1}{L^2}.$$

Again, rescaling the amplitudes in the form

$$X = -\frac{\sqrt{\zeta}A_{11}}{2\theta\sqrt{2\gamma(R-\zeta\chi)}},\ Y = \frac{\pi RB_{11}}{2\sqrt{2\gamma\zeta(R-\zeta\chi)}}\ \text{and}\ Z = -\frac{\pi RB_{02}}{(R-\zeta\chi)}$$

will provide the following set of equations

$$\begin{cases} \dot{X} = \sigma\zeta((1+\delta\sin(\Omega\tau))Y - X), \\ \dot{Y} = \frac{1}{\zeta}\left(R\left(\frac{4\pi^2}{P_e^2+4\pi^2}\right)X - \zeta\chi Y - (R-\zeta\chi)XZ\right), \\ \dot{Z} = 4\gamma(XY - Z), \end{cases} \tag{10}$$

Please cite this article in press as: Bhadauria BS, Singh A. Throughflow and G-jitter effects on chaotic convection in an anisotropic porous medium. Ain Shams Eng J (2017), http://dx.doi.org/10.1016/j.asej.2016.08.024

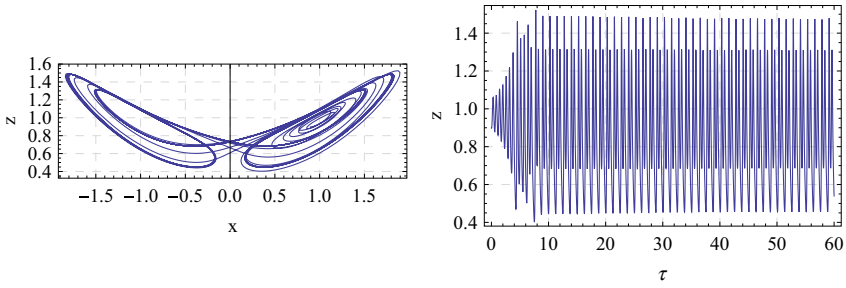

Fig. 5. Phase Portrait and time domain diagrams For the System (10) with parameters $R = 23$ and $\zeta = 0.4$, $\chi = 0.4$, $P_e = 1.0$, $\delta = 0.1$, $\Omega = 5$.

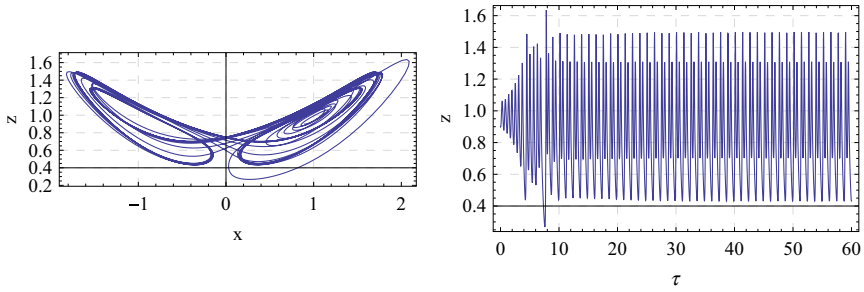

Fig. 6. Phase Portrait and time domain diagrams For the System (10) with parameters $R = 24$ and $\zeta = 0.4$, $\chi = 0.4$, $P_e = 1.0$, $\delta = 0.1$, $\Omega = 5$.

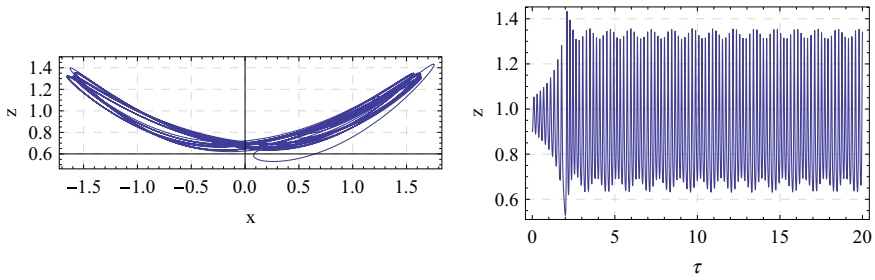

Fig. 7. Phase Portrait and time domain diagrams For the System (10) with parameters $R = 200$ and $\zeta = 0.4$, $\chi = 0.4$, $P_e = 1.0$, $\delta = 0.1$, $\Omega = 5$.

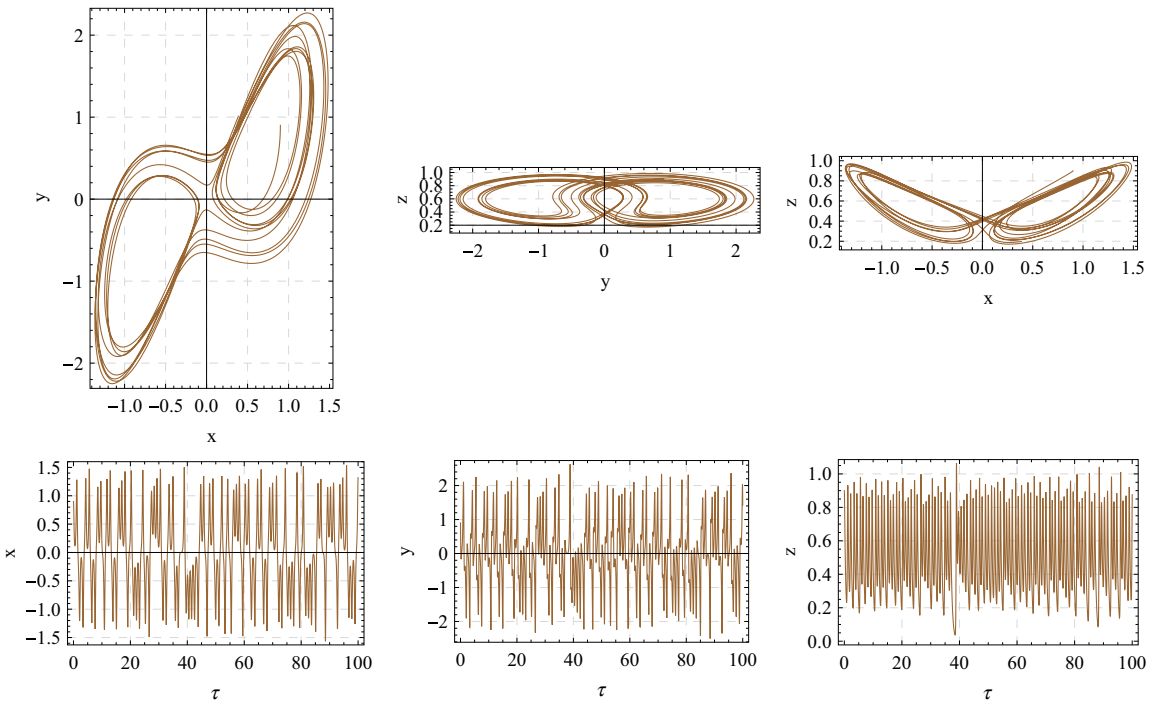

Fig. 8. Phase Portrait and time domain diagrams For the System (10) with parameters $P_e = 5$ and $\zeta = 0.4$, $\chi = 0.4$, $R = 15$, $\delta = 0.1$, $\Omega = 5$.

Please cite this article in press as: Bhadauria BS, Singh A. Throughflow and G-jitter effects on chaotic convection in an anisotropic porous medium. Ain Shams Eng J (2017), http://dx.doi.org/10.1016/j.asej.2016.08.024

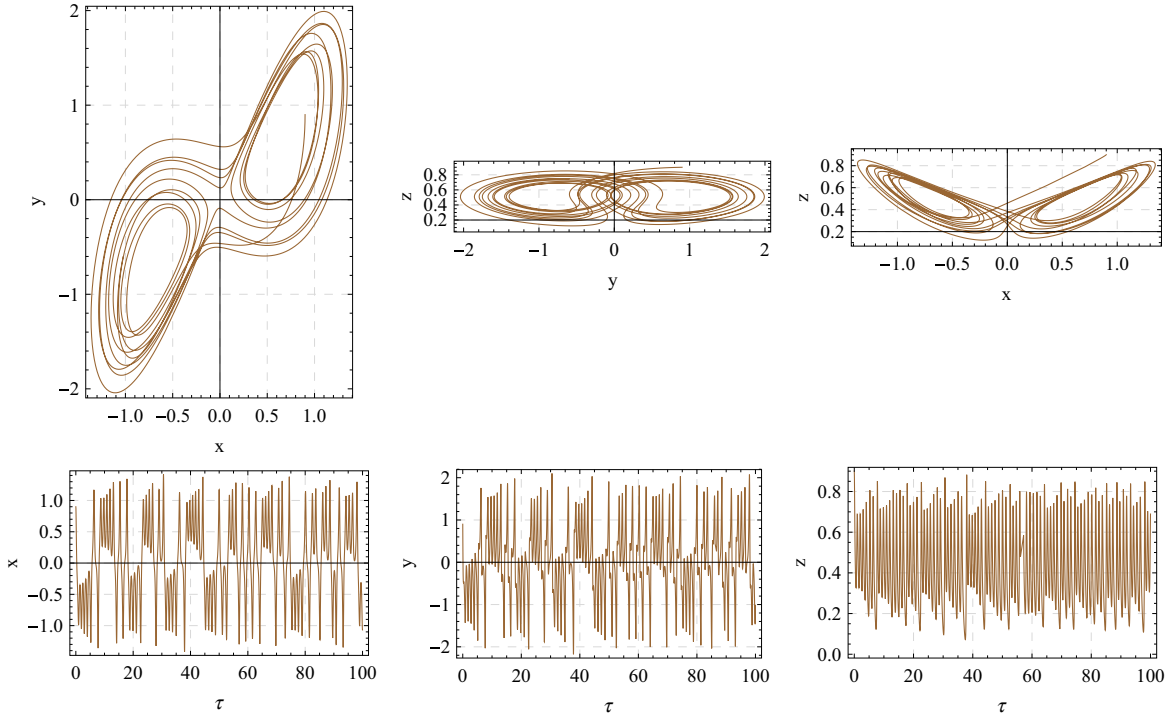

Fig. 9. Phase Portrait and time domain diagrams For the System (10) with parameters $P_e = 6$ and $\zeta = 0.4$, $\chi = 0.4$, $R = 15$, $\delta = 0.1$, $\Omega = 5$.

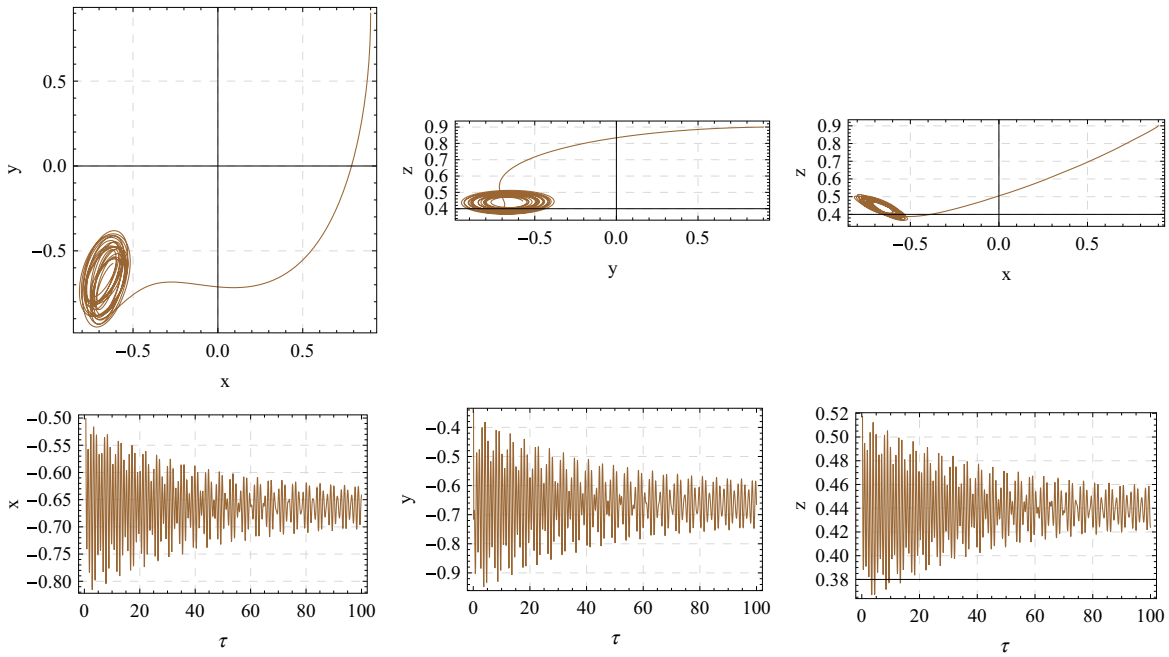

Fig. 10. Phase Portrait and time domain diagrams For the System (10) with parameters $P_e = 7$ and $\zeta = 0.4$, $\chi = 0.4$, $R = 15$, $\delta = 0.1$, $\Omega = 5$.

where the primes ($'$) denote time derivatives. If the amplitude of gravity modulation $\delta = 0$ and $P_e = 0$ then the system (10) reduces into Gupta et al. [53] model as

$$\begin{cases} \dot{X} = \sigma\zeta(Y - X), \\ \dot{Y} = \frac{1}{\zeta}(RX - \zeta\chi Y - (R - \zeta\chi)XZ), \\ \dot{Z} = 4\gamma(XY - Z). \end{cases} \tag{11}$$

4. Results and discussion

MATHEMATICA 7.0 has been used for the numerical simulation of the Lorenz system (10). In this simulation, we considered the initial conditions $\tau = 0 : X = Y = Z = 0.9$ and fixed the parameters $\sigma = 10, \gamma = 0.5$. The parameters $R, P_e, \delta, \Omega, \chi, \zeta$ are considered as variable to examine the behavior of modulated chaotic system.

Please cite this article in press as: Bhadauria BS, Singh A. Throughflow and G-jitter effects on chaotic convection in an anisotropic porous medium. Ain Shams Eng J (2017), http://dx.doi.org/10.1016/j.asej.2016.08.024

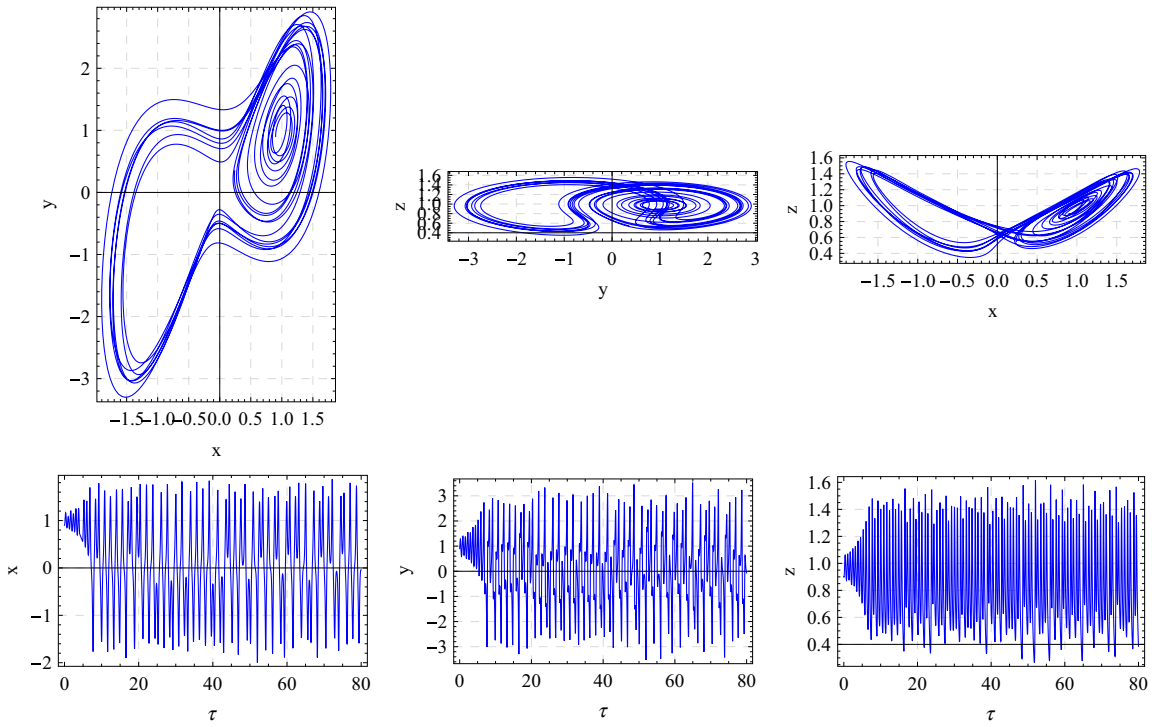

Fig. 11. Phase Portrait and time domain diagrams For the System (10) with parameters $\zeta = 0.4$ and $P_e = 1$, $\chi = 0.4$, $R = 15$, $\delta = 0.1$, $\Omega = 5$.

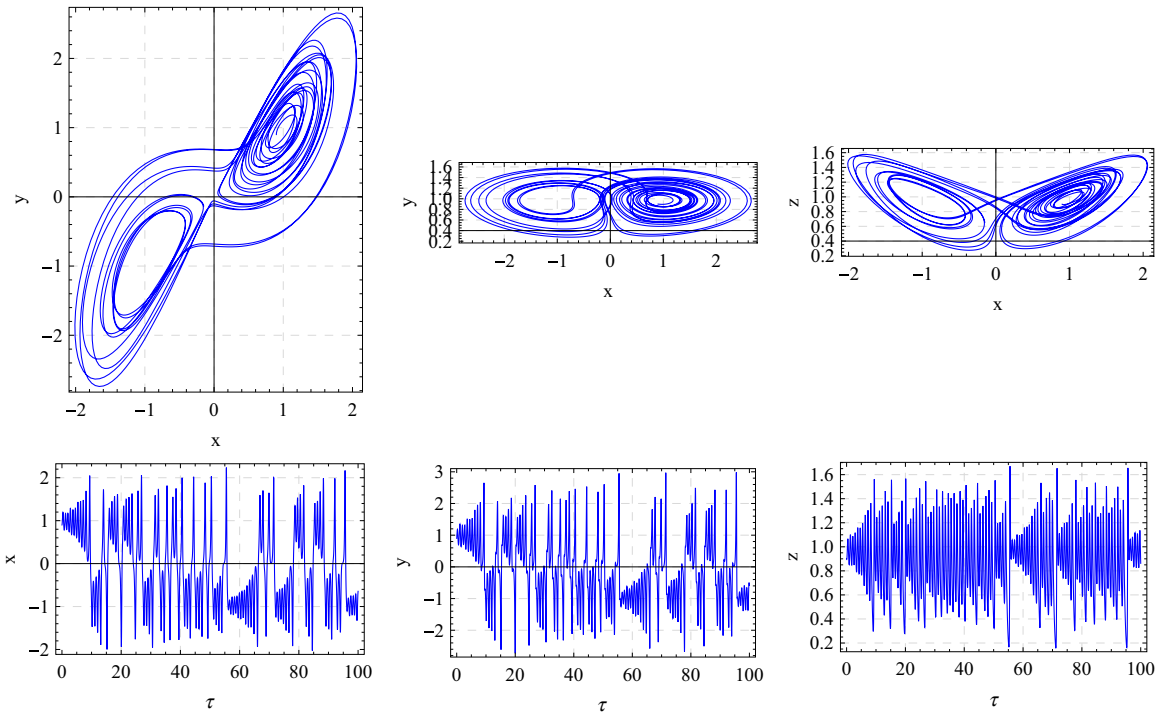

Fig. 12. Phase Portrait and time domain diagrams For the System (10) with parameters $\zeta = 0.7$ and $P_e = 1$, $\chi = 0.4$, $R = 15$, $\delta = 0.1$, $\Omega = 5$.

The phase-portrait diagrams depicts how modulation term affect the dynamics of the thermal convection for a combination of varied parameters. The results are further depicted in Figs. 2–26 to analyse the Lorenz model by using phase-portrait and time domain diagrams.

The effect of scaled Rayleigh number R on the system are depicted in Figs. 2–7, keeping fixed the other parameters. Fig. 2 shows a periodic solution ($R = 5$) and for ($R = 8.5$) system moves from periodic to weak chaotic solution in Fig. 3. Fig. 4 ($R = 15$) depicts a chaotic behaviour or aperiodic solution of the Lorenz

Please cite this article in press as: Bhadauria BS, Singh A. Throughflow and G-jitter effects on chaotic convection in an anisotropic porous medium. Ain Shams Eng J (2017), http://dx.doi.org/10.1016/j.asej.2016.08.024

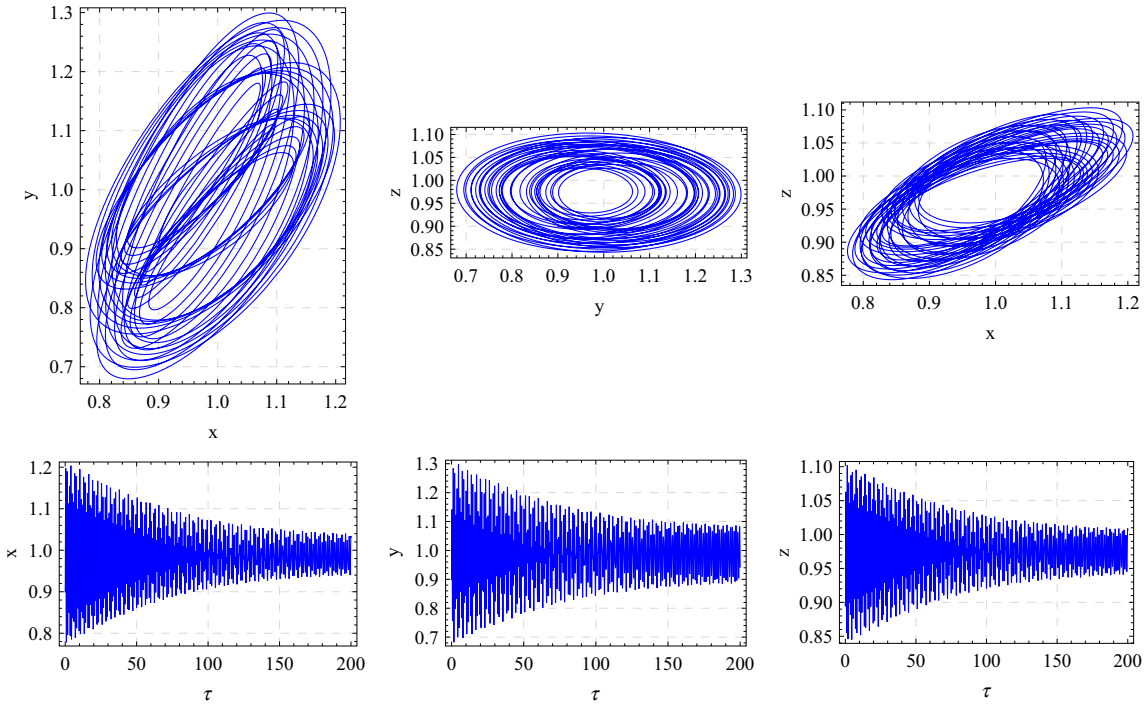

Fig. 13. Phase Portrait and time domain diagrams For the System (10) with parameters $\zeta = 0.9$ and $P_e = 1$, $\chi = 0.4$, $R = 15$, $\delta = 0.1$, $\Omega = 5$.

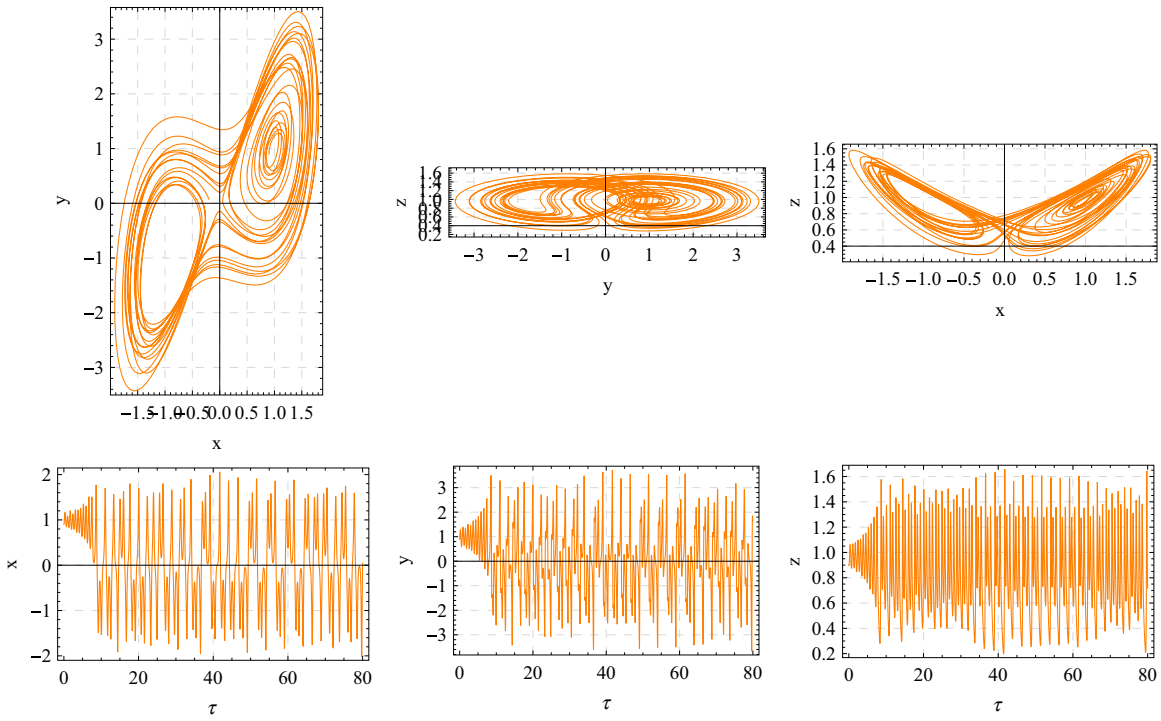

Fig. 14. Phase Portrait and time domain diagrams For the System (10) with parameters $\chi = 0.5$ and $P_e = 1$, $\zeta = 0.4$, $R = 15$, $\delta = 0.1$, $\Omega = 5$.

system which shows that heat transfer is more in this case in comparison to previous two case. Further in Figs. 5 and 6 system shows periodic solution for $(R = 23, R = 24)$ respectively. On increasing the higher value of $R > 100$ system always shows periodic solution depicts in Fig. 7. Hence, we conclude that the system has either periodic or chaotic behavior depending upon the value of scaled Rayleigh number which agrees with the results obtained by Long et al. [49]. The impact of Péclet number *Pe* on the system for different parametric values $Pe = 5, 6, 7$ keeping fixed the other parameters, is depicted in Figs. 8–10, respectively. From these figures we can see that the system transition from chaos to periodic i.e. heat transfer level down on increasing the value *Pe*, clear from the diagrams.

Please cite this article in press as: Bhadauria BS, Singh A. Throughflow and G-jitter effects on chaotic convection in an anisotropic porous medium. Ain Shams Eng J (2017), http://dx.doi.org/10.1016/j.asej.2016.08.024

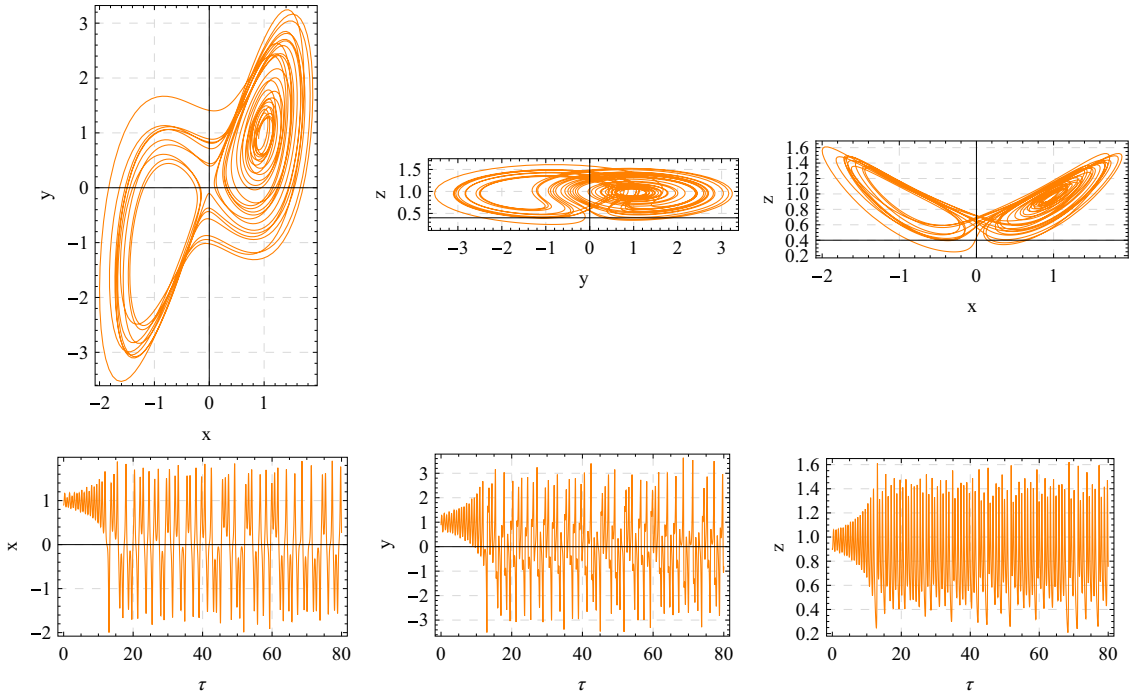

Fig. 15. Phase Portrait and time domain diagrams For the System (10) with parameters $\chi = 0.7$ and $P_e = 1$, $\zeta = 0.4$, $R = 15$, $\delta = 0.1$, $\Omega = 5$.

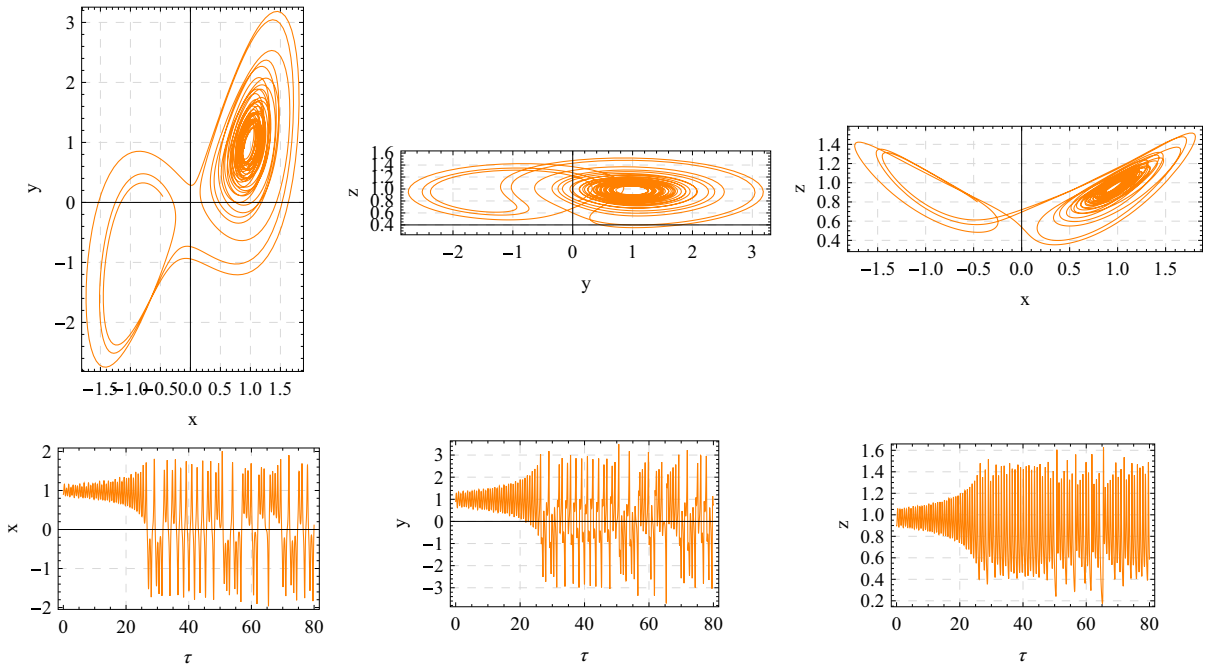

Fig. 16. Phase Portrait and time domain diagrams For the System (10) with parameters $\chi = 0.9$ and $P_e = 1$, $\zeta = 0.4$, $R = 15$, $\delta = 0.1$, $\Omega = 5$.

Figs. 11–13 depict the effect of different values of scaled mechanical anisotropic parameter $\zeta = 0.4, 0.7, 0.9$, keeping fixed the other parameters. The phase-portrait diagrams and time domain solutions show that the system has chaotic nature for $\zeta = 0.4$ and $= 0.7$ while the system shows a periodic nature for $\zeta = 0.9$. Thus, the system returns to periodic solution from the chaotic solution as ζ increases, and so, mechanical anisotropic parameter ζ delay the heat transfer, similar the result [53]. The another anisotropic parameter χ effects on the system are depicted in Figs. 14–16 for $\chi = 0.5, 0.7, 0.9$ respectively. Here we notice that

Please cite this article in press as: Bhadauria BS, Singh A. Throughflow and G-jitter effects on chaotic convection in an anisotropic porous medium. Ain Shams Eng J (2017), http://dx.doi.org/10.1016/j.asej.2016.08.024

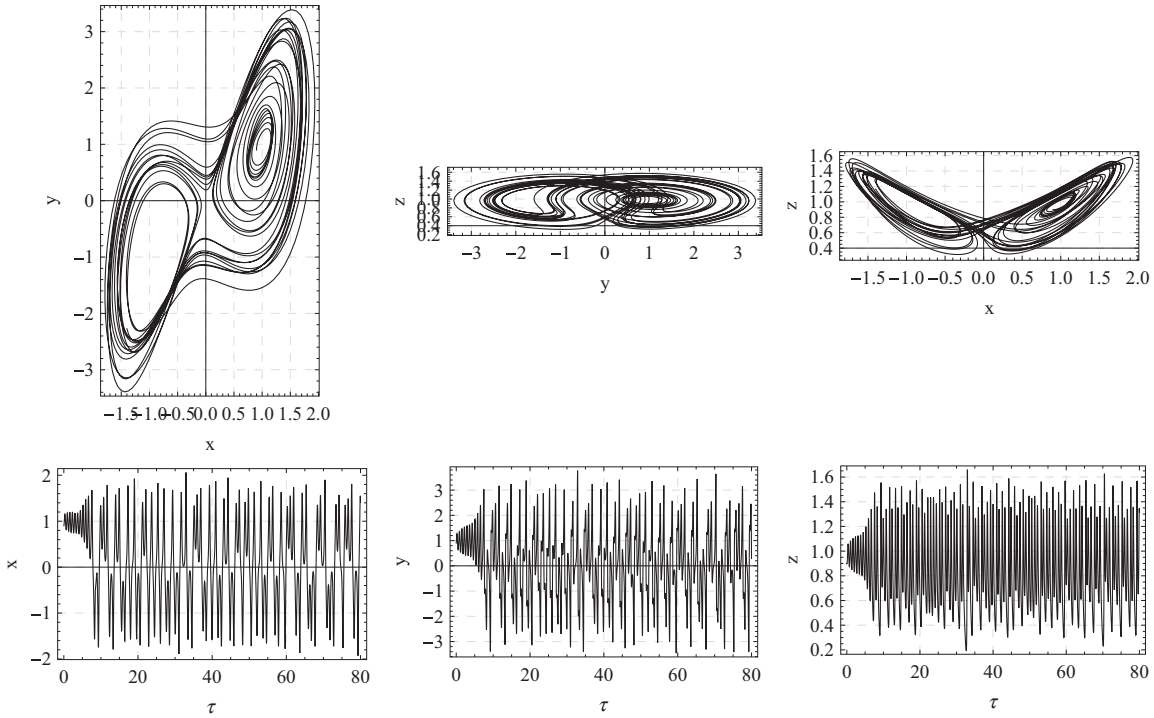

Fig. 17. Phase Portrait and time domain diagrams For the System (10) with parameters $\Omega = 10$ and $P_e = 1$, $\zeta = 0.4$, $R = 15$, $\delta = 0.1$, $\chi = 0.4$.

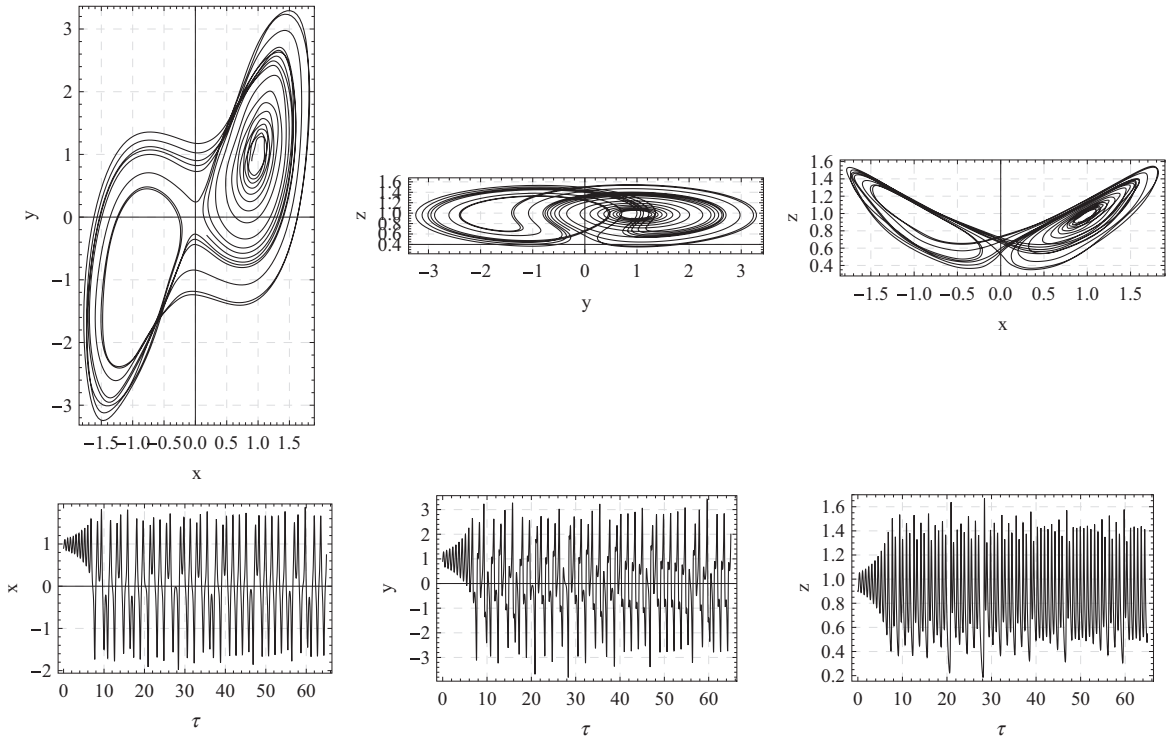

Fig. 18. Phase Portrait and time domain diagrams For the System (10) with parameters $\Omega = 40$ and $P_e = 1$, $\zeta = 0.4$, $R = 15$, $\delta = 0.1$, $\chi = 0.4$.

from the time domain solution, heat transfer decreases, finally system tends to periodic behavior on increasing χ compatible with result [53].

The effect of frequency of gravity modulation Ω is depicted in Figs. 17–19 for $\Omega = 10, 40, 80$, keeping fixed other parameters. In this case, the system looses its chaotic behaviour and shift into periodic behaviour, and so, heat transfer is delay the convection. The impact of amplitude of gravity modulation δ on the system for different parametric values $\delta = 0.01, 0.2, 0.4$ keeping fixed the other parameters, is depicted in Figs. 20–22, respectively. These

Please cite this article in press as: Bhadauria BS, Singh A. Throughflow and G-jitter effects on chaotic convection in an anisotropic porous medium. Ain Shams Eng J (2017), http://dx.doi.org/10.1016/j.asej.2016.08.024

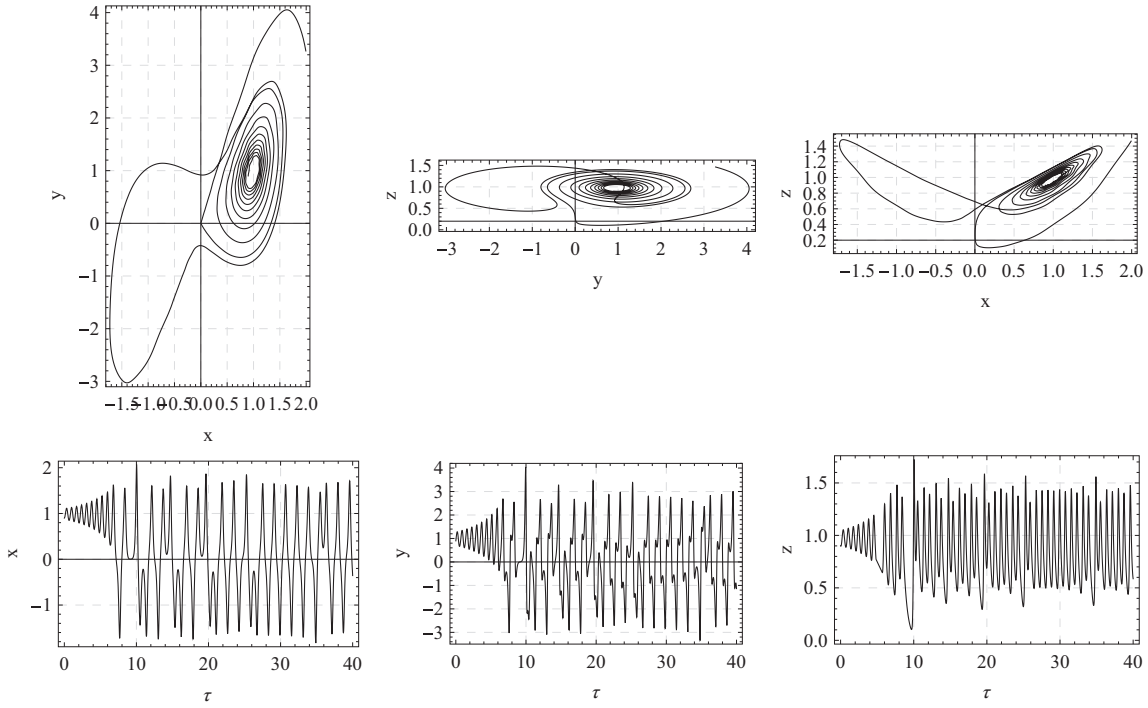

Fig. 19. Phase Portrait and time domain diagrams For the System (10) with parameters $\Omega = 80$ and $P_e = 1$, $\zeta = 0.4$, $R = 15$, $\delta = 0.1$, $\chi = 0.4$.

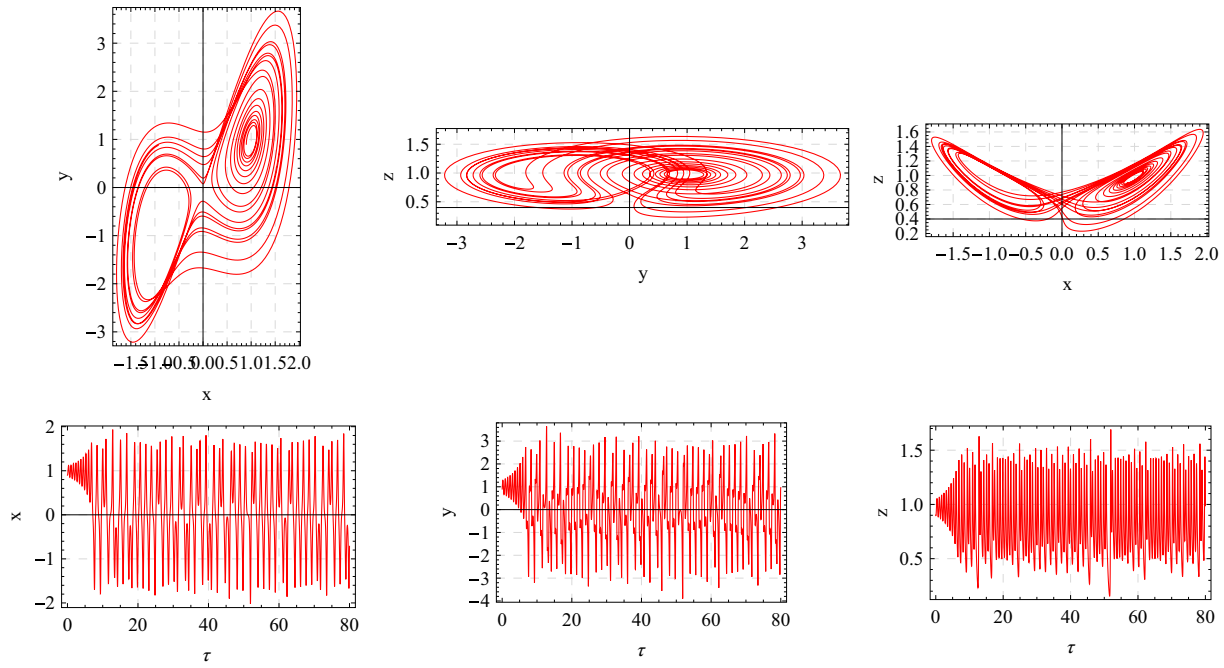

Fig. 20. Phase Portrait and time domain diagrams For the System (10) with parameters $\delta = 0.01$ and $P_e = 1$, $\zeta = 0.4$, $R = 15$, $\Omega = 5$, $\chi = 0.4$.

figures depict that the trajectories are much disturbed on increasing δ. Therefore, the chaotic behaviour advances, that is, the heat transfer is increases gradually. Both Results are analogous to [51].

Further, we compare the result of gravity modulated and unmodulated systems. For $\delta = 0, R = 5$ and fixed the other parameters Fig. 23 shows a stable solution while for $\delta = 0.1, R = 5$, the system has periodic solution, is depicted in Fig. 24. We noticed that in gravity modulated system heat transfer is more in comparison to unmodulated system. Lastly we also compare the our result from the result already obtained by Vinod et al. [53] depicted in Figs. 25. In Fig. 25 all the trajectories are moving into fixed point and time domain solution shows a stable solution for given parametric values. On the other hand all the trajectories are much disturbed in Fig. 26 due to present the modulation term δ and time domain solution depicted a periodic system, hence we analyse that in modulated system heat transfer is more.

Please cite this article in press as: Bhadauria BS, Singh A. Throughflow and G-jitter effects on chaotic convection in an anisotropic porous medium. Ain Shams Eng J (2017), http://dx.doi.org/10.1016/j.asej.2016.08.024

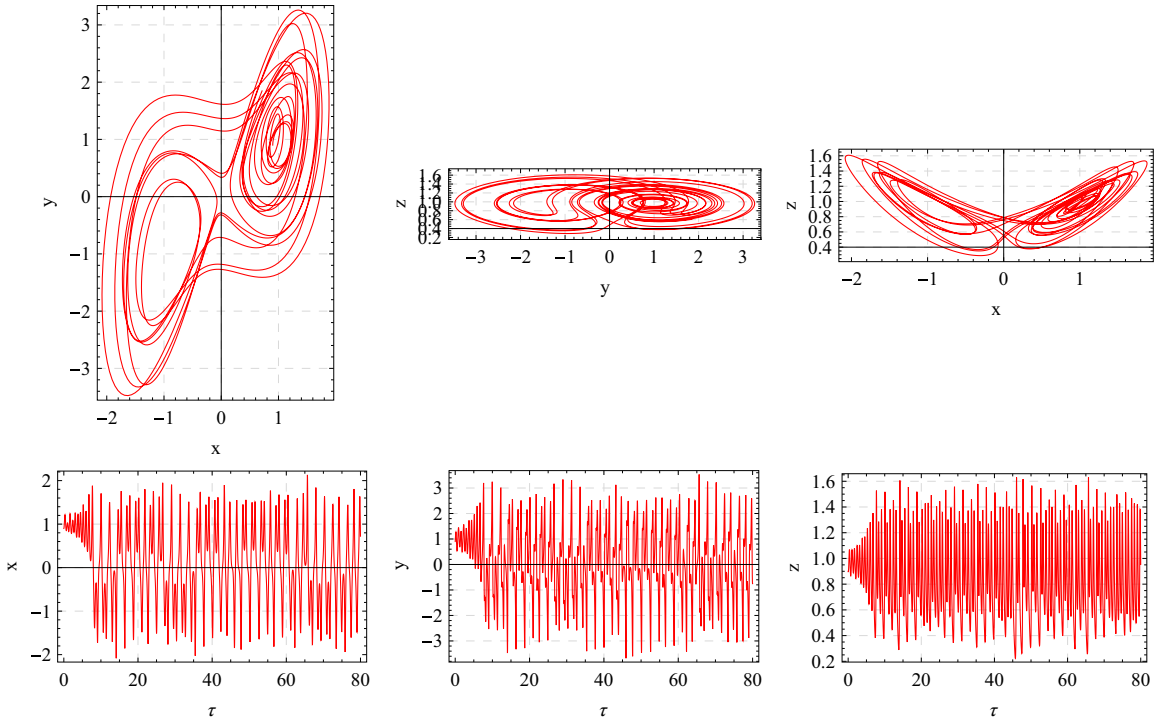

Fig. 21. Phase Portrait and time domain diagrams For the System (10) with parameters $\delta = 0.2$ and $P_e = 1$, $\zeta = 0.4$, $R = 15$, $\Omega = 5$, $\chi = 0.4$.

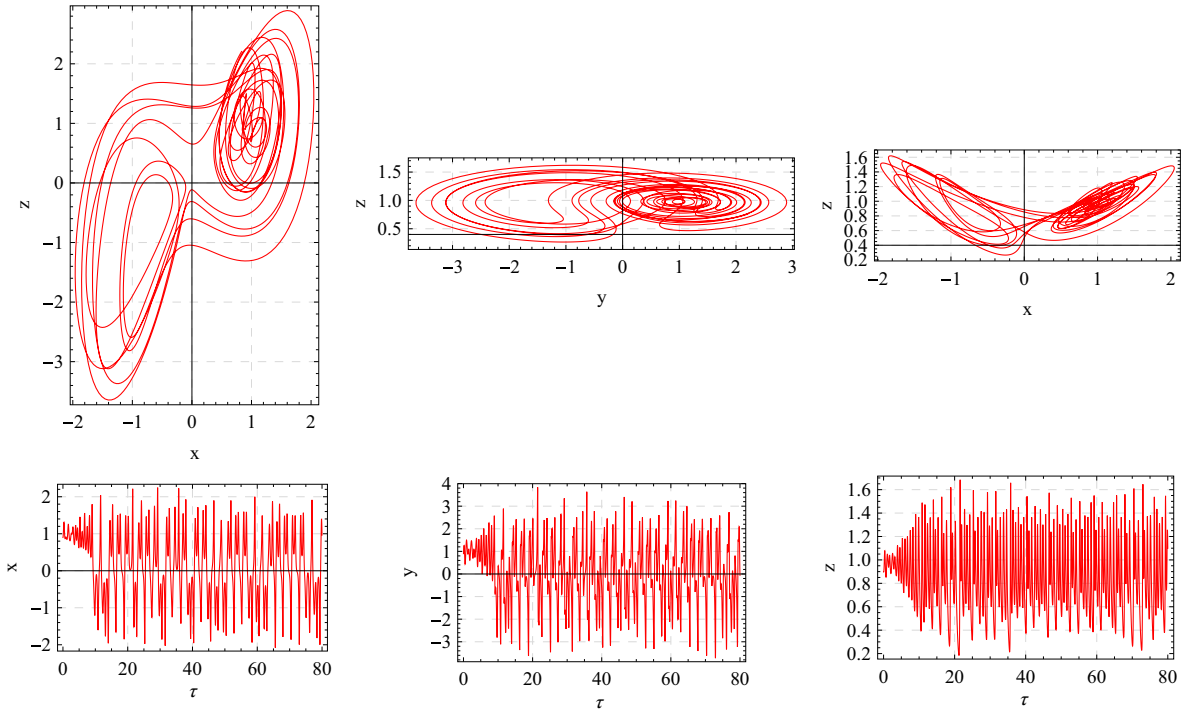

Fig. 22. Phase Portrait and time domain diagrams For the System (10) with parameters $\delta = 0.4$ and $P_e = 1$, $\zeta = 0.4$, $R = 15$, $\Omega = 5$, $\chi = 0.4$.

5. Conclusions

In this paper, throughflow and G-jitter effects on chaotic convection in an anisotropic porous medium are studied. The adopted model is firstly reduced into Lorenz system by employing truncated Galerkin expansion method. By using phase portrait and time domain diagrams the following findings are obtained.

(a) The effect of scaled Rayleigh number R is to either increase (chaotic) or decrease(periodic) the heat transport in the Lorenz system.

Please cite this article in press as: Bhadauria BS, Singh A. Throughflow and G-jitter effects on chaotic convection in an anisotropic porous medium. Ain Shams Eng J (2017), http://dx.doi.org/10.1016/j.asej.2016.08.024

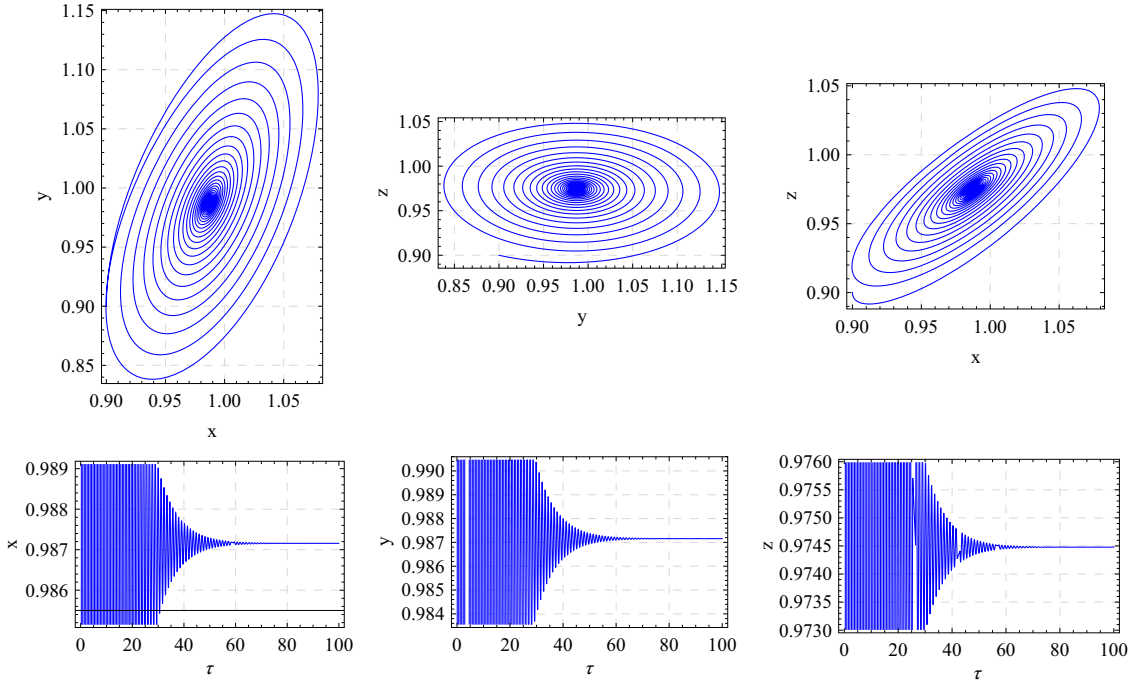

Fig. 23. Phase Portrait and time domain diagrams For the System (10) with parameters $\delta = 0.0$ and $P_e = 1$, $\zeta = 0.4$, $R = 5$, $\Omega = 5$, $\chi = 0.4$.

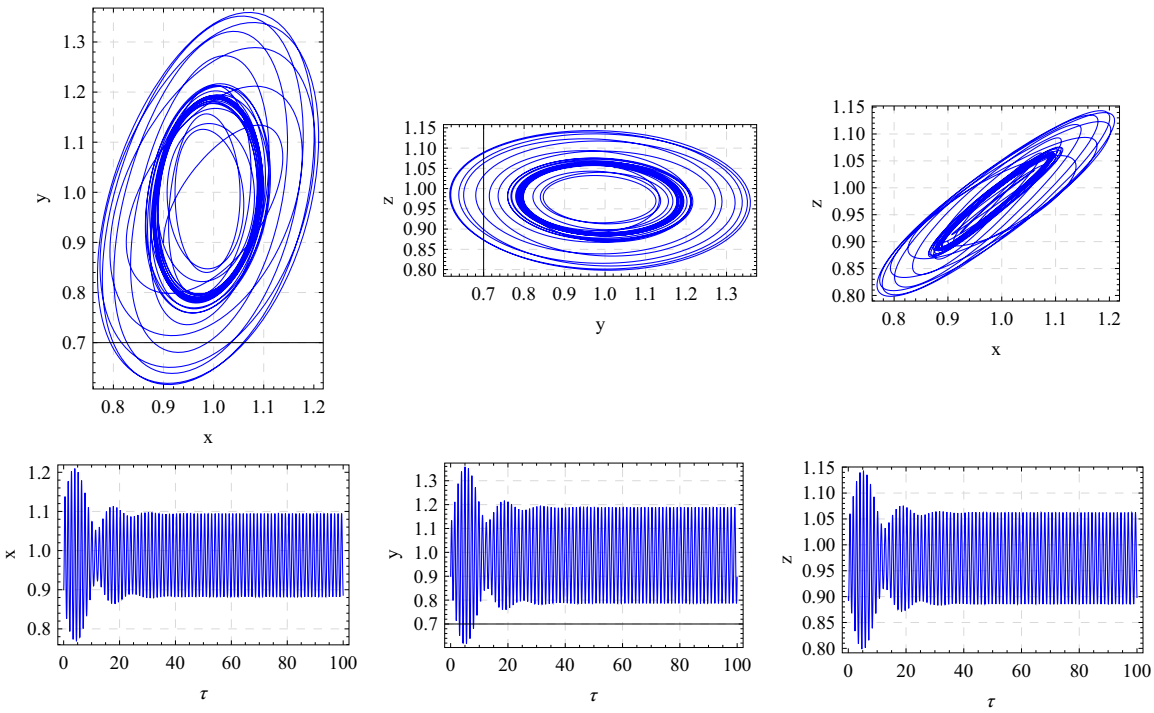

Fig. 24. Phase Portrait and time domain diagrams For the System (10) with parameters $\delta = 0.1$ and $P_e = 1$, $\zeta = 0.4$, $R = 5$, $\Omega = 5$, $\chi = 0.4$.

(b) The throughflow parameter *Pe* is to delay the chaotic convection i.e. heat transfer decreases in the system.
(c) The amplitude δ (frequency Ω) of modulation is to advance (delay) the heat transfer in the Lorenz system.
(d) The anisotropic parameters χ and ζ has tendency to delay the chaotic behaviour in the system.
(e) Finally, it is obtained that heat transfer is more in the modulated system in comparison to the without modulated system.

Please cite this article in press as: Bhadauria BS, Singh A. Throughflow and G-jitter effects on chaotic convection in an anisotropic porous medium. Ain Shams Eng J (2017), http://dx.doi.org/10.1016/j.asej.2016.08.024

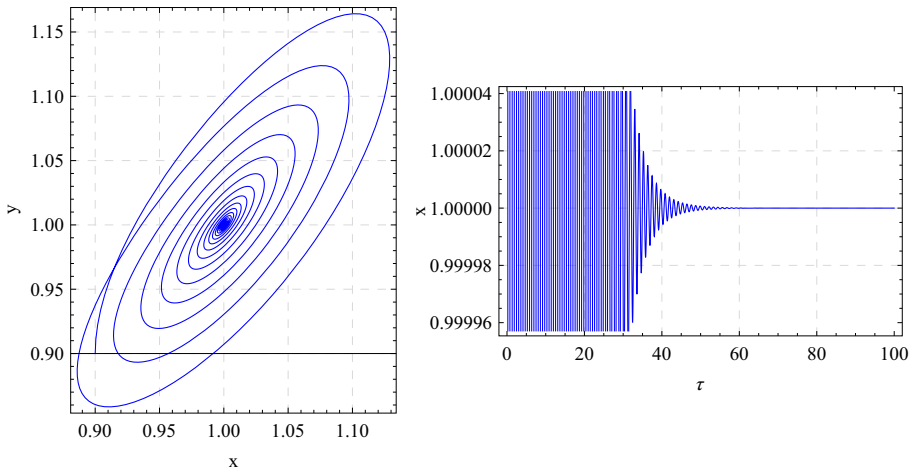

Fig. 25. Phase Portrait and time domain diagrams For the System (10) with parameters $\delta = 0.0$ and $\zeta = 1.5$, $R = 16$, $\chi = 0.6$, $\sigma = 5$.

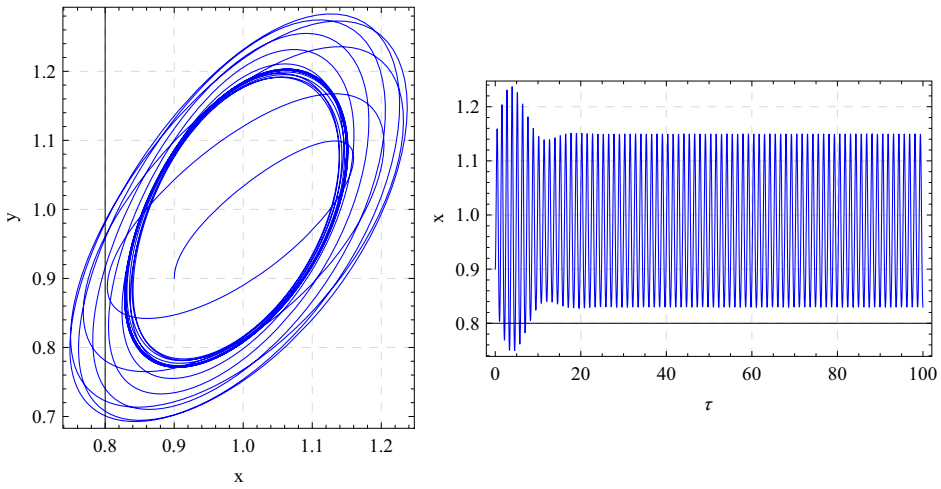

Fig. 26. Phase Portrait and time domain diagrams For the System (10) with parameters $\delta = 0.1$ and $P_e = 1$, $\zeta = 1.5$, $R = 16$, $\Omega = 5$, $\chi = 0.6$, $\sigma = 5$.

Acknowledgement

The authors Ajay Singh gratefully acknowledges the financial assistance from Babasaheb Bhimrao Ambedkar University, Lucknow, India as a research fellowship.

References

[1] Ingham DB, Pop I. Transport phenomena in porous media, 1st ed., vol. III. Oxford: Elsevier; 2005.
[2] Nield DA, Bejan A. Convection in porous media. 3rd ed. New York: Springer; 2006.
[3] Vafai K. Handbook of porous media. New York: Marcel Dekker; 2000.
[4] Epherre JF. Crit'ere d'apparition de la convection naturalle dans une couche poreuse anisotrope. Rev. Gn. Thermique, 1975;168: 949–950 English translation. Int Chem Eng 1977;17:615–6.
[5] Kvernvold O, Tyvand PA. Nonlinear thermal convection in anisotropic porous media. J Fluid Mech 1979;90:609–24.
[6] Nisen T, Storesletten L. An analytical study of natural convection in isotropic and anisotropic porous channels. Trans ASME J Heat Transf 1990;112:369–401.
[7] Tyvand PA, Storesletten L. Onset of convection in an anisotropic porous medium with oblique principal axes. J Fluid Mech 1991;226:371–82.
[8] Degan G, Vasseur P, Bilgen E. Convective heat transfer in a vertical anisotropic porous layer. Heat Mass Transf 1995;38(11):1975–87.
[9] Nield DA, Kuznetsov AV. Effects of gross heterogeneity and anisotropy in forced convection in a porous medium: layered medium analysis. J Porous Med 2003;6:51–7.
[10] Nield DA, Kuznetsov AV. The effects of combined horizontal and vertical heterogeneity and anisotropy on the onset of convection in a porous medium. Int J Therm Sci 2007;46:1211–8.
[11] Govender S. On line effect of anisotropy on the stability of convection in a rotating porous media. Transp Porous Med 2006;64:413–22.
[12] Govender S. Coriolise effect on the stability of centrifugally driven convection in a rotating anisotropic porous layer subject to gravity. Transp Porous Med 2007;69:55–66.
[13] Malashetty MS, Heera R. The effect of rotation on the onset of double diffusive convection in a horizontal anisotropic porous layer. Numer Heat Transf 2006;49:69–94.
[14] Malashetty MS, Swamy M. The effect of rotation on the onset of convection in a horizontal anisotropic porous layer. Int J Therm Sci 2007;46:1023–32.
[15] Simmons CT, Kuznetsov AV, Nield DA. Effect of strong heterogeneity on the onset of convection in a porous medium: importance of spatial dimensionality and geologic controls. Water Resour Res 2010;46:W09539. doi: http://dx.doi.org/10.1029/2009WR008606.
[16] Altawallbeh AA, Bhadauria BS, Hashim I. Linear and nonlinear double-diffusive convection in a saturated anisotropic porous layer with Soret effect and internal heat source. Int J Heat Mass Transf 2013;59:103–11.
[17] Alok et al. Heat transport in an anisotropic porous medium saturated with variable viscosity liquid under G-jitter and internal heating effects. Transp Porous Med 2013;99(2):359–76.
[18] Bhadauria BS, Kiran P. Heat transport in an anisotropic porous medium saturated with variable viscosity liquid under temperature modulation. Transp Porous Med 2013;100(2):279–95.

Please cite this article in press as: Bhadauria BS, Singh A. Throughflow and G-jitter effects on chaotic convection in an anisotropic porous medium. Ain Shams Eng J (2017), http://dx.doi.org/10.1016/j.asej.2016.08.024

[19] Gresho PM, Sani R. The effects of gravity modulation on the stability of a heated fluid layer. J Fluid Mech 1970;40:783–806.
[20] Malashetty MS, Padmavathi V. Effect of gravity modulation on the onset of convection in a fluid and porous layer. Int J Eng Sci 1997;35:829–83.
[21] Rees DAS, Pop I. The effect of G-jitter on vertical free convection boundary-layer flow in porous media. Int Commun Heat Mass Transf 2000;27(3):415–24.
[22] Govender S. Weak non-linear analysis of convection in a gravity modulated porous layer. Transp Porous Med 2005;60:33–42.
[23] Siddhavaram VK, Homsy GM. The effects of gravity modulation on fluid mixing Part 1. Harmonic modulation. J Fluid Mech 2006;562:445–75.
[24] Saravanan S, Sivakumar T. Thermo vibrational instability in a fluid saturated anisotropic porous medium. ASME J Heat Transf 2011;133(5):051601. doi: http://dx.doi.org/10.1115/1.4003013.
[25] Malashetty MS, Swamy M. Effect of gravity modulation on the onset of thermal convection in rotating fluid and porous layer. Phys Fluids 2011;23(6):064108.
[26] Wooding RA. Rayleigh instability of a thermal boundary layer in flow through a porous medium. J Fluid Mech 1960;9:183–92.
[27] Sutton FM. Onset of convection in a porous channel with net throughflow. Phys Fluids 1970;13:1931.
[28] Homsy GM, Sherwood AE. Convective instabilities in porous media with throughflow. AIChE J 1976;22:168–74.
[29] Jones MC, Persichetti JM. Convective instability in packed beds with throughflow. AIChE J 1986;32:1555–7.
[30] Nield DA. Convective instability in porous media with throughflow. AIChE J 1987;33:1222–4.
[31] Shivakumara IS. Effects of throughflow on convection in porous media. In: Proc. 7th Asian congr. fluid mech., vol. 2; 1997. p. 557–60.
[32] Khalili A, Shivakumara IS. Onset of convection in a porous layer with net throughflow and internal heat generation. Phys Fluids 1998;10:315.
[33] Shivakumara IS. Boundary and inertia effects on convection in a porous media with throughflow. Acta Mech 1999;137:151–65.
[34] Shivakumara IS, Nanjundappa CE. Effects of quadratic drag and throughflow on double diffusive convection in a porous layer. Int Commun Heat Mass Transf 2006;33:357–63.
[35] Shivakumara IS, Sureshkumar S. Convective instabilities in a viscoelastic-fluid-saturated porous medium with throughflow. J Geophys Eng 2007;4:104–15.
[36] Brevdo L. Three-dimensional absolute and convective instabilities at the onset of convection in a porous medium with inclined temperature gradient and vertical throughflow. J Fluid Mech 2009;641:475–87.
[37] Barletta A, di Schio ER, Storesletten L. Convective roll instabilities of vertical throughflow with viscous dissipation in a horizontal porous layer. Transp Porous Med 2010;81:461–77.
[38] Reza M, Gupta AS. Magnetohydrodynamics thermal instability in a conducting fluid layer with through flow. Int J Non-Linear Mech 2012;47:616–25.
[39] Nield DA, Kuznetsov AV. The effects of combined horizontal and vertical heterogeneity on the onset of convection in a porous medium with horizontal throughflow. Int J Heat Mass Transf 2010;54:5595–601.
[40] Bhadautria BS, Kiran P. Nonlinear throughflow effects on thermally modulated porous medium. Ain Shams Eng J 2016;7:473–82.
[41] Poincaré JH. Sur le probléme des trois corps et les équations de la dynamique. Acta Math 1890;13:01–279.
[42] Lorenz EN. Deterministic non-periodic flow. J Atmos Sci 1963;20:130–41.
[43] Sparrow C. The Lorenz equations: bifurcations, chaos, and strange attractors. New York: Springer-Verlag; 1982.
[44] Vadasz P, Olek S. Transition and chaos for free convection in a rotating porous layer. Int J Heat Mass Transf 1998;41(11):1417–35.
[45] Vadasz P, Olek S. Weak turbulence and chaos for low Prandtl number gravity driven convection in porous media. Transp Porous Med 1999;37(1):69–91.
[46] Vadasz P, Olek S. Computational recovery of the homoclinic orbit in porous media convection. Int J Non-Linear Mech 1999;34(6):89–93.
[47] Vadasz P, Olek S. Route to chaos for moderate Prandtl number convection in a porous layer heated from below. Transp Porous Med 2000;41(2):211–39.
[48] Vadasz P, Olek S. Convergence and accuracy of Adomian's decomposition method for the solution of Lorenz equations. Int J Heat Mass Transf 2000;43(10):1715–34.
[49] Long et al. Chaotic convection of viscoelastic fluid in porous media. Chaos Solitons Fractals 2008;37:113–24.
[50] Vadasz et al. Chaotic and Periodic natural convection for moderate and high Prandtl numbers in a porous layer subject to vibrations. Transp Porous Med 2014;103:279–94.
[51] Bhadauria BS, Kiran P. Chaotic and oscillatory magneto-convection in a binary viscoelastic fluid under G-jitter. Int J Heat Mass Transf 2015;84:610–24.
[52] Bhadauria BS, Kiran P. Chaotic convection in a porous medium under temperature modulation. Transp Porous Med 2015;107:745–63.
[53] Gupta VK, Singh AK. A study of chaos in an anisotropic porous cavity. Int J Energy Tech 2013;5(27):1–12.

Dr. B.S. Bhadauria is working as Professor in the Department of Applied Mathematics, Babasaheb Bhimrao Ambedkar University Lucknow-226025, India. Presently he is on leave from Department of Mathematics, Institute of Science, Banaras Hindu University, Varanasi-221005, India, where he works as Professor of Mathematics. His area of research interest is nonlinear thermal instability, numerical methods and mathematical modeling.

Ajay Singh is a research scholar in the Department of Applied Mathematics, in Babasaheb Bhimrao Ambedkar University Lucknow India. His research interest is Fluid Mechanics.

Please cite this article in press as: Bhadauria BS, Singh A. Throughflow and G-jitter effects on chaotic convection in an anisotropic porous medium. Ain Shams Eng J (2017), http://dx.doi.org/10.1016/j.asej.2016.08.024